UNIVERSIDADE
BEIRA INTERIOR

Biosynthesis and purification of DNA vectors as therapeutic approaches against Human Papillomavirus infection

Ana Margarida Cardoso Valério de Almeida

Tese para obtenção do Grau de Doutor em
Bioquímica
(3º ciclo de estudos)

Orientadora: Prof.ª Doutora Ângela Maria Almeida de Sousa
Co-orientadora: Prof.ª Doutora Fani Pereira de Sousa

julho de 2020

Dedicatory

To my mom, Zé and my best friends.

Acknowledgements

Firstly, I would like to express my profound gratitude to Professor Doctor Ângela Sousa and Professor Doctor Fani Sousa for all the support and guidance that both were able to provide me throughout these past years. To Professor Ângela, my deepest appreciation for all the valuable advices, both professional and personal, the scientific discussions, the shared knowledge, fun moments, patience, help, availability, faith, friendship and dedication in the past years. Without any doubt, your support was crucial for me. To Professor Fani, my sincere gratitude for all the insightful discussions, valuable advices, knowledge, expertise, help and availability shared with me in the past years.

To Professor Doctor João Queiroz, for all the scientific advices and insightful suggestions, which undoubtedly added value to this thesis.

To University of Beira Interior, especially to the Health Sciences Research Centre for providing the adequate conditions for the development of this research project. Also to Uhr Cernigoj and Bia Separations company, for kindly providing the monolithic supports used in this project and for the useful scientific discussions.

To Fundação para a Ciência e Tecnologia (FCT) for the financial support for my PhD fellowship (SFRH/BD/81914/2011), allowing me to experience this incredible opportunity.

I would also like to thank my lab colleagues, to whom I owe interesting scientific discussions, which allowed to put some results in different perspectives, and with whom I was able to share happy moments inside and outside the lab. For all the team-work, support, advices and good mood, I thank you all.

Moreover, I would like to thank my close friends, especially the ones that have been also working at CICS, for withstanding by my side throughout fun breaks, tearful results and heated scientific discussions. You were the ones that especially helped me keep my sanity throughout these hard-working years. To my hometown friends, thanks for understanding why I was so unwilling to talk about my thesis, I just needed a mental break when I was with you guys!

To Zé, my profound appreciation for your love and patience, especially in the last few months, for being able to endure my late nights and weekends working in this thesis. In this final stage, you were my rock.

E por fim, mas principalmente, gostaria de agradecer à minha Mãe, que de tudo fez para que nada me faltasse e para que eu pudesse ser a melhor versão de mim mesma.

List of scientific publications

Papers related with Doctoral thesis

I. HPV-16 Targeted DNA Vaccine Expression: The Role of Purification

A.M. Almeida, J. Tomás, P. Pereira, J.A. Queiroz, F. Sousa, A. Sousa

Biotechnology Progress (2018) 34: 546–551 (doi: 10.1002/btpr.2603).

II. Minicircle DNA purification: Performance of chromatographic monoliths bearing lysine and cadaverine ligands.

A.M. Almeida, J.A. Queiroz, F. Sousa, A. Sousa.

Journal of Chromatography B (2019) 1118–1119: 7-16 (doi: 10.1016/j.jchromb.2019.04.024).

III. Cervical cancer and HPV-Infection: ongoing therapeutic research to counteract the action of E6 and E7 oncoproteins.

A.M. Almeida, J.A. Queiroz, F. Sousa, A. Sousa.

Drug Discovery Today (2019) S1359-6446: 30310-1 (doi: 10.1016/j.drudis.2019.07.011).

IV. The use of size-exclusion chromatography in the isolation of supercoiled minicircle DNA from *Escherichia coli* lysate.

A.M. Almeida, D. Eusébio, J.A. Queiroz, F. Sousa, A. Sousa.

Journal of Chromatography A (2019) 460444 (doi: 10.1016/j.chroma.2019.460444).

V. Quality assessment of supercoiled minicircle DNA by cadaverine-modified analytical chromatographic monolith

A.M. Almeida, U. Černigoj, J.A. Queiroz, F. Sousa, A. Sousa

Journal of Pharmaceutical and Biomedical Analysis (2019) 180: 113037 (doi: 10.1016/ j.jpba.2019.113037)

VI. Minicircle DNA – The future for DNA-based vectors?

A.M. Almeida, J.A. Queiroz, F. Sousa, A. Sousa

Trends in Biotechnology (2020) S0167-7799(20)30113-X (doi: 10.1016/j.tibtech.2020.04.008)

VII. Enhancement of a biotechnological platform for the purification and delivery of a human papillomavirus supercoiled plasmid DNA vaccine.

A.M. Almeida, D. Costa, A.R. Simões, J.A. Queiroz, F. Sousa, A. Sousa

New Biotechnology (2020) 59: 1-9 (doi: 10.1016/j.nbt.2020.04.003)

VIII. Silencing Human Papillomaviruses E6 and E7 oncoproteins with a minicircle DNA vector encoding pri-miR-375

A.M. Almeida, J.A. Queiroz, F. Sousa, A. Sousa

(In preparation)

Papers not related with Doctoral thesis

I. Histamine monolith versatility to purify supercoiled plasmid deoxyribonucleic acid from Escherichia coli lysate.

A. Sousa, A.M. Almeida, U. Cernigoj, F. Sousa, J.A. Queiroz.

Journal of Chromatography A (2014) 1355: 125-133.

II. Optimization of supercoiled HPV-16 E6/E7 plasmid DNA purification with arginine monolith using design of experiment.

A.M. Almeida, J.A. Queiroz, F. Sousa, A. Sousa.

Journal of Chromatography B (2015) 978-979:145-50.

III. Preparation of Well-Defined Brush-Like Block Copolymers for Gene Delivery Applications Under Biorelevant Reaction Conditions.

J.R. Góis, F. Reis, A.M. Almeida, P. Pereira, F. Sousa, A.C. Serra, J.F.J. Coelho.

Colloids and Surfaces B: Biointerfaces (2018) 169: 107–117.

IV. Optimization of peptide-plasmid DNA vectors formulation for gene delivery in cancer therapy exploring design of experiments.

A. Sousa, A.M. Almeida, R. Faria, K. Konate, P. Boisguerin, J.A. Queiroz, D. Costa.

Colloids and Surfaces B: Biointerfaces (2019) 183: 110417

Chapters not related with Doctoral thesis

I. Minicircle DNA vaccine purification by size-exclusion chromatography and antigen detection with immunocytochemistry

A.M. Almeida, D. Eusébio, J.A. Queiroz, F. Sousa and A. Sousa

Methods and Protocols in DNA Vaccines - Methods in molecular biology (Springer)

(In production)

List of scientific communications

Oral communications related with Doctoral thesis

I. Supercoiled HPV16 E6/E7 plasmid DNA-based vaccine purified by affinity chromatography for in vitro transfection studies.

A.M. Almeida, P. Pereira, J. Tomás, V. Figueiredo, J. A. Queiroz, F. Sousa, A. Sousa.

VIII Jornadas sobre Tecnologia e Saúde. Guarda, Portugal, 2015

II. DNA vaccine development for HPV treatment: biotechnological production, purification and in vitro application.

A.M. Almeida, P. Pereira, J. Tomás, V. Figueiredo, J. A. Queiroz, F. Sousa, A. Sousa.

Microbiotec'15 - Congress of Microbiology and Biotechnology. Évora, Portugal, 2015

III. Versatility of arginine monolithic support in the purification of therapeutic DNA vectors.

A.M. Almeida, J. A. Queiroz, F. Sousa, A. Sousa.

XVI Congresso Latino-Americano de Cromatografia (COLACRO) e 9º Encontro Nacional de Cromatografia. Lisboa, Portugal, 2016

IV. DNA vaccines and gene therapy for treatment of HPV-induced cervical cancer.

A.M. Almeida, J.A. Queiroz, F. Sousa, A. Sousa.

Jornadas Nacionais de Ciências Biomédicas. Covilhã, Portugal, 2017.

Invited communication

V. Affinity chromatography for Minicircle DNA purification: lysine- and cadaverine-monoliths performance.

A.M. Almeida, J.A. Queiroz, F. Sousa, A. Sousa.

II International Congress in Health Sciences Research. Covilhã, Portugal, 2017

VI. Pri-miR-375 expressing mcDNA vector: reaching for HPV oncoproteins silencing.

A.M. Almeida, J.A. Queiroz, F. Sousa, A. Sousa.

ESBES 18. Lisboa, Portugal, 2018

Poster communications related with Doctoral thesis

I. Biotechnological approach to prepare a DNA vaccine for HPV induced cervical cancer treatment.

A. M. Almeida, P. Pereira, J. Tomás, V. Figueiredo, J. A. Queiroz, F. Sousa, A. Sousa.

HPV 2015, 30th International Papillomavirus Conference. Lisboa, Portugal, 2015

II. Implementation of biotechnological platform for the obtainment of HPV-16 E6 and E7 plasmid DNA vaccine.

A.M. Almeida, J. Tomás, P. Pereira, V. Figueiredo, J. A. Queiroz, F. Sousa, A. Sousa.

I Congress in Health Sciences Research: Towards Innovation and Entrepreneurship. Covilhã, Portugal, 2015

III. Purifying minicircle DNA: a comparison between the lysine and cadaverine affinity ligands.

A.M. Almeida, J.A. Queiroz, F. Sousa, A. Sousa.

Microbiotec 17. Porto, Portugal, 2017

IV. Biotechnological production and purification of minicircle DNA encoding pri-miR-375 for the potential treatment of cervical cancer.

A.M. Almeida, J.A. Queiroz, F. Sousa, A. Sousa.

XII Annual CICS-UBI Symposium. Covilhã, Portugal, 2018

V. Highly pure sc pDNA vaccine against HPV infection: Dendritic cell targeting with modified CaCO3 nanoparticle.

A. Sousa, A.M. Almeida, A.R. Simões, J.A. Queiroz, D. Costa.

ESBES 18. Lisboa, Portugal, 2018

Oral communications not related with Doctoral thesis

I. Purification of Human Papillomavirus16 E6/E7 plasmid DNA-based vaccine using an arginine modified monolithic support.

A. Soares, A. M. Almeida, J.A. Queiroz, F. Sousa, A. Sousa.

Micro Biotech'13 - Congress of Microbiology and Biotechnology. Aveiro, Portugal, 2013

II. Optimized purification strategy of supercoiled HPV16 E6/E7 plasmid DNA-based vaccine for in vitro transfection studies.

A.M. Almeida, P. Pereira, J. Tomás, J.A. Queiroz, F. Sousa, A. Sousa.

IX Annual CICS Symposium. Covilhã, Portugal, 2014

III. **Biosynthesis and purification of a minicircular DNA vector for cervical cancer therapy.**

J.M. Alves, A.M. Almeida, C.J. Maia, J.A. Queiroz, F. Sousa, A. Sousa.
XII Annual CICS Symposium. Covilhã, Portugal, 2017

IV. Therapeutic effect evaluation of minicircle DNA (mcDNA) vectors.

A. Resende-Pinto, D. Carvalho Pereira, D. Eusébio, A.M. Almeida, L.A. Passarinha, A. Sousa.
XIV Annual CICS Symposium. Covilhã, Portugal, 2019

Poster communications not related with Doctoral thesis

I. Arginine monolith in the purification of Human Papillomavirus16 E6/E7 plasmid DNA-based vaccine.

A. Soares, A. M. Almeida, J.A. Queiroz, F. Sousa, A. Sousa.

8º Encontro Nacional de Cromatografia. Covilhã, Portugal, 2013

II. Minicircular DNA as a potential gene therapy vector in cervical cancer.

J.M. Alves, A.M. Almeida, C. J. Maia, J.A. Queiroz, F. Sousa, A. Sousa.

II International Congress in Health Sciences Research. Covilhã, Portugal, 2017

III. Recombinant p53- minicircular DNA: from the design to the in vitro p53 expression.

J.M. Alves, A.M. Almeida, C. J. Maia, J.A. Queiroz, F. Sousa, A. Sousa.

Microbiotec 17. Porto, Portugal, 2017

IV. Recombinant p53-minicircular DNA: biopharmaceutical purification and re-establishing of the p53 levels in cancer cells.

D. Eusébio, A.M. Almeida, J.M. Alves, C.J. Maia, J.A. Queiroz, F. Sousa, A. Sousa.

XII Annual CICS-UBI Symposium. Covilhã, Portugal, 2018

V. Recombinant p53-minicircular DNA: a potential therapeutic strategy for cervical cancer.

D.Eusébio, A.M. Almeida, J.M. Alves, C.J. Maia, J.A. Queiroz, F. Sousa, A. Sousa.

ESBES 18. Lisboa, Portugal, 2018

Resumo Alargado

Introdução

O cancro do colo do útero é uma das principais causas de morte entre as mulheres, especialmente em países com acesso limitado a cuidados de saúde e higiene. Ao contrário da maioria dos cancros, que geralmente têm origem em mutações relacionadas com a ação de mutagénicos ou carcinogénicos, o desenvolvimento deste cancro em particular está fortemente associado à infeção pelo vírus do papiloma humano (HPV). Este vírus é responsável pela expressão de oncoproteínas que irão interferir com a regulação do ciclo celular, afetando os mecanismos de reparação e proliferação das células infetadas. As proteínas virais com maior ação oncogénica são as proteínas E6 e E7 do HPV, que por sua vez interferem com a expressão/ação das proteínas supressoras de tumor p53 e pRB, respetivamente. A alteração dos níveis de expressão/ação das proteínas supressoras de tumor pode levar à acumulação de erros irreparáveis nas células que se encontram em constante divisão, resultando na formação de massas celulares cancerígenas altamente proliferativas. Deste modo, identificando a expressão das proteínas E6 e E7 como as principais causas para o desenvolvimento do cancro do colo do útero, várias estratégias têm vindo a ser desenvolvidas no sentido de reverter ou controlar os efeitos associados a esta infeção, perspetivando o desenvolvimento de uma terapêutica efetiva.

Nas últimas décadas, estratégias inovadoras como vacinação por DNA ou terapia génica têm sido alvo de grande foco por parte dos investigadores na procura de uma cura para o cancro do colo do útero. Enquanto as vacinas de DNA permitem exercer uma ação tanto terapêutica como preventiva contra a infeção por HPV através da estimulação/mobilização do sistema imunitário, a terapia génica permite aumentar ou silenciar a expressão de proteínas envolvidas no desenvolvimento da patologia. No caso das vacinas de DNA, têm surgido vários estudos com o intuito de direcionar a expressão das proteínas E6 e/ou E7 em células apresentadoras de antigénios, de forma a criar uma resposta imunológica humoral e celular contra estas proteínas. Esta estratégia, para além de ativar o sistema imunitário para o reconhecimento das células que apresentam estes antigénios (ação terapêutica), permite também a produção de linfócitos de memória que poderão ser ativados aquando de uma posterior infeção por HPV (ação preventiva). Por outro lado, a terapia génica tem como intuito atuar diretamente na massa cancerígena, induzindo a expressão de proteínas supressoras de tumor (como o caso das proteínas p53 e pRB) ou silenciando a expressão de proteínas malignas (como o caso das proteínas E6 e E7). No segundo caso existem diversas metodologias pelas quais o mecanismo de silenciamento pode ocorrer, desde a utilização de moléculas sintetizadas quimicamente até à utilização de moléculas naturalmente expressas pelo organismo capazes de regular a expressão de diversas proteínas, como por exemplo os microRNAs (miRs). Estes pequenos RNAs são responsáveis por regular a expressão de diversas proteínas através do seu silenciamento. A

expressão de microRNAs tem sido recentemente associada ao cancro, dado que a sua desregulação pode levar a que haja uma maior apetência para desencadear os mecanismos responsáveis pelo desenvolvimento de cancro. Por exemplo, alguns trabalhos descrevem que os níveis de miR-375 estão significativamente diminuídos em amostras de cancro do colo do útero. Diferentes estudos identificaram que o aumento da expressão do miR-375 leva à diminuição dos níveis de expressão das proteínas E6 e E7, aliados ao aumento dos níveis de expressão das proteínas supressoras de tumor p53 e pRB. Em suma, tanto a estratégia de vacinas de DNA como terapia génica apresentam resultados promissores que poderão contribuir para o estabelecimento de uma abordagem terapêutica sólida e eficaz. No entanto existe uma problemática que afeta transversalmente estas estratégias e que se prende com o tipo de vetor utilizado para entregar e expressar a informação genética pretendida.

Atualmente, os vetores virais têm vindo a ser amplamente utilizados em detrimento de vetores não-virais, como o DNA plasmídeo (pDNA), devido à eficácia terapêutica diminuída demonstrada pelos últimos, apesar de serem mais seguros e biocompatíveis para o paciente. Esta realidade levou a que vários investigadores se focassem no desenvolvimento de vetores não-virais inovadores que apresentam maior efeito terapêutico. O DNA minicircular (mcDNA) consiste num vetor de DNA não-viral cuja popularidade tem vindo a aumentar incrivelmente nos últimos anos. Este vetor advém da recombinação de uma molécula semelhante ao pDNA convencional, denominada plasmídeo parental (PP). Contudo, o PP apresenta dois locais de recombinação que, após indução, dão origem à recombinação desta molécula em duas moléculas filhas: uma contendo toda a informação procariota necessária para a amplificação do PP em hospedeiros procariotas (miniplasmídeo – mP) e outra contendo toda a informação necessária para a expressão do gene terapêutico em células eucariotas (mcDNA). A eliminação do conteúdo procariota leva a que o vetor de mcDNA apresente um tamanho reduzido, permitindo maior facilidade na internalização das células alvo, uma maior biocompatibilidade, eficácia terapêutica e segurança. Isto porque, as sequências procariotas presentes nos plasmídeos são responsáveis por desencadear respostas imunológicas adversas e consequentemente o silenciamento da expressão do gene alvo, o que fica controlado com a utilização de mcDNA. Tendo em conta a sua tecnologia de produção inovadora, existe a necessidade de desenvolver estratégias adequadas para a obtenção de mcDNA cuja pureza se enquadre nos valores estabelecidos pelas agências reguladoras como a *European Medicines Agency* (EMA) ou a *Food and Drug Administration* (FDA).

Descrição do trabalho realizado

Este trabalho baseou-se, numa primeira fase, no desenvolvimento de uma vacina de pDNA para a produção simultânea das proteínas antigénicas E6 e E7 do HPV, e numa segunda fase, no desenvolvimento de uma estratégia de terapia génica para o silenciamento das proteínas referidas através da obtenção de um vetor de mcDNA capaz de codificar o miR-375.

Na abordagem sobre vacinas de pDNA, foram realizados estudos *in vitro* para perceber a importância que o método de purificação poderá ter na expressão das proteínas antigénicas codificadas na molécula de pDNA, seguindo-se o desenvolvimento de estratégias adequadas para a entrega da vacina em estudo. Para tal, a vacina de pDNA foi purificada por cromatografia de afinidade aplicando suportes monolíticos modificados com ligandos de arginina e posteriormente também foram explorados sistemas de carbonato de cálcio para avaliar a capacidade na entrega da vacina de pDNA às células apresentadoras de antigénio (células dendríticas).

Na abordagem de terapia génica, o estudo do silenciamento das oncoproteínas E6 e E7 foi realizado através da construção de um vetor mcDNA codificante para o pri-miR-375. Tendo em conta o carácter inovador do mcDNA, foram desenvolvidos vários estudos no sentido de implementar metodologias adequadas para a sua purificação e caracterização. Para tal, foi explorado pela primeira vez um suporte monolítico modificado com ligandos de cadaverina, no sentido de isolar mcDNA na isoforma superenrolada (sc) de outras isoformas e constituintes bacterianos, bem como de resquícios do seu precursor PP presentes na amostra. Por outro lado, também foi explorada a cromatografia de filtração em gel para a purificação desta molécula através da utilização da matriz Sephacryl SF-1000. Além disso, foi implementada pela primeira vez uma metodologia analítica, baseada em cromatografia com o monolito modificado com cadaverina, para a avaliação do conteúdo de mcDNA presente em amostras simples e complexas. Por último, a avaliação da potencial ação terapêutica deste vetor foi iniciada tendo por base a transfeção de células CaSki, uma linha celular modelo para o cancro do colo do útero.

Principais resultados alcançados

Este trabalho foi realizado com duas perspetivas diferentes para o tratamento do cancro do colo do útero, considerando nomeadamente as vacinas de DNA e terapia génica. Primeiramente, no que concerne às vacinas de DNA, o estudo de purificação da vacina de pDNA por cromatografia de afinidade permitiu perceber que a estratégia utilizada contribui significativamente para a eficiente transfeção e expressão do gene codificado na respetiva molécula de pDNA. A utilização de um monolito modificado com ligandos de arginina, comparativamente à utilização de estratégias comercialmente disponíveis, permitiu obter um maior conteúdo da isoforma sc presente na amostra final da vacina de DNA, contribuindo para uma maior expressão das proteínas alvo. Posteriormente, um monólito com ligandos de arginina acoplados a um braço espaçador foi desenvolvido com o intuito de melhorar a acessibilidade dos ligandos, em comparação ao método de purificação previamente estabelecido, e assim melhorar a estratégia de purificação usada para a vacina de pDNA. Verificou-se que a capacidade de ligação da estratégia com braço espaçador é menor do que sem braço espaçador, provavelmente devido à ocupação de uma área maior pelo braço espaçador. Contudo, observou-

se um aumento da pureza em condições de carregamento devido à eluição de isoformas não funcionais durante este passo, um fenómeno conhecido como *sample displacement*. Também se verificou que o desenvolvimento de nanossistemas compostos por carbonato de cálcio permitiu a encapsulação do pDNA e a transfeção de células dendríticas, não se revelando citotoxicidade para este tipo de sistemas.

No que diz respeito ao estudo para potencial aplicação em terapia génica, foi inicialmente realizada a construção e produção do vector mcDNA contendo o gene de interesse, pri-miR-375, sendo posteriormente avaliadas duas estratégias diferentes para a purificação do mcDNA. Inicialmente, foi preparado um suporte cromatográfico monolítico modificado com ligandos de cadaverina em colaboração com a empresa BIA Separations, Eslovénia. Este suporte foi explorado pela primeira vez em cromatografia e a sua utilização na purificação da isoforma sc de mcDNA permitiu uma recuperação de 78,6% desta molécula, acoplada a uma pureza de 98,4%. Estes resultados foram alcançados através da estudo da influência do pH nas condições de ligação e eluição e explorando gradientes por passos com aumento da concentração de NaCl. Estes valores revelaram-se bastante promissores considerando as estratégias implementadas até à data na purificação de mcDNA. Adicionalmente, também foi explorada a cromatografia de filtração em gel através da utilização da matriz Sephacryl SF-1000, no sentido de se poder aumentar a quantidade de amostra de lisado injetada, e consequentemente a quantidade de mcDNA purificada por ensaio. Esta estratégia baseou-se na utilização de uma coluna cromatográfica com 60 cm de altura e 121 mL de matriz aliada a um gradiente isocrático com uma concentração mínima de NaCl, de forma a impedir ligações inespecíficas à matriz. Após a injeção de 2 mL de uma amostra de lisado de mcDNA, foi possível obter-se uma recuperação de 66% de mcDNA sc, com uma pureza de 98,35%. Apesar de esta estratégia ter permitido aumentar cerca de 12 vezes a quantidade de mcDNA puro obtido por ensaio em relação à metodologia anteriormente estudada, o tempo de cada ensaio foi 8 vezes superior ao tempo gasto com o monolito modificado com cadaverina, sugerindo que a seleção do método de purificação deverá ser de acordo com o objetivo final. Desta forma, foram desenvolvidas e caracterizadas duas estratégias de purificação de mcDNA sc, aplicando uma simples estratégia cromatográfica, sem implicar modificações genéticas específicas na molécula de PP. Estes resultados reforçam a versatilidade destas estratégias de purificação e potencial aplicação a qualquer tipo de mcDNA, independentemente do seu tamanho e constituição nucleotídica. Contudo, a necessidade de implementar uma metodologia analítica que permita quantificar o conteúdo de mcDNA sc de forma rápida, economicamente vantajosa e eficaz levou ao desenvolvimento e validação de um método cromatográfico analítico com o monolito modificado com cadaverina. Assim, foi estabelecida uma estratégia por passos com o aumento da concentração de NaCl durante cerca de 40 minutos para permitir a eluição de todas as espécies da coluna, capaz de quantificar a concentração de mcDNA sc presente numa amostra complexa ou pura, num intervalo de 1-25 µg/mL. A validação deste método passou pela avaliação da sua linearidade, precisão, exatidão e reprodutibilidade de acordo com as normas

estabelecidas para o efeito. Para além disso, a utilização de diferentes pares de mcDNA-PP, de composição variada, permitiu observar a robustez deste método, dado que apenas pequenas alterações deverão ser feitas ao gradiente de forma a permitir a quantificação de diferentes moléculas de mcDNA.

Por último, de forma a estudar o potencial do miR-375 como possível tratamento do cancro do colo do útero, estudos *in vitro* foram realizados para avaliar o efeito do vetor mcDNA-miR-375 na expressão das oncoproteínas E6 e E7. Para tal, foi utilizado o modelo de células CaSki, que consiste em células metásticas do cancro do colo do útero infetadas com HPV-16. Por outro lado, uma linha celular de fibroblastos foi utilizada como controlo não cancerígeno. Inicialmente foi verificada a expressão correta de miR-375, acompanhada de uma diminuição da expressão de E6 e E7, tanto a nível de transcritos como de proteína, comparando as células cancerígenas transfetadas com mcDNA com as mesmas células não transfetadas. Além disso, verificou-se que este vetor não afetou a viabilidade celular dos fibroblastos, apesar de nas células CaSki se ter verificado uma diminuição da proliferação celular ao longo do tempo assim como da viabilidade celular das mesmas. Estes resultados são indicativos que a utilização de vetor de mcDNA-miR-375 pode ser proposta como uma possível estratégia terapêutica que deverá ser mais explorada no futuro. Assim, esta tese pretende contribuir junto da comunidade científica com informação útil para o potencial desenvolvimento de novas abordagens para o tratamento do cancro do colo do útero, através da implementação de duas plataformas biotecnológicas. Uma das estratégias baseia-se no desenvolvimento de uma vacina de pDNA que codifica para os antigénios E6 e E7 do HPV com objetivo de ativar as duas vias do sistema imune, a via preventiva/humoral e principalmente a via terapêutica/celular, possibilitando consequentemente a eliminação das células do organismo que expressarem estes antigénios. A segunda estratégia tem como foco a obtenção de um vetor inovador de terapia génica, o mcDNA que codifica para o pri-miR-375 no sentido de silenciar as oncoproteínas E6 e E7 do HPV, permitindo uma ação direta sobre as células cancerígenas do colo do útero, por reposição da expressão ou função de proteínas supressoras de tumor.

Palavras-chave

Cromatografia de afinidade; DNA minicircular; Sistemas de entrega; Terapia génica; Vacinas de DNA; Vírus do papiloma humano

Abstract

Cervical cancer is one of the leading causes of death amongst women, especially in countries lacking suitable access to health and hygiene care. Contrarily to most cancers, which usually take origin in mutations related with the action of mutagenic or carcinogenic agents, the development of cervical cancer is strongly associated with infection by Human Papillomavirus (HPV). This virus is responsible for the expression of E6 and E7 oncoproteins, which interfere with the cell cycle regulation, affecting the cellular mechanisms of repair and proliferation of infected cells. In the last decades, DNA-based therapies, such as DNA vaccines or gene therapy, have been highly explored by researchers in the search of an efficient non-viral vector for the cervical cancer treatment. Plasmid DNA (pDNA) is a popular non-viral vector, which has been widely studied in the past decades for the development of a variety of DNA vaccines and gene therapy strategies. However, the presence of CpG motifs necessary to its amplification in prokaryotic hosts may lead to the activation of the immune system and to the degradation of this molecule before it can reach the target cells, in a gene therapy perspective. However, these same motifs may contribute to the recognition of this bioproduct by antigen presenting cells, facilitating the processing of pDNA as a DNA vaccine. Minicircle DNA (mcDNA) consists in a non-viral vector whose popularity has been largely increasing in the last years. This vector results from the recombination of a molecule, which is similar to conventional pDNA, named parental plasmid (PP). However, PP presents two recombination sites which, upon induction, give origin to the recombination of this molecule into two different molecules: one containing all the prokaryotic information necessary for PP amplification in prokaryotic hosts (miniplasmid – mP) and another containing all the information necessary for the therapeutic gene expression in eukaryotic cells (mcDNA). Considering its innovative character, it is crucial to develop suitable strategies for mcDNA preparation, with a purity that fits the requirements established by regulatory agencies such as European Medicines Agency (EMA) or Food and Drug Administration (FDA).

Thus, this work was performed with two different perspectives regarding cervical cancer treatment, namely DNA vaccines and gene therapy. Firstly, concerning DNA vaccines, the application of an adequate purification strategy allowed to understand that the purity degree of the pDNA sample can significantly contribute for the increased expression of the target antigen. The application of a monolith modified with arginine ligands, comparatively to the use of commercially available techniques, allowed to retrieve a final DNA vaccine sample with higher supercoiled (sc) content, leading to a higher expression of the target proteins. Concomitantly, the development of nanocarriers composed by calcium carbonate and gelatin allowed the delivery of pDNA vaccine to dendritic cells, also known as antigen presenting cells, without detecting cytotoxicity. On the other hand, two different strategies for mcDNA purification were explored. Firstly, the preparation of a monolith modified with cadaverine

ligands and its use in the purification of sc mcDNA allowed a recovery yield of 78.6% coupled with 98.4% purity. These results turned out to be very interesting considering the current mcDNA purification scenario in the literature. On the other side, size exclusion chromatography was also explored through the use of Sephacryl SF-1000 matrix. This strategy allowed to obtain a sc mcDNA yield of 66% alongside a purity of 98.35%. Despite 12 times more mass of pure sc mcDNA was obtained in one assay, the assay turned out to be approximately 8 times longer than the assays performed with the cadaverine modified monolith. In the end, two strategies were developed for sc mcDNA purification, each presenting its advantages and disadvantages. Nonetheless, both allowed the purification of mcDNA without resorting to PP specific genetic modifications, which implies that these strategies can be universally used for mcDNA purification. However, the need to implement an analytical methodology that allows to quantify sc mcDNA content in a fast, low cost and effective way led to the study of cadaverine-modified monolith with this purpose. Thus, a chromatographic method was implemented and validated to quantify sc mcDNA concentration present in a complex or pure sample, within a range of 1-25 μg/mL. Lastly, to study the effectiveness of miR-375 in the treatment of cervical cancer, *in vitro* studies were performed to evaluate the effect displayed by mcDNA-pri-miR-375 in the expression of E6 an E7 oncoproteins. Therefore, CaSki cell line model was used, which consists in metastatic cervical cancer cells infected by HPV-16. Also, a fibroblast cell line was used as a non-carcinogenic model for control. It was possible to identify the correct expression of miR-375, coupled with a decrease in E6 and E7 transcript and protein levels. Furthermore, it was observed that fibroblast viability was not affected, instead observing a decrease in transfected CaSki proliferation and viability. Thus, the application of mcDNA-pri-miR-375 as a possible therapeutic strategy should be more amply studied in the future. In the end, this thesis presents a scientific work that intends to contribute towards the scientific community with useful information for the potential development of new approaches for cervical cancer treatment, through the implementation of two biotechnological platforms. One of the strategies is based on the obtainment of a DNA vaccine, encoding E6 and E7 HPV antigens with the aim of activating two pathways of the immune system, the preventive/humoral and the therapeutic/cellular pathways, allowing the consequent elimination of the antigen-expressing and HPV-infected cervical cancer cells. The second strategy is focused on the obtainment of innovative gene therapy mcDNA vector, encoding pri-miR-375, to silence E6 and E7 HPV oncoproteins, allowing the direct targeting of infected cervical cancer cells, through the re-establishment of tumor suppressor proteins expression or function.

Keywords

Affinity chromatography; Delivery systems; DNA vaccine; Gene therapy; Human Papillomavirus; Minicircle DNA

Thesis overview

This thesis is structured in five main chapters. The first chapter accounts for a literature review of the main topics, which will be addressed in the thesis, to contextualize the reader, and comprises two different sections. The first section provides a literature review of E6 and E7 oncoprotein actions in the development of cervical cancer and discusses different biotechnological strategies, which have been studied and explored for the treatment of this disease, presented in a paper review form (Paper I. Cervical cancer and HPV-Infection: ongoing therapeutic research to counteract the action of E6 and E7 oncoproteins). The second section consists in a brief literature review of minicircle DNA vectors, explaining the main differences presented by minicircle DNA and plasmid DNA vectors, while providing a succinct review in the different methodologies currently implemented for mcDNA manufacturing. This section will also be presented as a paper review form (Paper II. Minicircle DNA – The future for DNA-based vectors?).

The second chapter includes the global aims established for the current thesis project.

The third chapter presents the main results obtained for the application of a DNA vaccine targeting E6 and E7 oncoproteins, with the respective discussion. This chapter comprises two sections in the form of original research papers, respectively:

Paper III. HPV-16 Targeted DNA Vaccine Expression: The Role of Purification

Paper IV. Purification and delivery of a Human Papillomavirus supercoiled plasmid DNA vaccine

The fourth chapter presents the implementation of suitable methodologies to obtain pure sc mcDNA, as well as an analytical methodology for its recovery and quality assessment and finally the evaluation of sc mcDNA-miR-375 therapeutic potential in the silencing of E6 and E7 oncoproteins. Thus, this chapter comprises four sections in the form of original research papers, respectively:

Paper V. Minicircle DNA purification: Performance of chromatographic monoliths bearing lysine and cadaverine ligands

Paper VI. The use of size-exclusion chromatography in the isolation of supercoiled minicircle DNA from Escherichia coli lysate.

Paper VII. Quality assessment of supercoiled minicircle DNA by cadaverine-modified analytical chromatographic monolith

Paper VIII. Silencing Human Papillomaviruses E6 and E7 oncoproteins with a minicircle DNA vector encoding pri-miR-375

Finally, the fifth chapter summarizes the results obtained throughout this research project and comprises two different sections. These sections are the concluding remarks and the future trends for this thesis, alongside additional research work that should be performed to culminate the findings achieved within this project.

Index

CHAPTER I

Paper I

Cervical cancer and HPV-Infection: ongoing therapeutic research to counteract the action of E6 and E7 oncoproteins

A.M. Almeida, J.A. Queiroz, F. Sousa, A. Sousa*

CICS-UBI – Centro de Investigação em Ciências da Saúde, Universidade da Beira Interior, Av. Infante D. Henrique, 6200-506 Covilhã, Portugal

Drug Discovery Today S1359-6446: 30310-1

Short description: A literature review focused on E6 and E7 oncoproteins action in cervical tissue and the use of DNA vaccines and gene therapy to target these proteins

ELSEVIER

Teaser Novel nucleic acid-based therapeutic approaches as a promising non-invasive solution for the treatment of cervical cancer caused by Human Papillomavirus.

Cervical cancer and HPV infection: ongoing therapeutic research to counteract the action of E6 and E7 oncoproteins

Ana M. Almeida, João A. Queiroz, Fani Sousa and Ângela Sousa

CICS-UBI — Centro de Investigação em Ciências da Saúde, Universidade da Beira Interior, Av. Infante D. Henrique, 6200-506 Covilhã, Portugal

Cervical cancer is the fourth most common cancer among women worldwide and its development is mainly associated with human papillomavirus infection, a highly sexually transmissible virus. The expression of E6 and E7 viral oncoproteins deregulates cell repairing mechanisms through impairment of tumor suppressor protein functions, such as p53 or retinoblastoma protein. Although the implementation of new preventive vaccines has decreased the infection rate and cervical cancer progression, there are still many women who are affected by this pathology. Nowadays, the main treatment often requires the use of invasive techniques. From well-established strategies, like DNA vaccines and gene therapy, to innovative gene silencing technologies; different methodologies are currently under scrutiny that target the E6 and E7 oncoproteins and/or their modes of action.

Introduction

The connection between human papillomavirus (HPV) and cancer development, more specifically cervical cancer, was first established in 1983 by Harald zur Hausen and co-workers [1]. At the time, it had already been possible to correlate the development of certain carcinomas in animals with the infection of specific viruses – leading scientists to pursue the same line of thought and study HPV in cancer biopsies, given that HPV DNA had been reported in genital warts [2]. Hence, for the first time, zur Hausen was able to identify HPV type 16 and demonstrated its presence in several malignant tumor biopsies [1]. Later on, zur Hausen's research group found the presence of HPV-16 and HPV-18 DNA in cervical cancer cell lines, as well as in cervical carcinoma biopsies [3]. The first steps to understand the development of cervical cancer were taken, and the groundbreaking work performed by the German scientist was later recognized in the form of a Nobel prize. Ever since such scientific discoveries were performed, many efforts have been made toward the establishment of new detection, screening, preventive and therapeutic methodologies against cervical cancer, mainly by exploring the crucial role of HPV in the development of this pathology.

Although the incidence of cervical cancer has been slowly decreasing with the advances in this field, it still represents one of the most common cancers among women nowadays and it is

Corresponding author: Sousa, F. (angela@fcsaude.ubi.pt)

Ana Margarida Almeida has an MS in biomedical sciences from Universidade da Beira Interior (2014) and is currently finishing her PhD, financed by the Foundation for Science and Technology, in biochemistry, at the same university. Her research activities take place at the CICS-UBI – Health Sciences Research Centre and are focused on the production and purification of DNA vaccines and gene silencing vectors for the treatment of cervical cancer induced by human papillomavirus.

João Queiroz is Full Professor of Biochemistry/Biotechnology at Universidade da Beira Interior, since 2003. He received his degree in biochemistry from University of Coimbra, 1986, his MS in biotechnology (biochemical engineering) from Instituto Superior Técnico, 1991, and his PhD in chemistry from Universidade da Beira Interior, 1996. He obtained the Habilitation in Biochemistry from Universidade da Beira Interior, 2002. He was Director of CICS-UBI – Health Sciences Research Centre, Universidade da Beira Interior. His research interests are related mainly to biotechnology, biomolecular sciences, analytical chromatography, preparative chromatography, protein purification and nucleic acid purification. He has supervised eight post-doctoral fellows in the areas of health sciences and biotechnology, and supervised (or co-supervised) with success a total of 21 PhD students in the areas of biochemistry, biotechnology and biomedicine. He is author/co-author of one international patent, three national patents, six book chapters and >230 scientific papers in international journals with peer review.

Fani Sousa completed her PhD in biochemistry in 2008 and is Assistant Professor at the Faculty of Health Sciences, Universidade da Beira Interior, since 2009. She is vice-coordinator of the CICS-UBI – Health Sciences Research Centre, since 2015, and coordinator of the Biopharmaceuticals and Biomaterials Research Group in the same research unit. Her research interests are related to the

https://doi.org/10.1016/j.drudis.2019.07.011

mandatory to search for new methodologies that will help to overcome this problem. To fully understand the ultimate treatment for this disease, it is first necessary to unveil the background of cervical cancer, to decode the mechanisms responsible for the development and progression of HPV infection and to explore different and promising therapeutic approaches.

Cervical cancer worldwide

Cancers are some of the deadliest pathological conditions globally. In particular, cervical cancer is considered the fourth most common cancer in women, accounting for 266 000 deaths in 2012 [4]. When consulting data collected and provided by GLOBOCAN 2018, it is possible to infer that the cervical cancer burden is higher in less developed countries [5]. Actually, in Eastern and Central Africa, this cancer is known as the primary cancer found in women. This might be strongly associated with the fact that less developed countries present very poor health resources in comparison to developed countries, perhaps leading to a late diagnosis [6]. In addition, the recent distribution of several HPV vaccines worldwide probably contributed to a decrease in HPV infection, and a consequent decrease in the number of the cervical cancer cases in countries with easy access to vaccination, such as developed countries. Given its severe implication in the development of cervical cancer, it is therefore very important to understand the biological mechanisms by which HPV operates within the cervical epithelium and further develop suitable strategies that might prevent or overturn its infection and tumorigenicity.

HPV infection and cervical cancer development

According to World Cancer Reports, 'persistent epithelial infection with one or more oncogenic types of HPV may lead to the development of precancerous lesions . . . which may progress to invasive cervical cancer' [6]. As a matter of fact, between 79% and 100% of invasive cervical cancer cases worldwide account with the presence of DNA belonging to high-risk HPV types, from which ~70% are related to HPV-16 and HPV-18 [7,8]. Even though HPV is directly associated with cervical cancer, other cancers have also been found to be correlated with HPV infection such as anal, vaginal, vulvar, penile and head and neck cancers [9]. Indeed, there are about 200 HPV genotypes currently documented; however, only some present carcinogenic potential and are known to have the ability of inducing cancer [10]. The fact that different HPV types are related to different clinical symptoms has led scientists to classify each HPV type according to the severity of the clinical outcomes, namely by low, intermediate and high risk. The high-risk types encompass HPV that can induce the development of tumor cells [11]. The severity of the symptoms is usually associated with the affinity presented by E6 and E7 oncoproteins within each HPV type toward the target proteins: tumor suppressors p53 and retinoblastoma protein (pRB), respectively.

HPV is a small double-stranded DNA virus, belonging to the family *Papillomaviridae*, and one of the most common sexually transmissible viruses worldwide. It presents a nonenveloped icosahedral structure and its genome contains eight open reading frames (ORFs) [12]. These ORFs are responsible for coding eight proteins, which can be divided into early stage (E1, E2, E4-E7) and late stage (L1 and L2). As the name implies, early proteins are the proteins to be first expressed upon virus infection of the host cell and are associated with the infection itself and the possible transformation of infected cells. By contrast, late proteins constitute the viral capsid and contribute to the spreading of the infection through the host system, via the release of virus particles within the superficial epithelial cells [12].

Figure 1a illustrates the normal cell repairing pathway. Viral infection with HPV begins when the virus can penetrate the cervical epithelium through micro-abrasions. Then, the E1 and E2 protein expression leads to regulation of the viral replication within infected cells, resulting on the expression of other early-stage proteins. At this point, E5, E6 and E7 oncoproteins begin to be expressed, contributing to cell survival and uncontrolled proliferation, as presented in Fig. 1b [13–15]. Such a carcinogenic mechanism is strongly dependent on the HPV ability in mainly expressing E6 and E7 viral oncoproteins. Both proteins are known to interfere with cell-cycle regulation, affecting the signaling pathways for cell repair and apoptosis [13,14].

The E6 protein can induce tumor suppressor p53 degradation, hindering its function as an apoptosis signaling cascade regulator, through E6AP protein binding. The latter is unable to bind itself to p53, in normal circumstances. However, in the presence of E6 protein, E6AP and E6 form a protein complex that can recognize and bind to p53. Such attachment can impair transcriptional activation or repression of p53-responsive promoters by preventing its binding to specific DNA

development of new biotechnological platforms to obtain biopharmaceuticals (mainly plasmid DNA, minicircle DNA and RNA) with potential therapeutic applications. In particular, the purification of plasmid DNA and RNA is being largely investigated through the design and development of specific technologies. Moreover, considering the formulation of the bioproducts enabling their stabilization, protection and delivery to cellular models. The main therapeutic areas addressed in these studies have been cancer and neurodegenerative diseases, through the evaluation of gene therapy or gene silencing approaches.

Ângela Sousa received her PhD in biochemistry at the Universidade da Beira Interior (UBI), Portugal, in 2011, and was awarded two postdoctoral grants in 2012 and 2015. From 2017 to 2018 was Invited Auxiliary Professor and since september 2018 is auxiliary researcher at UBI. Her main scientific interests include biotechnological processes for the biosynthesis, isolation and purification of biopharmaceuticals (plasmids, minicircle DNA and RNA), with particulated or monolithic chromatographic supports modified with amino acids and derivative ligands, to be used as DNA vacines or gene therapy. Her work is also focused on the development of nanosystems for plasmid targeted delivery to dendritic or cervical cancer cells, as well as the study of the therapeutic action of nucleic-acid-based vectors in the treatment of cancer.

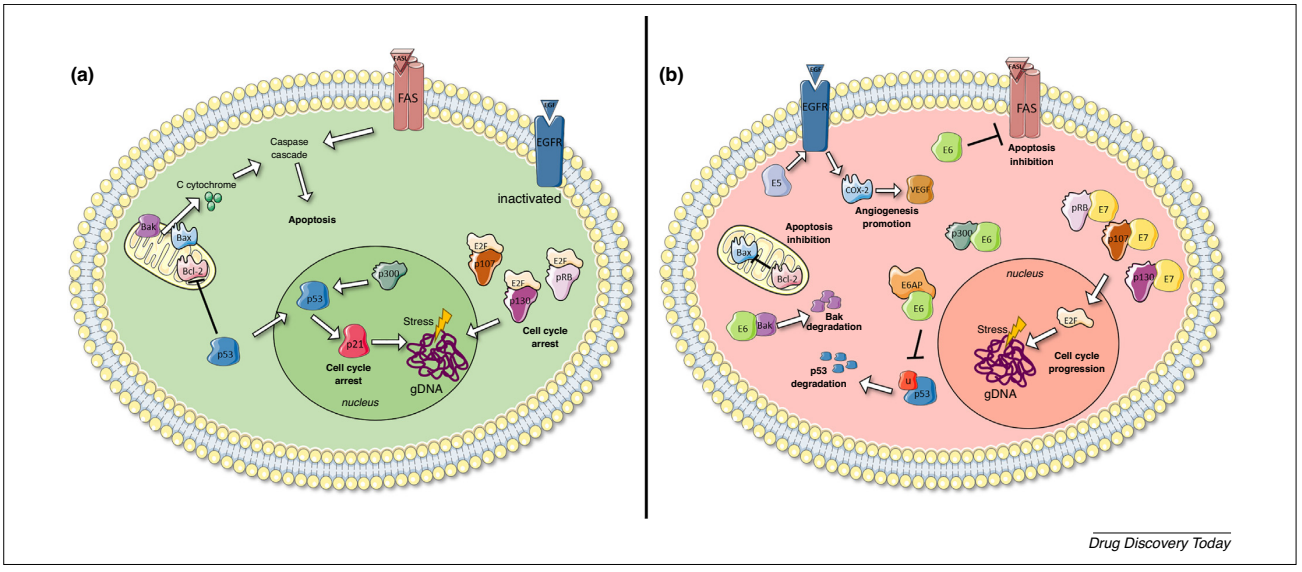

FIGURE 1

Schematic representation of cell-repairing systems in normal cells vs cells infected with human papilloma virus (HPV). **(a)** Normal cell. When a stressful event leads to cell damage, different mechanisms are triggered to induce cell quiescence or death. Tumor suppressor protein p53 is expressed at high levels and different targets are either activated or repressed. In the nucleus, p300 acetylates p53 and induces its ability to act as a transcription promoter for p21 (between other targets) expression. Then, p21 triggers a series of events that will result in cell-cycle arrest. p53 represses the transcription of Bcl-2, an antiapoptotic protein. Thus, Bak and Bax apoptotic proteins induce C cytochrome production, which will in turn trigger the caspase cascade, leading to apoptosis induction. FAS receptors are also able to trigger the caspase cascade when triggered by FASL binding. Additionally, pRB, p107 and p130 bind to E2F transcription factor, impeding its action as a cell-cycle promoter. **(b)** HPV-infected cell. Upon production of E5, E6 and E7 HPV oncoproteins, the cell repairing systems are altered. E5 presence leads to inappropriate activation of EGFR, triggering a series of events that culminate in VEGF production, thus promoting angiogenesis, one of the hallmarks of cancer progression. E6 production leads to the repression of several signaling systems. E6 can form a complex with E6AP able to mark p53 for degradation, thus decreasing the levels of this tumor suppressor protein. Such degradation of p53 leaves Bcl-2 expression deregulated, leading to Bax inhibition. Moreover, E6 can mark Bak for degradation, an important proapoptotic protein, and can bind to p300, thus inhibiting its p53 activation mechanism. Besides, E6 has the ability to bind to FAS and accelerate its degradation. All these mechanisms triggered by E6 result in apoptosis protection. E7 has the ability to bind to tumor suppressors pRB, p107 and p130, which are regulator proteins of the E2F transcription factor. This binding frees E2F, which in turn can continuously induce cell-cycle progression. Overall, HPV protein interference leads to the uncontrolled proliferation of cells. Abbreviations: E6AP, E6AP ubiquitin-protein ligase; EGF, epidermal growth factor; EGFR, EGF receptor; FAS, Fas receptor; FASL, Fas ligand; gDNA, genomic DNA; VEGF, vascular endothelial growth factor; pRB, retinoblastoma protein.

motifs and ultimately lead p53 to degradation through ubiquitination, resulting in a decrease in p53 levels [13,16]. The inactivation of p53 function favors the continuous replication of damaged DNA and abnormal cell survival, which would otherwise be repaired or eliminated by apoptosis induction if p53 was expressed in normal levels (Fig. 1a) [13]. Moreover, E6 has been shown to be able to interact with other proteins that also regulate cell signaling pathways. For instance, E6 can also interact with p300, a promoter that activates p53 through acetylation in an E6AP-independent manner [17]. Also, E6 can target for degradation of other proteins involved in the signaling cascade for apoptosis, namely Bak, the adaptor molecule Fas-associated death domain (FADD) and procaspase 8 [17]. Taking these interactions altogether, the disruptive effect that E6 can exert on the regulation of cell-cycle proliferation and repair is notorious. By contrast, E7 protein is involved in the impairment of tumor suppressor pRB function. As portrayed in Fig. 1a, whereas p53 activates apoptosis, pRB functions mainly rely on the inactivation of transcription factors, such as E2F. This molecule, when freely available, stimulates cellular cycle transition to S phase. Thus, upon viral infection, E7 is expressed and binds to pRB, disrupting its complex with E2F and contributing to continuous cell proliferation (Fig. 1b) [14,18]. Moreover, E7 oncoprotein is also involved with the interference of p107 and p130 functions, two proteins that also regulate cell-cycle proliferation through E2F transcription factor binding. The ultimate inhibition of pRB, p107 and p130 by E7 viral protein contributes to the uncontrolled cell proliferation and progression to malignant transformation seen in HPV-infected cervical epithelium [14,19]. Although E6 and E7 proteins are considered the main causative agents for HPV-infected cell transformation, E5 also presents carcinogenic activity. This protein has the ability to enhance cell proliferation through interaction with epidermal growth factor (EFG), a known stimulator of cell growth, therefore contributing to tumor progression (Fig. 1b) [15].

With the evolution of HPV infection, normal cervical tissue begins to lose its normal features and cells become more undifferentiated. The progression of the disease leads to the establishment of cervical intraepithelial neoplasia (CIN), which can be mild (CIN1) or moderate (CIN2) and characterized by cytologic abnormalities in the tissue. Without suitable treatment and as a result of persistent infections, CIN2 can evolve into high-grade lesions such as severe CIN (CIN3) or invasive carcinoma [20]. Therefore, given

the timeline of HPV infection and possible progression into cervical cancer, it is crucial to detect and treat the HPV infection before its evolution into more serious conditions.

HPV infection and cervical cancer: prevention and therapy

With the understanding of the HPV role in the development of cervical cancer, and other genital diseases, researchers have focused on developing suitable strategies to detect and prevent the disease. Suitable screening techniques are currently available, such as Papanicolaou stain or HPV DNA testing, allowing physicians to detect HPV infection at an early stage and prevent its evolution into invasive cervical cancer [21]. In 2002 a monovalent vaccine was studied, which consisted in the development of HPV-16 L1 capsid virus-like particles (VLPs) [22]. Scientists were able to verify a decrease in the incidence of HPV-16 infection in the population vaccinated with this particular vaccine, suggesting this vaccine was able to confer protection against this particular type of HPV and reduce the risk of developing cervical cancer [22–24]. Considering the fact that there is a wide range of HPV types associated with serious infections that can ultimately lead to the onset of cancer, HPV vaccine research began to focus on developing new vaccines that could provide protection against multiple HPV types. In 2005, a Phase II clinical trial was published regarding the administration of a quadrivalent HPV vaccine, which could supposedly confer protection against four HPV types, responsible for 70% of cervical cancer cases (HPV-16 and HPV-18) and 90% of genital warts (HPV-6 and HPV-11) [25]. According to the data, vaccinated women presented a 90% reduction of combined incidence of persistent infection or disease with the four HPV types, in comparison to women assigned with the placebo [25]. Given the success demonstrated in Phase II and Phase III clinical trials [25–29], this quadrivalent vaccine was later approved and licensed by the FDA, followed by its launch under the name of Gardasil®, by Merck. Simultaneously, a bivalent vaccine was developed with the main goal of preventing cervical cancer, therefore containing only L1 VLPs of HPV-16 and HPV-18 [30,31]. Some studies revealed that the bivalent vaccine could elicit higher antibody production than the quadrivalent vaccine, suggesting that it could persist longer [32]. The bivalent vaccine was launched as Cervarix® by GlaxoSmithKline in Europe and the USA in 2007 and 2009, respectively. Cervarix® and Gardasil® have been shown to be protective over 10 years (time that has elapsed since the initial clinical trials) [33,34]. More recently, Merck developed a new vaccine named Gardasil®-9 which confers protection against nine HPV types (HPV−6, −11, −16, −18, −31, −33, −45, −52 and −58) that, together, have been found in 85% of invasive cervical cancers worldwide [7,35,36]. By expanding the vaccination coverage worldwide, cervical cancer and other HPV-associated cancer rates are expected to decrease. However, to increase the protection and possibly eradicate these high-risk HPV types, vaccination of men must also be considered, given that HPV can also be responsible for the development of anal or penile cancers [37]. As a matter of fact, some countries have implemented a gender-neutral vaccination system with this purpose. Nevertheless, modern antivaccination movements, led by organizations who believe in a cause–effect relationship between immunization and development of severe adverse reactions, has been contributing to a decrease in the adherence to vaccination programs through the influence of general opinion [38,39]. Also, considering that HPV virions can infect the epithelium through the existence of micro-abrasions, it is very important to vaccinate individuals at an early age, preferably before initiating an active sexual life, given these vaccines do not exert any therapeutic effect against an ongoing HPV infection. Therefore, it is also necessary to focus on the development of suitable cervical cancer treatment options.

Currently, the main guidelines for cervical cancer treatment at an early disease state describe the use of surgery to remove the cancerous tissue, sometimes accompanied by chemotherapy or radiotherapy [40]. Surgery can vary from conization to radical hysterectomy, sometimes implying loss of fertility. The coupling with radiotherapy is very common in the treatment of several cancers, presenting satisfactory results in numerous cases and currently representing the most suitable treatment for local and nonmetastatic cancer [40]. When the treatment turns out to be ineffective or it is necessary to expand its range to the entire body, owing to tumor metastasis, chemotherapy is the next logical step [41]. Chemotherapy involves the administration of cytotoxic substances that can interfere with cell-cycle proliferation, therefore preventing tumor growth and leading to cancer cell death [41]. However, given that radiotherapy and chemotherapy treatments are unable to differentiate cancerous tissue from healthy tissue, there is a significant cytotoxicity associated that usually leads to the appearance of side effects and can cause significant discomfort to the patient [41]. Therefore, the design and development of anticancer therapeutics that are efficient and targeted toward the unhealthy tissue is imperative.

Cervical cancer and HPV infection: ongoing therapeutic research

DNA is, without doubt, a crucial molecule in all living organisms owing to its coding functions within the cell, providing the necessary information for protein synthesis as well as for regulation of cell mechanisms. With advances in biotechnology, DNA recombinant technology was born and continues to grow. The possibility for rearranging different genes and manipulating their functions has led scientists to dedicate their research to the development of new gene-based therapies. RNA has also been gaining attention because of the discoveries made, regarding its ability to control gene expression, allowing modification and regulation of cell signaling pathways. With the knowledge acquired through the study of these molecules, researchers were able to propose and explore innovative strategies for the treatment of different pathologies. Currently, several of these cutting-edge technologies are under study to prevent or treat cervical cancer.

DNA vaccines

DNA vaccines have been categorized as the third generation of vaccines, promising humoral and cellular immune responses, with low cost production, thermostability and easy distribution in comparison to conventional vaccines [42]. Such immunological technology is based on the delivery of genetic information with the intent of inducing an immune response against a specific antigen. After inoculation, the treated individual should be capable of producing a strong immune response against the antigen for which genetic information was previously delivered. The antigen

chosen to be encoded in the DNA vaccine must be related with a given pathology [43]. Such an immune response is triggered mainly as a result of the transfection of antigen-presenting cells (APCs) and non-APCs that will later express the antigen encoded in the DNA vaccine. As depicted in Fig. 2, there are two pathways that can lead to antigen presentation. In Fig. 2a, cells transfected with the DNA vaccine can directly present the antigen to $CD8^+$ T lymphocytes, through major histocompatibility complex (MHC) class I [43,44]. This activation leads to the maturation of cytotoxic T lymphocytes (CTLs), effector cells, which can identify cells that present the target antigen through MHC class I. Once these cells are found by the CTLs, cell death is triggered via different pathways. Such a pathway represents the therapeutic effect of the DNA vaccine [45]. By contrast, antigen production by non-APCs can lead to APCs taking up the antigen exogenously, resulting in the presentation of the latter to $CD4^+$ T lymphocytes via MHC class II, as portrayed in Fig. 2b. Such activated lymphocytes can activate B cells, which are white blood cells that can produce antibodies against specific antigens. The secretion of such antibodies can lead to neutralization of the microbe responsible for the production of the target antigen (in this case, the virus) [46]. Also, memory B cells are formed from this activation. Such cells are responsible for the induction of a strong immune response when reinfection occurs, thus representing the preventive effect of the DNA vaccine [46]. The combination of both pathways leads to the emergence of a strong humoral and cellular immune response, contrarily to prophylactic vaccines [43,44].

Although one of the advantages of DNA vaccines over prophylactic vaccines is the broad range of the elicited immune response, this is not the only great feature presented by this technology. DNA vaccines are much more economic to manufacture than prophylactic vaccines, considering the simplicity of its production process [47]. DNA vaccines can be easily obtained in large quantities and high-grade purity, owing to the fact that DNA is a molecule easier to manipulate than the peptides from which prophylactic vaccines are made [48]. This also accounts the fact that DNA is more stable, facilitating its transportation and storage. Moreover, DNA vaccines have the potential of providing longer *in vivo* exposure to antigens, which could lead to the increase of immunogenicity and to a decrease in the number of required immunizations [49].

Given that DNA vaccines can exert preventive and therapeutic effects, they are being currently explored in the treatment of cancer. Many cancers exhibit specific antigens that could be used in the development of a DNA vaccine to elicit a specific immune response against those antigens [50]. Thus, given all the advantages inherent to DNA vaccines, much effort has been devoted to developing suitable DNA vaccines for cervical cancer. Considering the main role that E6 and E7 oncoproteins display in cancer development, therapeutic DNA vaccines are currently being developed by using these oncoproteins as antigenic agents. So far, there are many research studies that have been conducted with the aim of developing a suitable DNA vaccine against HPV. From codon optimization to the inclusion of different fusion proteins to facilitate the antigen-presenting process, many approaches have been studied for this matter [51–53]. Such approaches are crucial to induce a strong immune response, because they can significantly alter the immunogenicity for a given DNA vaccine [54]. Codon optimization is used to increase antigen production, principally in heterologous expression systems. This need emerges with the fact that different sets of nucleotides can code for the same amino acid, thus constituting a codon. However, not all organisms are known to make use of all the existing codons. As a matter of fact, a preference for some codons has been shown for different organisms. This can lead to an ineffective translational

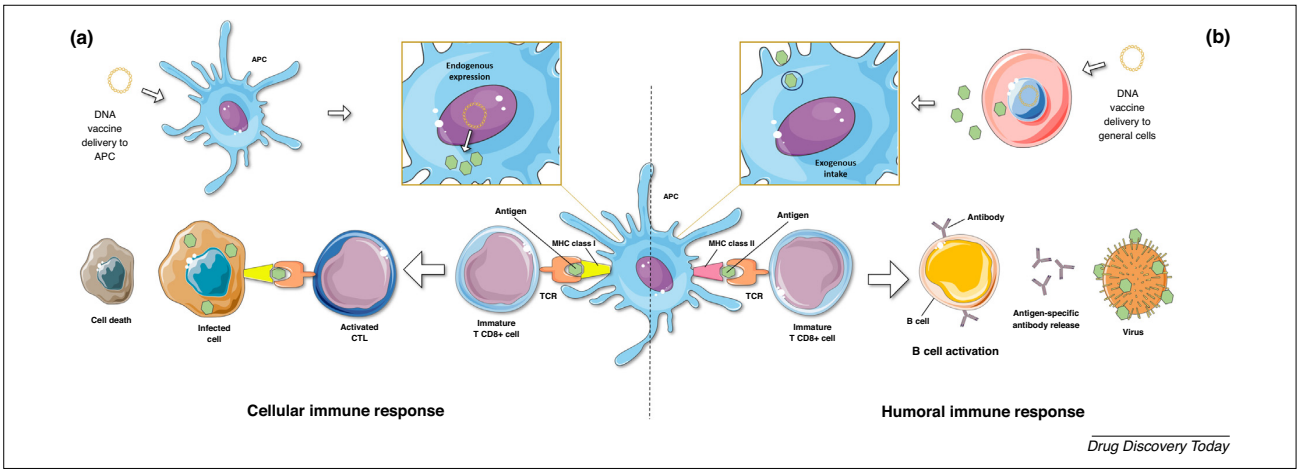

FIGURE 2

Antigen presentation schematics. **(a)** Endogenous antigen presentation. APCs transfected with DNA vaccine can endogenously produce the target antigen. This antigen will be presented by MHC class I to naive $CD8^+$ T cells, activating them as CTLs. Then, CTLs identify cells expressing MHC class I coupled with the antigen that is used for their activation. When such identification is successful, the cell presenting the antigen is destroyed by CTLs as a result of the activation of different paths that mainly lead to apoptosis induction. **(b)** Exogenous antigen presentation. APCs can take exogenous antigens, produced by other cells transfected with the DNA vaccine, and present them by MHC class II to naive $CD4^+$ T cells, activating them. Then, these cells activate B cells into the producing antigen-specific antibodies. These antibodies are released and can trigger different pathways that lead to virus neutralization. Abbreviations: APC, antigen-presenting cell; CTL, cytotoxic T Lymphocyte; MHC, major histocompatibility complex; TCR, T cell receptor.

process and result in decreased protein expression [43]. Thus, codon optimization might be necessary to improve antigen expression and increase immune response. Adjuvants can also be used to improve the outcome of DNA vaccines. These adjuvants might come in as separate molecules or can be included in the antigen design as fusion proteins [43]. Whereas the former might be obtained through the concomitant administration of a plasmid encoding these adjuvants, for example, the latter are constructed by genetically engineering the gene encoding the antigen to produce a protein fused to one, or more, proteins. Such engineering can be used to take advantage of different protein domains. For instance, it can be used to increase the uptake or the stability of a given antigen [43,52]. Table 1 lists a few selected examples of proteins that have been included in the design of different DNA vaccines and their functions in the optimization of this strategy. Some of these proteins have been included in the design of DNA vaccines that have reached clinical trials, such as HSP70, a heat shock protein that facilitates antigen presentation and concomitantly exhibits antiproliferation effects, or the more recently studied interleukin (IL)-10 receptor, which can inhibit the action of IL-10, which can interfere with triggering of the immune response [53,55]. As mentioned above, different molecules with different roles can be used to optimize the therapeutic effect of a DNA vaccine, altering significantly the performance of the immunological response.

Although several DNA vaccines have been designed in the past years toward E6 and E7 antigens, few have reached clinical trials for cervical cancer. Cornelia Trimble and her research group have been dedicating their research to developing and improving DNA vaccines for cervical cancer treatment, having published a Phase I clinical trial (NCT00121173) regarding the use of pNGVL4a-Sig/E7 (detox)-HSP70 in 2009 [53]. This DNA vaccine encodes the HPV-16 E7 oncoprotein modified, so that it is unable to bind to pRB. The DNA vaccine was also coupled to a signal peptide to facilitate the release from cells through a secretory pathway, coupled to HSP70 [53]. In this study it was found that 33% of the patients presented histologic regression. Later on, in 2014, another Phase I study (NCT00788164) was conducted with this particular vaccine, where a robust, localized and effective immune response was detected in the treated patients [56]. Recently, a Phase II trial began to explore the effect of this vaccine coupled with TA-CIN vaccine, a protein vaccine that comprises L2/E6/E7 proteins from HPV-16 (NCT03911076). In 2015, Trimble's research group conducted a Phase II clinical trial (NCT01304524) in patients with CIN2/3 by using VGX-3100, a DNA vaccine consisting of an equal mixture of two plasmid DNAs, each containing the optimized sequence for an

TABLE 1

Examples of proteins that have been selected to improve DNA vaccine therapeutic action in recent years

Year	Protein	Function	Antigens used	Targeted HPV type	Clinical trials (cervix-related diseases)	Refs
2008–2017	CRT	Ca^{2+}-binding protein able to associate with ER transportation molecules, aiding in the antigen presentation through MHC class I	E6, E7, E6/E7	HPV-16 HPV-11	NCT00988559	[59,100,101]
2009–2014	Flt3L	Growth factor able to expand DC and increase population of lymphocytes, improving $CD8^+$ T cell and NK cell activation	E7, E6/E7	HPV-16 HPV-18	NCT02139267, NCT02596243, NCT01634503, NCT02100085, NCT03206138, NCT02411019, NCT03444376	[51,102,103]
2009	HSP70	Heat-shock protein able to improve the uptake of the linked antigen by APC and aid in the antigen presentation through MHC class I and class II, eliciting proinflammatory responses	E7	HPV-16	NCT03911076, NCT00788164, NCT00121173	[53]
2017	IL-2	Interleukin able to induce T and B cell proliferation as well as immunoglobulin synthesis, eliciting strong and robust immune response	E7	HPV-16	–	[104]
2011–2017	TTFC	Foreign molecule able to elicit $CD4^+$ T helper response and provide more stability to the antigen, improving its half life	E6, E7	HPV-16	–	[52,105]
2018	MLT	Immunomodulatory hormone able to induce lymphocyte activation and exert proapoptotic effects	E7	HPV-16	–	[106]
2019	SA-4-1BBL	Artificial ligand for TNF receptor that promotes the proliferation and survival of CD8 + T cells and induces production of different proinflammatory cytokines	E7	HPV-16	–	[107]
2019	IL-10 receptor	Inhibits IL-10, which is an interleukin that interferes with antigen presentation and reduces $CD8^+$ T responses	E7	HPV-16	–	[55]

Abbreviations: APC, antigen-presenting cells; CRT, calreticulin; DC, dendritic cells; ER, endoplasmic reticulum; Flt3L, Fms-related tyrosine kinase 3 ligand; gp, glycoprotein; HSP, heat-shock protein; IL, interleukin; NK, natural killer; MLT, melatonin; TNF, tumor necrosis factor; TTFC, tetanus toxin fragment C.

E6/E7 fusion protein of HPV-16 or HPV-18 [57]. This particular vaccine had the advantage of possibly being offered as a treatment for two of the HPV strains most associated with cervical cancer: HPV-16 and HPV-18. The results were shown to be promising, given that histologic regression was observed in 49.5% of treated patients, without major adverse reactions. These findings suggested that this DNA vaccine could be a suitable alternative to more-invasive techniques such as surgery [57]. Following this line of thought, a Phase III clinical trial, entitled REVEAL 1 – Evaluation of VGX-3100 and Electroporation for the Treatment of Cervical HSIL (NCT03185013), was initiated in 2017 by Inovio Pharmaceuticals with the intent of further proving the safety and effectiveness of the VGX-3100 vaccine. This study is expected to end in 2021 and bring support to the commercialization of this vaccine [58].

In 2016, Trimble and co-workers also published data regarding a Phase I clinical trial (NCT00988559) that was conducted with pNGVL4a-CRT/E7 (detox), a DNA vaccine specifically designed to target HPV-16 E7 oncoprotein. This pDNA molecule expresses the E7 protein, with a modification that prevents its ability to transform healthy cells, coupled to calreticulin, a heat-shock protein similar to HSP70 [59]. In the conducted study, 30% of the patients, who exhibited CIN2/3, demonstrated histologic regression and well tolerability toward the vaccine administration [59]. However, in comparison to VGX-3100, this DNA vaccine is limited to HPV-16 infections, which can be considered as a disadvantage by not targeting HPV-18 infections as well, limiting its coverage.

Another DNA vaccine that has reached clinical trials, this time developed by Kim and co-workers, is the GX-188E HPV DNA vaccine. This DNA vaccine was designed to express shuffled HPV-16 E6 and E7 proteins, to prevent the interaction with tumor suppressors p53 and pRB, coupled to an extracellular domain of Flt3L and the signal sequence of tissue plasminogen activator (tpa) [51]. The latter sequences were included to promote antigen presentation and to enhance the release of the fused protein through the secretory pathway, respectively [51]. In this Phase I study (NCT01634503), which was also conducted in patients with CIN2/3, 78% of treated patients demonstrated histologic regression and 89% displayed enhanced HPV-specific CD8 T cell response, suggesting this DNA vaccine can be a promising noninvasive therapeutic strategy for patients with cervical dysplasia [51]. A Phase Ib/II study is currently being carried out to assess the effect of GX-188E coupled with pembrolizumab, a monoclonal antibody, in patients with advanced and nonresectable HPV-positive cervical cancer (NCT03444376).

Overall, DNA vaccine research is evolving accompanied by very interesting results, suggesting that this therapeutic pathway can be promising to cervical cancer treatment. Nevertheless, researchers have generally found that the majority of DNA vaccines developed so far do not present the high-level immunogenicity observed in mouse models, thus justifying the lack of DNA vaccines approved for human use [48,60]. New methodologies are currently under study to improve the clinical outcome of DNA vaccines. These methodologies derive from the outstanding progress that has been observed in the past years for this field of studies [60]. Moreover, cases like VGX-3100, which stands out as the current HPV DNA vaccine with most promising results, are proof that the first DNA vaccine to be commercially available for humans might be launched in the near future.

Gene therapy

Gene therapy has been in the research spotlight for years. The gene therapy premise involves the delivery of a foreign DNA sequence to the host cells with the intent of altering the function of a given molecule that could play an important part in disease development [61]. The potential of this field for the treatment of 'incurable' diseases resultant from inherited mutations has led researchers to focus their efforts on the search for the next 'miracle' cure. Although its popularity has been affected owing to the threat posed by some severe adverse reactions that occurred in some initial clinical studies and as a result of the lack of significant therapeutic results, researchers have been able to turn the tables through the knowledge acquired during the past decades [62,63]. In recent years, more efforts have been made in the development of gene therapy strategies suitable for cancer treatment. As a matter of fact, the majority of the gene therapy clinical trials performed to date have been directed toward cancer treatment (65%) [64]. Therefore, there has been an increased interest in studying tumor suppressor proteins in the development of such strategies. For instance, pRB is a tumor suppressor protein, the action of which is inhibited owing to HPV viral activity, more precisely the expression of oncoprotein E7. As stated before, its function is mainly involved in regulating cell-cycle proliferation through the inactivation of transcription factor E2F. In 2001, Ip and co-workers designed a gene therapy study to evaluate the therapeutic potential of an adenovirus (AV) expressing pRB [65]. However, their findings suggested that pRB is not a suitable candidate for the development of a cervical cancer therapy because no inhibitory effect was found in the cell growth of three different cervical cancer cell lines, as opposed to an osteosarcoma cell line [65]. Moreover, they evaluated the use of a p53-expressing AV in the same cell lines and apoptosis induction was detected through flow cytometry [65]. The main reason for such different outcomes is probably related to the fact that p53 activates a signaling pathway responsible for apoptosis induction, whereas pRB is mainly involved in regulating cell proliferation, leading to G1 phase arrest and cell senescence but not necessarily contributing to cell death [18]. Additionally, a few reports state that E2F activates apoptosis p53-independently, and normal function can be impaired in the presence of overexpressed pRB [66]. Nevertheless, the poor results obtained with the pRB-based gene therapy protocol for the treatment of cervical cancer led this strategy to fall into oblivion.

By contrast, the p53 gene has been considered the main tumor suppressor gene chosen for the development of gene therapy strategies, sometimes combined with other conventional therapies such as chemotherapy or radiotherapy [64]. Although 50% of the cancer cases worldwide result from mutations in the p53 gene, rendering the protein unable to regulate cell proliferation and to activate the apoptosis cascade [67], in cervical cancer p53 is degraded because of the presence of E6 viral oncoprotein [13]. Restoring p53 levels could be a suitable strategy for inducing tumor cell apoptosis, which could be accomplished by transfecting malignant cells with a p53 expression vector. The use of such a strategy has been controversial according to the literature, given that some researchers claim that this type of gene therapy might

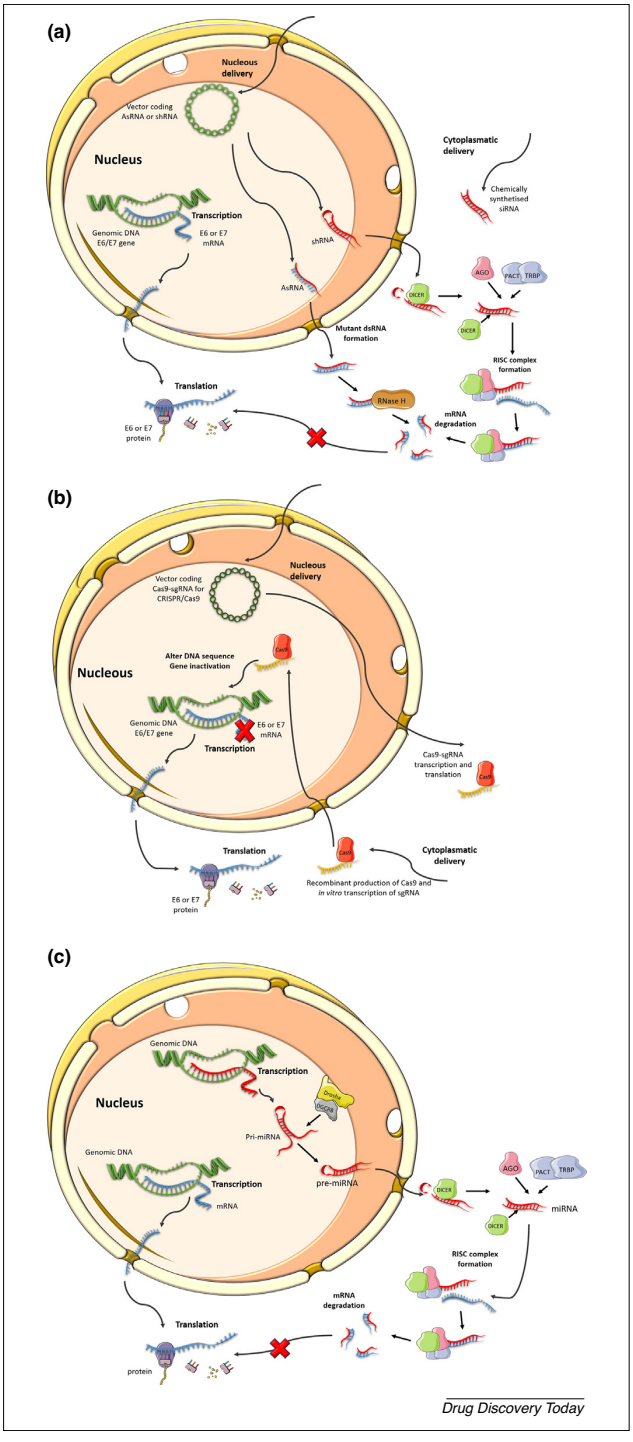

FIGURE 3

Schematic representation of different gene silencing strategies. **(a)** Artificial RNA-based therapies. Such therapies include AsRNA, shRNA and siRNA. AsRNA and shRNA must be delivered to the nucleus via a vector encoding these molecules, whereas siRNA molecules are delivered directly to the cytoplasm. Upon excretion to the cytoplasm, AsRNA binds to the target mRNA, forming a mutant dsRNA that will be marked to degradation by RNase H. By contrast, shRNA will be excreted and processed by Dicer before forming the RISC complex. shRNA and siRNA follow the same process after RISC complex formation, leading to target mRNA identification and degradation. Such a strategy might be used to mark E6 and E7 mRNA to degradation. **(b)** CRISPR/cas9 systems. Cas9-sgRNA can be delivered to the nucleus, via an encoding vector, or directly delivered to the cytoplasm, when produced *in vitro*. Its assembly and nucleus entering will allow editing of the target sequence to which the sgRNA was designed, leading to genomic DNA definitive alteration. Such genomic editing might be used to delete the human papilloma virus (HPV)-integrated genome, preventing the translation of E6 and E7 mRNA, thus preventing the protein production. **(c)** miRNA biogenesis. miRNAs

not be completely effective owing to E6-mediated degradation of p53 protein resulting from *de novo* synthesis [68]. To surpass this problem and avoid the E6 direct action on the p53 expressed by the gene therapy vector, in 1998, Prabhu and co-workers published a study regarding the development of an AV that could express p73β, a homolog for p53 protein that displays similar functions to the p53 tumor suppressor [68]. This protein can induce apoptosis in a p53-dependent manner but is usually expressed in low levels, because its activation is generally a response to stress. In the study, HPV-E6-expressing cells were transfected with either p53- or p73β-expressing AV. Cellular proliferation was only suppressed in cells transfected with p73β-AV, as opposed to cells transfected with p53-AV. In addition, p73β-AV displayed apoptosis induction in transfected cells, suggesting that the E6 mechanisms responsible for p53 degradation are unable to interfere with p73β signaling [68]. In 2003, such findings were sustained by a study conducted by Das and co-workers, where they developed a nonreplicating p73β-AV, for biosafety purposes, and compared its efficiency with a p53-AV, recording very similar data to those reported previously by Prabhu [68,69]. In 2006, Das *et al.* gave continuity to the research and published a study based on the use of nonreplicating p73β-AV *in vitro* and *in vivo* [70]. The growth inhibition of HPV-positive cervical cancer cells was accomplished with administration of this biopharmaceutical product, followed by apoptosis induction, in *in vitro* and *in vivo* models. Overall, these results suggested that p73β might be a promising strategy for scientists to pursue a next generation HPV-induced cancer treatment. However, no new information regarding the use of this vector has been released to date.

Despite the studies developed by Prabhu and Das, other researchers kept on exploring the use of p53 gene therapy in HPV-induced cervical cancer and good results have been obtained. As a matter of fact, Gendicine, the first known gene therapy product to be released for cancer treatment, the approval of which was restricted to China, consists of a recombinant AV that expresses human p53 protein [71,72]. Twelve years since its market release, >30 000 patients have received this biopharmaceutical drug as cancer treatment. No serious adverse reactions have been reported so far, except high fevers in the first hours upon receiving the treatment [73]. Nevertheless, its approval in other countries was controversial because the methodology used for data collection in China was not comparable to that used by the FDA [73]. In the particular case of cervical cancer, it was demonstrated that the coadministration of Gendicine with radiotherapy resulted in the significant increase of 5-year survival rate in comparison to radiotherapy alone, suggesting that the use of this gene therapy approach can have a synergistic effect in the treatment of this cancer [72]. Although there are interesting results published regarding the use of p53 expressing AV in cervical cancer, the fact that E6-positive cells can interfere with the production of p53 can be hiding the full potential of this method. To overcome this issue, the use of a gene therapy strategy targeting the overexpression of p53 or pRB concomitantly with the silencing of E6 or E7 oncoproteins could be very promising in unravelling the full potential of this approach in the future.

Gene silencing

With the fast and innovative advances in the gene therapy field, a new approach has been taken into consideration: why not directly silence the expression of proteins involved in the disease emergence? Since the discovery of antisense RNA technology in 1981 by Tomizawa and co-workers [74], followed by the accidental discovery of RNA interference by Guo *et al.* [75] and the study of its implication in gene expression by Fire *et al.* [76], such a strategy became easier to pursue. Thus, many scientists have been exploring the implementation of this technology in different diseases. In cervical cancer induced by HPV, the most obvious pathway to follow is the downregulation of E6 and E7 oncoproteins. With this in mind, several HPV oncoprotein silencing studies have been performed in the past years. In Fig. 3 the main technologies used for this purpose are represented: antisense RNA (AsRNA), small interfering RNA (siRNA), short hairpin RNA (shRNA), the clustered regularly interspaced short palindromic repeats associated with Cas9 (CRISPR/cas9) system and microRNA. In next subsections, the promising roles of these technologies will be discussed for the treatment of HPV-induced cancer.

Artificial RNA-based therapies

Artificial RNA-based therapies encompass antisense RNA (AsRNA), a single-stranded antisense RNA complementary to the target mRNA; siRNA, a double-stranded RNA complementary to mRNA; and shRNA, a double-stranded RNA that originates siRNA. As schematized by Fig. 3a, these systems can interfere with protein expression by binding to the mRNA of the target protein through perfect complementarity, targeting this molecule to degradation. In 1988, the first attempt at silencing the expression of E6 and E7 oncoproteins was performed, when von Knebel Doeberitz and co-workers transfected a C4-1 cell line, a cervical carcinoma bearing HPV-18, with a plasmid containing HPV-18 E6 and E7 AsRNA sequences [77]. Here, they were able to verify that cell growth was affected by such an experiment, given that, in the presence of dexamethasone, transfected cells revealed a reduction in its growth rate comparatively to nontransfected cells. Since then, many studies have been conducted regarding the silencing of E6 and E7 oncoproteins in an independent manner or simultaneously. It is noteworthy to mention that E6 and E7 mRNAs are bicistronically transcribed from the same promoter in HPV-infected cells. Thus, some silencing sequences can be designed to simultaneously target both oncoproteins.

are naturally produced by the cellular organism and are known to regulate different cellular pathways. Thus, these molecules are first transcribed in the nucleus, from the cell's genomic DNA, presenting a primary miRNA transcript named pri-miRNA. In the nucleus, this transcript is processed by Drosha and DGCR8 proteins, resulting in a precursor miRNA known as pre-miRNA. Following this, the pre-miRNA molecule is exported to the cytoplasm, where it is processed by DICER, as mature miRNA, to integrate into the RISC complex, an RNA-induced silencing complex formed by DICER, AGO, PACT and TRBP. Such a complex is able to identify the mRNA targets of the miRNA to which it is bound, leading to the degradation of these mRNAs. Abbreviations: AGO, argonaute; AsRNA, antisense RNA; Cas9, CRISPR associated protein 9; CRISPR, clustered regularly interspaced short palindromic repeats; DGCR8, protein DiGeorge syndrome critical region gene 8; dsRNA, double-stranded RNA; miRNA, microRNA; mRNA, messenger RNA; PACT, kinase R-activating protein; RISC, RNA-induced silencing complex; sgRNA, single guide RNA; shRNA, short-hairpin RNA; siRNA, small interfering RNA; TRBP, Tar RNA-binding protein.

In 2000, Choo and co-workers developed a retrovirus for an AsRNA strategy targeted against HPV-16 E7 oncoprotein, with the intent of studying its impact in the tumorigenicity of HPV-16-positive cervical cancer cells [78]. In that study, cell growth inhibition was observed, from a decrease in E7 oncoprotein levels. However, such inhibition was unable to result in tumor cell death, rather resulting in cell differentiation, a cell feature that is lost in cancer progression [78]. By contrast, Cho and co-workers conducted a study in 2002 by using a plasmid encoding an AsRNA for HPV-16 E6 oncoprotein in the same cell model used in Choo's research [79]. They were able to verify that, after transfection, cell growth was inhibited and an apoptotic morphology was acquired by the cells, which was confirmed by an increase in p53 levels [79]. These results suggested that E6 silencing leads to a more preeminent function in tumor suppression than E7 silencing.

Curiously, Yamato and co-workers took advantage of the bicistronic transcript and conducted a study with two synthetic siRNAs, designed to target different splicing variants of HPV-18 E6 mRNA. One of them was able to knockdown E6 and E7 expression and the other could successfully knockdown E6 levels but was unable to inhibit E7 as efficiently as the former [80]. Their findings showed that the isolated E6 suppression exerted a more significant tumor cell death effect comparatively to concomitant suppression of E6 and E7, suggesting that targeting E6 oncoprotein could be crucial when developing a siRNA-based strategy for cervical cancer induced by HPV [80]. Although these results seem to be in accordance with the investigation previously conducted by either Choo and Cho's research groups [78,79], it goes against the work developed by Jiang and Milner [81]. In 2002, the researchers published a study reporting the comparative use of synthetic siRNAs against either E6 or E7 HPV-16 oncoproteins. However, in contrast to what Choo *et al.* and Yamato *et al.* found in their studies [78,80], Jiang and Milner reported a reduced cell growth derived from E6 silencing and apoptosis induction from E7 inhibition [81]. These apparently contradictory results can be explained by the differences shown in study design, namely because different types of HPV were studied, distinct methods were used for silencing, the bicistronic nature of the transcription of which E6 and E7 mRNA are originated from, and considering the diverse splicing variants that can arise from such process. Moreover, as presented in Fig. 3a, the artificial RNA-based therapies integrate different pathways before interfering with E6 and E7 oncoprotein translation, which can result in different mRNA degradation levels. The delivery of these molecules, which can occur directly to the nucleus, through the use of an expression vector (such as shRNA), or to the cytoplasm after chemical synthesis (like siRNA molecules), can result in different outcomes, because it can lead to different levels of the intended RNA molecule [82]. In addition, different RNA structures present different stability and resistance to degradation, which can also affect the therapeutic outcome of these molecules [83]. Still, the use of shRNA appears to be more advantageous given that it can express, in a continuous form, silencing molecules that naturally integrate the endogenous miRNA pathway, leading to a stronger and more effective silencing effect than chemically synthetized siRNA [84]. Nevertheless, many studies have been dedicated in the past decade to the concomitant silencing of E6 and E7 oncoproteins with artificial RNA-based therapies. The most recent studies that have been performed by using AsRNA, siRNA or shRNA for simultaneous E6 and E7 silencing, as well as any major findings, are represented in Table 2. However, several obstacles have been found that can impair the implementation of these techniques. These limitations rely on the fact that RNA molecules are very unstable and can be rapidly degraded because of host RNase action [83]. Also, exogenous RNA molecules can present motifs that trigger immune responses owing to interferon stimulation, which can result in the development of severe adverse reactions [85]. To overcome this problem, many efforts have been focused on chemically altering the RNA structure to make it more stable and disable the stimulation of interferon [85]. Moreover, the development of suitable delivery strategies that protect the RNA molecule and direct it to the target tissue is crucial to increase the bioavailability of these biopharmaceuticals, and is currently the main goal of researchers working in this field [83,85]. Thus, further studies are necessary before proceeding with this strategy to clinical trials.

TABLE 2

Recent E6 and E7 silencing studies performed for AsRNA, shRNA and siRNA

Year	Silencing type	Antigen silencing	TargetedHPV type	Findings	Refs
2007	AsRNA	Simultaneous	HPV-16	p53 expression was significantly increased, followed by apoptosis and senescence detection in SiHa cells	[108]
2013	shRNA	Simultaneous	HPV-16	Tumor suppressor protein levels were increased in HPV-positive cell models and treated mice demonstrated lower tumor growth and higher survival rates than control	[109]
2016	siRNA	Simultaneous	HPV-16 HPV-18	Growth of subcutaneously injected HPV-positive cancer cells was suppressed in mice through systemic administration of siRNA by actively targeted polyion complex micelles	[110]
2017	siRNA	Simultaneous	HPV-16 HPV-18	Coupled with cisplatin or paclitaxel, tumor growth was suppressed in mice owing to synergistic effect between siRNA and chemotherapeutics	[111]
2018	shRNA	Simultaneous	HPV-16	Almost complete eradication of tumor mass in mice without adverse reactions	[112]
2018	AsRNA	Separate	HPV-16	AsRNA-E7 demonstrated higher inhibitory effects in tumor growth than AsRNA-E6	[113]

Abbreviations: AsRNA, antisense RNA; shRNA, short hairpin RNA; siRNA, small interfering RNA.

Gene editing with CRISPR/cas9 systems

More recently, CRISPR/cas9 systems have been described as the new cutting-edge technology of gene silencing strategies. The technology consists of a programmable RNA-guided endonuclease system that can be used to edit defective genes [86]. This technology, as represented in Fig. 3b, allows disruption of the DNA sequence of a target gene with the help of an RNA-guide strand, rendering the gene unable to be expressed.

Its application in HPV-induced cancers is more recent, Hu and co-workers developed a study, in 2014, regarding the use of CRISPR technology for the disruption of HPV-16 E7 gene in HPV-16-positive human cancer cell lines [87]. Apoptosis induction and decreased E7 oncoprotein levels were found in HPV-16-positive cancer cell lines such as CaSki and SiHa as opposed to HPV-16-negative cancer cell lines (C33A and HEK293). These findings highlighted the promising future of CRISPR/cas9 in HPV-induced cancer treatment. In a different approach, Zhen and co-workers used this system for the disruption of the HPV-16 E6/E7 promoter coupled with cisplastin, a chemical drug, in the HPV-16-positive cancer cell line SiHa. In this study, it was possible to verify that cell viability was lower in cells transfected with CRISPR/cas9 in comparison with cells only treated with cisplatin. However, when combining both strategies, a synergistic effect was detected, suggesting CRISPR/Cas was able to sensitize cells to cisplatin [88]. This study showed that CRISP/cas9 could be used concomitantly with chemotherapeutic drugs to potentiate its effect. Nevertheless, suitable delivery systems should be considered given that chemotherapeutic drugs are known to affect healthy tissues. Later on, Kennedy and co-workers also developed a CRISPR/cas9 system targeting E6 or E7 genes that was able to decrease the content of these oncoproteins and thus activate the p53 or pRB signaling pathway, respectively, in HPV-16- and HPV-18-positive cancer cell lines [89]. The CRISPR/cas9 systems used in this study were designed specifically for each type of protein (E6 and E7) and each type of HPV (16 and 18), resulting in four different CRISPR/cas9 systems.

More recently, Zhu *et al.* developed nanoparticles for the delivery of plasmid DNA encoding either CRISPR/cas9 or shRNA specific for E7 silencing [90]. Their findings suggested that shRNA is more effective in silencing the target protein owing to its functional status right upon plasmid transcription, whereas CRISPR/cas9 technology requires protein translation to function. Also, considering the permanent knockout condition of CRISPR/cas9 technology, and considering the possible off-targets that this technology can present, the use of shRNA is considered safer [90]. Nevertheless, despite the overall popularity and promising features of this technology, new findings suggest that its utilization could lead to large rearrangements in the genome, posing a severe threat to the regular cell function and perhaps leading to the emergence of pathological conditions [91]. Therefore, new studies must be performed accompanied by exhaustive genome examination, to guarantee the safe use of CRISPR/cas9 in humans.

microRNAs: an emergent silencing alternative

Lately, the study of microRNA profiling in cancer has been very important in detecting these molecules, because their expression levels can be used as prognostic markers. Several studies have revealed that, in different tissues, microRNAs can present significant alterations in the expression pattern and therefore contribute to a phenotypic cancer state. For instance, microRNA upregulation can contribute to the downregulation of proteins where function is fundamental for cell growth regulation, and *vice versa* [92]. Besides the fact that miRNA levels provide crucial information regarding the cellular mechanisms that can contribute to the onset of the disease, it can also indicate useful pathways to explore when trying to find a cure. These small noncoding RNAs that present 19–25 nucleotides are naturally expressed from miRNA-encoding genomic sequences [93,94]. First, as portrayed in Fig. 3c, its expression renders a long primary transcript (pri-miRNA), which will be cleaved by a complex formed by Drosha and protein DiGeorge syndrome critical region gene 8 (DGCR8) [93]. The processing of pri-miRNA by this complex results in a long hairpin molecule, the precursor of miRNA (pre-miRNA). As presented in Fig. 3c, this whole process occurs in the nucleus. Then, pre-miRNA is exported into the cytoplasm so that it can be cleaved by Dicer, which is coupled with Tar RNA-binding protein (TRBP) and kinase R-activating protein (PACT) [93]. This process presents a double-stranded mature miRNA. The antisense miRNA strand consists in the guide-strand for RNA-induced silencing complex (RISC), which will be loaded onto this complex once Dicer processing is complete. Then, the complex is able to identify target mRNAs that present some complementarity to the miRNA sequence [93]. Different outcomes can result according to the complementarity between RNA molecules, namely: degradation, destabilization or translation repression of target mRNA [93,95]. The main difference between siRNA and miRNA systems is the fact that miRNA can regulate hundreds of different target molecules whereas siRNA is only able to interfere with the expression of molecules with 100% complementarity [93,95]. This feature might be seen as a threat, given that miRNA interaction with off-targets can lead to severe cell deregulation. However, considering that miRNAs can regulate molecules and processes within similar functions and signaling pathways, the exploration of these molecules in therapy could also pose as an advantage in comparison to siRNA technology, because it could be used to simultaneously regulate different oncotargets. For instance, the research work developed by Wei and co-workers demonstrated that miR-17-5p was able to target tumor protein p53-induced nuclear protein 1 (TP53INP1) in cervical cancer cells – a protein that is usually upregulated in this type of tumor and is responsible for regulation of p53 transcriptional activity [96]. In this study, a plasmid expressing pri-miR-17-5p was able to inhibit the proliferation and the viability of cervical cancer cells.

Another microRNA where the tumor-suppressive function has been studied in cervical cancer is miR-125. *In vivo* studies performed by Cui *et al.* demonstrated that overexpression of miR-125b would decrease the ability of injected HeLa cells to form tumors in mice [97]. Moreover, Fan and co-workers were able to prove that miR-125a overexpression was able to suppress the metastasis of cervical cancer cells by targeting STAT3, leading to tumor growth inhibition and impairing metastasis formation in mice [98]. In this study, it was also possible to verify that the presence of HPV viral oncoproteins E6 and E7 would suppress the p53-mediated activation of miR-125a, suggesting that the downregulation of this microRNA is caused by the presence of the viral oncoproteins. Although these studies provide remarkable path-

ways that could be used for the treatment of cervical cancer, it still suggests that HPV infection might offer resistance to such treatments. Nevertheless, Jung *et al.* were able to prove that overexpression of miR-375 was able to directly downregulate E6 and E7 expression in HPV-16- and HPV-18-positive cervical cancer cell lines, rescuing p53 and pRB pathway signaling [99]. Moreover, the downregulation of E6AP, CIP2A and 14-3-3ζ oncogenic proteins was also seen in this study, contributing to a reduction of 35% telomerase activity and ultimately leading to cell-cycle arrest and inhibition of tumor cell proliferation [99]. The fact that this particular microRNA is able to silence E6 and E7 expression while downregulating other oncogenic proteins that are upregulated in cervical cancer cells suggests that the role of miR-375 in HPV-positive cervical cancer might be crucial. The exploration of therapeutic approaches that involve the expression of microRNAs able to regulate HPV-16 and HPV-18 transcripts and promote tumor suppressor protein expression, such as miR-375, can pose as a promising option in the future search for the ultimate HPV-induced cervical cancer treatment. Nevertheless, such a deed might still be remote, considering the amount of study and research that is necessary before exploring this strategy in humans.

Concluding remarks and future perspectives

The HPV impact in women's health is undeniable. It is crucial to invest in the prevention of this infection through the development of vaccines that cover the high-risk HPV types. It is also necessary to make sure these are affordable and can be easily distributed in less developed countries, which are currently the most affected by this virus. Given that vaccination has become a controversial issue recently, owing to increasing popular belief in a link between vaccines and severe adverse reactions, one must consider that full vaccination coverage and HPV eradication might be difficult to achieve in the near future. Therefore, suitable noninvasive and effective strategies should be explored to provide a comfortable and burden-free cervical cancer treatment to patients, as opposed to the currently available treatments. Here, we discussed three approaches that are currently being explored by researchers as a possible pathway that can lead to the discovery of such treatment. Each of these technologies: DNA vaccines, gene therapy and gene silencing, present their advantages and drawbacks. Currently, DNA vaccines stand as the most likely strategy to be implemented more rapidly for HPV treatment, when comparing their achievements in clinical trials with the remaining approaches. Nevertheless, the potential of gene therapy and gene silencing is undeniable and is currently under intensive study. Thus, the exploration and combination of these approaches poses as a fruitful and promising strategy in the future of HPV-induced cervical cancer treatment.

Acknowledgments

This work was supported by FEDER funds through the POCI – COMPETE 2020 – Operational Programme Competitiveness and Internationalization in Axis I – Strengthening Research, Technological Development and Innovation (Project POCI-01-0145-FEDER-007491) and National Funds by FCT – Foundation for Science and Technology (Project UID/Multi /00709/2013). A.M.A. and A.S. acknowledge the doctoral and post-doctoral fellowships (SFRH/BD/102284/2014 and SFRH/BPD/102716/2014, respectively) from FCT.

References

1 Dürst, M. *et al.* (1983) A papillomavirus DNA from a cervical carcinoma and its prevalence in cancer biopsy samples from different geographic regions. *Proc. Natl. Acad. Sci. U. S. A* 80, 3812–3815
2 zur Hausen, H. (1974) *Condylomata acuminata* and human genital cancer. *Cancer Res.* 36, 794
3 Schwarz, E. *et al.* (1985) Structure and transcription of human papillomavirus sequences in cervical carcinoma cells. *Nature* 314, 111–114
4 Bray, F. *et al.* (2013) Global estimates of cancer prevalence for 27 sites in the adult population in 2008. *Int. J. Cancer* 132, 1133–1145
5 Ferlay, J. *et al.* (2018) Estimating the global cancer incidence and mortality in 2018: GLOBOCAN sources and methods. *Cancer Epidemiol.* 144, 1941–1953. http://dx.doi.org/10.1002/ijc.31937
6 Stewart, B.W. and Wild, C.P. (2014) *World Cancer Report 2014*. doi: 92832042982014
7 de Sanjose, S. *et al.* (2010) Human papillomavirus genotype attribution in invasive cervical cancer: a retrospective cross-sectional worldwide study. *Lancet Oncol.* 11, 1048–1056
8 Rogovskaya, S.I. *et al.* (2013) Human papillomavirus prevalence and type-distribution, cervical cancer screening practices and current status of vaccination implementation in Russian Federation, the Western countries of the former Soviet Union, Caucasus Region and Central Asia. *Vaccine* 31 . http://dx.doi.org/10.1016/j.vaccine.2013.06.043
9 Stern, P.L. *et al.* (2012) Therapy of human papillomavirus-related disease. *Vaccine* 30 . http://dx.doi.org/10.1016/j.vaccine.2012.05.091
10 van Doorslaer, K. *et al.* (2017) The papillomavirus episteme: a major update to the papillomavirus sequence database. *Nucleic Acids Res* 45, D499–506
11 Chan, P.K.S. *et al.* (2012) Laboratory and clinical aspects of human papillomavirus testing. *Crit. Rev. Clin. Lab. Sci.* 49, 117–136
12 Doorbar, J. *et al.* (2015) Human papillomavirus molecular biology and disease association. *Rev. Med. Virol.* 25, 2–23
13 Vande Pol, S.B. and Klingelhutz, A.J. (2013) Papillomavirus E6 oncoproteins. *Virology* 445, 115–137
14 Roman, A. and Munger, K. (2013) The papillomavirus E7 proteins. *Virology* 445, 138–168
15 DiMaio, D. and Petti, L.M. (2013) The E5 proteins. *Virology* 445, 99–114. http://dx.doi.org/10.1016/j.virol.2013.05.006
16 Thomas, M. *et al.* (1999) The role of the E6-p53 interaction in the molecular pathogenesis of HPV. *Oncogene* 18, 7690–7700. http://dx.doi.org/10.1038/sj.onc.1202953
17 Tomaić, V. (2016) Functional roles of E6 and E7 oncoproteins in HPV-induced malignancies at diverse anatomical sites. *Cancers* 8, 95. http://dx.doi.org/10.3390/cancers8100095
18 Duronio, R.J. and Xiong, Y. (2013) Signaling pathways that control cell proliferation. *Cold Spring Harb. Perspect. Biol.* 5, a008904. http://dx.doi.org/10.1101/cshperspect.a008904
19 Pang, C.L. and Thierry, F. (2013) Human papillomavirus proteins as prospective therapeutic targets. *Microb. Pathog* 58, 55–65. http://dx.doi.org/10.1016/j.micpath.2012.11.002
20 Shah, S.S. *et al.* (2016) Current technologies and recent developments for screening of HPV-associated cervical and oropharyngeal cancers. *Cancers* 8, 85. http://dx.doi.org/10.3390/cancers8090085
21 Ronco, G. *et al.* (2014) Efficacy of HPV-based screening for prevention of invasive cervical cancer: follow-up of four European randomised controlled trials. *Lancet* 383, 524–532
22 La, K. *et al.* (2002) A controlled trial of a human papillomavirus type 16 vaccine. *N. Engl. J. Med.* 2002, 1645–1651
23 Mao, C. *et al.* (2006) Efficacy of human papillomavirus-16 vaccine to prevent cervical intraepithelial neoplasia: a randomized controlled trial. *Obstet. Gynecol.* 107, 18–27
24 Rowhani-Rahbar, A. *et al.* (2009) Longer term efficacy of a prophylactic monovalent human papillomavirus type 16 vaccine. *Vaccine* 27, 5612–5619

25 Villa, L.L. *et al.* (2005) Prophylactic quadrivalent human papillornavirus (types 6, 11, 16, and 18) L1 virus-like particle vaccine in young women: a randomiseddouble-blind placebo-controlled multicentre Phase II efficacy trial. *Lancet Oncol* 6, 271–278

26 Villa, L.L. *et al.* (2006) High sustained efficacy of a prophylactic quadrivalent human papillomavirus types 6/11/16/18 L1 virus-like particle vaccine through 5 years of follow-up. *Br. J. Cancer* 95, 1459–1466

27 Garland, S.M. *et al.* (2007) Quadrivalent vaccine against human papillomavirus to prevent anogenital diseases. *N. Engl. J. Med.* 356, 1928–1943

28 FUTURE II Study Group (2007) Quadrivalent vaccine against human papillomavirus to prevent high-grade cervical lesions. *N. Engl. J. Med.* 356, 1915–1927

29 Ault, K.A. (2007) Effect of prophylactic human papillomavirus L1 virus-like-particle vaccine on risk of cervical intraepithelial neoplasia grade 2, grade 3, and adenocarcinoma *in situ*: a combined analysis of four randomised clinical trials. *Lancet* 369, 1861–1868. http://dx.doi.org/10.1016/S0140-6736(07)60852-6

30 Harper, D.M. *et al.* (2006) Sustained efficacy up to 4.5 years of a bivalent L1 virus-like particle vaccine against human papillomavirus types 16 and 18: follow-up from a randomised control trial. *Lancet* 367, 1247–1255

31 Paavonen, J. *et al.* (2009) Efficacy of human papillomavirus (HPV)-16/18 AS04-adjuvanted vaccine against cervical infection and precancer caused by oncogenic HPV types (PATRICIA): final analysis of a double-blind, randomised study in young women. *Lancet* 374, 301–314

32 Einstein, M.H. *et al.* (2014) Comparison of long-term immunogenicity and safety of human papillomavirus (HPV)-16/18 AS04-adjuvanted vaccine and HPV-6/11/16/18 vaccine in healthy women aged 18-45 years: end-of-study analysis of a Phase III randomized trial. *Hum. Vaccines Immunother* 10, 3435–3445

33 Naud, P.S. *et al.* (2014) Sustained efficacy, immunogenicity, and safety of the HPV-16/18 AS04-adjuvanted vaccine: final analysis of a long-term follow-up study up to 9.4 years post-vaccination. *Hum. Vaccines Immunother* 10, 2147–2162

34 Nygård, M. *et al.* (2015) Evaluation of the long-term anti-human papillomavirus 6 (HPV6), 11, 16, and 18 immune responses generated by the quadrivalent HPV vaccine. *Clin. Vaccine Immunol.* 22, 943–948

35 Joura, E.A. *et al.* (2015) A 9-valent HPV vaccine against infection and intraepithelial neoplasia in women. *Obstet. Gynecol. Surv.* 70, 446–448

36 Luxembourg, A. *et al.* (2015) Phase III, randomized controlled trial in girls 9–15 years old to evaluate lot consistency of a novel nine-valent human papillomavirus L1 virus-like particle vaccine. *Hum. Vaccines Immunother.* 11, 1306–1312

37 van Damme, P. *et al.* (2016) A Phase III clinical study to compare the immunogenicity and safety of the 9-valent and quadrivalent HPV vaccines in men. *Vaccine* 34, 4205–4212

38 Lefèvre, H. *et al.* (2018) HPV vaccination rate in French adolescent girls: an example of vaccine distrust. *Arch. Dis. Child.* 103, 740–746. http://dx.doi.org/10.1136/archdischild-2017-313887

39 Larson, H.J. *et al.* (2014) Tracking the global spread of vaccine sentiments: the global response to Japan's suspension of its HPV vaccine recommendation. *Hum. Vaccines Immunother.* . http://dx.doi.org/10.4161/21645515.2014.969618

40 Marth, C. *et al.* (2017) Cervical cancer: ESMO Clinical Practice Guidelines for diagnosis, treatment and follow-up. *Ann. Oncol* 28, iv72–83

41 Pérez-Herrero, E. and Fernández-Medarde, A. (2015) Advanced targeted therapies in cancer: drug nanocarriers, the future of chemotherapy. *Eur. J. Pharm. Biopharm.* 93, 52–79

42 Hasson, S.S.A.A. *et al.* (2015) The past, current and future trends in DNA vaccine immunisations. *Asian Pac. J. Trop. Biomed.* 5, 344–353

43 Li, L. and Petrovsky, N. (2016) Molecular mechanisms for enhanced DNA vaccine immunogenicity. *Expert Rev. Vaccines* 15, 313–329

44 Lee, J. *et al.* (2018) Engineering DNA vaccines against infectious diseases. *Acta Biomater.* 80, 31–47

45 Yang, B. *et al.* (2014) DNA vaccine for cancer immunotherapy. *Hum. Vaccines Immunother.* . http://dx.doi.org/10.4161/21645515.2014.980686

46 Lichtor, T. and Glick, R.P. (2012) Immunogene therapy. *Adv. Exp. Med. Biol.* 746, 151–165

47 Almeida, A.M. *et al.* (2015) Optimization of supercoiled HPV-16 E6/E7 plasmid DNA purification with arginine monolith using design of experiments. *J. Chromatogr. B Anal. Technol. Biomed. Life Sci.* 978–979, 145–150

48 Hancock, G. *et al.* (2018) Therapeutic HPV vaccines. *Best Pract. Res. Clin. Obstet. Gynaecol.* 47, 59–72

49 Gulce-Iz, S. and Saglam-Metiner, P. (2019) Current state of the art in DNA vaccine delivery and molecular adjuvants: Bcl-xL anti-apoptotic protein as a molecular adjuvant. *Immune Response Act. Immunomodulation IntechOpen* . http://dx.doi.org/10.5772/intechopen.82203 https://www.intechopen.com/books/immune-response-activation-and-immunomodulation/current-state-of-the-art-in-dna-vaccine-delivery-and-molecular-adjuvants-bcl-xl-anti-apoptotic-prote

50 Yang, B. *et al.* (2014) DNA vaccine for cancer immunotherapy. *Hum. Vaccines Immunother.* 10, 3153–3164

51 Kim, T.J. *et al.* (2014) Clearance of persistent HPV infection and cervical lesion by therapeutic DNA vaccine in CIN3 patients. *Nat. Commun* 5 . http://dx.doi.org/10.1038/ncomms6317

52 Samuels, S. *et al.* (2017) HPV16 E7 DNA tattooing: safety, immunogenicity, and clinical response in patients with HPV-positive vulvar intraepithelial neoplasia. *Cancer Immunol. Immunother.* . http://dx.doi.org/10.1007/s00262-017-2006-y

53 Trimble, C.L. *et al.* (2009) A Phase I trial of a human papillomavirus DNA vaccine for HPV16+ cervical intraepithelial neoplasia 2/3. *Clin. Cancer Res* 15, 361–367

54 Chandra, J. *et al.* (2017) DNA vaccine encoding HPV16 oncogenes E6 and E7 induces potent cell-mediated and humoral immunity which protects in tumor challenge and drives E7-expressing skin graft rejection. *J. Immunother.* 40, 62–70

55 Silva, J.R. *et al.* (2019) Expression of a soluble IL-10 receptor enhances the therapeutic effects of a papillomavirus-associated antitumor vaccine in a murine model. *Cancer Immunol. Immunother.* 68, 753–763

56 Maldonado, L. *et al.* (2014) Vaccination: intramuscular therapeutic vaccination targeting HPV16 induces T cell responses that localize in mucosal lesions. *Sci. Transl. Med.* 6, 221ra13. http://dx.doi.org/10.1126/scitranslmed.3007323

57 Trimble, C.L. *et al.* (2015) Safety, efficacy, and immunogenicity of VGX-3100, a therapeutic synthetic DNA vaccine targeting human papillomavirus 16 and 18 E6 and E7 proteins for cervical intraepithelial neoplasia 2/3: a randomised, double-blind, placebo-controlled Phase 2b trial. *Lancet* 386, 2078–2088. http://dx.doi.org/10.1016/S0140-6736(15)00239-1

58 Inovio Pharmaceuticals (2019) *Inovio Completes Enrollment of VGX-3100 Phase 3 Trial (REVEAL 1) for the Treatment of HPV-Related Cervical Pre-cancer*. 2019 Available at: http://ir.inovio.com/news-and-media/news/press-release-details/2019/Inovio-Completes-Enrollment-of-VGX-3100-Phase-3-Trial-REVEAL-1-for-the-Treatment-of-HPV-Related-Cervical-Pre-cancer/default.aspx

59 Alvarez, R.D. *et al.* (2016) A pilot study of pNGVL4a-CRT/E7(detox) for the treatment of patients with HPV16 + cervical intraepithelial neoplasia 2/3 (CIN2/3). *Gynecol. Oncol.* 140, 245–252

60 Hobernik, D. and Bros, M. (2018) DNA vaccines – how far from clinical use? *Int. J. Mol. Sci.* 19, 3605

61 Wang, W. *et al.* (2013) Non-viral gene delivery methods. *Curr. Pharm. Biotechnol.* 14, 46–60

62 Naldini, L. (2015) Gene therapy returns to centre stage. *Nature* 526, 351–360

63 Sheridan, C. (2011) Gene therapy finds its niche. *Nat. Biotechnol.* 29, 121–128

64 Ginn, S.L. *et al.* (2018) Gene therapy clinical trials worldwide to 2017: an update. *J. Gene Med.* 20, e3015

65 Ip, S.M. *et al.* (2001) pRb-expressing adenovirus Ad5-Rb attenuates the p53-induced apoptosis in cervical cancer cell lines. *Eur. J. Cancer* 37, 2475–2483. http://dx.doi.org/10.1016/S0959-8049(01)00308-2

66 Hunt, K.K. *et al.* (1997) Adenovirus-mediated overexpression of the transcription factor E2F-1 induces apoptosis in human breast and ovarian carcinoma cell lines and does not require p53. *Cancer Res.* 57, 4722–4726

67 Valente, J.F. *et al.* (2018) p53 as the focus of gene therapy: past, present and future. *Curr. Drug Targets* 19 . http://dx.doi.org/10.2174/1389450119666180115165447

68 Prabhu, N.S. *et al.* (1998) p73beta, unlike p53, suppresses growth and induces apoptosis of human papillomavirus E6-expressing cancer cells. *Int. J. Oncol.* 13, 5–14

69 Das, S. *et al.* (2003) Efficient growth inhibition of HPV 16 E6-expressing cells by an adenovirus-expressing p53 homologue p73β. *Oncogene* 22, 8394–8402. http://dx.doi.org/10.1038/sj.onc.1206908

70 Das, S. and Somasundaram, K. (2006) Therapeutic potential of an adenovirus expressing p73 beta, a p53 homologue, against human papilloma virus positive cervical cancer *in vitro* and *in vivo*. *Cancer Biol. Ther.* 5, 210–217

71 Guan, Y.S. *et al.* (2005) Successful management of postoperative recurrence of hepatocellular carcinoma with p53 gene therapy combining transcatheter arterial chemoembolization. *World J. Gastroenterol* 11, 3803–3805. http://dx.doi.org/10.3748/wjg.v11.i24.3803

72 Su, X. *et al.* (2016) Effect and safety of recombinant adenovirus-p53 transfer combined with radiotherapy on long-term survival of locally advanced cervical cancer. *Hum. Gene Ther.* 27, 1008–1014

73 Zhang, W.-W. *et al.* (2018) The first approved gene therapy product for cancer Ad-p53 (Gendicine): 12 years in the clinic. *Hum. Gene Ther.* 29, 160–179. http://dx.doi.org/10.1089/hum.2017.218

74 Tomizawa, J. *et al.* (1981) Inhibition of ColE1 RNA primer formation by a plasmid-specified small RNA. *Proc. Natl. Acad. Sci. U. S. A.* 78, 1421–1425. http://dx.doi.org/10.1073/pnas.78.3.1421

75 Guo, S. and Kemphues, K.J. (1995) par-1, a gene required for establishing polarity in *C. elegans* embryos, encodes a putative Ser/Thr kinase that is asymmetrically distributed. *Cell* 81, 611–620. http://dx.doi.org/10.1016/0092-8674(95)90082-9

76 Fire, A. *et al.* (1998) Potent and specific genetic interference by double-stranded RNA in *Caenorhabditis elegans*. *Nature* 391, 806–811. http://dx.doi.org/10.1038/35888

77 von Knebel Doeberitz, M. *et al.* (1988) Correlation of modified human papilloma virus early gene expression with altered growth properties in C4-1 cervical carcinoma cells. *Cancer Res.* 48, 3780–3786

78 Choo, C.K. *et al.* (2000) Retrovirus-mediated delivery of HPV16 E7 antisense RNA inhibited tumorigenicity of CaSki cells. *Gynecol. Oncol.* 78, 293–301. http://dx.doi.org/10.1006/gyno.2000.5916

79 Cho, C.W. *et al.* (2002) HPV E6 antisense induces apoptosis in CaSki cells via suppression of E6 splicing. *Exp. Mol. Med.* 34, 159–166. http://dx.doi.org/10.1038/emm.2002.23

80 Yamato, K. *et al.* (2006) Induction of cell death in human papillomavirus 18-positive cervical cancer cells by E6 siRNA. *Cancer Gene Ther.* 13, 234–241. http://dx.doi.org/10.1038/sj.cgt.7700891

81 Jiang, M. and Milner, J. (2002) Selective silencing of viral gene expression in HPV-positive human cervical carcinoma cells treated with siRNA, a primer of RNA interference. *Oncogene* 21, 6041–6048. http://dx.doi.org/10.1038/sj.onc.1205878

82 Tang, S. *et al.* (2006) Short-term induction and long-term suppression of HPV16 oncogene silencing by RNA interference in cervical cancer cells. *Oncogene* 25, 2094–2104. http://dx.doi.org/10.1038/sj.onc.1209244

83 Castanotto, D. and Rossi, J.J. (2009) The promises and pitfalls of RNA-interference-based therapeutics. *Nature* 457, 426–433. http://dx.doi.org/10.1038/nature07758

84 Rao, D.D. *et al.* (2009) siRNA vs. shRNA: similarities and differences. *Adv. Drug Deliv. Rev.* 61, 746–759. http://dx.doi.org/10.1016/j.addr.2009.04.004

85 De Vincenzo, J.P. (2012) The promise, pitfalls and progress of RNA-interference-based antiviral therapy for respiratory viruses. *Antivir. Ther.* 17, 213–225. http://dx.doi.org/10.3851/IMP2064

86 Zhen, S. *et al.* (2014) *In vitro* and *in vivo* growth suppression of human papillomavirus 16-positive cervical cancer cells by CRISPR/Cas9. *Biochem. Biophys. Res. Commun.* 450, 1422–1426. http://dx.doi.org/10.1016/j.bbrc.2014.07.014

87 Hu, Z. *et al.* (2014) Disruption of HPV16-E7 by CRISPR/Cas system induces apoptosis and growth inhibition in HPV16 positive human cervical cancer cells. *Biomed. Res. Int.* 2014 . http://dx.doi.org/10.1155/2014/612823

88 Zhen, S. *et al.* (2016) *In vitro* and *in vivo* synergistic therapeutic effect of cisplatin with human papillomavirus16 E6/E7 CRISPR/CAS9 on cervical cancer cell line. *Transl. Oncol.* 9, 498–504. http://dx.doi.org/10.1016/j.tranon.2016.10.002

89 Kennedy, E.M. *et al.* (2014) Inactivation of the human papillomavirus E6 or E7 gene in cervical carcinoma cells by using a bacterial CRISPR/Cas RNA-guided endonuclease. *J. Virol.* 88, 11965–11972. http://dx.doi.org/10.1128/JVI.01879-14

90 Zhu, D. *et al.* (2018) Nanoparticles based on poly (β-amino ester) and HPV16 targeting CRISPR/shRNA as potential drugs for HPV16 related cervical malignancy. *Mol. Ther.* 26, 2443–2455. http://dx.doi.org/10.1016/J.YMTHE.2018.07.019

91 Kosicki, M. *et al.* (2018) Repair of double-strand breaks induced by CRISPR–Cas9 leads to large deletions and complex rearrangements. *Nat. Biotechnol.* 36, 765–771. http://dx.doi.org/10.1038/nbt.4192

92 Li, J. *et al.* (2017) Deregulated miRNAs in human cervical cancer: functional importance and potential clinical use. *Fut. Oncol.* 13, 743–753. http://dx.doi.org/10.2217/fon-2016-0328

93 Pereira, P. *et al.* (2017) Current progress on microRNAs-based therapeutics in neurodegenerative diseases. *Wiley Interdiscip. Rev. RNA* 8, e1409. http://dx.doi.org/10.1002/wrna.1409

94 Konicke, K. *et al.* (2018) The microRNA landscape of cutaneous squamous cell carcinoma. *Drug Discov. Today* 23, 864–870. http://dx.doi.org/10.1016/j.drudis.2018.01.023

95 Díaz-González, S.D.M. *et al.* (2015) Utility of microRNAs and siRNAs in cervical carcinogenesis. *Biomed. Res. Int.* 2015 . http://dx.doi.org/10.1155/2015/374924

96 Wei, Q. *et al.* (2012) miR-17-5p targets TP53INP1 and regulates cell proliferation and apoptosis of cervical cancer cells. *IUBMB Life* 64, 697–704. http://dx.doi.org/10.1002/iub.1051

97 Cui, F. *et al.* (2012) miR-125b inhibits tumor growth and promotes apoptosis of cervical cancer cells by targeting phosphoinositide 3-kinase catalytic subunit delta. *Cell. Physiol. Biochem.* 30, 1310–1318. http://dx.doi.org/10.1159/000343320

98 Fan, Z. *et al.* (2015) miR-125a suppresses tumor growth, invasion and metastasis in cervical cancer by targeting STAT3. *Oncotarget* . http://dx.doi.org/10.18632/oncotarget.4457

99 Jung, H.M. *et al.* (2014) miR-375 activates p21 and suppresses telomerase activity by coordinately regulating HPV E6/E7, E6AP, CIP2A, and 14-3-3ζ. *Mol. Cancer* 13 . http://dx.doi.org/10.1186/1476-4598-13-80

100 Kim, D. *et al.* (2008) Enhancement of DNA vaccine potency through coadministration of CIITA DNA with DNA vaccines via gene gun. *J. Immunol.* 180, 7019–7027. http://dx.doi.org/10.4049/jimmunol.180.10.7019

101 Ahn, J. *et al.* (2017) Immunologic responses to a novel DNA vaccine targeting human papillomavirus-11 E6E7. *Laryngoscope* 127, 2713–2720. http://dx.doi.org/10.1002/lary.26737

102 Seo, S.H. *et al.* (2009) Optimal induction of HPV DNA vaccine-induced CD8+ T cell responses and therapeutic antitumor effect by antigen engineering and electroporation. *Vaccine* 27, 5906–5912. http://dx.doi.org/10.1016/j.vaccine.2009.07.033

103 Zurkova, K. *et al.* (2009) The expression of the soluble isoform of hFlt3 ligand by recombinant vaccinia virus enhances immunogenicity of the vector. *Oncol. Rep.* 21, 1335–1343. http://dx.doi.org/10.3892/or_00000359

104 Sun, Y. *et al.* (2017) Coinjection of IL2 DNA enhances E7-specific antitumor immunity elicited by intravaginal therapeutic HPV DNA vaccination with electroporation. *Gene Ther* 24, 408–415. http://dx.doi.org/10.1038/gt.2017.38

105 Oosterhuis, K. *et al.* (2011) Preclinical development of highly effective and safe DNA vaccines directed against HPV 16 E6 and E7. *Int. J. Cancer* 129, 397–406. http://dx.doi.org/10.1002/ijc.25894

106 Baghban Rahimi, S. *et al.* (2018) Enhancement of therapeutic DNA vaccine potency by melatonin through inhibiting VEGF expression and induction of antitumor immunity mediated by CD8+ T cells. *Arch. Virol.* 163, 587–597

107 Garza-Morales, R. *et al.* (2019) A DNA vaccine encoding SA-4-1bbl fused to HPV-16 E7 antigen has prophylactic and therapeutic efficacy in a cervical cancer mouse model. *Cancers* 11, 96

108 Sima, N. *et al.* (2007) Antisense targeting human papillomavirus type 16 E6 and E7 genes contributes to apoptosis and senescence in SiHa cervical carcinoma cells. *Gynecol. Oncol* 106, 299–304. http://dx.doi.org/10.1016/j.ygyno.2007.04.039

109 Zhou, J. *et al.* (2013) Inhibition of cervical cancer cell growth *in vitro* and *in vivo* by lentiviral-vector mediated shRNA targeting the common promoter of HPV16 E6 and E7 oncogenes. *Antiviral Res.* 98, 305–313. http://dx.doi.org/10.1016/j.antiviral.2013.03.010

110 Nishida, H. *et al.* (2016) Systemic delivery of siRNA by actively targeted polyion complex micelles for silencing the E6 and E7 human papillomavirus oncogenes. *J. Control. Release* 231, 29–37. http://dx.doi.org/10.1016/j.jconrel.2016.03.016

111 Rajasekaran, N. *et al.* (2017) Effect of HPV E6/E7 siRNA with chemotherapeutic agents on the regulation of TP53/E2F dynamic behavior for cell fate decisions. *Neoplasia* 19, 735–749. http://dx.doi.org/10.1016/j.neo.2017.07.005

112 Sato, N. *et al.* (2018) Eradication of cervical cancer in vivo by an AAV vector that encodes shRNA targeting human papillomavirus type 16 E6/E7. *Int. J. Oncol* 52, 687–696. http://dx.doi.org/10.3892/ijo.2018.4245

113 Kojima, Y. *et al.* (2018) Adenovirus-mediated transfer of HPV 16 E6/E7 antisense RNA combined with cisplatin inhibits cellular growth and induces apoptosis in HPV-positive head and neck cancer cells. *Cancer Gene Ther* 25, 274–283. http://dx.doi.org/10.1038/s41417-018-0024-3

Paper II

Minicircle DNA – The future for DNA-based vectors?

A.M. Almeida, J.A. Queiroz, F. Sousa, A. Sousa*

CICS-UBI – Centro de Investigação em Ciências da Saúde, Universidade da Beira Interior, Av. Infante D. Henrique, 6200-506 Covilhã, Portugal

Trends in Biotechnology (2020) S0167-7799(20)30113-X

Short description: A succinct literature review focused on explaining the main differences between minicircle DNA and plasmid DNA, concomitantly presenting the methodologies currently available for minicircle DNA production and purification

Trends in Biotechnology

CellPress REVIEWS

Forum

Minicircle DNA: The Future for DNA-Based Vectors?

Ana Margarida Almeida [1], João António Queiroz [1], Fani Sousa [1] and Ângela Sousa [1,*]

Minicircle DNA (mcDNA) is a smaller and safer version of non-viral DNA vectors that results from a cutting-edge *in vivo* recombination process to excise prokaryotic sequences from plasmid DNA (pDNA). Considering the molecule's potential and increasing interest as a non-viral DNA-based therapeutic, biomanufacturing methodologies need to be improved, especially in downstream processing.

mcDNA

mcDNA has attracted significant attention as a gene therapy vector, DNA vaccine, or intermediate in cell-based therapies due to its strong performance and safety as a non-viral DNA vector [1], especially in comparison with the popular pDNA vector (Box 1). Although mcDNA was designed specifically to overcome the limitations of pDNA, its origin derives from a pDNA-like structure called a parental plasmid (PP). A PP contains specific sequences, such as *att*, *loxP*, *MRS*, or *attP*/*attB* recombination sites, that allow its recombination into two different molecules: mcDNA and miniplasmid (mP) (Box 2) [2]. Despite the well-documented potential of this outstanding biopharmaceutic, showing better performance than pDNA in cell transfection and gene expression in different fields, little attention has been given to mcDNA manufacturing restrictions and recent progress that has been made to overcome them. These points are crucial to understand how to further improve the yield and purity and reduce the costs of mcDNA manufacturing to reach its large-scale potential.

mcDNA Processing

Upstream Processing

While a mP inherits all the prokaryotic sequences necessary for PP amplification within the prokaryotic system, including the replication origin and selection markers, mcDNA retains the eukaryotic sequences required for the therapeutic effect, such as the promoter and gene of interest [2]. PP production begins similarly to pDNA production, and induced *in vivo* recombination of the PP into mP and mcDNA follows. Simultaneously, in some particular systems, certain events can occur to promote the cleavage and elimination of mP and unrecombined PP impurities (Box 2). Each system can have a different impact on its downstream processing since variable mcDNA, PP, and mP content can result from the recombination process, affecting not only the final mcDNA yield but also its contamination degree.

Downstream Processing

Due to its peculiar production features, mcDNA upstream processing still requires optimization since mcDNA is often contaminated with the PP. Moreover, the methods used to purify pDNA are not as efficient for purifying mcDNA. This unfortunate situation is mainly due to the similar genetic composition of the mcDNA, PP, and mP molecules. The PP and mP impurities contain analogous structural and chemical properties to mcDNA, which hampers the purification process because the impurities interact similarly with the chromatographic matrix. These drawbacks have prompted the use of affinity chromatography to isolate mcDNA.

Backbone Modification

Until 2016, the methods used to purify mcDNA strongly depended on custom backbone modification. For instance, in 2008, a strategy for mcDNA purification was developed that involved modifying the PP backbone to include a lactose operator (LacOp) sequence in the mcDNA template [3]. The sample would be loaded onto a chromatographic column modified with a LacOp repressor protein. Given the specific LacOp sequence, mcDNA would bind to the column, while the remaining contaminants would be eluted. However, this approach requires full PP recombination since the presence of the PP would impair the purity of mcDNA due to the shared LacOp sequence.

In 2015, a different approach, based on the negative purification of mcDNA, was

Box 1. mcDNA versus pDNA Biomanufacturing

pDNA is the most popular non-viral vector, having been widely studied and characterized for delivering foreign genetic information [12]. Despite being regarded as safer than most known viral strategies, pDNA contains bacterial sequences that may trigger immunological reactions after administration, and its efficiency in eliciting therapeutic effects is often lower than that of viral vectors [1,2]. These bacterial sequences can contribute to antibiotic resistance, given that this expression pattern is widely used as a selection marker for pDNA production [2]. pDNA manufacturing is less expensive than the manufacture of viral vectors, so there have been numerous studies regarding pDNA production and purification. Thus, mcDNA, which is a smaller molecule devoid of potentially harmful sequences, has emerged as an improved non-viral vector that can overcome the difficulties presented by pDNA (Figure I). This innovative molecule can enter eukaryotic cells more easily than pDNA. Some studies suggest that pDNA expression is often silenced by cellular mechanisms related to the presence of bacterial sequences whose absence renders prolonged expression for mcDNA vectors (Figure I). However, upstream and downstream processes can lead to mcDNA contamination with PP, and the similarity between these molecules is on the basis of low selectivity and yields rendered by common pDNA purification methodologies.

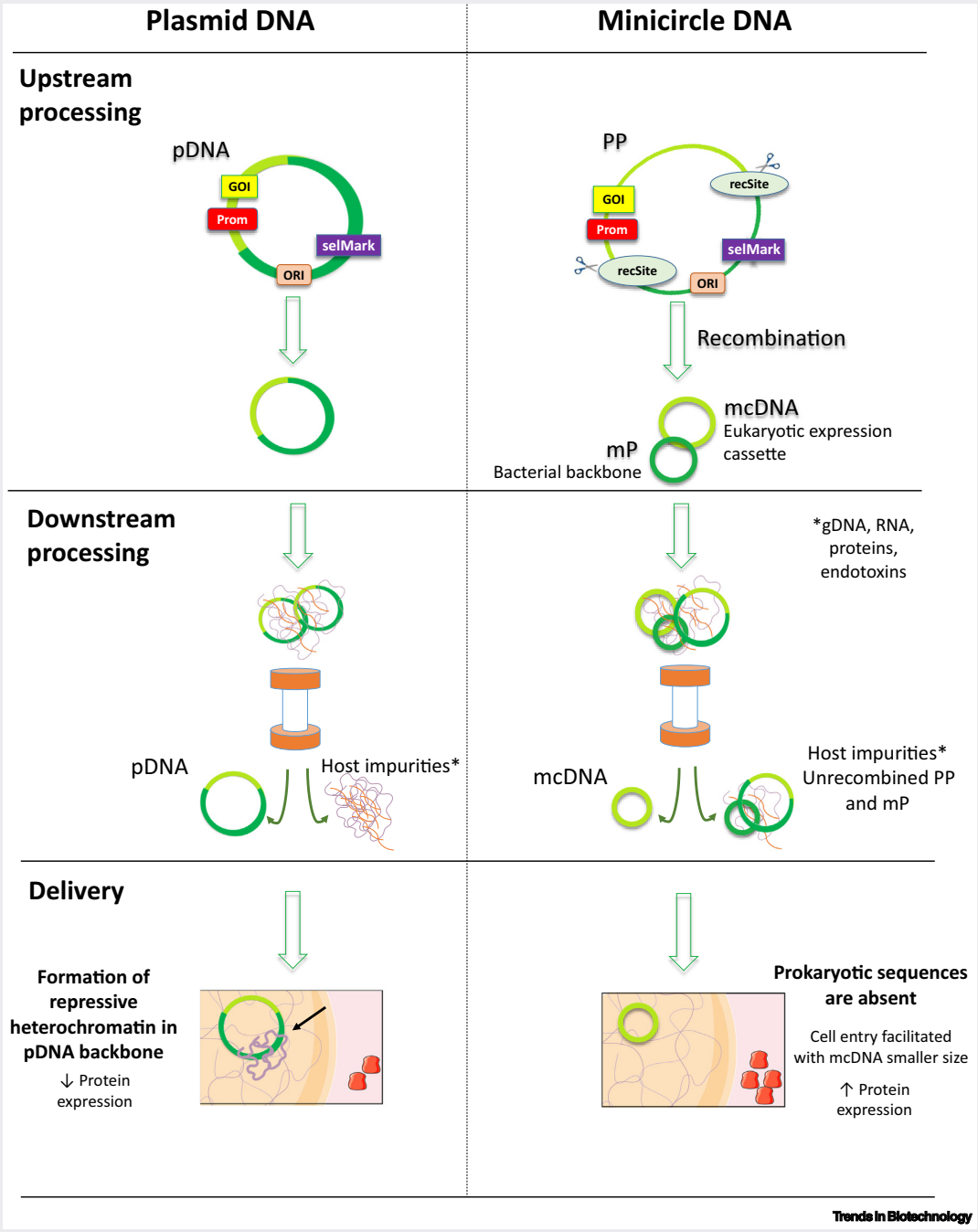

Figure I. Biomanufacturing Comparison between Plasmid DNA (pDNA) and Minicircle DNA (mcDNA) Vectors, from Production to Purification and Delivery. Abbreviations: gDNA, genomic DNA; GOI, gene of interest; mP, miniplasmid; ORI, origin of replication; PP, parental plasmid; Prom, promotor; recSite, recombination site; selMark, selection marker.

Box 2. mcDNA Recombination Systems

Four major PP–mcDNA recombination systems have been explored, each presenting different outcomes in recombination efficiency and contaminant elimination. Table I gives a comparative analysis of current mcDNA production systems [13]. Despite these interesting results, there have been several more successful strategies for producing the rival molecular pDNA in the biopharmaceutical market. In general, mcDNA yields in published studies vary between 0.1 and 8.84 mg/l of fermentation. Compared with pDNA yields, which can reach 2.2 g/l, mcDNA yields are very low, which constitutes a drawback for this technology. Despite the innovative character of mcDNA technology, the yield of mcDNA is presently controlled by the yield of PP and by its recombination efficiency. The fact that full recombination might not occur automatically hampers the mcDNA yield, which is illustrated by the yield disparity observed between these molecules under similar production conditions. Nonetheless, with its increasing popularity, some studies have recently proposed improvements to mcDNA production by adjusting fermentation conditions, such as temperature and induction time [14], or by genetically improving the strains for better yields [15]. These results suggest that further efforts should be focused on overcoming mcDNA upstream processing limitations.

Table I. mcDNA Production Systems to Induce PP *In Vivo* Recombination

	Phage λ integrase	Phage P1 Cre recombinase	ParA resolvase	PhiC31 integrase/I-SceI
Recombination mechanism	Tyrosine recombinase, which catalyzes the recombination of *att* hybrid sites with the aid of accessory proteins FIS and IHF	Site-specific tyrosine recombinase, which performs a bidirectional recombination when binding to *loxP* sites	Serine recombinase, which performs an irreversible and unidirectional recombination between two identical *MRS* sites	Serine recombinase, which mediates unidirectional recombination between *attP/attB* binding sites, while I-SceI endonuclease cleaves the mP and unrecombined PP molecules
Unrecombined PP and mP degradation	No	No	No	Yes
Recombination yields	Medium–low (60%) due to intrinsic toxicity	Medium–low (60%)	Very high (99.5%)	Medium–high (75%)
Limitations	Requires the expression of host factors FIS and IHF; intrinsic toxicity; PP and mP contamination must be addressed	PP and mP contamination must be addressed	mP contamination must be addressed	PP degradation may reduce mcDNA yield; residual PP molecules found in final sample

developed by capturing the impurities from the sample. The PP backbone was modified to include a specific triplex DNA (TriD) sequence in the mP region template [4]. Magnetic beads were modified with specific oligonucleotides that would recognize the TriD sequence. Upon sample incubation, both PP and mP molecules would bind to the magnetic beads and be extracted from the sample, yielding 94–95% mcDNA. However, both strategies raised a similar issue: prepurification with a commercial anion-exchange column was necessary to eliminate host impurities.

To address this issue, in a different approach, the PP backbone was designed to contain a recognition site for Nb.BbvCI enzyme in the PP/mP template [5,6]. After bacterial lysis, the sample is digested with the nicking Nb.BbvCI enzyme to convert supercoiled (sc) mP and PP to the respective open circular (oc) forms. This digestion step helps to separate sc mcDNA from mP and unrecombined PP through hydrophobic interaction chromatography (HIC). One adaptation of this method substitutes HIC for multimodal chromatography with Capto adhere ligand [7]. Using increasing NaCl gradients, this strategy allowed a near 40% mcDNA recovery with 93.5% purity. Although prepurification is not required in this strategy, the need for PP backbone modification and the use of enzyme digestion render this process costly for effective industrial scale-up.

A Universal Purification Approach

To overcome these hurdles, a method was implemented in 2016 that used a monolithic column coupled with diethylaminoethyl ligand [8]. sc mcDNA was purified from mP, PP, and host impurities with a single chromatographic run, requiring little NaCl gradient manipulation, and representing a great advance towards developing a cost-effective mcDNA purification strategy with reduced environmental impact. However, the mcDNA elution was distributed in two different peaks, lowering the mcDNA recovery (~50%) compared with some other strategies.

In 2019, a different strategy was implemented to increase mcDNA recovery yield by exploring cadaverine as a new chromatographic ligand. After recombination, sc mcDNA was purified from all contaminants and host impurities by using a cadaverine-modified monolith and a smooth NaCl gradient [9]. This approach resulted in a sc mcDNA recovery yield of 78.6% with 98.4% purity in a single peak. Nonetheless, small amounts of

pure sc mcDNA were recovered (1.97 μg), requiring this process to be repeated many times to obtain high amounts of purified sc mcDNA.

Later, size-exclusion chromatography was explored for sc mcDNA isolation from a clarified lysate sample [10]. In this study, sc mcDNA was isolated by a Sephacryl SF-1000 matrix with a recovery yield of 66%. Although a slightly lower yield was observed, higher sc mcDNA mass was recovered (24.02 μg) despite the long chromatographic runs [10]. Moreover, this strategy was implemented with two differently sized PP–mcDNA pairs, highlighting the universal applicability of this approach. Overall, it has become clear that mcDNA isolation and purification methodologies have been evolving. Nonetheless, more effort should be placed on developing more specific, selective, robust, and low-cost strategies, which can be easily implemented for high-yield recovery of pure mcDNA from different complex samples, so that the full potential of mcDNA can be reached in an affordable way.

Quantitative Analysis

Many strategies to detect host impurities are currently commercially available. However, methodologies to evaluate and characterize the sc mcDNA quality and purity with respect to other nucleic acids are expensive and limited. PP, mP, and mcDNA content has been evaluated by real-time polymerase chain reaction (qPCR) and horizontal electrophoresis [8,9]. While qPCR is quantitative, accurate, expensive, and time consuming, electrophoretic analysis is fast and cheap but mainly qualitative and unable to quantify mcDNA content. In 2020, a chromatographic methodology for sc mcDNA quantitative analysis was implemented for the first time, using the previously developed cadaverine modified monolith [11]. This methodology quantified sc mcDNA from a complex lysate sample in 40 minutes and could be easily adapted for differently sized mcDNA–PP pairs. This hallmark in mcDNA downstream processing was only possible due to the recent interest in pursuing lower costs for mcDNA biomanufacturing.

Concluding Remarks and Future Perspectives

mcDNA has outstanding therapeutic outcomes that highlight the versatility of innovative vector design and open the door to a new generation of DNA vectors. The potential utility of mcDNA will ideally prompt further research into overcoming some challenges associated with its manufacture, especially regarding its production yield and purification costs. Pursuing genetic strain modifications and exploring different culture conditions is useful to increase the overall mcDNA yield in different systems. It is important to place more effort into studying the recombination process in order to decrease the degree of PP and mP contamination in the upstream process. This will allow investments in simple, robust, and cost-effective purification strategies to obtain large amounts of pure sc mcDNA and can promote the success of this molecule within the pharmaceutical industry for biomedical applications.

Scaling up currently available purification strategies still represents an increased cost and adds more variability for mcDNA manufacturing due to the use of very specific ligands, backbone modifications, and enzyme digestion, along with time consumption and underachieved yields. More validation and reproducibility assays regarding the preparation of these methods and their use in different mcDNA samples should be performed. This will assure the development of suitable and robust techniques that can be applied to different types of mcDNA. Improvements to these strategies should be coupled with the study of faster, cheaper, and more sensitive techniques for mcDNA quality control. It could be interesting to explore emerging techniques, such as aqueous two-phase systems or microfluidic devices, in the extraction, isolation, or even detection of mcDNA. Once mcDNA mechanisms have become well understood and strategies for manufacturing it have been widely implemented, mcDNA can replace pDNA as the most popular non-viral DNA vector for clinical assays.

Acknowledgments

This work was supported by FEDER funds through the POCI – COMPETE 2020 – Operational Programme Competitiveness and Internationalization in Axis I – Strengthening research, technological development, and innovation (project POCI-01-0145-FEDER-007491) and National Funds by FCT – Foundation for Science and Technology (project UID/Multi/00709/2019). Also, A.M.A acknowledges a doctoral fellowship (SFRH/BD/102284/2014) from FCT.

[1]CICS-UBI – Health Sciences Research Centre, University of Beira Interior, Av. Infante D. Henrique, 6200-506 Covilhã, Portugal

*Correspondence:
angela@fcsaude.ubi.pt (Â. Sousa).

https://doi.org/10.1016/j.tibtech.2020.04.008

References

1. Foldvari, M. *et al.* (2016) Non-viral gene therapy: gains and challenges of non-invasive administration methods. *J. Control. Release* 240, 165–190
2. Mayrhofer, P. *et al.* (2009) Use of minicircle plasmids for gene therapy. *Methods Mol. Biol.* 542, 87–104
3. Mayrhofer, P. *et al.* (2008) Minicircle-DNA production by site specific recombination and protein–DNA interaction chromatography. *J. Gene Med.* 10, 1253–1269
4. Hou, X.H. *et al.* (2015) Increasing the minicircle DNA purity using an enhanced triplex DNA technology to eliminate DNA contaminants. *Mol. Ther. Methods Clin. Dev.* 1, 14062
5. Alves, C.P.A. *et al.* (2016) Development of a nicking endonuclease-assisted method for the purification of minicircles. *J. Chromatogr. A* 1443, 136–144
6. Alves, C.P.A. *et al.* (2018) Production and purification of supercoiled minicircles by a combination of *in vitro* endonuclease nicking and hydrophobic interaction chromatography. *Hum. Gene Ther. Methods* 29, 157–168
7. Silva-Santos, A.R. *et al.* (2019) Multimodal chromatography of supercoiled minicircles: a closer look into DNA–ligand interactions. *Sep. Purif. Technol.* 212, 161–170
8. Diamantino, T. *et al.* (2016) Minicircle DNA purification using a CIM® DEAE-1 monolithic support. *J. Sep. Sci.* 39, 3544–3549

9. Almeida, A.M. *et al.* (2019) Minicircle DNA purification: performance of chromatographic monoliths bearing lysine and cadaverine ligands. *J. Chromatogr. B Anal. Technol. Biomed. Life Sci.* 1118–1119, 7–16
10. Almeida, A.M. *et al.* (2020) The use of size-exclusion chromatography in the isolation of supercoiled minicircle DNA from *Escherichia coli* lysate. *J. Chromatogr. A* 1609, 460444
11. Almeida, A.M. *et al.* (2020) Quality assessment of supercoiled minicircle DNA by cadaverine-modified analytical chromatographic monolith. *J. Pharm. Biomed. Anal.* 180, 113037
12. Schmeer, M. *et al.* (2017) Plasmid DNA manufacturing for indirect and direct clinical applications. *Hum. Gene Ther.* 28, 856–861
13. Gaspar, V. *et al.* (2015) Minicircle DNA vectors for gene therapy: advances and applications. *Expert. Opin. Biol. Ther.* 15, 353–379
14. Gaspar, V.M. *et al.* (2014) Improved minicircle DNA biosynthesis for gene therapy applications. *Hum. Gene Ther. Methods* 25, 93–105
15. Šimčíková, M. *et al.* (2016) Improvement of DNA minicircle production by optimization of the secondary structure of the 5′-UTR of ParA resolvase. *Appl. Microbiol. Biotechnol.* 100, 6725–6737

CHAPTER II

Global aims

Considering the impact of Human Papillomavirus (HPV) infection has in our society, especially in the development of cervical cancer, the global aim of this thesis is to explore different therapeutic strategies that could potentially be used on the treatment of HPV infection. Such aim will rely on the implementation of two different biotechnological platforms for the production and purification of a DNA vaccine and a silencing gene therapy. Also, the assessment of the therapeutic potential displayed by these systems, coupled with the optimization of the transfection conditions to maximize such therapeutic potential, will be performed. While the DNA vaccine will be based on a pDNA molecule encoding E6 and E7 antigens and delivered to dendritic cells into a calcium carbonate system coupled with gelatin, the silencing strategy will be carried out with innovative minicircle DNA non-viral vector. Considering the newfound role of miR-375 in silencing E6 and E7 transcripts, pri-miR-375 gene will be inserted into a mcDNA vector and its effect in E6 and E7 protein will be assessed. Nonetheless, suitable downstream strategies for mcDNA processing will be explored and assessed to guarantee the optimized preparation of this innovative vector.

Thus, to accomplish the proposed aims, the following tasks should be carried out:

1 – Analysis of the impact that vector purity might present in the therapeutic outcome of the DNA vector through the comparison of E6 and E7 *in vitro* expression displayed by the DNA vaccine purified by two different methodologies.
2 – Development and characterization of suitable nanocarriers to deliver the DNA vaccine to cells by exploring the formulation of calcium carbonate systems coupled with gelatin and assessing its ability to deliver DNA vaccine to dendritic cells.
3 – Study of different chromatographic matrices to appropriately purify mcDNA in its supercoiled isoform accordingly with the purity specifications imposed by regulatory agencies, resorting to affinity chromatography and size-exclusion chromatography.
4 – Implementation of an analytical chromatographic method able to characterize mcDNA content in a complex sample, to further decrease costs associated with downstream mcDNA processing, by exploring cadaverine-modified monolith performance as an analytical technique.
5 – Construction of mcDNA vector able to express miR-375 to evaluate the effect presented by this vector in silencing E6 and E7 proteins upon transfection of cervical cancer cell line infected by HPV.

CHAPTER III

Paper III

HPV-16 targeted DNA vaccine expression: the role of purification

A.M. Almeida, J. Tomás, P. Pereira, J.A. Queiroz, F. Sousa, A. Sousa

CICS-UBI – Centro de Investigação em Ciências da Saúde, Universidade da Beira Interior, Av. Infante D. Henrique, 6200-506 Covilhã, Portugal

Biotechnology Progress 34: 546-551

Short description: An original research paper focusing the comparison between differently purified DNA vaccine samples in the expression of target E6 and E7 antigens

AIChE

HPV-16 Targeted DNA Vaccine Expression: The Role of Purification

Ana M. Almeida
CICS-UBI – Centro de Investigação em Ciências da Saúde, Universidade da Beira Interior, Av. Infante D. Henrique, Covilhã 6200-506, Portugal

Joana Tomás
CICS-UBI – Centro de Investigação em Ciências da Saúde, Universidade da Beira Interior, Av. Infante D. Henrique, Covilhã 6200-506, Portugal

Patrícia Pereira
CICS-UBI – Centro de Investigação em Ciências da Saúde, Universidade da Beira Interior, Av. Infante D. Henrique, Covilhã 6200-506, Portugal

João A. Queiroz
CICS-UBI – Centro de Investigação em Ciências da Saúde, Universidade da Beira Interior, Av. Infante D. Henrique, Covilhã 6200-506, Portugal

Fani Sousa
CICS-UBI – Centro de Investigação em Ciências da Saúde, Universidade da Beira Interior, Av. Infante D. Henrique, Covilhã 6200-506, Portugal

Ângela Sousa
CICS-UBI – Centro de Investigação em Ciências da Saúde, Universidade da Beira Interior, Av. Infante D. Henrique, Covilhã 6200-506, Portugal

DOI 10.1002/btpr.2603
Published online January 19, 2018 in Wiley Online Library (wileyonlinelibrary.com)

DNA vaccines have come to light in the last decades as an alternative method to prevent many infectious diseases, but they can also be used for the treatment of specific diseases, such as cervical cancer caused by Human Papillomavirus (HPV). This virus produces E6 and E7 oncoproteins, which alter the cell cycle regulation and can interfere with the DNA repairing system. These features can ultimately lead to the progression of cervical cancer, after cell infection by HPV. Thus, the development of a DNA vaccine targeting both proteins arises as an interesting option in the treatment of this pathology. Nonetheless, before evaluating its therapeutic potential, the purity levels of a biopharmaceutical must meet the regulatory agency specifications. Previously, our research group successfully purified the supercoiled isoform of the recombinant HPV-16 E6/E7 DNA vaccine with virtual 100% purity by affinity chromatography. The present work was designed to evaluate the effect that pDNA sample purity levels may exert in the expression of a target protein. Thus, in vitro studies were performed to assess the vaccine ability to produce the target proteins and to compare the expression efficiency between the pDNA sample obtained by affinity chromatography, which only presents the sc isoform and fulfils the regulatory agency recommendations, and the same DNA vaccine retrieved by a commercial purification kit, which contains different pDNA isoforms. Our achievements suggest that the E6/E7 DNA vaccine purified by affinity chromatography promotes higher E6 and E7 mRNA and protein expression levels than the DNA vaccine purified with the commercial kit. Overall, these results underline the importance that a purification strategy may present in the therapeutic outcome of recombinant DNA vaccines, envisaging their further application as biopharmaceuticals. © 2018 American Institute of Chemical Engineers *Biotechnol. Prog.*, 34:546–551, 2018
Keywords: affinity chromatography, HPV16 E6/E7 DNA vaccine, supercoiled pDNA isoform, protein expression

Introduction

Human Papillomavirus (HPV) is a sexually transmitted virus highly known for its tumorigenic role in cervical cancer development and progress. So far, over 100 subtypes have been identified, each presenting different outcome in infection and disease development. The different subtypes can be classified by either low, probable high-risk and high risk, accordingly to its ability to induce cancer.[1] HPV DNA has been found in a range of 77.2 to 100% of invasive

Correspondence concerning this article should be addressed to A. Sousa at angela@fcsaude.ubi.pt.

cervical cancer cases worldwide, to which 70% are estimated to be associated with high risk subtypes HPV-16 and HPV-18.[1–3] Both subtypes have been subjected to an intensive study in the past decades with the intent of unravelling the pathways by which infection and carcinogenesis are induced. E6 and E7 proteins were identified as the major contributors to the development of a cancer disease state in HPV-infected cells, due to its inhibitory role over tumor suppressor proteins p53 and pRB, respectively.[4,5] These oncoproteins are responsible for modulating keratinocyte differentiation, and stimulating cell proliferation and survival.[4] As a matter of fact, the ability of both proteins to interfere with the cell cycle proliferation mechanisms is correlated with the low to high risk classification of the different existing HPV subtypes.[5]

DNA vaccines arise as an immunological therapeutic approach whose popularity has increased in the past years, presenting many advantages when compared to conventional vaccines. While conventional vaccines are only able to trigger an immune response mediated by T helper cells, preventing the intended infection through antibody production, DNA vaccines can induce different immune responses, which culminate in a preventive and therapeutic effect against the infection, once they also stimulate CD8+ T cells.[6] Considering the importance of E6 and E7 HPV oncoproteins in the induction of invasive cervical cancer, the selection of both proteins as antigens for the implementation of a new immunotherapy method seems the next logical step in cervical cancer treatment.

To accomplish this, improved biotechnological processes are required to obtain highly pure and effective DNA vaccines. Affinity chromatography is a purification technique that takes advantage of different naturally occurring interactions between a ligand and a target biomolecule, allowing its isolation and purification. This procedure becomes essential in the development of new biopharmaceuticals, as its production must comply with several specifications, to be safely considered for therapeutic administration. Regarding plasmid DNA (pDNA), the supercoiled (sc) conformation is not only the most produced isoform by *Escherichia coli* (*E.coli*), as it is also responsible for a more pronounced and desired biological function, providing greater transfection and gene expression rates than other isoforms.[7] Thereby, the isolation of sc isoform from other less-effective pDNA topologies, such as open circular (oc), and from bacterial components is extremely important to enhance the transfection rate as well as the effectiveness and biosafety for therapeutic administration.

In the past few years, our research group has been focused on the production and purification of the recombinant pDNA vaccine encoding E6 and E7 HPV16 oncoproteins.[8–10] Thereby, the main purpose of this work was to conduct a differential *in vitro* comparison study to assess the expression of E6 and E7 proteins, resorting to the transfection of mammalian cells with pDNA samples obtained by different methods. For this, it was our interest to compare a pDNA with 100% sc isoform homogeneity obtained with arginine monolith with a native pDNA sample, containing oc and sc isoform, retrieved by a commercial anion-exchange purification kit. First, cell live imaging was performed to follow the pDNA entry into the cell and nucleus. Subsequently, to further comprehend the ability of these different pDNA samples to correctly express the intended oncoproteins, real-time quantitative polymerase chain reaction (RT-qPCR) and immunocytochemistry techniques were performed for the detection of E6 and E7 transcripts and proteins, respectively.

Materials and Methods

Bacterial growth and pDNA isolation

HPV-16 E6/E7 pDNA (plasmid 8641 from Addgene, Cambridge, MA)[11] was amplified through *E. coli* DH5α culture, as previously described.[10] To obtain the native pDNA sample (containing oc and sc isoform), NZYMaxiprep commercial kit (NZYTech, Lisbon, Portugal) was used accordingly to the manufacturer's instructions. Several extractions were performed and homogenized before transfections for more reliable results. For affinity chromatographic experiments, a complex pDNA sample was isolated by resorting to the modified alkaline lysis method.[12] Then, concentration and clarification of the resulting sample was carried out as described by Diogo et al.[13] Finally, ammonium sulfate present in the supernatant was removed from the sample using PD-10 desalting columns (GE Healthcare, Buckinghamshire, UK) according to manufacturer's instructions.

Affinity chromatography and purity assessment

All chromatographic experiments were carried out using an AKTA Püre system (GE Healthcare, Buckinghamshire, UK), a compact separation unit and a personal computer with UNICORN™ 6.3 software. The arginine monolith used for pDNA separation was prepared and kindly provided by BIA Separations (Ajdovščina, Slovenia). The purification strategy was previously developed and optimized by our research group.[8,10] All chromatographic peak fractions were collected, concentrated, and desalted by Vivaspin® 6 Centrifugal Concentrator (Vivaproducts, Littleton, MA), at 800 g for further analysis and experiments. The evaluation of purity and recovery was carried out resorting to CIMac™ analytical column, as described by Sousa et al.[14] In similarity to native pDNA preparation, several purified sc pDNA samples were homogenized before transfection.

Cell culture and transfection

Mouse Fibroblasts and Chinese hamster ovary (CHO) cells were cultured in Dulbecco's Modified Eagle Medium-F12 High Glucose supplemented with 10% (v:v) of fetal bovine serum (FBS) and a mixture of penicillin (100 μg/mL) and streptomycin (100 μg/mL). Cells were seeded at 2×10^5 cellscper well and grown at 37°C in a humidified atmosphere with 5% of CO_2 in 12-well plates for equal time in each experiment, until reaching an 80–90% confluence. Then, cells were incubated with medium without antibiotic and FBS for 24 h. Cells transfection with native and sc pDNA samples was performed with Lipofectamine 2000 (Invitrogen, Life Technology) transfection reagent, accordingly to the manufacturer's protocol. On transfection, cells were cultured for 24, 48, and 72 h to perform RNA extraction and analysis or immunocytochemistry. For each technique, three independent transfections were performed ($N = 3$).

Live cell imaging

Fibroblasts cells were grown in μ-slide 8 well (Ibidi, Martinsried, Germany) until 80–90% confluence was reached. Before transfection, the purified sc pDNA sample was labeled with fluorescein isothiocyanate isomer I (FITC, Invitrogen, Life Technology). Briefly, FITC was prepared with

sterile anhydrous dimethyl sulfoxide (500 mg/mL) and added to a reaction mixture containing labeling buffer (0.1 M Sodium Tetraborate, pH = 8.5), deionized water and sc pDNA, followed by 4 h incubation at room temperature in a shaker oscillating at low speed. The resulting FITC-labeled pDNA was encapsulated with Lipofectamine 2000 and real live transfection was visualized using a LSM710 confocal laser scanning microscope (Carl Zeiss, Germany) under a 63× magnification and analyzed with the Zeiss LSM 710 laser scanning confocal microscope (Carl Zeiss SMT, Inc., Oberkochen, Germany) Throughout this experiment, cells were maintained at 37°C with 5% of CO_2.

E6 and E7 mRNA expression detection by RT-qPCR

Total RNA extraction was performed with TripleXtractor reagent (Grisp Research Solutions, Porto, Portugal), following the manufacturer's instructions. RNA quantification was performed by spectrophotometry at 260 nm and its integrity assessed by agarose gel electrophoresis (data not shown). 1μg of total RNA was reversed transcribed into cDNA with the RevertAid First Strand cDNA Synthesis Kit (Thermo Scientific, Molecular Biology), according to the manufacturer's instructions. RT-qPCR reactions were performed with 1 μL cDNA in a final volume of 20 μL with the Maxima SYBR Green/Fluorescein qPCR Master Mix (2×) (Thermo Scientific, Molecular Biology) and 0.3 μM of each primer in a CFX Connect Real-time System (Bio-Rad Laboratories, Hercules, CA). Primers were designed specifically for E6 (Fw: 5′-CAGGAGCGAAGAAAGCCCTT-3′, Rv: 5-ATAGTCTACCAGCTCACGTCGT-3) and E7 (Fw: 5′-TCCACAAGCAGCTGGACCGGA-3′, Rv: 5′-GCACACA-ATTCCTGTTAGGCCCAT-3′). GADPH (Fw: 5′-TGACGTGCCGCCTGGAGAAA-3′, Rv: 5′-AGTGTAGC-CGCCCAAGATCAGCTT-3′) was used as the housekeeping gene. Cycling parameters were: denaturation at 95°C for 3 min; 35 cycles of denaturation at 95°C for 30 s, annealing at 60°C for 30 s and extension at 72°C for 30 s. Relative quantification was performed based on the comparative threshold cycle (C_T) method, in which the amount of the target was determined to be $2^{-(\Delta CT\ \text{target} - \Delta CT\ \text{calibrator})}$ normalized to levels of GADPH and relative to the native pDNA transfected cells.

Immunocytochemistry

CHO cells were cultured in 12-well plates with glass coverslips. Transfection protocol was performed, as previously described, with sc and native pDNA. Immunocytochemistry protocol was performed 72 h after transfection.[15] Mouse anti-E6 IgG monoclonal antibody sc-460 or mouse anti-E7 IgG monoclonal antibody sc-6981 (Santa Cruz Biotechonology, Heidelberg, Germany) were used (1:50). Alexa 488 goat anti-mouse and Alexa goat anti-mouse 546 (Life Technologies, CA, United States of America) were applied for E6 or E7 primary antibody stained cells, respectively. Coverslips were placed on glass slides and analyzed using a Zeiss LSM 710 laser scanning confocal microscope (Carl Zeiss SMT, Inc., Oberkochen, Germany) under a 63× amplification with the Zeiss Zen software (2010). Immunofluorescence analysis was performed with ImageJ 1.48u software. Statistical analysis was performed with GraphPad Prism version 6.04 trial software.

Results and Discussion

Non-viral DNA vectors have been studied for safe and alternative treatments of several diseases. However, soon it was perceived that many factors could interfere with the expression of the target molecule, leading to a decay of its therapeutic effect.[16] The elimination of impurities resultant from the production of these biopharmaceuticals in the recombinant host, such as gDNA, endotoxins, and other biomolecules is mandatory, because these impurities may restrict the transfection efficiency by inducing toxicity and secondary effects such as inflammation, septic shock and organ failure.[17–20] Conversely, sc pDNA is more compact than other pDNA isoforms, resulting in higher ability to penetrate the eukaryotic cell membrane, and does not present any structural damage that might impair the expression cassette functioning. Thereby, the sc molecule is considered more biologically active than other isoforms, such as oc or linear,[7] and regulatory agencies have established that recombinant DNA used for therapy should present at least 97% of sc pDNA content. Thus, the lack of impurities coupled with the increased sc homogeneity can contribute to higher expression efficiency.

To answer this challenge, our research group has spent the past years studying and developing purification strategies to isolate the sc pDNA, by exploiting its specific interaction with several amino acids, used as affinity ligands.[21] As a matter of fact, we were previously able to purify the sc isoform of the recombinant HPV-16 E6/E7 pDNA vaccine using an arginine monolith, based on a biorecognition mechanism toward sc pDNA.[8,10] In Figure 1A, it is presented the chromatogram of this approach and in the Figure 1B1 is the corresponding electrophoresis of the peak of interest, showing the sc pDNA isolated from other impurities, which were eliminated in the binding and washing steps. The use of arginine monolith allowed to develop a suitable purification strategy, by applying a smooth salt increasing step gradient for sc pDNA elution. With this strategy, 83% of sc pDNA was recovered with 100% virtual purity.[8] For comparison, in Figure 1B2 is depicted an electrophoresis of a pDNA sample retrieved by a commercial purification kit, presenting both sc and oc pDNA isoforms. Usually, the purification strategies available on the market are based on the use of anion-exchange chromatography. This approach relies on binding the target molecule to a ligand with opposite charge, allowing the fractionation of several molecules present in the sample by charge differences.[22] However, with this technique it is more difficult to separate molecules that present similar chemical and physical properties, for example the sc and oc pDNA isoforms.[21] Also, such commercial strategies make use of RNase enzyme for easier RNA elimination.[23] This impairs the use of such samples for therapeutic studies, as regulatory agencies do not allow the use of animal originated enzymes, to prevent harmful effects.[24]

Hence, *in vitro* comparative transfection studies were designed to assess the effect that overall pDNA purity can display in the expression of E6 and E7 proteins, and to prove the added value of this purification strategy in comparison to commercially available pDNA purification kits. Initially, and considering that the target DNA vaccine presents a significant size (7.9 kb) because it encodes two proteins, it was important to assess if the pDNA molecule can reach the cell nucleus. This study was accomplished using live cell imaging to follow the pDNA passage through the cell membrane

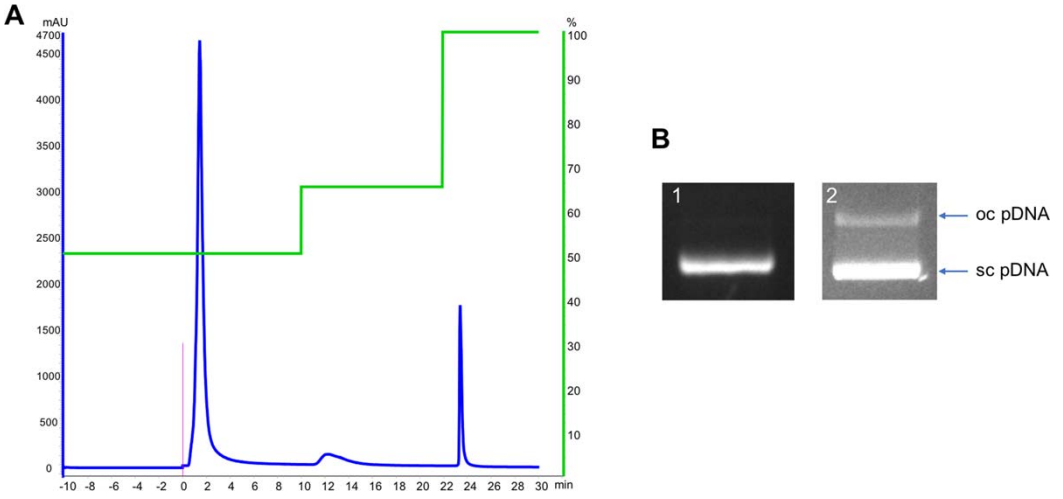

Figure 1. Purification of HPV 16 E6/E7 DNA vaccine by arginine monolith.

(A) Arginine monolith chromatogram performed with 501 mM NaCl in 10 mM Tris-EDTA (pH = 7.9) for binding step, 650 mM NaCl in 10 mM Tris-EDTA (pH = 7.9) for washing step and 1 M NaCl in 10 mM Tris-EDTA (pH = 7.9) for elution step. (B) Electrophoresis of different pDNA samples. 1 – sc pDNA sample purified by arginine monolith; 2 - pDNA sample purified by the commercial kit, presenting oc and sc isoforms.

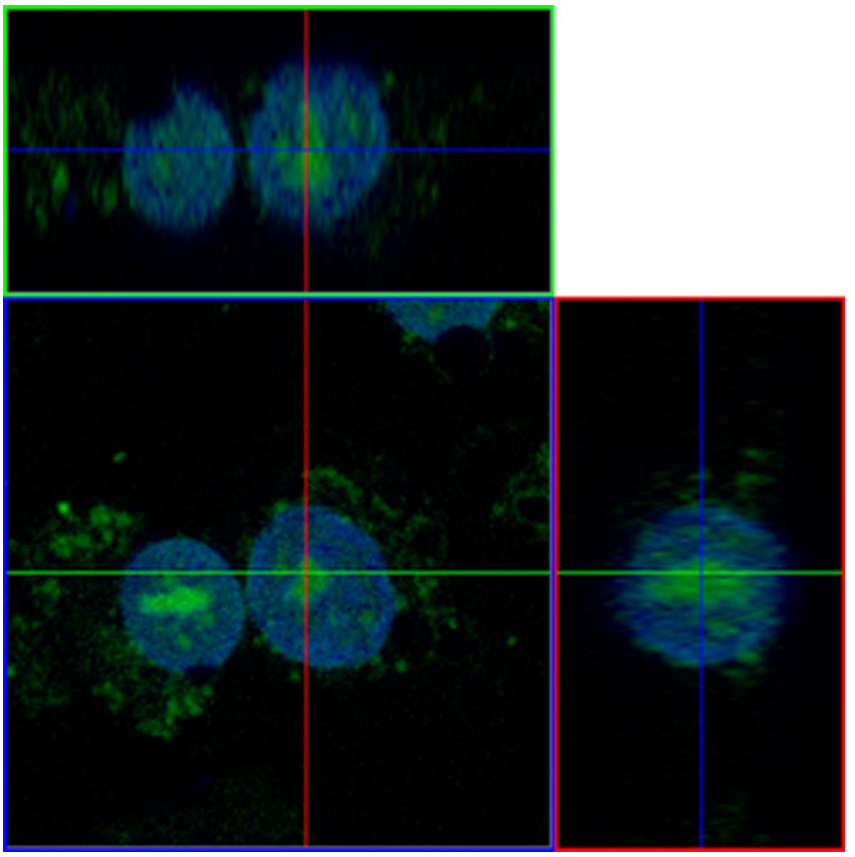

Figure 2. Orthogonal view of live cell imaging 1 h after pDNA complexes addition to fibroblasts cells.

The blue staining represents the cell's nucleus and the green staining represents FITC-labeled pDNA.

and the access to nucleus. Figure 2 presents an orthogonal view of cells 1 h after addition of the DNA-stained complexes. In this image, it is possible to identify FITC-labeled pDNA in the nucleus of fibroblasts suggesting that fibroblasts are transfected with the target sc pDNA vaccine, and that it enters the nucleus regardless of its larger size.

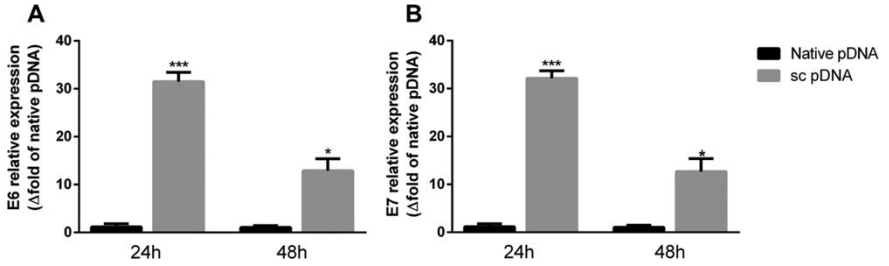

Figure 3. E6 (A) and E7 (B) mRNA relative expression between native and sc pDNA transfected cells, 24 and 48 h after transfection ($N = 3$, Unpaired *t*-test * $P < 0.05$; *** $P < 0.001$).

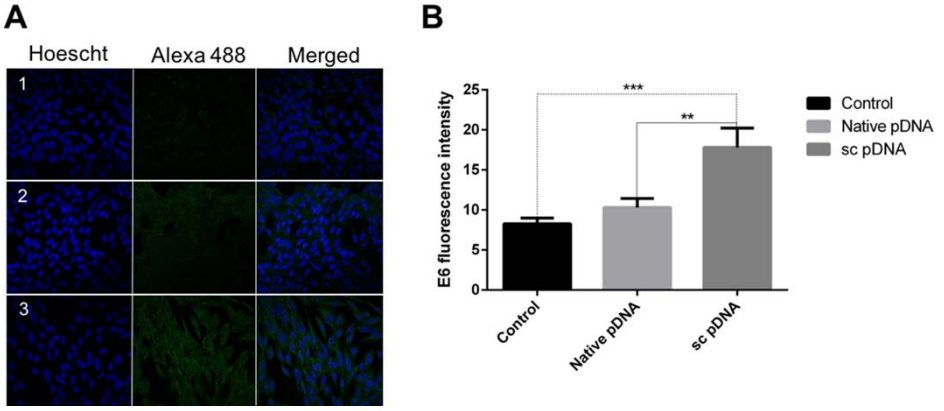

Figure 4. E6 protein levels analysis by immunofluorescence.

(A) CHO-1 cells immunocytochemistry images for E6 staining. 1: Control group; 2: native pDNA transfected cells; 3: sc pDNA transfected cells. (B) E6 protein immunofluorescence comparison between the different groups by one-way ANOVA test ($N = 3$, ** $P < 0.01$, *** $P < 0.001$).

Therefore, it was also inferred that these transfection conditions are suitable for further experiments.

E6 and E7 gene expression was evaluated, after cell transfection, to compare pDNA samples obtained with the two purification strategies: commercial kit and arginine monolith. As depicted in Figure 3A,B, RT-qPCR results revealed a significant difference in E6 and E7 expression in cells transfected with native pDNA (obtained with the commercial kit) and sc pDNA (obtained with Arg-monolith), both at 24 and 48 h. At these time points, sc pDNA transfected cells presented higher levels of E6 and E7 transcripts than native pDNA transfected cells, highlighting the importance of delivering highly pure sc pDNA. Such differences may be explained by the fact that oc isoform is damaged in comparison to sc isoform, presenting nicks in its structure that can interfere with important gene location, such as eukaryotic expression cassette genes.[25] Concomitantly, the damaging of this molecule leads to a more relaxed form, contributing to an increased size of the nanocarrier.[26] In addition, these results suggest that 24 h after transfection, the expression of both mRNA transcripts is higher than after 48 h, a pattern that it is usually associated with transient transfection, as the effect brought by transfected cells begins to dilute between cells newly originated by mitosis.[27]

Although these results strongly indicate that protein expression is higher in cells transfected with sc pDNA than cells transfected with native pDNA, mRNA translation into protein sometimes can be impaired by different mechanisms.[28] Therefore, to evaluate if the E6 and E7 protein levels follow the same tendency previously observed for mRNA, their quantification was performed using immunocytochemistry. In Figure 4A, it is portrayed the E6 fluorescent staining of non-transfected cells (control cells), and cells transfected with native and sc pDNA. According to these results, it can be perceived that cells transfected with sc pDNA present higher immunofluorescence (green staining) than the remaining samples. In Figure 4B, it is represented the total immunofluorescence quantification for E6 fluorescent staining of images taken from the different assays ($N = 3$, for each N were taken 5 images). As it can be observed, cells transfected with sc pDNA present immunofluorescence significantly higher than control cells and cells transfected with native pDNA for E6 protein staining, suggesting higher protein production levels and thus corroborating the results previously obtained for mRNA quantification. After confirming the sc pDNA ability to express higher levels of E6 protein than native pDNA, and given that this pDNA vector is expected to express both E6 and E7 proteins, immunocytochemistry was also performed, only for control and sc pDNA transfected cells, to verify E7 concomitant expression. As predicted, on quantification of total immunofluorescence it was verified that cells transfected with sc pDNA presented significantly higher immunofluorescence for E7 protein staining than control cells (data not shown). Overall, these results suggest that E6 and E7 mRNAs are being correctly translated into E6 and E7 proteins.

Altogether, HPV-16 E6/E7 pDNA vaccine provided the correct E6 and E7 protein expression. Also, a difference was observed regarding their expression levels when studying differently obtained pDNA samples. Actually, it was possible to verify that the pDNA biopharmaceutical purity is extremely important, affecting mRNA and protein expression levels. Confirmed the efficiency of the DNA vaccine at inducing E6 and E7 expression, in the future, *in vitro* and *in vivo* studies should be carried out to assess its ability to induce an immune response against the target proteins.

Acknowledgments

This work was supported by FEDER funds through the POCI - COMPETE 2020 - Operational Programme Competitiveness and Internationalization in Axis I - Strengthening research, technological development and innovation (Project POCI-01-0145-FEDER-007491) and National Funds by FCT - Foundation for Science and Technology (Project UID/Multi/00709/2013). A.M. Almeida and A. Sousa acknowledge doctoral and post-doctoral fellowships (SFRH/BD/102284/2014 and SFRH/BPD/102716/2014, respectively) from FCT. The authors also acknowledge to BIA Separations for the monolithic support and to Karl Münger for HPV-16 E6/E7 Addgene plasmid.

Literature Cited

1. Chelimo C, Wouldes TA, Cameron LD, Elwood JM. Risk factors for and prevention of human papillomaviruses (HPV), genital warts and cervical cancer. *J Infect.* 2013;66:207–217.
2. Rogovskaya SI, Shabalova IP, Mikheeva IV, Minkina GN, Podzolkova NM, Shipulina OY, Sultanov SN, Kosenko IA, Brotons M, Buttmann N, Dartell M, Arbyn M, Syrjänen S, Poljak M. Human papillomavirus prevalence and type-distribution, cervical cancer screening practices and current status of vaccination implementation in Russian Federation, the Western countries of the former Soviet Union, Caucasus region and Central Asia. *Vaccine.* 2013;31:H46–H58.
3. Bosch FX, Robles C, Diaz M, Arbyn M, Baussano I, Clavel C, Ronco G, Dillner J, Lehtinen M, Petry KU, Poljak M, Kjaer SK, Meijer CJ, Garland SM, Salmerón J, Castellsagué X, Bruni L, de Sanjosé S, Cuzick J. HPV-FASTER: broadening the scope for prevention of HPV-related cancer. *Nat Rev Clin Oncol.* 2016;13:119–132.
4. Roman A, Munger K. The papillomavirus E7 proteins. *Virology.* 2013;445:138–168.
5. Vande Pol SB, Klingelhutz AJ. Papillomavirus E6 oncoproteins. *Virology.* 2013;445:115–137.
6. Li L, Saade F, Petrovsky N. The future of human DNA vaccines. *J Biotechnol.* 2012;162:171–182.
7. Sousa F, Prazeres DM, Queiroz JA. Improvement of transfection efficiency by using supercoiled plasmid DNA purified with arginine affinity chromatography. *J Gene Med.* 2009;11:79–88.
8. Almeida AM, Queiroz JA, Sousa F, Sousa A. Optimization of supercoiled HPV-16 E6/E7 plasmid DNA purification with arginine monolith using design of experiments. *J Chromatogr B.* 2015;978–979:145–150.
9. Amorim LF, Sousa F, Queiroz JA, Cruz C, Sousa A. Screening of L-histidine-based ligands to modify monolithic supports and selectively purify the supercoiled plasmid DNA isoform. *J Mol Recognit.* 2015;28:349–358.
10. Soares A, Queiroz JA, Sousa F, Sousa A. Purification of human papillomavirus 16 E6/E7 plasmid deoxyribonucleic acid-based vaccine using an arginine modified monolithic support. *J Chromatogr A.* 2013;1320:72–79.
11. Munger K, Phelps WC, Bubb V, Howley PM, Schlegel R. The E6 and E7 genes of the human papillomavirus type 16 together are necessary and sufficient for transformation of primary human keratinocytes. *J Virol.* 1989;63:4417–4421.
12. Sambrook J, Fritsch EF, Maniatis T. *Molecular Cloning*, 2nd ed. Cold Spring Harbor, NY: Cold Spring Harbor Laboratory Press; 1989.
13. Diogo MM, Queiroz JA, Monteiro GA, Martins SA, Ferreira GN, Prazeres DM. Purification of a cystic fibrosis plasmid vector for gene therapy using hydrophobic interaction chromatography. *Biotechnol Bioeng.* 2000;68:576–583.
14. Sousa A, Almeida AM, Cernigoj U, Sousa F, Queiroz JA. Histamine monolith versatility to purify supercoiled plasmid deoxyribonucleic acid from Escherichia coli lysate. *J Chromatogr A.* 2014;1355:125–133.
15. Pereira PA, Tomas JF, Queiroz JA, Figueiras AR, Sousa F. Recombinant pre-miR-29b for Alzheimer s disease therapeutics. *Sci Rep.* 2016;6:19946.
16. Colosimo A, Goncz KK, Holmes AR, Kunzelmann K, Novelli G, Malone RW, Bennett MJ, Gruenert DC. Transfer and expression of foreign genes in mammalian cells. *BioTechniques.* 2000;29:314–318. 320-312, 324 passim.
17. Wei Z, Huang W, Li J, Hou G, Fang J, Yuan Z. Studies on endotoxin removal mechanism of adsorbents with amino acid ligands. *J Chromatogr B.* 2007;852:288–292.
18. Wooddell CI, Subbotin VM, Sebestyen MG, Griffin JB, Zhang G, Schleef M, Braun S, Huss T, Wolff JA. Muscle damage after delivery of naked plasmid DNA into skeletal muscles is batch dependent. *Hum Gene Ther.* 2011;22:225–235.
19. Magalhaes PO, Lopes AM, Mazzola PG, Rangel-Yagui C, Penna TC, Pessoa A Jr. Methods of endotoxin removal from biological preparations: a review. *J Pharm Pharm Sci.* 2007;10:388–404.
20. Bazzani RP, Cai Y, Hebel HL, Hyde SC, Gill DR. The significance of plasmid DNA preparations contaminated with bacterial genomic DNA on inflammatory responses following delivery of lipoplexes to the murine lung. *Biomaterials.* 2011;32:9854–9865.
21. Sousa F, Prazeres DM, Queiroz JA. Affinity chromatography approaches to overcome the challenges of purifying plasmid DNA. *Trends Biotechnol.* 2008;26:518–525.
22. Matos T, Queiroz JA, Bulow L. Binding and elution behavior of small deoxyribonucleic acid fragments on a strong anion-exchanger multimodal chromatography resin. *J Chromatogr A.* 2013;1302:40–44.
23. Koontz L. Explanatory chapter: how plasmid preparation kits work. *Methods Enzymol.* 2013;529:23–28.
24. Prazeres DMF. Considerations on the use of enzymes in the downstream processing of biopharmaceuticals. *Pharma Bioprocess.* 2016;4:95–99.
25. Urthaler J, Schuchnigg H, Garidel P, Huber H. Industrial manufacturing of plasmid-DNA products for gene vaccination and therapy. In: Thalhamer J, Weiss R, Scheiblhofer S, editors. *Gene Vaccines.* Vienna, Austria: Springer Vienna; 2012:311–330.
26. Dhanoya A, Chain BM, Keshavarz-Moore E. Role of DNA topology in uptake of polyplex molecules by dendritic cells. *Vaccine.* 2012;30:1675–1681.
27. Al-Dosari MS, Gao X. Nonviral gene delivery: principle, limitations, and recent progress. *AAPS J.* 2009;11:671–681.
28. Roy B, Jacobson A. The intimate relationships of mRNA decay and translation. *Trends Genet.* 2013;29:691–699.

Manuscript received Sep. 14, 2017, and revision received Nov. 23, 2017.

Paper IV

Enhancement of a biotechnological platform for the purification and delivery of a human papillomavirus supercoiled plasmid DNA vaccine

A.M. Almeida, D. Costa, A.R. Simões, J.A. Queiroz, F. Sousa, A. Sousa

CICS-UBI – Centro de Investigação em Ciências da Saúde, Universidade da Beira Interior, Av. Infante D. Henrique, 6200-506 Covilhã, Portugal

New Biotechnology (2020) 59: 1-9

Short description: An original research paper focusing a new chromatographic strategy for DNA vaccine purification and the development of suitable nanocarriers for DNA vaccine delivery to dendritic cells

New BIOTECHNOLOGY 59 (2020) 1–9

Contents lists available at ScienceDirect

New BIOTECHNOLOGY

journal homepage: www.elsevier.com/locate/nbt

Full length Article

Enhancement of a biotechnological platform for the purification and delivery of a human papillomavirus supercoiled plasmid DNA vaccine

Ana M. Almeida, Diana Costa, Ana R. Simões, João A. Queiroz, Fani Sousa, Ângela Sousa*

CICS-UBI – Health Sciences Research Centre, University of Beira Interior, Av. Infante D. Henrique, 6200-506 Covilhã, Portugal

ARTICLE INFO

Keywords:
Arginine monolith
Biotechnological platform
$CaCO_3$ nanoplexes
DNA vaccine
Spacer arm
Supercoiled plasmid DNA

ABSTRACT

New biotechnological strategies are being explored, aimed at rapid and economic manufacture of large quantities of DNA vaccines with the required purity for therapeutic applications, as well as their correct delivery as biopharmaceuticals to target cells. This report describes the purification of supercoiled (sc) HPV-16 E6/E7 plasmid DNA (pDNA) vaccine from a bacterial lysate, using an arginine-based monolith, presenting a spacer arm in its configuration. To enhance the performance of the purification process, monolith modification with the spacer arm can improve accessibility of the arginine ligand. By using a low NaCl concentration at pH 7.0, a condition to eliminate the RNA impurity directly in the flow through was established. The pH increase to 7.5 allowed the elimination of non-functional pDNA isoforms, the sc pDNA being recovered by increasing the ionic strength. As well as a binding capacity of 2.53 mg/mL obtained with a pre-purified sc pDNA sample, the column also purified sc pDNA from high lysate loading, with capacities above 1 mg/mL. Due to the sample displacement phenomena, non-functional pDNA isoforms were eliminated throughout column loading, favoring the degree of purity of final sc pDNA of 93.3%–98.5%. Thereafter, purified sc pDNA was successfully encapsulated into $CaCO_3$-gelatin nano-complexes. Delivery of the pDNA-carriers to THP-1 cells was assessed through pDNA cellular uptake evaluation and correct E6 expression was verified by mRNA and protein detection. A biotechnological platform was established for sc pDNA purification and delivery to dendritic cells, stimulating further *in vivo* studies.

Introduction

Human papillomavirus (HPV) infection is a widespread sexually transmitted disease, that can ultimately lead to different cancer types [1,2]. Cancer progression is caused by expression of the E6 and E7 oncoproteins, which are responsible for viral replication and host cell transformation and immortalization [3]. Popularity of plasmid DNA (pDNA) vaccines for treatment of HPV infection has increased exponentially, due to their dual role as a preventive and therapeutic approach for cancer treatment, as well their safety, lack of toxicity, simple manufacture and application of this biomolecule compared to conventional prophylactic vaccines [4–6]. Nevertheless, some of the currently employed plasmid purification techniques involve multiple chromatographic steps, leading to low recoveries and high operating costs. For instance, three chromatographic procedures (ion exchange chromatography, hydrophobic interaction chromatography and size exclusion chromatography) were employed sequentially for the purification of large amounts of a pharmaceutical-grade pDNA with a global recovery yield of 48 % [7]. Hence, efficient purification strategies are essential to maximize the purity and recovery of pDNA vaccines and minimize manufacturing costs.

Convective interaction media (CIM®) monoliths are innovative chromatographic supports, suited to fast purification of large biomolecules due to continuous and highly porous beds with interconnected network channels, which confer high dynamic binding capacity (DBC) and good mass transfer properties to the support [8]. However, the success of pDNA purification mostly depends on selectivity towards the target biomolecule and the interactions promoted by the ligands immobilized on the chromatographic supports. Affinity chromatography exploits the selective biorecognition of target biomolecules by specific

Abbreviations: arg-spacer, arginine with a spacer arm; CIM, convective interaction media; DBC, dynamic binding capacity; DLS, dynamic light scattering; ECF, enhanced chemifluorescence; EE, encapsulation efficiency; FITC, fluorescein isothiocyanate isomer I; HPV, human papillomavirus; MCPBA, 2-chlorometaperoxybenzoic acid; oc, open circular; gDNA, genomic DNA; pDNA, plasmid DNA; sc, supercoiled; RT, retention time; SEM, scanning electron microscopy; SP, streptomycin/penicillin; TEM, transmission electron microscopy; Tris-EDTA, 10 mM Tris-HCl and 10 mM EDTA

* Corresponding author.
E-mail address: angela@fcsaude.ubi.pt (Â. Sousa).

https://doi.org/10.1016/j.nbt.2020.04.003
Received 26 March 2019; Received in revised form 30 March 2020; Accepted 13 April 2020
Available online 02 July 2020

ligands based on their biological function or chemical structure [8,9]. Amino acids have been often used as ligands, since they are natural and safe compounds that promote specific interactions with nucleic acids [9]. The immobilization of these ligands or derivatives in monolithic supports has been demonstrated to be a successful combination for pDNA purification [8,10,11]. The performance of histidine-, histamine- and agmatine-based monoliths was dependent on the use of harsh binding and elution conditions, such as acid pH and high ammonium sulphate concentrations, which can represent an economic and environmental impact when applied industrially. Arginine monolith have allowed the isolation of supercoiled (sc) pDNA under mild ionic conditions, with recovery improved from 39 % to 83.5 % by using an experimental design tool [12]. The present work takes advantage of the versatility of the monolithic support and selectivity and specificity of the arginine ligand, to evaluate the impact of ligand accessibility, due to the presence of a spacer arm, on establishing additional interactions. The influence of spacer arm in the arginine modified monolith was explored in sc HPV-16 E6/E7 pDNA vaccine purification from 200 µL of *Escherichia coli* lysate, by manipulating the salt concentration and pH of the elution buffer. Column performance in sc pDNA purification from a loading of 68 mL of lysate was also tested. Purity and recovery of sc pDNA obtained by different loading approaches were evaluated. The dynamic binding capacity (DBC) of the arginine monolith with a spacer arm (arg-spacer monolith) was determined by using a pre-purified sc pDNA sample.

Although sc pDNA content has been shown to influence target gene expression highly [13], the formulation of pDNA in specific delivery systems can also affect its therapeutic outcome [14]. After successful sc pDNA purification, pDNA-$CaCO_3$-gelatin formulations were prepared to deliver the DNA vaccine to dendritic cells. $CaCO_3$-gelatin nanoplexes were characterized by scanning electron microscopy (SEM) and transmission electron microscopy (TEM). The size and zeta-potential of the nanoplexes were also evaluated, alongside the pDNA encapsulation efficiency (EE). To determine the $CaCO_3$-gelatin carrier ability to transfect cells and direct the pDNA to the nucleus, THP-1 cells were transfected, cellular uptake of pDNA was assessed, and mRNA and protein expression evaluated.

Material and methods

Bacterial growth conditions

The HPV-16 E6/E7 plasmid (plasmid 8641) was purchased from Addgene (Cambridge, USA) [15] and amplified through *E. coli* DH5α fermentation, as described elsewhere [12].

Sample preparation

The lysate sample was obtained using the modified alkaline lysis method [16] and the supernatant was prepared as previously described [17]. The final sample was desalted by passing through PD-10 desalting columns (GE Healthcare, Uppsala, Sweden), following the manufacturer's instructions and applying 10 mM Tris-HCl and 10 mM EDTA buffer (Tris-EDTA buffer), pH 8.0. The pre-purified pDNA sample was prepared with the NZYMaxiprep commercial kit from NZYTech (Lisbon, Portugal), according to manufacturer's instructions.

Affinity chromatography

All chromatographic experiments were performed on an AKTA Pure system (GE Healthcare Biosciences Uppsala, Sweden) and Unicorn 6.3 software. Four epoxy monoliths, (i) non-modified, (ii) modified with 2-allyloxyethanol spacer arm, (iii) modified with arginine and (iv) modified with 2-allyloxyethanol spacer arm and arginine, 0.34 mL column bed volume, were kindly prepared and provided by BIA Separations (Ajdovščina, Slovenia). Spacer arm immobilization was performed by washing two epoxy monoliths with 3 mL of 1,4-dioxane reagent using a syringe and further incubating with the same reagent for 2 h at room temperature. Each monolith was inserted into a housing and rinsed with 3 mL of 2-allyloxyethanol solution (4 mL 2-allyloxyethanol + 0.2 mL BF_3xEt_2O dissolved in 10 mL 1,4-dioxane), with subsequent incubation in the same solution for 2 h at 30 °C. Each disk was then rinsed with 2-chlorometaperoxybenzoic acid (MCPBA) solution (5.151 g MCPBA in 15 mL of 1,4-dioxane) and incubated in the same solution for 24 h at 60 °C. Finally, the disks modified with the 2-allyloxyethanol spacer arm were washed with 1,4-dioxane. One of the monoliths was used for arginine immobilization by pumping an arginine solution (4 g arginine, 16 mL H_2O, 0.64 mL HCl) and subsequent incubation for 48 h at 60 °C. Both monoliths were washed with water and 0.5 M H_2SO_4 to deactivate the remaining epoxy groups. To assess ionic density of arg-spacer and arginine modified monoliths, the protocol implemented in [18] was used. To characterize the chromatographic behavior of each monolith with a pre-purified pDNA sample, linear gradients were performed with decreasing $(NH_4)_2SO_4$ concentration from 3 M to 0 M (hydrophobic elution conditions) or increasing the NaCl concentration from 0 to 3 M (ionic elution conditions) in Tris-EDTA, pH 8.0, during 15 min.

Several elution strategies were explored with the arg-spacer monolith, by increasing the NaCl concentration and pH manipulation from 7 to 9, to determine the optimal conditions for sc pDNA isolation. Thus, sc pDNA purification was achieved after equilibrating the arg-spacer monolith at 680 mM NaCl in Tris-EDTA, pH 7.0, injection of 200 µL (7.2 µg of pDNA/mL) of lysate sample and two elution steps by increasing pH to 7.5, maintaining the NaCl concentration (680 mM NaCl in Tris-EDTA buffer, pH 7.5) and then increasing the NaCl concentration to 1 M maintaining the pH (1 M NaCl in Tris-EDTA, pH 7.5), at 1 mL/min.

Purification of sc pDNA was also conducted with the arg-spacer monolith with larger volumes of lysate sample.The column was equilibrated as previously described and overloaded with 68 mL of lysate sample (5 µg of pDNA/mL), prepared in the same buffer. All experiments were carried out at room temperature and absorbance was constantly monitored at 260 nm. Fractions were concentrated and desalted with 3 mL Tris-EDTA in Vivaspin® 6 Centrifugal Concentrator (Vivaproducts, Littleton, MA, USA) cut-off 10,000 MW, at 1000 g.

Agarose gel electrophoresis

Samples were analyzed by horizontal electrophoresis in a 15 cm long 0.8 % agarose gel (Hoefer, Holliston, MA, USA) and stained with 0.012 µL/mL greensafe (NZYTech, Lisbon, Portugal) as previously described [12].

Plasmid DNA quantification

The sc pDNA purity and recovery evaluation was carried out with CIMac™ pDNA analytical column, by applying a modified analytical method [18].

Dynamic binding capacity

Capacity experiments were carried out at 1 mL/min and a pDNA concentration of 0.05 mg/mL. The arg-spacer column was equilibrated with Tris-EDTA, pH 8.0 and overloaded with the plasmid sample in the same buffer. DBC was determined by the amount of bound pDNA/mL of support at 10 % breakthrough curve, discounting the void volume. Finally, to elute the bound plasmid, ionic strength was increased to 1 M NaCl.

Plasmid DNA quality assessment

Protein and endotoxin concentrations were measured by the micro-

bicinchoninic acid (BCA) protein assay kit from Pierce (Rockford, USA) and ToxinSensor™ Chromogenic Limulus Amoebocyte Lysate (LAL) Endotoxin Assay Kit from GenScript (Piscataway, USA, Inc.), respectively, following the manufacturer's instructions. Genomic DNA quantification was measured by real-time PCR in an iQ5 Multicolor Real-Time PCR Detection System (Bio-Rad, Hemel Hempstead, UK), as previously described [19].

pDNA-$CaCO_3$ formulation and characterization

For nanoplex formulation, an optimization of the methodology previously established [20] was performed through modification of the co-precipitation method previously described [21]. 5 µL (5 µg) of purified pDNA was added to 245 µL of 0.5 M $CaCl_2$ as solution A. For solution B, 187.5 µL of 0.005 M Na_2CO_3 were mixed with 62.5 µL of gelatin (gel strength 160, Fluka/ Sigma-Aldrich, Steinheim, Germany) (5 mg/mL). Solution A was added dropwise to solution B, while the latter was placed in a vortex. The pDNA/$CaCO_3$ complexes were recovered by centrifugation throughout 30 min. at 20,000 × *g*. The resulting supernatant was used to calculate the encapsulation efficiency:

EE (%) = [(Total pDNA amount-pDNA supernatant amount)/Total pDNA amount] ∗ 100

The pellet of nanoplexes was resuspended in water. Size and surface charge (zeta potential) were measured by Dynamic Light Scattering (DLS), with a Zetasizer NanoZS particle analyzer (Malvern Instruments, Worcestershire, UK), equipped with a He-Ne laser, as described by others [22]. Freshly prepared samples were used to measure particle diameters at 25 °C, with 173° scattering angle in fully automatic mode. Moreover, the surface charges (zeta potential) of the nanoparticles were determined in disposable capillary cells and computed by using Henry's [F(Ka)1.5], and Smoluchowsky models, at 25 °C [23–26]. In both cases, the average values of size and zeta potential measurements were calculated with the data obtained from three samples ± SD. For the nanoparticle morphology assessment, (SEM) (Hitachi S-2700, Tokyo, Japan) was used (20 kV) after treating the nanoplexes with tungsten (1 %) and drying overnight. TEM (Hitachi, Japan) was also performed after resuspension of nanoplexes in deionized water and sonication.

Cell culture

THP-1 dendritic cells, kindly provided by Professor Maria Rosete, Center for Neurosciences and Cell Biology, University of Coimbra, Portugal, were grown in suspension with RPMI medium supplemented with 10 % fetal bovine serum and 1 % streptomycin/penicillin (SP) solution. For transfection purposes, cells were previously differentiated with 10 ng/mL phorbol 12-myristate 13-acetate and SP was withdrawn the day before transfection.

pDNA cellular uptake

To follow the entry of pDNA/$CaCO_3$ complexes into THP-1 cells, pDNA was stained with fluorescein isothiocyanate isomer I (FITC) before transfection, as described [13]. Prior to transfection, cells were seeded in 12-well plates with glass coverslips. Cells were transfected with the labeled FITC pDNA-$CaCO_3$-gelatin complexes for 8, 16 and 24 h. Coverslips were placed on glass slides and visualized using a Zeiss LSM710 laser scanning confocal microscope (Carl Zeiss SMT, Inc., Oberkochen, Germany) under 63 × amplification with the Zeiss Zen software (2010).

PCR and RT-PCR

To confirm pDNA nuclear delivery by nanoplexes, cells were recovered 24 h after transfection as described in [27], followed by PCR for E6 gene detection of transfected cells. To detect E6 mRNA expression, total RNA extraction was performed 24 h after transfection followed by cDNA synthesis. PCR detection of E6 mRNA was carried out according to conditions previously described [13].

Western blot

To detect E6 protein expression, western blotting was used. Briefly, 12.5 % polyacrylamide gel electrophoresis was performed with pooled fractions of total protein extracted from transfected and control cells. Samples were prepared with 30 µg of each protein sample, the volume of which was calculated from the calibration curve constructed by protein quantification. Electroblotting was carried out for 10 min in the standard protocol of the TransBlot Turbo system (Bio-Rad, Hemel Hempstead, UK). Mouse anti-E6 IgG monoclonal antibody (Santa Cruz Biotechonology, Heidelberg, Germany) was incubated overnight (1:200 dilution) at 4 °C, followed by washing and incubation with mouse anti-β-actin monoclonal antibody (Sigma-Aldrich, MO, United States of America) (1:20000) for 8 h at 4 °C. After, membrane was washed and incubated with goat anti-mouse IgG polyclonal antibody (Santa Cruz Biotechnology) for 1 h at room temperature. Membrane was finally incubated for 5 min with enhanced chemifluorescence (ECF) (GE Healthcare, Buckinghamshire, United Kingdom) and visualized in a BioRad FX-Pro-plus (Bio-Rad, Hemel Hempstead, UK).

Results and discussion

Plasmid DNA purification

For the pharmaceutical application of sc isoform HPV-16 E6/E7 pDNA vaccine, elimination of impurities must be assured according to regulatory agency criteria: sample homogeneity > 97 % of supercoiled pDNA, proteins and RNA undetectable by the micro-bicinchoninic acid (BCA) method and 0.8 % agarose gel electrophoresis, respectively, genomic (g) DNA under 2 ng/µg plasmid by real-time PCR and endotoxins under 0.1 EU/µg plasmid by limulus amebocyte lysate (LAL) assay [28]. To purify sc pDNA isoform from a complex *E. coli* lysate sample, different strategies can be explored, such as the use of a competitive ligand or the manipulation of pH, ionic strength or polarity, depending on the ligand and target biomolecule characteristics [5].

Epoxy monolith modifications

The chromatographic behavior of pDNA was evaluated on different monoliths to further understand the influence of each ligand configuration. Thus, decreasing linear gradients from 3.0 to 0 M $(NH_4)_2SO_4$ (hydrophobic elution conditions) and increasing linear gradients from 0 to 3.0 M NaCl (ionic elution conditions) in Tris-EDTA, pH 8.0, were performed for 15 min. Through retention time (RT) analysis summarized in Table 1, the non-modified epoxy monolith retained pDNA only under hydrophobic binding and elution conditions, eluting at around 11 min. This chromatographic behavior was expected, resulting from the presence of hydrophobic epoxy groups that retain nucleic acids in the presence of $(NH_4)_2SO_4$ [29]. The addition of a 2-allyloxyethanol

Table 1
Evaluation of the retention time (min) of four epoxy monoliths (non-modified, modified with 2-allyloxyethanol spacer arm, modified with arginine amino acid and modified with 2-allyloxyethanol spacer arm and arginine), under hydrophobic (decreasing linear gradient from 3 to 0 M of $(NH_4)_2SO_4$) and ionic (increasing linear gradient from 0 to 3 M of NaCl) elution conditions in Tris-EDTA buffer, pH 8.0, during 15 min (mean ± SD, n = 3).

Monoliths	Hydrophobic conditions	Ionic conditions
Epoxy	10.7 ± 0.2	0
Epoxy with spacer arm	12.0 ± 0.3	0
Epoxy with arginine	0	10.0 ± 0.1
Epoxy with spacer arm and arginine	0	8.6 ± 0.2

spacer arm resulted in a pDNA RT of 12 min solely under hydrophobic elution conditions, suggesting a slight increase in the ligand hydrophobicity and additional hydrogen bonds. The epoxy monolith modification with arginine resulted in an altered chromatographic behavior, retaining pDNA only under ionic conditions, which eluted after 10 min. Finally, the epoxy monolith modified with 2-allyloxyethanol spacer and arginine showed a lower RT (8.6 min) than arginine monolith, also only under ionic elution conditions, suggesting a mild influence on the pDNA interaction by the spacer arm. The electronegative character of the 2-allyloxyethanol group may repel pDNA phosphate groups, decreasing the interaction strength with the arginine ligand. A similar behavior was observed in previous studies with arginine and agmatine monoliths [8,11]. The agmatine ligand derives from arginine decarboxylation. The absence of the electronegative carboxyl group favored multiple non-covalent interactions, leading to higher pDNA retention and requiring a higher NaCl concentration (> 1.8 M) for pDNA elution [11], compared to the arginine ligand (795 mM NaCl) [8]. The arg-spacer monolith was explored further for sc pDNA purification.

pDNA vaccine purification

pH manipulation can improve arginine ligand selectivity and increase sc pDNA recovery yield [12]. Thus, a strategy to purify sc pDNA was explored with different pH values (9, 8, 7.5 and 7), since previous studies have indicated that a pH increase can reduce pDNA retention [12]. Hence the arg-spacer monolith was equilibrated with 680 mM NaCl in Tris-EDTA, pH 7.0, at 1 mL/min, and after injection of 200 µL lysate sample (7.2 µg of pDNA/mL), the unbound species were eluted in the flowthrough. However, non-functional pDNA isoforms remained bound to the matrix. Thereafter, two steps were performed, either by increasing NaCl concentration or using different pH buffers, to study the elution profile of the retained biomolecules. Although pH 7.0 was essential to eliminate RNA and simultaneously bind pDNA, this strategy was found to lack enough selectivity for sc pDNA isolation. The best outcome for sc pDNA purification was at pH 7.5, which allowed elimination of non-functional pDNA isoforms. Thus, a chromatographic method was established comprising a binding step at 680 mM NaCl in Tris-EDTA buffer, pH 7.0, and after the elimination of RNA in the flowthrough, two elution steps were applied at 680 mM and 1 M NaCl in Tris-EDTA, pH 7.5 (**Figure 1**A). Agarose gel electrophoresis shows selective elution of non-functional pDNA isoforms in the second peak, with increased pH in the elution buffer, and the sc pDNA recovery in the third peak, by increasing the NaCl concentration (Fig. 1B, lanes 2 and 3).

The differential interactions between nucleic acids present in the lysate sample and the arg-spacer monolith complied with that previously described [8,12]. Given that the pKa of arginine is 12 [30], the lower working pH can increase the effectiveness of arginine positive charges, leading to predominant electrostatic interactions, mostly with nucleic acids negative phosphate groups. However, such ionic interactions can be weakened by competition with increased NaCl concentration in the elution buffer, reducing the effective net charge between the ligand and the species with lower affinity [31]. RNA was eluted in the flowthrough with 680 mM NaCl, due to its small size and lower charge density associated with the single stranded structure. Furthermore, the specific biorecognition of the sc pDNA compared to other pDNA isoforms can be explained by the involvement of additional non-covalent interactions with arginine, such as cation-π interactions, bifurcate hydrogen bonds and hydrogen-π interactions, mainly with the more exposed bases of this conformation caused by the supercoiled structure [32,33]. Therefore, the slight increase in buffer pH allowed the elution of species with lower affinity (oc and linear pDNA isoforms) and the increase ionic strength induced the final recovery of sc pDNA in the last peak.

The purity and recovery of a sc pDNA sample obtained from the injection of a 200 µL volume of lysate into the arg-spacer monolith were evaluated by CIMac™ pDNA analytical column, according to the previously adapted method [18]. The purity of 93.3 % reinforces the fact that the arg-spacer monolith can purify sc pDNA more efficiently from a lysate sample. The recovery yield of 72 % indicated that some pDNA can be loss during the recovery, concentration and desalting steps [8,34]. Nonetheless, such loss cannot be quantified separately considering that all steps must be performed before the analytical evaluation, since ionic strength would interfere with pDNA interaction with the CIMac™ column and a much diluted sample would render the pDNA undetectable by this method. Though this recovery yield is lower than the 86 % obtained with the arginine monolith [8], it is satisfactory compared to other chromatographic strategies, such as the 62 % of recovery yield obtained with anion exchange [35] and the triplex affinity chromatography [36], as well as 70 % attained with hydrophobic interaction chromatography [17].

The limitation of several chromatographic matrices for sc pDNA purification is related to the translation of laboratory to preparative scale, given that high loading generally affects final sample purity and

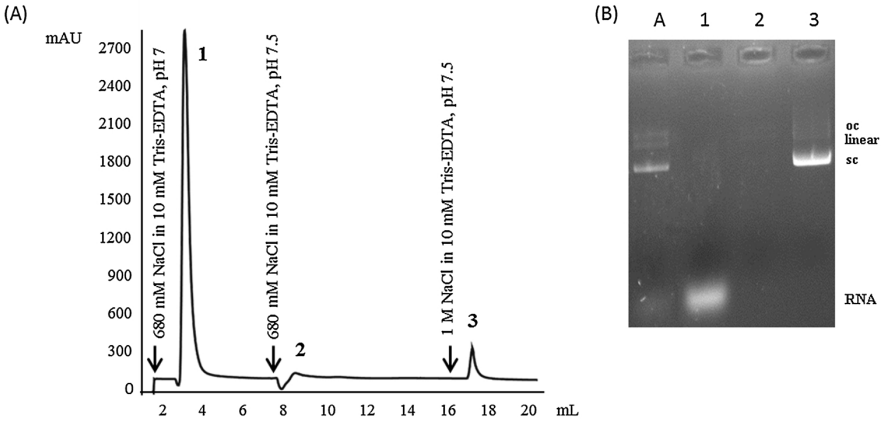

Fig. 1. (A) Chromatographic profile of sc pDNA purification from lysate sample (loading of 200 µL), through an arg-spacer monolith. (B) Corresponding agarose gel electrophoresis: lane A: lysate sample; lane 1-3: peaks 1–3, respectively.

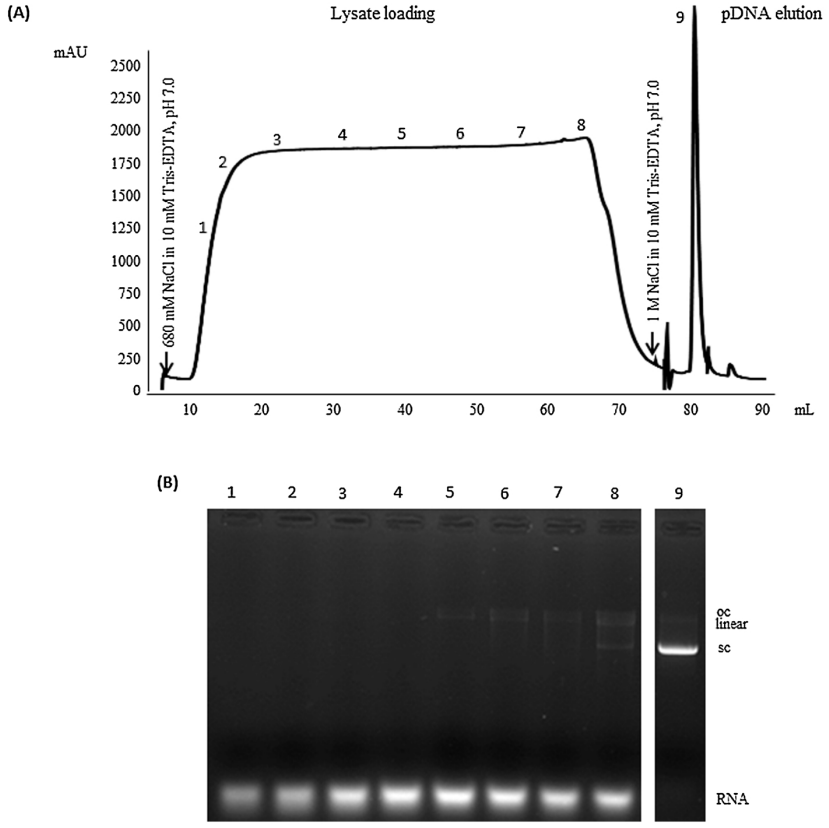

Fig. 2. (A) Chromatographic profile of lysate loading (68 mL) onto arg-spacer monolith, prepared in 680 mM NaCl in Tris-EDTA, pH 7.0. Plasmid elution with 1 M NaCl in Tris-EDTA, pH 7.0. (B) Corresponding agarose gel electrophoresis: lane A: lysate sample; lane 1-9: fractions 1–9, respectively.

Table 2
Measurement of proteins, gDNA and endotoxins in sc pDNA recovered fractions from 200 µL- and 68 mL-loading approaches.

Approach	Sample	Proteins (mg/mL)	RNA (mg/mL)	gDNA (ng/µg of pDNA)	Endotoxins (EU/µg of pDNA)
Small volume injection	sc pDNA	Undetectable	Undetectable	0.090	0.011
Column loading	sc pDNA	Undetectable	Undetectable	0.680	0.003

process productivity. However, the principle of sample displacement chromatography has led to successful purity results at large pDNA-sample loading [10,37]. Thus, this principle was explored here, when the column was loaded with 68 mL of diluted *E. coli* lysate (5 µg of pDNA/mL), prepared in equilibrium buffer (680 mM NaCl in Tris-EDTA, pH 7.0), corresponding to 1 mg pDNA loaded per mL of column (Fig. 2A). Agarose electrophoresis showed RNA continuous elution from start of the loading step, followed by elution of non-functional pDNA species with lower affinity towards the column during the loading step and finally the partial elution of sc pDNA (Fig. 2B). Considering the elution behavior and the sample displacement observed throughout loading, an elution step was performed subsequently only by increasing the ionic strength (1 M NaCl in Tris-EDTA, pH 7.0) to elute bound species. Lane 9 of Fig. 2B shows the sc pDNA recovery in the elution step, almost free from other pDNA isoforms. In fact, the results obtained in the analytical column indicated a sc pDNA homogeneity of 98.5 %. Also, in this assay, sc pDNA preferential retention was verified, recovered by a simple elution step, since non-functional pDNA isoforms were previously eluted during the loading. This suggests the involvement of sample displacement chromatography, since the high loading did not affect final sample purity [10,37]. Contrary to what was observed with lower injection volumes, no intermediate step was necessary to remove non-biologically active pDNA isoforms from the sample, causing pH alteration to be unnecessary. Moreover, it was verified that this monolith can be successfully adapted to preparative chromatography, taking advantage of its DNA binding capacity.

Host impurity assessment

To reduce adverse reactions, pDNA samples for therapeutic application should be free from contaminants and host impurities [38]. The analysis in Table 2 indicates a significant reduction of impurities in the purified samples. The protein and RNA content were undetectable and residual amounts of gDNA and endotoxins were below the limits recommended by regulatory agencies [28]. Thus, both samples could be applied in further *in vitro* and *in vivo* studies, minimizing the possibility of bacterial impurities provoking adverse reactions, such as inflammation, septic shock and organ failure [39,40].

Dynamic Binding Capacity (DBC)

As described previously, monoliths have higher DBC than particulate chromatographic supports [8].The arg-spacer monolith was characterized in terms of DBC. Breakthrough experiments were performed at 1 mL/min, with 0.05 mg/mL of a pre-purified pDNA sample (data not shown). The DBC at 10 % of breakthrough curve was 2.53 mg/mL, which is lower than the 3.55 mg/mL of the arginine monolith [8]. This difference can be related to the lower number of available ligands, since the arg-spacer occupies a larger area than simple arginine. To confirm this hypothesis, ionic density was evaluated for both monoliths with a technique developed in [41]. This relies on the determination of ionic groups available for interaction by assessing a pH transient with two solutions at different salt concentrations (20 and 500 mM phosphate) but at the same pH (6.8). Regeneration with NaOH was necessary before saturating monoliths with the more concentrated solution, in order to guarantee that all ionic groups were available for interaction. After achieving saturation, the mobile phase was suddenly changed to the less concentrated solution for pH transient measurement. The time between alteration of the mobile phases and the 50 % breakthrough achievement was assessed to determine the ionic capacity of each monolith. The arg-spacer monolith presented an ionic capacity of 135 mM phosphate/L column, while arginine monolith presented 146 mM phosphate/L column. The latter displays a higher ionic capacity than arg-spacer monolith, supporting the results obtained for DBC.

Plasmid DNA delivery

Nanoparticle characterization

When developing DNA-based therapies, an obstacle usually arises regarding safe delivery of the designed biomolecule to the intended cell niche. A carrier system lacking any cytotoxicity towards healthy cells and concomitantly very specific in identifying and delivering its content to the target tissue must be developed [42,43]. At the same time, DNA delivery must be high and efficient to exert a reasonable therapeutic effect. $CaCO_3$ systems are popular nanosystems due to its simplicity, biocompatibility and economical preparation [44]. Here, $CaCO_3$ nanoplexes were formulated by co-precipitation, including the purified sc pDNA sample, and modified with gelatin, as a natural and biodegradable biopolymer. Gelatin has been shown to add stability to pDNA nanoplexes and to increase compaction, allowing the formation of smaller nanoparticles [20]. Fig. 3A,B shows SEM and TEM images of the pDNA-$CaCO_3$-gelatin systems, presenting a spherical shape, which is an important feature as this morphology allows a rapid absorption by the cell membrane, facilitating vector internalization. Table 3 shows the average of size, zeta potential and pDNA EE determined for pDNA-$CaCO_3$-gelatin formulated complexes. The nanoparticles were approximately 200 nm in size, with a negative surface charge, and were able to load and encapsulate pDNA to a high degree. With some exception for the zeta potential, where a negative value can disfavor cell membrane interaction, pDNA-based carrier properties seem to be adequate for cellular uptake, internalization and consequently transfection. It has been documented that spherical vectors with sizes < 300 nm can promote cellular uptake. Nevertheless, vector internalization success and, therefore, gene transfection efficiency are at the same time dependent on the set of physicochemical vehicle properties and the cell type [45].

Table 3
Average encapsulation efficiency, zeta potential and size of pDNA-$CaCO_3$-gelatin nanoplexes (mean ± SD, n = 3).

Characterization parameters	Values
Encapsulation Efficiency (%)	81.5 ± 2.88
Zeta Potential (mV)	−2.07 ± 0.45
Size (nm)	203.2 ± 9.0

EE demonstrated that nearly 81 % of the pDNA was successfully encapsulated, indicating that each nanoparticle batch carried approximately 4.05 µg of pDNA. Thus, the quantity of nanoparticles prepared can be suitably adjusted accordingly with the surface area of the well for *in vitro* transfection studies. Compared to a previous study, in which pDNA was encapsulated into rhodamine-$CaCO_3$-gelatin nanoplexes for mitochondrial targeting, a higher EE was achieved with rhodamine-free $CaCO_3$-gelatin nanoparticles [20]. Moreover, the nanoplexes as formulated here presented an average size that was slightly higher than rhodamine-$CaCO_3$-gelatin. This might be explained by the fact that rhodamine presents positive charges that may help pDNA condensation through electrostatic binding, leading to smaller nanoplexes. However, the average size of $CaCO_3$-gelatin complexes is still within the range for optimal cell transfection. The $CaCO_3$-gelatin vectors formulated were of lower zeta potential than the former nanoplexes, perhaps because rhodamine is a positively charged fluorochrome. Rhodamine has been applied to direct delivery systems towards mitochondria in a gene therapy protocol, which is not the current aim. Overall, the $CaCO_3$-gelatin nanoplexes presented suitable characteristics for sc pDNA delivery to target cells.

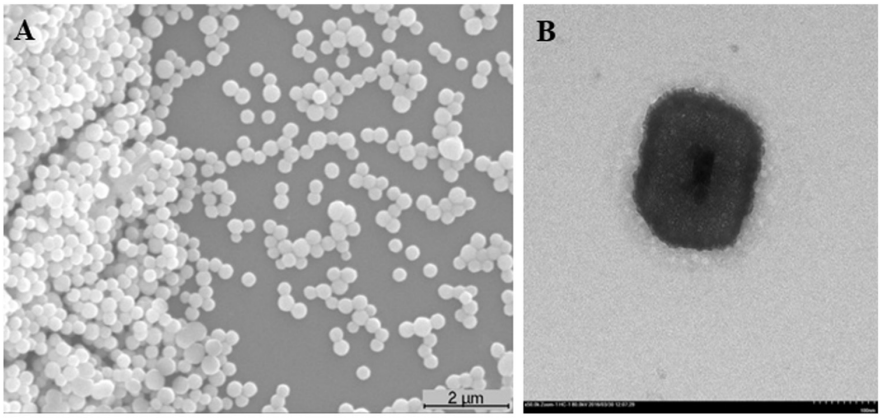

Fig. 3. (A) pDNA-$CaCO_3$-gelatin complexes by scanning electron microscopy (Magnification x10,000). (B) pDNA-$CaCO_3$-gelatin complexes by transmission electron microscopy.

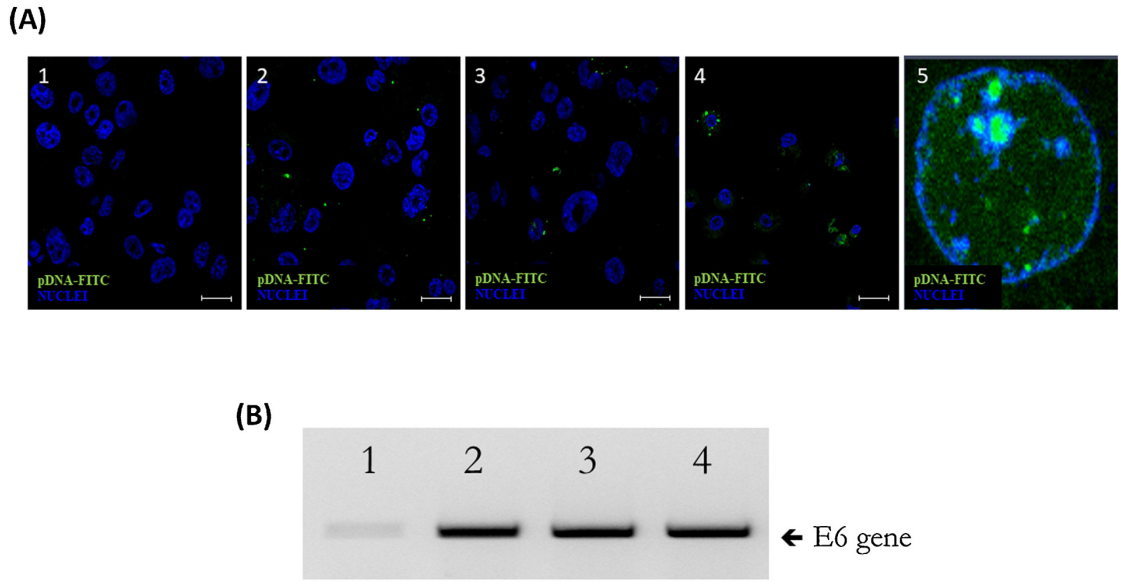

Fig. 4. (A) Fluorescence detection of FITC-labeled pDNA-$CaCO_3$-gelatin complexes upon different transfection periods (green – pDNA/FITC staining; blue – nucleus staining). 1 - Non-transfected THP-1 cells; 2 - THP-1 cells 8 h post-transfection; 3 - THP-1 cells 16 h post- transfection; 4 - THP-1 cells 24 h post-transfection. 5 – THP-1 cell nucleus 24 h post-transfection. (B) PCR for pDNA detection in cells 24 h post-transfection. 1 - Non-transfected THP-1 cells; 2–4 -Cells transfected with $CaCO_3$ modified systems.

DNA vaccine cell delivery

To increase therapeutic potential, DNA vaccine administration should target dendritic cells, the professional antigen presenting cells activating cytotoxic and humoral immune responses [46,47]. Thus, it is essential to develop efficient, biocompatible transfection systems that can specifically identify dendritic cells, which are known to be difficult to transfect [48]. To investigate the ability of pDNA-$CaCO_3$-gelatin complexes to undergo dendritic cell internalization, pDNA was labeled with FITC and its entry into THP-1 cells, a human monocyte cell line that can be differentiated into macrophages and dendritic cells, was monitored. As shown in Fig. 4A, fluorescence was found within cells 24 h after transfection, suggesting that the $CaCO_3$-gelatin complexes were able to deliver pDNA into the cell successfully. These results indicate potential of the $CaCO_3$-gelatin nanoparticle as a new nanocarrier for pDNA delivery to dendritic cells. To further assess pDNA cell entry, 24 h after transfection, PCR was performed for E6 gene detection. As shown in Fig. 4B, the E6 gene was found in 3 independent transfections of THP-1 cells with pDNA-$CaCO_3$-gelatin nanoplexes (lanes 2–4), compared to the control (lane 1). The presence of the gene, only found in HPV-infected cells, adds more evidence that the pDNA was correctly delivered, supporting the ability of these nanoplexes to deliver pDNA vaccines. Viability studies showed no cytotoxic effect, as previously described [20].

DNA vaccine antigen expression

To verify the pDNA expression, cells were transfected and recovered after 24 h for total RNA extraction. After cDNA synthesis, RT-PCR was performed for E6 mRNA detection. Fig. 5A shows the resulting gel electrophoresis, with the presence of E6 mRNA in transfected THP-1 cells (lane 2) compared to non-transfectants (lane 1). A positive control was also performed with CaSki cells (lane 3), HPV-16 infected cervical cancer cells. The data suggests that the gene is correctly transcribed into E6 mRNA, highlighting the $CaCO_3$-gelatin complexes capacity to deliver the sc pDNA vaccine to the nucleus. E6 protein detection was performed by western blotting. Cells were transfected and recovered after 48 h for protein extraction. Fig. 5B shows a western blot representing E6 protein staining in non-transfected cells (lane 3) and cells transfected with pDNA-$CaCO_3$-gelatin complexes (lane 4). The band density difference between samples, compared to housekeeping β-actin staining for both samples (lanes 1 and 2, respectively), indicates that the E6 mRNA was correctly translated into protein. Overall, these data underline the potential of $CaCO_3$-gelatin nanoplexes as a new pDNA delivery system, suggesting a promising feature for DNA vaccine therapeutic application.

Conclusion

This work presents a biotechnological platform for HPV-16 E6/E7 pDNA vaccine purification followed by *in vitro* evaluation of its delivery. The use of an arg-spacer monolith confirmed the ligand accessibility and its capability to efficiently remove RNA, oc and linear pDNA isoforms by two purification strategies of different lysate sample loading (200 µL and 68 mL). Open circular and linear pDNA isoform displacement during column loading favored the elimination of these impurities throughout the assay with pDNA binding capacities above 1 mg/mL. Moreover, the sc pDNA obtained from large sample loading eluted in a single step by ionic strength increase, with a higher degree of purity than in a previous approach. This monolith offers rapid and successful sc pDNA separation by different loading approaches, indicating its applicability for future industrial scale-up without affecting process effectiveness and productivity. $CaCO_3$-gelatin complexes were found to successfully encapsulate sc pDNA. Characterization of nanoplexes demonstrated good size and zeta-potential features, suggesting good transfection ability, which was demonstrated by the successful transfection of dendritic cells, a cell line model which is usually difficult to transfect. Overall, the $CaCO_3$-gelatin complexes present a promising future in DNA vaccine delivery. The combination of an innovative biotechnological strategy to purify sc pDNA with a suitable and high-performance pDNA delivery system contributes towards progress in the clinical application of pDNA vaccines.

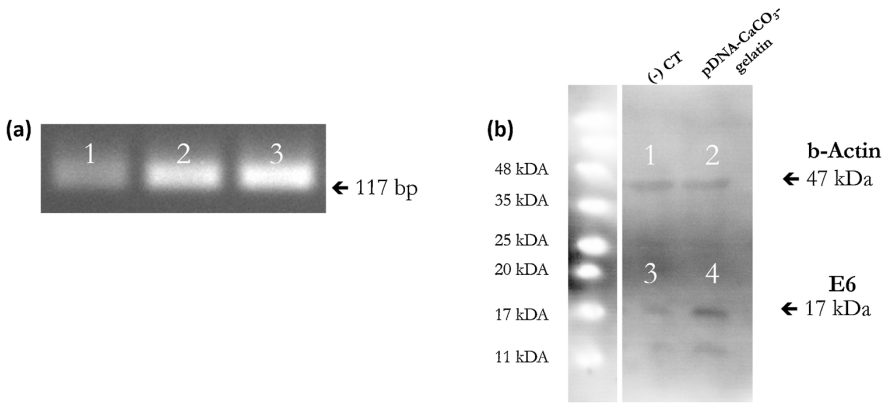

Fig. 5. (A) RT PCR for detection of E6 mRNA. 1 - Non-transfected THP-1 cells; 2 - Cells transfected with pDNA-$CaCO_3$-gelatin systems; 3 - CaSki cells (positive control). (B) Western blot for β-actin and E6 protein 48 h after transfection. 1- β-actin in non-transfected THP-1 cells; 2 – β-actin in cells transfected with pDNA-$CaCO_3$-gelatin systems; 3– E6 in non-transfected THP-1 cells; 4 – E6 in cells transfected with pDNA-$CaCO_3$-gelatin systems.

Declaration of Competing Interest

None.

Acknowledgements

This work was supported by FEDER funds through the POCI - COMPETE 2020 - Operational Programme Competitiveness and Internationalisation in Axis I - Strengthening research, technological development and innovation (Project POCI-01-0145-FEDER-007491) and National Funds by FCT - Foundation for Science and Technology (Project UID/Multi/00709/2019). A.M Almeida acknowledges the PhD fellowship (SFRH/BD/102284/2014) from FCT. D. Costa acknowledges the FCT program contract IF/01459/2015 supported by Fundo Social Europeu e Programa Operacional Potencial Humano. The authors also acknowledge John Blenis for the pcDNA3-myc-FLNa S2152A Addgene plasmid, BIA Separations for having kindly provided monolithic disks and especially to Dr. Urh Černigoj for the valuable help in epoxy monolith modifications.

References

[1] Pereira N, Kucharczyk KM, Estes JL, Gerber RS, Lekovich JP, Elias RT, et al. Human papillomavirus infection, infertility, and assisted reproductive outcomes. J Pathog 2015;2015:1–8. https://doi.org/10.1155/2015/578423.
[2] Paavonen J. Human papillomavirus infection and the development of cervical cancer and related neoplasias. Int J Infect Dis 2007;11(Suppl 2):S3–9.
[3] Motoyama S, Ladines-llave CA, Villanueva SL, Maruo T. The role of human papilloma virus in the molecular biology of cervical carcinogenesis. Kobe J Med Sci 2004;50:9–19.
[4] Han Y, Liu S, Ho J, Danquah MK, Forde GM. Using DNA as a drug—bioprocessing and delivery strategies. Chem Eng Res Des 2009;87:343–8. https://doi.org/10.1016/j.cherd.2008.09.010.
[5] Sousa F, Prazeres DMF, Queiroz JA. Affinity chromatography approaches to overcome the challenges of purifying plasmid DNA. Trends Biotechnol 2008;26:518–25. https://doi.org/10.1016/j.tibtech.2008.05.005.
[6] Josefsberg JO, Buckland B. Vaccine process technology. Biotechnol Bioeng 2012;109:1443–60. https://doi.org/10.1002/bit.24493.
[7] Sun B, Yu XH Yin Y, Liu X, Wu Y, Chen Y, et al. Large-scale purification of pharmaceutical-grade plasmid DNA using tangential flow filtration and multi-step chromatography. J Biosci Bioeng 2013;116:281–6. https://doi.org/10.1016/j.jbiosc.2013.03.015.
[8] Soares A, Queiroz JA, Sousa F, Sousa A. Purification of human papillomavirus 16 E6/E7 plasmid deoxyribonucleic acid-based vaccine using an arginine modified monolithic support. J Chromatogr A 2013;1320:72–9. https://doi.org/10.1016/j.chroma.2013.10.053.
[9] Ghanem A, Healey R, Adly FG. Current trends in separation of plasmid DNA vaccines: a review. Anal Chim Acta 2013;760:1–15. https://doi.org/10.1016/j.aca.2012.11.006.
[10] Amorim LFA, Gaspar R, Pereira P, Černigoj U, Sousa F, Queiroz JA, et al. Chromatographic HPV-16 E6/E7 plasmid vaccine purification employing L-histidine and 1-benzyl-L-histidine affinity ligands. Electrophoresis 2017;38:2975–80. https://doi.org/10.1002/elps.201700147.
[11] Sousa Â, Pereira P, Sousa F, Queiroz JA. Binding mechanisms for histamine and agmatine ligands in plasmid deoxyribonucleic acid purifications. J Chromatogr A 2014;1366:110–9. https://doi.org/10.1016/j.chroma.2014.09.031.
[12] Almeida AM, Queiroz JA, Sousa F, Sousa A. Optimization of supercoiled HPV-16 E6/E7 plasmid DNA purification with arginine monolith using design of experiments. J Chromatogr B Anal Technol Biomed Life Sci 2015;978–979:145–50. https://doi.org/10.1016/j.jchromb.2014.12.004.
[13] Almeida AM, Tomás J, Pereira P, Queiroz JA, Sousa F, Sousa Â. HPV-16 targeted DNA vaccine expression: the role of purification. Biotechnol Prog 2018;34:546–51. https://doi.org/10.1002/btpr.2603.
[14] Blanco E, Shen H, Ferrari M. Principles of nanoparticle design for overcoming biological barriers to drug delivery. Nat Biotechnol 2015;33:941–51. https://doi.org/10.1038/nbt.3330.
[15] Münger K, Phelps WC, Bubb V, Howley PM, Schlegel R. The E6 and E7 genes of the human papillomavirus type 16 together are necessary and sufficient for transformation of primary human keratinocytes. J Virol 1989;63:4417–21. doi:2476573.
[16] Sambrook J, Fritsch TM EF. Molecular cloning. New York: Cold Spring Harb Press; 1989.
[17] Diogo MM, Queiroz J, Monteiro G, Martins S, Ferreira GN, Prazeres DM. Purification of a cystic fibrosis plasmid vector for gene therapy using hydrophobic interaction chromatography. Biotechnol Bioeng 2000;68:576–83. https://doi.org/10.1002/(SICI)1097-0290(20000605)68:5<576::AID-BIT13>3.0.CO;2-5 [pii].
[18] Sousa A, Almeida AM, Černigoj U, Sousa F, Queiroz JA. Histamine monolith versatility to purify supercoiled plasmid deoxyribonucleic acid from Escherichia coli lysate. J Chromatogr A 2014;1355:125–33. https://doi.org/10.1016/j.chroma.2014.06.003.
[19] Martins SAM, Prazeres DMF, Cabral JMS, Monteiro GA. Comparison of real-time polymerase chain reaction and hybridization assays for the detection of Escherichia coli genomic DNA in process samples and pharmaceutical-grade plasmid DNA products. Anal Biochem 2003;322:127–9. https://doi.org/10.1016/j.ab.2003.07.004.
[20] Coutinho E, Batista C, Sousa F, Queiroz J, Costa D. Mitochondrial gene therapy: advances in mitochondrial gene cloning, plasmid production, and nanosystems targeted to mitochondria. Mol Pharm 2017;14:626–38. https://doi.org/10.1021/acs.molpharmaceut.6b00823.
[21] Zhao D, Zhuo RX, Cheng SX. Alginate modified nanostructured calcium carbonate with enhanced delivery efficiency for gene and drug delivery. Mol Biosyst 2012;8:753–9. https://doi.org/10.1039/c1mb05337j.
[22] Góis JR, Reis F, Almeida AM, Pereira P, Sousa F, Serra AC, et al. Preparation of well-defined brush-like block copolymers for gene delivery applications under biorelevant reaction conditions. Colloids Surf B Biointerfaces 2018;169:107–17. https://doi.org/10.1016/j.colsurfb.2018.05.004.
[23] Milling AJ. Surface characterization methods: principles, techniques, and applications. New York: Marcel Dekker; 1999.
[24] Tiwari A, Mishra YK, Kobayashi H, Turner APF. Intelligent nanomaterials. second edition Wiley; 2016. https://doi.org/10.1002/9781119242628.
[25] Bhattacharjee S. DLS and zeta potential - what they are and what they are not? J Control Release 2016;235:337–51. https://doi.org/10.1016/j.jconrel.2016.06.017.
[26] Van De Voorde M, Werner M, Fecht HJ. The nano-micro interface: bridging the Micro and nano worlds. second edition Ulm, Germany: Wiley-vch; 2015. https://doi.org/10.1002/9783527679195.
[27] De La Vega J, Ter Braak B, Azzoni AR, Monteiro GA, et al. Impact of plasmid quality

on lipoplex-mediated transfection. J Pharm Sci 2013;102:3932–41. https://doi.org/10.1002/jps.23709.
[28] Ferreira GN, Monteiro G, Prazeres DM, Cabral JM. Downstream processing of plasmid DNA for gene therapy and DNA vaccine applications. Trends Biotechnol 2000;18:380–8. https://doi.org/10.1016/S0167-7799(00)01475-X.
[29] Diogo MM, Queiroz J, Prazeres DM. Studies on the retention of plasmid DNA and Escherichia coli nucleic acids by hydrophobic interaction chromatography. Bioseparation 2001;10:211–20. https://doi.org/10.1023/A:1016361721316.
[30] Lee D, Lee J, Seok C. What stabilizes close arginine pairing in proteins? Phys Chem Chem Phys 2013;15:5844–53. https://doi.org/10.1039/c3cp00160a.
[31] Ongkudon CM, Danquah MK. Process optimisation for anion exchange monolithic chromatography of 4.2kbp plasmid vaccine (pcDNA3F). J Chromatogr B Anal Technol Biomed Life Sci 2010;878:2719–25. https://doi.org/10.1016/j.jchromb.2010.08.011.
[32] Diogo MM, Queiroz JA, Prazeres DMF. Chromatography of plasmid DNA. J Chromatogr A 2005;1069:3–22. https://doi.org/10.1016/j.chroma.2004.09.050.
[33] Giovannini R, Freitag R, Tennikova TB. High-performance membrane chromatography of supercoiled plasmid DNA. Anal Chem 1998;70:3348–54.
[34] Sousa A, Tomaz CT, Sousa F, Queiroz JA. Successful application of monolithic innovative technology using a carbonyldiimidazole disk to purify supercoiled plasmid DNA suitable for pharmaceutical applications. J Chromatogr A 2011;1218:8333–43. https://doi.org/10.1016/j.chroma.2011.09.033.
[35] Prazeres DMF, Schluep T, Cooney C. Preparative purification of supercoiled plasmid DNA using anion-exchange chromatography. J Chromatogr A 1998;806:31–45. https://doi.org/10.1016/S0021-9673(97)01254-5.
[36] Schluep T, Cooney CL. Purification of plasmids by triplex affinity interaction. Nucleic Acids Res 1998;26:4524–8. https://doi.org/10.1093/nar/26.19.4524.
[37] Černigoj U, Martinuč U, Cardoso S, Sekirnik R, Krajnc NL, Štrancar A. Sample displacement chromatography of plasmid DNA isoforms. J Chromatogr A 2015;1414:103–9. https://doi.org/10.1016/j.chroma.2015.08.035.
[38] Diogo MM, Queiroz JA, Prazeres DMF. Purification of plasmid DNA vectors produced in Escherichia coli for gene therapy and DNA vaccination applications. Methods Biotechnol 2005;18:165–78.
[39] Bazzani RP, Cai Y, Hebel HL, Hyde SC, Gill DR. The significance of plasmid DNA preparations contaminated with bacterial genomic DNA on inflammatory responses following delivery of lipoplexes to the murine lung. Biomaterials 2011;32:9854–65. https://doi.org/10.1016/j.biomaterials.2011.08.092.
[40] de Oliveira Magalhães P, Lopes AM, Mazzola PG, Rangel-Yagui C, Penna TCV, Pessoa A. Methods of endotoxin removal from biological preparations: a review. J Pharm Pharm Sci 2007;10:388–404.
[41] Lendero N, Vidič J, Brne P, Podgornik A, Štrancar A. Simple method for determining the amount of ion-exchange groups on chromatographic supports. J Chromatogr A 2005;1065:29–38. https://doi.org/10.1016/j.chroma.2004.10.072.
[42] Cortesi R, Campioni M, Ravani L, Drechsler M, Pinotti M, Esposito E. Cationic lipid nanosystems as carriers for nucleic acids. N Biotechnol 2014;31:44–54. https://doi.org/10.1016/j.nbt.2013.10.001.
[43] González-Domínguez I, Grimaldi N, Cervera L, Ventosa N, Gòdia F. Impact of physicochemical properties of DNA/PEI complexes on transient transfection of mammalian cells. N Biotechnol 2019;49:88–97. https://doi.org/10.1016/j.nbt.2018.09.005.
[44] Maleki Dizaj S, Barzegar-Jalali M, Zarrintan MH, Adibkia K, Lotfipour F. Calcium carbonate nanoparticles as cancer drug delivery system. Expert Opin Drug Deliv 2015;12:1649–60. https://doi.org/10.1517/17425247.2015.1049530.
[45] Liu X, Wu F, Tian Y, Wu M, Zhou Q, Jiang S, et al. Size dependent cellular uptake of rod-like bionanoparticles with different aspect ratios. Sci Rep 2016;6:24567. https://doi.org/10.1038/srep24567.
[46] Su JH, Wu A, Scotney E, Ma B, Monie A, Hung CF, et al. Immunotherapy for cervical cancer: research status and clinical potential. BioDrugs 2010;24:109–29. https://doi.org/10.2165/11532810-000000000-00000.
[47] Mantia-Smaldone GM, Chu CS. A review of dendritic cell therapy for cancer: progress and challenges. BioDrugs 2013;27:453–68. https://doi.org/10.1007/s40259-013-0030-9.
[48] Maeß MB, Wittig B, Lorkowski S. Highly efficient transfection of human THP-1 macrophages by nucleofection. J Vis Exp 2014:e51960https://doi.org/10.3791/51960.

CHAPTER IV

Paper V

Minicircle DNA purification: Performance of chromatographic monoliths bearing lysine and cadaverine ligands

A.M. Almeida, J.A. Queiroz, F. Sousa, A. Sousa

CICS-UBI – Centro de Investigação em Ciências da Saúde, Universidade da Beira Interior, Av. Infante D. Henrique, 6200-506 Covilhã, Portugal

Journal of Chromatography B 1118-1119: 7-16

Short description: An original research paper based on the comparison of two different affinity chromatographic strategies for the purification of minicircle DNA in its supercoiled isoform.

Journal of Chromatography B 1118–1119 (2019) 7–16

Contents lists available at ScienceDirect

Journal of Chromatography B

journal homepage: www.elsevier.com/locate/jchromb

Minicircle DNA purification: Performance of chromatographic monoliths bearing lysine and cadaverine ligands

A.M. Almeida, J.A. Queiroz, F. Sousa, A. Sousa*

CICS-UBI – Centro de Investigação em Ciências da Saúde, Universidade da Beira Interior, Av. Infante D. Henrique, 6200-506 Covilhã, Portugal

ARTICLE INFO

Keywords:
Cadaverine
Lysine
mcDNA
Monoliths
Pseudo-affinity chromatography

ABSTRACT

Minicircle DNA (mcDNA) technology is in the vanguard of vectors designed for gene therapy, since the absence of prokaryotic sequences confers to mcDNA higher biosafety in comparison to other DNA vectors. However, the presence of other isoforms and non-recombined parental molecules hampers the isolation of supercoiled (sc) mcDNA with the chromatographic methods already established for plasmid purification. In this work, two monolithic supports were modified with lysine and its decarboxylated derivative, cadaverine, to explore their performance in the sc mcDNA purification. Increasing NaCl gradients and different pH values (from 6 to 9) were tested in both modified monoliths. In general, cadaverine modified support established stronger interactions with mcDNA than lysine modified monolith, at acidic pH. For instance, at pH 6.0 the retention time for RNA and DNA molecules in lysine modified monolith was 11.58 and 14.59, respectively, while for cadaverine modified monolith was 20.32 and 27.12, respectively. The lysine modified monolith was able to successfully isolate sc mcDNA from the lysate sample. However, recovery yield was significantly sacrificed to guarantee high purity levels of sc mcDNA. The cadaverine modified monolith showed better selectivity than the previous monolith, achieving the successful sc mcDNA isolation from the lysate sample. The final sc mcDNA sample, obtained by the column that showed the best performance, was characterized by real-time PCR, presenting 98.4% purity and 78.6% recovery yield. The impurities content, namely genomic DNA, proteins and endotoxins, was found within the criteria established by regulatory agencies. Overall, a simple and practical chromatographic strategy to purify sc mcDNA was for the first time implemented by exploring a modified monolithic column, with no significant reduction on the purity and recovery and without resorting to backbone modification or specific enzymatic digestion. Such features will surely be crucial in the industrial scale-up of this chromatographic strategy since it will not be associated with significant cost-increase.

1. Introduction

Minicircle DNA (mcDNA) is the newest trend in DNA vectors that can overcome some limitations presented by conventional plasmid DNA (pDNA). This cutting edge technology has the ability of excising the prokaryotic sequences when the vector amplification is completed, resulting in a smaller DNA vector composed mainly by eukaryotic sequences [1]. These physical and structural differences result in higher transfection efficiency, biocompatibility and prolonged expression of the target gene, when using mcDNA in comparison to pDNA [2]. Briefly, the mcDNA molecule is derived from a parental plasmid (PP), which contains site-specific sequences recognized by PhiC31 integrase, in a specifically engineered *E. coli* strain (ZYCY10P3S2T) [3]. Also, PP presents several I-*Sce*I restriction sites that lead to the endonuclease-induced cleavage of the molecule [3,4]. Upon induction with L-arabinose, PhiC31 integrase is expressed and the recombination of PP begins, originating the mcDNA and the miniplasmid (mP) molecules [3,4]. While mcDNA contains the eukaryotic sequences needed for mammalian gene expression, the mP contains the remaining bacterial sequences from the PP [3]. Simultaneously, the expression of I-*Sce*I is induced, leading to the digestion of mP and PP molecules [3]. Nonetheless, the elimination of mP and PP is not totally effective and trace quantities may be found even after *in vivo* recombination [4]. Hence, chromatographic strategies must be explored to retrieve mcDNA with a purity degree suitable for therapeutic application.

Different chromatographic strategies have been explored for

Abbreviations: gDNA, genomic DNA; mcDNA, minicircle DNA; mP, miniplasmid; oc, open circular; PP, parental plasmid; pDNA, plasmid DNA; PCR, polymerase chain reaction; sc, supercoiled

* Corresponding author.
E-mail address: angela@fcsaude.ubi.pt (A. Sousa).

https://doi.org/10.1016/j.jchromb.2019.04.024
Received 9 November 2018; Received in revised form 11 March 2019; Accepted 11 April 2019
Available online 14 April 2019
1570-0232/

supercoiled (sc) mcDNA purification. Mayrhofer and co-workers [5] described a protocol based on the insertion of a specific sequence into the PP backbone, corresponding to a mcDNA portion after recombination. Then, through affinity chromatography, mcDNA is isolated by exploiting its binding to a specific ligand, the lactose operon repressor protein, which will recognize the sequence previously inserted [5]. In a similar way, Hou and colleagues [6] published a study regarding the purification of mcDNA using specific recognition sequences. However, in that work, the sequences were inserted in the region corresponding to the mP, which, in the presence of biotinylated DNA oligonucleotides, led to a reversible triple-helix structure. Then, these undesirable molecules were eliminated by binding them to streptavidin-coated magnetic beads, resulting in the isolation of mcDNA by negative chromatography. On the other hand, Alves and co-workers [7] established a purification strategy for sc mcDNA by resorting to *in vitro* enzymatic digestion of mP and PP molecules using a specific nicking endonuclease. Then, after nicking these molecules, sc mDNA isolation was achieved by using hydrophobic interaction chromatography. Although these studies provide good results for mcDNA isolation, it requires the use of PP molecules modified with specific sequences. Consequently, this approach cannot be used in other PP molecules available in the market. Also, some of these strategies do not have enough selectivity to allow sc isolation from other different mcDNA isoforms since they are designed to either recognize the contaminants or to bind to specific sequences shared by all mcDNA isoforms. Ultimately, considering the characteristics of such strategies, the scale-up would be too expensive to allow therapeutic mcDNA to be easily affordable. Therefore, the use of a unique chromatographic strategy that can be applied to mcDNA vectors with different backbones has great interest, allowing to reduce some of the purification costs [8]. To overcome these hurdles, our research group previously published a chromatographic strategy in which the successful sc mcDNA purification was achieved using CIM DEAE-1 monolith [9]. Nonetheless, this method presented some limitations associated with the sc mcDNA recovery yield [9], given that only 50% of the sc mcDNA content was recovered. These results emphasized the need to explore other options for sc mcDNA purification. Actually, the lack of selectivity can be related to the fact that weak anion exchange ligands only establish ionic interactions with the target molecule. In the presence of other molecules with similar surface charge, the selectivity of these chromatographic matrices may significantly decrease. In Table 1 it is presented a comparison between all the strategies here described for mcDNA purification.

Affinity chromatography has been pointed out as a fruitful technique in the separation of biomolecules due to the selectivity towards the target molecule [10]. Such approach exploits the specific recognition of the target molecule by matrix-attached ligands, based on its biological function or chemical structure. Thus, given the fact that sc isoform has specific exposed bases in its compact structure, in comparison to other isoforms, affinity chromatography can explore the selectivity of affinity ligands towards these bases for sc isolation. In fact, our research group has been exploring the role of different amino acids as ligands for the purification of nucleic acids. These ligands often resulted in high purity and recovery yields for target molecules [11–14]. Chromatographic monoliths are advantageous for large molecules separation due to convection-based mass transfer, enabling high and flow-independent dynamic binding capacity and resolution [15]. A combination of monolith with amino acid-based ligands seems to be a logical step forward in nucleic acid purification activities. Thus, the aim of the present study was to explore two purification strategies for sc mcDNA isolation from a bacterial lysate. For the first time, lysine and its decarboxylated derivative, cadaverine, were used as ligands immobilized in monolithic supports for the purification of sc mcDNA. Such ligands are usually manipulated for the exploration of electrostatic interactions. However, these molecules are known to present other elemental interactions, such as hydrogen bonds, hydrogen-π or cation-π interactions, water mediated bonds, hydrophobic interactions or van

Table 1
Comparison between different mcDNA purification approaches. (HIC – Hydrophobic Interaction Chromatography. + + much more, + more, − less, − - much less).

Ref	Purification strategy	Cost	Time	Separation	Recovery
[5]	PP backbone was modified so that mcDNA contains a lactose operator sequence, which will be recognized by a chromatographic column bearing the lactose operon repressor protein as a ligand. Requires full recombination of PP into mcDNA and mP as well as pre-purification with a commercial anion-exchange column.	+ + Given the expensive nature of the chromatographic column (necessary to produce and purify recombinant lactose operon repressor protein) and the requirement to modify the PP backbone	- Given the chromatographic run takes 50 min	Separates mcDNA from mP	There is no info regarding recovery
[6]	PP backbone was modified so that PP and mP present a specific TriD sequence, which will be recognized by specific oligonucleotides immobilized in magnetic beads. Requires pre-purification with a commercial anion-exchange column.	- Given the requirement to modify the PP backbone and the utilization of streptavidin-coated magnetic beads, which can be costly	+ Given the magnetic bead incubation time for sc mcDNA isolation is 2 h	Separates mcDNA from mP and PP	94–95% of recovery
[7]	PP backbone was modified so that PP and mP contain a Nb.*Bbv*CI recognition site. Upon bacterial lysis, the sample is incubated with Nb.BbvCI enzyme for sc mP conversion into oc mP. Afterwards, HIC is used for sc mcDNA separation. Requires full recombination of PP into mcDNA and mP.	+ Given the requirement to utilize enzymes for this chromatographic procedure and to modify the PP backbone. Also, the use of high salt concentrations in HIC approach will add cost to this procedure	+ + Given the lengthy process necessary for sc mcDNA isolation since the bacterial lysis (enzyme digestion, HIC, desalting)	Separates mcDNA from mP, PP and bacterial RNA	There is no info regarding recovery
[9]	CIM DEAE column from Biaseparations was used for the sc mcDNA isolation from a complex clarified lysate sample. No PP backbone alterations were necessary.	- - Given the lack of need in PP backbone modification and the use of a commercially available column	- - Given the chromatographic run takes 30 min	Separates mcDNA from mP, PP and bacterial RNA	Over 50% of recovery, the sc mcDNA co-elutes in two different chromatographic peaks

der Waals forces, which may ultimately contribute to more selectivity towards the target molecule, comparatively to commercially available weak anion exchangers.

2. Materials and methods

2.1. Materials

Lysine and cadaverine ligands were purchased from Alfa Aesar (Karlsruhe, Germany) and Tokyo Chemical Industry (Tokyo, Japan), respectively, and immobilized on Convective Interaction Media® (CIM®) epoxy monoliths with bed volume of 0.1 mL, kindly prepared and provided by BIA Separations (Ajdovščina, Slovenia). Briefly, the target ligand was dissolved in water and 5 M NaOH was added to adjust pH to 10.5. Then, 2 mL of ethanol was added and the resulting solution was pumped into an epoxy monolith. The monoliths were incubated along with the immobilization solution during 48 h hours at 60 °C, washed with water and the remaining epoxy groups were deactivated with 0.5 M H_2SO_4. Ionic density capacity was evaluated as described by Lendero and co-workers [16]. Sodium chloride was purchased from Panreac (Barcelona, Spain) and tris(hydroxymethyl)aminomethane (Tris) from Merck (Darmstadt, Germany). All solutions used in chromatographic experiments were freshly prepared by using deionized ultra-pure grade water, purified with a Milli-Q system from Millipore (Billerica, MA, USA), filtered through a 0.2 µm pore size membrane (Schleicher Schuell, Germany) and degassed ultrasonically. The *E. coli* strain ZYCY10P3S2T and pMC.CMV-MCS-EF1-GFP-SV40 PolyA vector of 7.06 Kbp were purchased from System Biosciences.

2.2. Methods

2.2.1. Minicircle DNA production and extraction

PP amplification was performed by culturing the *E. coli* strain ZYCY10P3S2T, harboring the pMC.CMV-MCS-EF1-GFP-SV40 PolyA vector, in Terrific Broth medium (20 g/L of tryptone, 24 g/L of yeast extract, 4 mL/L of glycerol, 0.017 M KH_2PO_4, 0.072 M K_2HPO_4) at 42 °C, followed by mcDNA (3.8 Kbp) synthesis induction by adding an induction mixture containing 0.01% L-arabinose. The induction was then carried out for 3 h, as previously described by Gaspar and co-workers [3]. This induction step also leads to expression of I-*Sce*I by this strain, which is responsible for the mP digestion. In the end, cells were recovered by centrifugation and stored at −20 °C. A complex mcDNA sample was prepared making use of the modified alkaline lysis method described by Diogo and co-workers [17]. The resulting supernatant was desalted with PD-10 desalting columns (GE Healthcare, Buckinghamshire, UK). Subsequently, the clarified lysate sample was used for the chromatographic assays.

2.2.2. Minicircle DNA purification

All chromatographic experiments were performed in an AKTA Püre system (GE Healthcare, Buckinghamshire, UK), which consists in a compact separation unit and a personal computer with UNICORN™ 6.3 software. The purification procedure was based on the use of two monolithic supports modified with lysine and cadaverine ligands, both with a bed volume of 100 µL. A 100 µL loop was used for sample injection and all experiments were carried out with a 1 mL/min flow rate.

For screening purposes, the chromatographic behavior of the different molecules of the sample was evaluated in both columns, by applying an increasing linear gradient from 0 to 2 M NaCl in 10 mM Tris-EDTA buffer (pH 7.0) for 30 min.

Upon several assays, the mcDNA purification was achieved by establishing a three-step elution strategy in each monolith. In the case of lysine modified monolith, the equilibration and sample injection were carried out at 190 mM NaCl in 10 mM Tris-EDTA buffer (pH 7.0), followed by a stepwise increase of ionic strength to 250 mM NaCl in 10 mM Tris-EDTA buffer (pH 7.0) for mcDNA recovery. Finally, 1 M NaCl in 10 mM Tris-EDTA buffer (pH 7.0) was applied to the column for the elution of molecules that remained bound. On the other hand, cadaverine modified monolith equilibration and sample injection were performed at 1.07 M NaCl in 10 mM Tris-EDTA buffer (pH 7.0), followed by a salt increase adjustment to 1.16 M NaCl in 10 mM Tris-EDTA buffer (pH 7.0).

All experiments were carried out at room temperature and the absorbance was continuously monitored at 260 nm. Fractions were recovered, according to the chromatograms, concentrated and desalted with Vivaspin® 6 Centrifugal Concentrator (Vivaproducts, Littleton, MA, USA), for further analysis. Agarose gel electrophoresis was performed [9] and each sample was analyzed for band density through Quantity software (Bio-Rad Laboratories, Hercules, CA, USA).

2.2.3. mcDNA purity and recovery assessment

To assess the purity and recovery levels of the mcDNA recovered from the chromatographic assays, real-time polymerase chain reaction (PCR) was performed in a CFX Connect Real-time System (Bio-Rad Laboratories, Hercules, CA) [3,5]. For PP detection, primers were designed for pUC19 origin (ColE1) (forward [fw]: 5′-TCCTGTTACCAGT GGCTGCT; reverse [rv]: 5′-AGTTCGGTGTAGGTCGTTCG), to amplify a fragment of 151 bp. For mcDNA detection, primers were designed for the GFP gene, (forward [fw]: 5′- ATGGAGAGCGACGAGAGCGG; reverse [rv]: 5′-TTAGCGAGATCCGGTGGAGC), amplifying a fragment of 759 bp. For mP detection, primers were designed for the kanamycin antibiotic resistance gene, (forward [fw]: 5′-TCACGACGAGATCCTCG CCGTC; reverse [rv]: 5′-CGTTAGGTAGAACAAGTTAGTA), amplifying a fragment of 561 bp. A calibration curve for each set of primers in the range of 50–0.5 ng/µL was performed with PP purified with NZYMaxiprep commercial kit (NZYTech, Lisbon, Portugal), according to the manufacturer's instructions. Real-time PCR was carried out with 20 µL reactions containing 10 µL of SYBR green mastermix, 3 µM of each primer and 1 µL of DNA. The parameters were: denaturation at 95 °C for 10 min; 35 cycles of denaturation at 95 °C for 10 s, annealing at 60 °C for 30 s and extension at 72 °C for 10 s. The PP, mP and mcDNA content was calculated resorting to the calibration curve. For mP and mcDNA quantification, the PP was subtracted, similarly to what has been previously described by Mayrhofer and co-workers [5].

2.2.4. Genomic DNA, endotoxins and protein quantification

Purified sc mcDNA concentration was determined by spectrophotometric quantification (A 260 nm). Genomic DNA was quantified through real time-PCR, with Maxima SYBR Green/Fluorescein qPCR Master Mix (Thermo Fisher Scientific), as described by Sousa and co-workers [18]. The calibration curve for gDNA concentration was constructed by serial dilutions of the *E. coli* gDNA in the range of 0.005 to 50 ng/µL. The ToxinSensor™Chromogenic Limulus amoebocyte lysate assay kit from GenScript (USA, Inc.) was used for endotoxin quantification, according to the manufacturer's instructions. The calibration curve was constructed with 10 endotoxin units (EU)/mL stock solution provided by the kit (0.005–0.1 EU/mL). For protein assessment, the Micro-BCA (bicinchoninic acid) protein assay kit from Pierce (Rockford, USA) was used, according to the manufacturer's instructions. The calibration curve was constructed with Bovine Serum Albumin (BSA) as a standard protein (0.01–0.1 mg/mL).

2.2.5. Assessment of selectivity in different loading conditions and dynamic binding capacity

For the evaluation of the effect that different loading conditions may have in the purification of sc mcDNA, different sample volumes (200 µL, 500 µL and 1 mL) from the same initial batch were loaded onto the cadaverine monolith, under the optimized chromatographic conditions previously established.

To perform the dynamic binding capacity, purified mcDNA solution was prepared with a 20 µg/mL concentration in 10 mM Tris-EDTA buffer. Cadaverine monolith was equilibrated with 10 mM Tris-EDTA

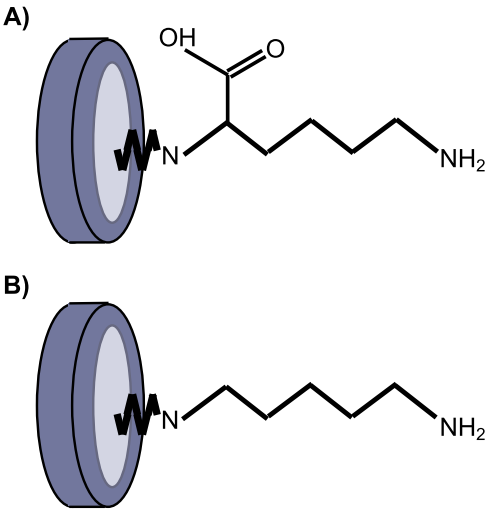

Fig. 1. Representation of the monoliths modified with: A) Lysine ligand; B) Cadaverine ligand.

buffer (pH 7.0), followed by mcDNA solution overloading. Determination of dynamic binding capacity was carried out as described by Soares and co-workers [19]. Afterwards, the elution of the bound mcDNA was achieved by increasing the ionic strength to 2 M NaCl in 10 mM Tris-EDTA buffer.

3. Results and discussion

Lysine and cadaverine were the ligands explored in the present work to purify sc mcDNA from a lysate sample. Lysine agarose was already successfully used by our research group in pDNA and pre-miRNA-29 purification [11,20]. Since cadaverine results from lysine decarboxylation, its application as a ligand appears to be very promising as it can favor some interactions with DNA, minimizing some repulsive effects. Thus, this study allows the evaluation of the carboxyl group influence in established interactions, by comparing the retention behavior of mcDNA in both supports. Two monolithic columns were modified with lysine and cadaverine ligands (Fig. 1) and, to qualitatively evaluate the monolith modification, several binding studies were performed with mcDNA lysate by using ionic and hydrophobic conditions (data not shown). It is known that the epoxy monolith (non-modified) is capable of binding nucleic acids under hydrophobic conditions, but this retention does not occur when exploring ion-exchange conditions [19,21]. After coupling the ligands to the column surface, cadaverine and lysine modified monoliths allowed the retention of DNA molecules, when loaded in low-conductivity buffers, thus proving the presence of ligands of ionic character. Also, ionic density of each monolithic column was evaluated to determine the total number of ionic groups available for interaction. This method consists in measuring a pH transient by using two solutions with the same pH but with different salt concentrations (500 mM phosphate and 20 mM Phosphate, pH 6.8). All chromatographic supports were regenerated before equilibration with the higher concentration buffer, until saturation was achieved. Then, the mobile phase was abruptly changed to the solution with lower ionic strength and the pH transient was evaluated. The time passed between switching the mobile phases and reaching 50% of breakthrough allows to determine the ionic capacity for the chromatographic support under study [16]. We were able to verify that the unmodified epoxy monolith presented 141 mM phosphate/L column, while lysine and cadaverine modified monoliths presented 414 mM phosphate/L and 526 mM phosphate/L, respectively (data not shown). Given that this relative measure of available ionic groups results from the coexistence of positive amino groups in cadaverine and lysine ligands and negative carboxyl groups in lysine ligand, we can infer that both monoliths have been correctly modified with the target ligands. Also, this result may serve as an indicative that cadaverine modified monolith presents more available ionic groups, when comparing to lysine modified monolith.

In an attempt of understanding the different interactions displayed by each column, lysate samples were loaded in both columns and eluted by using linear gradients of 30 min from 0 to 2 M of NaCl at different pH values (from 6 to 9). As observed in Fig. 2, the decrease of pH generally leads to an increased retention of the different molecules present in the initial sample. This effect can be correlated with the pKa of both ligands. While lysine amine groups present a pKa that varies between 8.95 and 10.5, cadaverine amine groups show a pKa that varies between 9.13 and 10.25. Also, carboxyl group of lysine presents a pKa of 2.2 [22]. Presumably, at lower pH, both ligands are more positively charged, strengthening the interactions and the binding of the negatively charged nucleic acids [23]. In addition, it can also be observed in Fig. 2 that nucleic acids generally present higher retention times in the cadaverine modified support than in the lysine modified monolith, suggesting that stronger interactions are involved. Briefly, at pH 6.0 the retention time (RT) for the lysine modified monolith was 11.58 for RNA and 14.59 for DNA molecules (Fig. 2A), although a small amount of

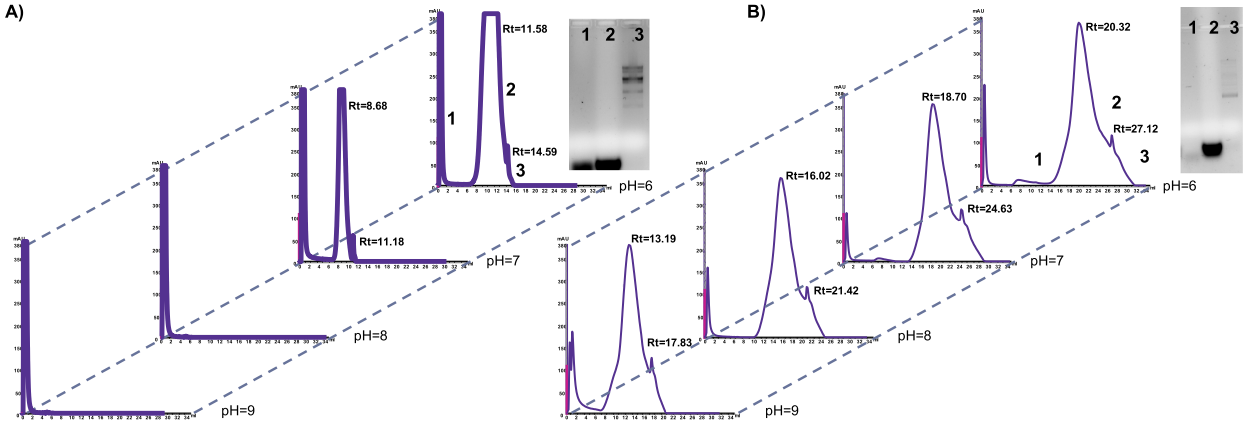

Fig. 2. Chromatographic profile and retention times (RT) of mcDNA-containing lysate sample loaded onto lysine (A) and cadaverine (B) monoliths, when subjected to buffers with different pH values. Chromatographic runs were performed with linear gradients of 30 min from 0 M to 2 M of NaCl in 10 mM Tris-HCl/EDTA at pH 9, 8, 7 and 6. Next to chromatogram at pH 6 it is the electrophoresis of the corresponding peaks (1, 2 and 3).

RNA was eluted in the flowthrough (lane 1 from agarose electrophoresis). However, cadaverine modified monolith presented a RT of 20.32 for RNA and a RT of 27.12 for DNA molecules (Fig. 2B). These results are also in agreement with the ionic density data.

In this first approach, it was observed a significant difference in the chromatographic profiles obtained with both columns. In a first glance, the fact that lysine modified monolith does not interact with the sample at pH 8.0 and pH 9.0 stands out, while cadaverine modified monolith promotes the interaction with the sample at all studied pH conditions. Considering the pKa of lysine amine groups, working at lower pH can increase the effectiveness of lysine positive charges and lead to a stronger interaction with nucleic acids, while higher pH can lead to a weaker ionic interaction (not disregarding the involvement of other multiple non-covalent interactions). Also, considering the fact that the carboxyl group is de-protonated in the studied pH range, the lack of interaction perceived between the sample and the chromatographic matrix at pH 8.0 and pH 9.0 may be explained by the electrostatic repulsion displayed by such group towards the phosphate groups of nucleic acids. Some studies have shown that lysine ligand is able to bind to small DNA fragments in very acidic conditions (pH 4.0), losing this ability with the pH increase [23].

At pH 6.0 the carboxylic group is de-protonated, therefore inhibiting the interaction between small RNA molecules and the chromatographic ligand through electrostatic repulsion [23]. On the other hand, our research group has previously studied the behavior of nucleic acid interaction with histidine and arginine decarboxylated amino acid derivatives, namely histamine and agmatine [21]. Such study allowed the identification of a higher pseudo-affinity between pDNA and histamine/agmatine ligands than with histidine/arginine precursors, probably due to the absence of electrostatic repulsion from the carboxyl group [21]. Therefore, the collected data suggest that the lysine decarboxylation also enables a stronger interaction with nucleic acids, perhaps avoiding the phosphate group repulsion through carboxyl group absence. Simultaneously, the cadaverine ligand can promote additional non-covalent interactions due to the higher availability of the carbon chain, which culminates in the higher retention of biomolecules.

Taking advantage of the weak interaction between the lysine ligand and RNA molecules, few attempts were performed in order to achieve the purification of sc mcDNA. At first, it seemed the most suitable strategy, considering the possibility to eliminate the bacterial RNA impurity directly in the flowthrough, maintaining the ligands available to bind to other sample components, namely the target mcDNA. Considering the fact that mcDNA does not interact with the lysine modified monolith at pH 8.0, and that at pH 7.0 it is possible to eliminate more RNA quantity in the flowthough than at pH 6.0, the following studies were performed at pH 7.0. A three-step salt increasing gradient was used, establishing the column equilibration at 190 mM NaCl, at a flow rate of 1 mL/min and injecting 100 µL of clarified lysate sample. After the elution of unbound species in the flowthough, ionic strength was increased to 240 mM, followed by 1 M NaCl for complete molecule removal from the support. In Fig. 3, it is presented the chromatogram (A) and the corresponding electrophoresis (B) regarding the purification of sc mcDNA with the lysine modified monolith. As it is shown, the isolation of the sc mcDNA was achieved by first promoting total RNA elution at 190 mM NaCl and simultaneously binding the remaining DNA species. With the increase of ionic strength to 240 mM NaCl, a small fraction of sc mcDNA was able to elute in peak 2 apart from the parental plasmid and open circular isoforms. However, as it is perceived in lane 3 of the electrophoresis of Fig. 3, a great part of the sc mcDNA still continued attached to the matrix, eluting together with other impurities in the third peak, suggesting the purity of the remaining mcDNA is not adequate. This elution profile may be related with the mcDNA smaller size, in comparison to PP molecule, and its more compact structure, regarding the open circular isoform. Such compaction degree can lead to different interactions between the lysine ligand and both isoforms [24].

In an attempt to improve the mcDNA recovery, a similar chromatographic assay was performed with lysine modified monolith only by changing the second step from 240 to 250 mM NaCl. This adjustment allowed to improve the recovery of sc mcDNA in the second peak, despite a considered amount still remained attached to the matrix and only eluted in the third peak (Appendices, Fig. A.1). In addition, this adjustment in the elution gradient also resulted in the co-elution of some impurities with the mcDNA, diminishing the purity degree of the second peak. These data suggest that the selectivity degree of this ligand is not totally suitable for the purification of sc mcDNA, as it would be necessary to greatly sacrifice the recovery to achieve good purity levels, and *vice-versa*. Such lack of selectivity can rely on the fact that, although both PP and mcDNA present different sizes, these molecules have very similar properties. By sharing common DNA sequences, its compaction and torsional strain can lead to the exposition of similar bases that can hamper the distinction of these two molecules. Moreover, previous works have shown that arginine ligand displays stronger interactions with pDNA than the lysine ligand [25]. The difference of ionic strength used in each matrix can be associated with the fact that arginine presents three available amine groups while lysine, as depicted in Fig. 1, presents solely one amine group available for the exploitation of several pseudo-affinity interactions, such as electrostatic, multiple hydrogen bonds or cation-π interactions. Following this line of thought, lysine limitation to one available amine group can be associated with the lack of selectivity and difficulty in the establishment of stronger interactions towards these two similar molecules, PP and mcDNA. Also, lysine-DNA interaction can be weakened due to the presence of the carboxyl group, which can cause repulsion of the negatively charged DNA phosphate groups.

With the intent of improving the sc mcDNA recovery and purity, the cadaverine modified monolith was also explored. Before proceeding, it was necessary to consider the results previously obtained in the pH screening, which are presented in Fig. 2. These experiments demonstrate the involvement of a multiple non-covalent interaction between the sample and the cadaverine matrix, suggesting an interaction towards the sample stronger than the one presented by lysine modified monolith. As a matter of fact, the electrophoresis of the different molecules eluted from lysine support at pH 6 (Fig. 2A) demonstrates that a considerable amount of RNA does not bind in salt-free conditions. Thus, these results indicate that lysine modified monolith promotes a weaker interaction with RNA, leading to some elution in the flowthrough even at the lowest pH (6.0). Therefore, higher salt concentrations must be used with cadaverine ligand, as nucleic acids bind strongly to this ligand than to lysine. Thus, preliminary experiments were carried out in the cadaverine modified monolith by using the same pH and buffer composition optimized in the lysine modified monolith (Fig. 3), in order to compare its chromatographic behavior. However, salt concentrations were adjusted accordingly to the information withdrawn from Fig. 2. To avoid RNA retention and to allow more ligand availability for target molecule binding, few screening studies were performed to establish the NaCl concentration to be used for column equilibration (data not shown).

Therefore, cadaverine modified monolith was equilibrated with 1 M NaCl for RNA elution, followed by the application of a linear gradient from 1 M to 1.19 M NaCl, to understand the interaction behavior of sc mcDNA towards the cadaverine ligand. Then, the salt concentration was increased to 1.3 M NaCl, to elute the species that remained bound to the column. In Fig. 4 it is presented the chromatogram (A) and the corresponding electrophoresis (B). As shown in lanes 4 and 5 of the electrophoresis, most of sc mcDNA was eluted earlier than PP molecules, suggesting that a small adjustment of salt concentration can lead to the complete isolation of sc mcDNA. The sample elution pattern also suggested that the cadaverine ligand can distinguish between both sc mcDNA and sc PP. Taking these results into consideration, a 3-step elution strategy was applied, similarly to the lysine modified monolith

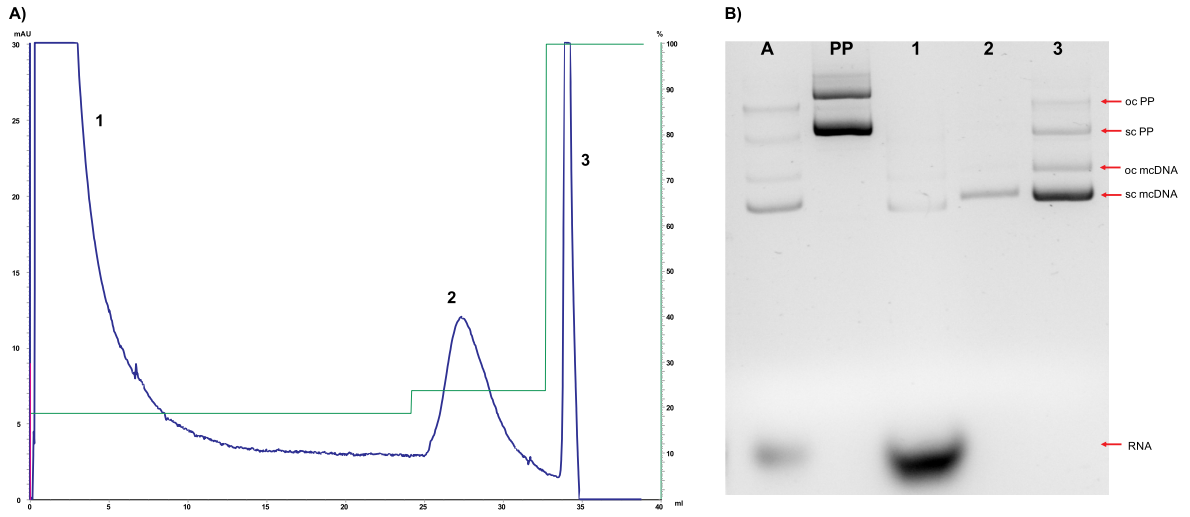

Fig. 3. Chromatographic profile and electrophoretic characterization of the clarified *E. coli* lysate injected onto the lysine monolith. A) Chromatographic run performed with 190 mM NaCl in 10 mM Tris-HCl/EDTA (pH 7.0), followed by 240 mM NaCl in 10 mM Tris-HCl/EDTA (pH 7.0) and 1 M NaCl in 10 mM Tris-HCl/EDTA (pH 7.0). B) Agarose gel electrophoresis of the different peaks. Lane A – Initial Sample; lane PP – Parental Plasmid Sample; Lane 1–3 - Samples corresponding to the respective chromatographic peaks.

approach but with higher ionic strength.

Considering that in the previous strategy RNA was still eluting during the linear gradient, the ionic strength of equilibrium step was increased in an attempt to eliminate all RNA content in the first step of the assay. Then, the salt concentration used in the second step of the gradient was slightly decreased to promote sc mcDNA elution while maintaining other DNA impurities bound to the matrix. Therefore, 1.07 M NaCl was first used to elute RNA species, allowing to bind the DNA molecules at the same time. Afterwards, salt concentration was increased to 1.16 M NaCl, for the recovery of sc mcDNA, followed by ionic strength increase to 1.3 M NaCl for elution of the remaining species. In Fig. 5 is portrayed the chromatogram (A) and the electrophoresis (B) for this result. In contrast to what was observed with the lysine modified monolith, higher sc mcDNA content appears to be retrieved completely isolated from other molecules. In comparison to initial and PP samples (Fig. 5B, lane A and PP), the sc mcDNA sample recovered from the cadaverine modified monolith presents a unique band (Fig. 5B, lane 3), suggesting that it is isolated from other

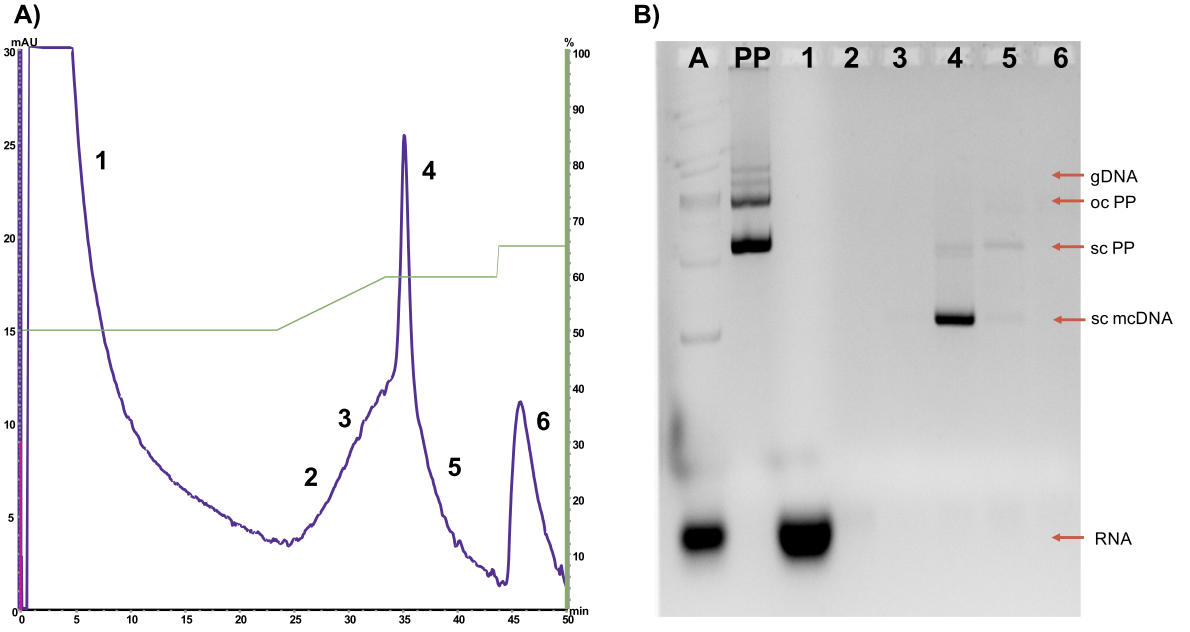

Fig. 4. Chromatographic profile and electrophoresis of the clarified *E. coli* lysate injected in the cadaverine monolith. A) Chromatographic run performed with 1 M NaCl in 10 mM Tris-HCl/EDTA (pH 7.0), followed by a 10 min-linear gradient up to 1.19 M NaCl in 10 mM Tris-HCl/EDTA (pH 7.0) and finally 1.3 M NaCl in 10 mM Tris-HCl/EDTA (pH 7.0). B) Agarose gel electrophoresis of the different peaks. Lane A – Initial Sample; Lane PP – Parental Plasmid Sample; Lane 1–6 - Samples corresponding to the respective chromatographic peaks.

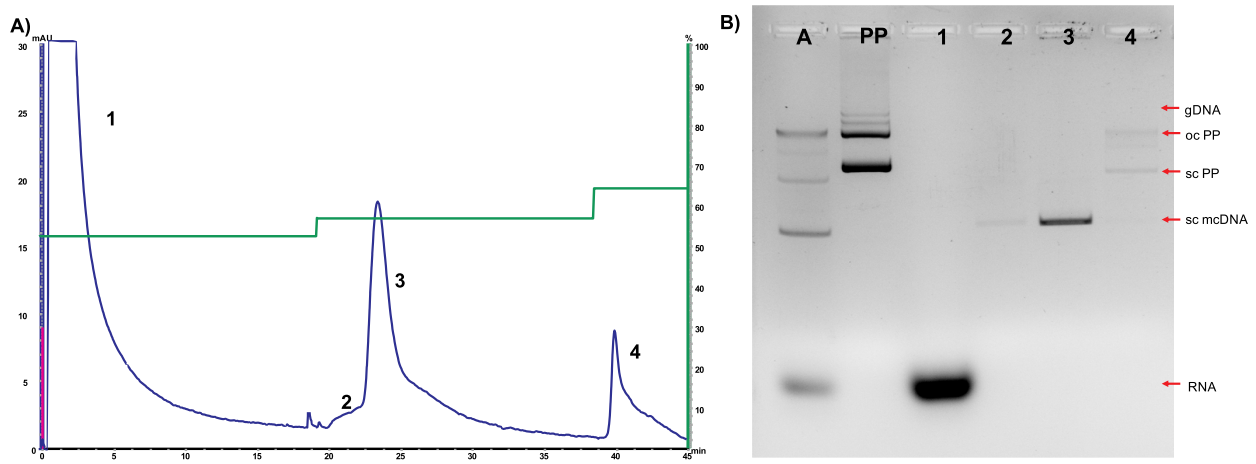

Fig. 5. Chromatographic profile and electrophoresis of the clarified *E. coli* lysate injected in the cadaverine monolith. A) Chromatographic run performed with 1.07 M NaCl in 10 Mm Tris-HCl/EDTA (pH 7.0), followed by 1.16 M NaCl in 10 mM Tris-HCl/EDTA (pH 7.0) and 1.3 M NaCl in 10 mM Tris-HCl/EDTA (pH 7.0). B) Agarose gel electrophoresis of the different peaks. Lane A – Initial Sample; lane PP – Parental Plasmid Sample; Lane 1–4 - Samples corresponding to the respective chromatographic peaks.

contaminants, such as PP molecules and RNA. Concomitantly, the recovery appears to have significantly increased in comparison to the lysine column strategy. Actually, it was not detected any sc mcDNA eluting in other steps (Fig. 5B, lane 4), suggesting that the recovery in the second step is very satisfactory.

Given that no analytical method is available for purity and recovery yield assessment of sc mcDNA, and considering that currently implemented pDNA analytical methods do not allow the separation between PP and mcDNA, real-time PCR was performed to evaluate the purity and the recovery of the obtained mcDNA sample. By designing specific primers for the PP origin, kanamycin and GFP genes, it was possible to perform a calibration curve using a PP sample, a molecule that contains all these sequences. With the PP origin set of primers, it was possible to determine the specific amount of PP in the sample and subtract its amount from the calculations performed either for mcDNA or mP. Thereby, we were able to retrieve the total amount of mcDNA present in the sample. By using this technique, it was possible to determine the purity of the final sc mcDNA as 98.4% and the recovery as 78.6%. Given that the electrophoresis result does not suggest any loss of mcDNA in other peak fractions, the recovery determined by real-time PCR (78.6%) experiments can be related with the fact that the eluted sample was desalted and concentrated, a process that usually resorts to the use of concentrators and that may add up to the loss of target molecule. Regardless, such recovery percentage is relevant and similar to the recovery percentages usually obtained with monoliths for other molecules, such as pDNA [13,14].

These distinctive results obtained with each monolith can be related with cadaverine and lysine structures (Fig. 1). Lysine and cadaverine ligands are composed by a terminal amine group, which can establish electrostatic interactions, hydrogen bonds, hydrogen-π interactions, cation-π interactions and water mediated bonds due to the nitrogen atom that may act as hydrogen bond donor and acceptor [21]. Both ligands also present a carbon chain, which can allow additional interactions, such as hydrophobic or van der Waals forces. These interactions occur preferentially with sc mcDNA, which presents higher charge density of phosphate groups per surface area and more exposed aromatic bases due to the supercoiling phenomenon. Considering that cadaverine does not present a carboxyl group, sc mcDNA can be closer to this ligand and establish molecular forces (which needs the right geometry and close distance) in a great extent, such as hydrogen bonding, van der Walls bonding and others. Therefore, cadaverine ligand presents stronger and more selective interactions than lysine, ultimately facilitating the biorecognition and separation of sc mcDNA from a complex lysate sample.

To complete the purity characterization, host gDNA, protein, RNA and endotoxin content of the isolated sc mcDNA sample was assessed to assure it complies with the regulatory agencies' criteria. In Table 2 is presented a comparison between the accepted impurity levels and the impurity levels evaluated in the sc mcDNA purified by cadaverine modified monolith. As it is perceived, all impurity content is within the range accepted by FDA for biopharmaceuticals (gDNA < 0.01 μg/μg pDNA, proteins undetectable, RNA undetectable, endotoxins < 0.01 EU/μg pDNA). This data underlines the ability of cadaverine modified monolith to purify sc mcDNA from a complex sample. This is a very important feature that a chromatographic strategy must fulfill when aiming to obtain biomolecules for further therapeutic application. Actually, the presence of such contaminants can contribute with harmful secondary effects such as inflammation, septic shock and organ failure [26–28]. Comparatively to the literature (Table 1), this study allowed to establish a purification strategy transposable to other mcDNA backbones, without resorting to its modification with specific recognition sequences or the use of specific enzymatic digestion [5–7]. Besides isolating mcDNA from PP, mP and bacterial contaminants, thus providing a high-grade purity level, this approach also allowed high recovery of the target molecule (78.6%). This is an enormous advantage in comparison to the strategy already established by Diamantino and co-workers (~50%), which was also meant to isolate mcDNA with different backbones [9].

Nonetheless, it is important to assess the sample volume influence in the purity of mcDNA, when developing purification strategies for a future industrial application. Thus, different sample loading assays, from the same initial batch, were performed with the optimized chromatographic conditions. In Fig. 6 is presented the resultant

Table 2
Comparison between FDA criteria and impurity levels evaluated in sc mcDNA sample obtained from cadaverine monolith [29]. EU – Endotoxin unit.

Impurities	FDA criteria	sc mcDNA isolated with cadaverine monolith
gDNA	< 0.01 μg/μg pDNA	0.00158 μg/μg mcDNA
Proteins	undetectable	undetectable
RNA	undetectable	undetectable
Endotoxins	< 0.01 EU/μg pDNA	0.0097 EU/μg mcDNA

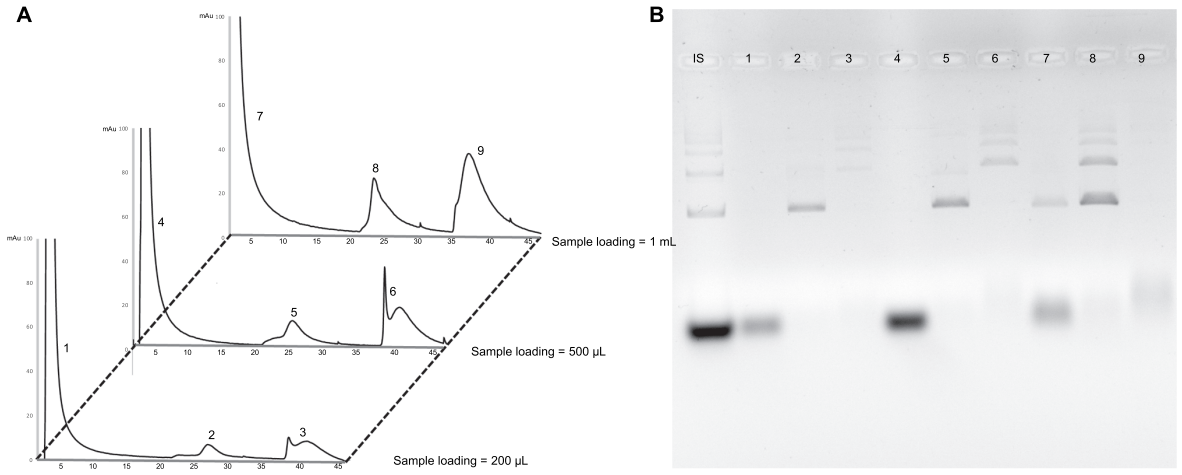

Fig. 6. Evaluation of sample volume effect in mcDNA selectivity. A – Chromatographic runs performed with 1.07 M NaCl in 10 mM Tris-HCl/EDTA (pH = 7.0), followed by 1.16 M NaCl in 10 mM Tris-HCl/EDTA (pH = 7.0) and 1.3 M NaCl in 10 mM Tris-HCl/EDTA (pH = 7.0), under different sample loading conditions (200 µL, 500 µL and 1 mL) in the cadaverine monolith. B - Electrophoresis of the respective chromatographic runs. Lane IS – Initial Sample; Lane 1–9 – Samples corresponding to the respective chromatographic peaks.

electrophoresis of the different assays. It can be perceived that mcDNA purity does not alter when loading 200 and 500 µL of sample (lanes 2 and 5). However, mcDNA does not fully bind to the matrix when using a sample volume of 1 mL, partially eluting with RNA in the first gradient step (lane 7). This might be related with the fact that, with such high sample loading, contaminants may be occupying the available sites for mcDNA binding, leading to its elution in the first step gradient. Then, purity is compromised as high weight molecules elute with mcDNA in the second step of the gradient (lane 8). Such occurrence may also be related with the fact that different amounts of high weight contaminants preferably bind to the matrix, interfering with the separation of mcDNA. Consequently, the conditions previously established for the purification of mcDNA demonstrate its inefficiency under high sample loading conditions, such as 1 mL. However, it must be highlighted the fact that these assays were performed with a monolithic disk of 100 µL volume. The increase of the monolithic disk volume may increase the sample loading volume without compromising mcDNA purity, thus circumventing this problem. Finally, dynamic binding capacity was performed with cadaverine monolith. Monoliths are expected to present higher binding capacity than particulate chromatographic supports [19]. Breakthrough experiments were performed at 1 mL/min, with 0.02 mg/mL purified mDNA sample. The dynamic binding capacity at 10% of breakthrough curve was 2 mg/mL and 2.44 mg/mL at 50% of breakthrough. Thus, it is here described for the first time the dynamic binding of a support utilized for the purification of mcDNA [5,7,9].

4. Conclusion

In the present work, lysine and cadaverine modified monoliths were explored in the sc mcDNA isolation. First, the monolith modification was confirmed by considering the ionic density capacity of lysine and cadaverine modified monoliths (414 mM phosphate/L and 526 mM phosphate/L, respectively) and the epoxy monolith (141 mM phosphate/L). Then, the pH influence in the sample chromatographic behavior was studied for both columns. It was possible to observe an increase of interaction between the sample and both monoliths with the pH decrease. Also, it was shown that cadaverine modified monolith presented higher retention times than lysine modified monolith, suggesting a stronger interaction between the sample and the matrix. This distinct chromatographic behavior can be explained by the presence of a carboxyl group in the lysine modified monolith, which can display electrostatic repulsion towards the phosphate groups of the nucleic acids in the sample. The exploitation of several elution strategies in both monoliths allowed to understand that different interactions were displayed, which ultimately led to different outcomes for each monolith. At first, lysine modified monolith showed to be able to isolate sc mcDNA, although rendering low sc mcDNA recovery. However, the attempt to increase sc mcDNA recovery yield resulted in loss of purity degree, suggesting low selectivity presented by lysine towards mcDNA. On the other hand, cadaverine modified monolith was also able to separate sc mcDNA, presenting better recovery yield than lysine column (78.6%), without loss of purity (98.4%). The stronger and selective interactions established by cadaverine ligand can be due to the absence of the carboxyl group exhibited by lysine. In this way, cadaverine modified monolith has no electrostatic repulsion towards the sc mcDNA phosphate groups, enabling a closer contact of this molecule with the ligand. Consequently, some molecular forces (which need the right geometry and close distance) occur in a great extent, such as hydrogen bonding, van der Walls bonding, between other. Moreover, the level of impurities was shown to fulfill the regulatory agency recommendations. Finally, the dynamic binding capacity for a chromatographic approach regarding the isolation of mcDNA was evaluated for the first time in the literature. In general, here is described a low-cost purification strategy for mcDNA, comparatively to the studies that have been developed so far. The present work allowed to underline cadaverine modified monolith potential as a chromatographic strategy for sc mcDNA purification, given its simplicity and practical use. Also, this ligand seems suitable to be explored for the implementation of an analytical method for quantification of sc mcDNA, which does not exist at the moment.

Acknowledgements

This work was supported by FEDER funds through the POCI - COMPETE 2020 - Operational Programme Competitiveness and Internationalization in Axis I - Strengthening research, technological development and innovation (Project POCI-01-0145-FEDER-007491) and National Funds by FCT - Foundation for Science and Technology (Project UID/Multi/00709/2013). A.M, Almeida and A. Sousa acknowledge the doctoral and post-doctoral fellowships (SFRH/BD/102284/2014 and SFRH/BPD/102716/2014, respectively) from FCT.

The authors acknowledge to BIA Separations for having kindly provided the monolithic supports and particularly to Dr. Uhr Černigoj for the monoliths' immobilization. The authors have no competing interests to declare.

Appendix A

Chromatographic profile and electrophoretic characterization of the clarified *E. coli* lysate injected onto the lysine monolith. A) Chromatographic run performed with 190 mM NaCl in 10 mM Tris-HCl/EDTA (pH 7.0), followed by 250 mM NaCl in 10 mM Tris-HCl/EDTA (pH 7.0) and 1 M NaCl in 10 mM Tris-HCl/EDTA (pH 7.0). B) Agarose gel electrophoresis of the different peaks. Lane A – Initial Sample; lane PP – Parental Plasmid Sample; Lane 1–3 - Samples corresponding to the respective chromatographic peaks.

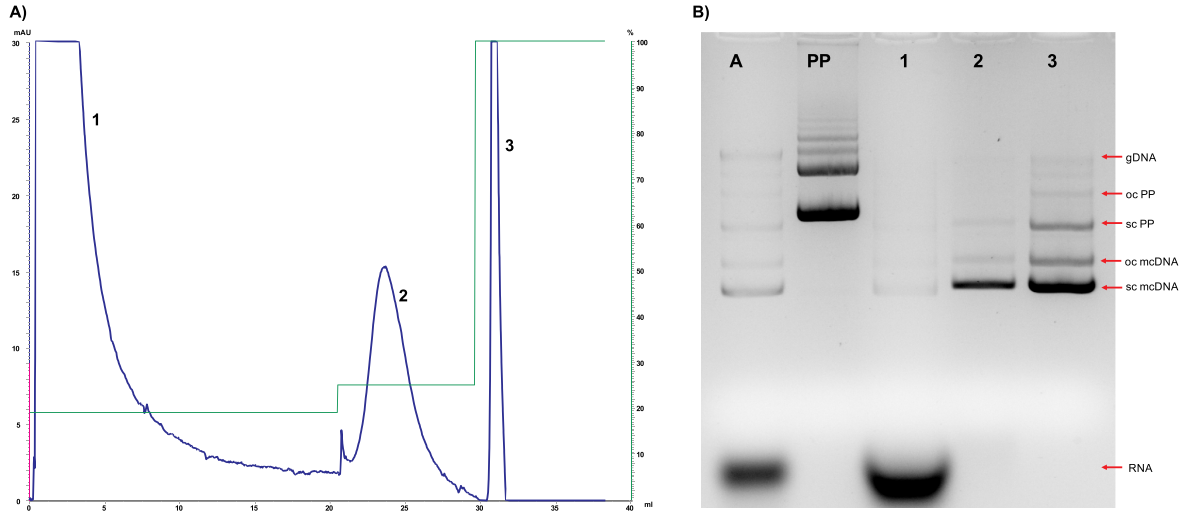

Fig. A.1. Chromatographic profile and electrophoretic characterization of the clarified E. coli lysate injected onto the lysine monolith. A) Chromatographic run performed with 190 mM NaCl in 10 mM Tris-HCl/EDTA (pH 7.0), followed by 250 mM NaCl in 10 mM Tris-HCl/EDTA (pH 7.0) and 1 M NaCl in 10 mM Tris-HCl/EDTA (pH 7.0). B) Agarose gel electrophoresis of the different peaks. Lane A – Initial Sample; lane PP – Parental Plasmid Sample; Lane 1-3 - Samples corresponding to the respective chromatographic peaks. gDNA - genomic DNA; mcDNA - minicircle DNA; oc - open circular; PP - parental plasmid; sc - supercoiled;

References

[1] V. Gaspar, D. de Melo-Diogo, E. Costa, A. Moreira, J. Queiroz, C. Pichon, I. Correia, F. Sousa, Minicircle DNA vectors for gene therapy: advances and applications, Expert. Opin. Biol. Ther. 15 (2015) 353–379, https://doi.org/10.1517/14712598.2015.996544.

[2] M.M. Munye, A.D. Tagalakis, J.L. Barnes, R.E. Brown, R.J. McAnulty, S.J. Howe, S.L. Hart, Minicircle DNA provides enhanced and prolonged transgene expression following airway gene transfer, Sci. Rep. 6 (2016) 23125, , https://doi.org/10.1038/srep23125.

[3] V.M. Gaspar, C.J. Maia, J.A. Queiroz, C. Pichon, I.J. Correia, F. Sousa, Improved minicircle DNA biosynthesis for gene therapy applications, Hum. Gene Ther. Methods. 25 (2014) 93–105, https://doi.org/10.1089/hgtb.2013.020.

[4] Z.-Y. Chen, C.-Y. He, M.A. Kay, Improved production and purification of minicircle DNA vector free of plasmid bacterial sequences and capable of persistent transgene expression *In Vivo*, Hum. Gene Ther. 16 (2005) 126–131, https://doi.org/10.1089/hum.2005.16.126.

[5] P. Mayrhofer, M. Blaesen, M. Schleef, W. Jechlinger, Minicircle-DNA production by site specific recombination and protein-DNA interaction chromatography, J. Gene Med. 10 (2008) 1253–1269, https://doi.org/10.1002/jgm.1243.

[6] X.H. Hou, X.Y. Guo, Y. Chen, C.-Y. He, Z.-Y. Chen, Increasing the minicircle DNA purity using an enhanced triplex DNA technology to eliminate DNA contaminants, Mol. Ther. Methods Clin. Dev. 1 (2015) 14062, , https://doi.org/10.1038/mtm.2014.62.

[7] C.P.A. Alves, M. Šimčíková, L. Brito, G.A. Monteiro, D.M.F. Prazeres, Development of a nicking endonuclease-assisted method for the purification of minicircles, J. Chromatogr. A 1443 (2016) 136–144, https://doi.org/10.1016/j.chroma.2016.03.035.

[8] J. Stadler, R. Lemmens, T. Nyhammar, Plasmid DNA purification, J. Gene Med. 6 (2004) S54–S66, https://doi.org/10.1002/jgm.512.

[9] T. Diamantino, P. Pereira, J.A. Queiroz, Â. Sousa, F. Sousa, Minicircle DNA purification using a CIM® DEAE-1 monolithic support, J. Sep. Sci. 39 (2016) 3544–3549, https://doi.org/10.1002/jssc.201600375.

[10] F. Sousa, D.M.F. Prazeres, J.A. Queiroz, Affinity chromatography approaches to overcome the challenges of purifying plasmid DNA, Trends Biotechnol. 26 (2008) 518–525, https://doi.org/10.1016/j.tibtech.2008.05.005.

[11] A. Sousa, F. Sousa, J.A. Queiroz, Impact of lysine-affinity chromatography on supercoiled plasmid DNA purification, J. Chromatogr. B Anal. Technol. Biomed. Life Sci. 879 (2011) 3507–3515, https://doi.org/10.1016/j.jchromb.2011.09.032.

[12] J.F.A. Valente, A. Sousa, J.A. Queiroz, F. Sousa, Selective purification of supercoiled p53-encoding pDNA with l-methionine-agarose matrix, Anal. Biochem. 459 (2014) 61–69, https://doi.org/10.1016/j.ab.2014.05.011.

[13] A.M. Almeida, J.A. Queiroz, F. Sousa, A. Sousa, Optimization of supercoiled HPV-16 E6/E7 plasmid DNA purification with arginine monolith using design of experiments, J. Chromatogr. B Anal. Technol. Biomed. Life Sci. 978–979 (2015) 145–150, https://doi.org/10.1016/j.jchromb.2014.12.004.

[14] L.F.A. Amorim, R. Gaspar, P. Pereira, U. Černigoj, F. Sousa, J.A. Queiroz, Â. Sousa, Chromatographic HPV-16 E6/E7 plasmid vaccine purification employing L-histidine and 1-benzyl-L-histidine affinity ligands, Electrophoresis 38 (2017) 2975–2980, https://doi.org/10.1002/elps.201700147.

[15] Â. Sousa, F. Sousa, J.A. Queiroz, Advances in chromatographic supports for pharmaceutical-grade plasmid DNA purification, J. Sep. Sci. 35 (2012) 3046–3058, https://doi.org/10.1002/jssc.201200307.

[16] N. Lendero, J. Vidič, P. Brne, A. Podgornik, A. Štrancar, Simple method for determining the amount of ion-exchange groups on chromatographic supports, J. Chromatogr. A 1065 (2005) 29–38, https://doi.org/10.1016/j.chroma.2004.10.072.

[17] M.M. Diogo, J.A. Queiroz, G.A. Monteiro, S.A. Martins, G.N. Ferreira, D.M. Prazeres, Purification of a cystic fibrosis plasmid vector for gene therapy using hydrophobic interaction chromatography, Biotechnol. Bioeng. 68 (2000) 576–583, https://doi.org/10.1002/(SICI)1097-0290(20000605)68:5<576::AID-BIT13>3.0.CO;2-5 (pii).

[18] A. Sousa, C.T. Tomaz, F. Sousa, J.A. Queiroz, Successful application of monolithic innovative technology using a carbonyldiimidazole disk to purify supercoiled plasmid DNA suitable for pharmaceutical applications, J. Chromatogr. A 1218 (2011) 8333–8343, https://doi.org/10.1016/j.chroma.2011.09.033.

[19] A. Soares, J.A. Queiroz, F. Sousa, A. Sousa, Purification of human papillomavirus 16 E6/E7 plasmid deoxyribonucleic acid-based vaccine using an arginine modified monolithic support, J. Chromatogr. A 1320 (2013) 72–79, https://doi.org/10.1016/j.chroma.2013.10.053.

[20] P. Pereira, Â. Sousa, J. Queiroz, A. Figueiras, F. Sousa, New approach for purification of pre-miR-29 using lysine-affinity chromatography, J. Chromatogr. A 1331 (2014) 129–132, https://doi.org/10.1016/j.chroma.2014.01.033.

[21] Â. Sousa, P. Pereira, F. Sousa, J.A. Queiroz, Binding mechanisms for histamine and agmatine ligands in plasmid deoxyribonucleic acid purifications, J. Chromatogr. A 1366 (2014) 110–119, https://doi.org/10.1016/j.chroma.2014.09.031.

[22] D.R. Lide, CRC Handbook of Chemistry and Physics, 84th edition, 2003–2004,

Handb. Chem. Phys, (2003), https://doi.org/10.1136/oem.53.7.504.
[23] L. Liu, Z. Guo, Z. Huang, J. Zhuang, W. Yang, Size-selective separation of DNA fragments by using lysine-functionalized silica particles, Sci. Rep. 6 (2016) 22029, , https://doi.org/10.1038/srep22029.
[24] A. Sousa, F. Sousa, J.A. Queiroz, Biorecognition of supercoiled plasmid DNA isoform in lysine-affinity chromatography, J. Chromatogr. B Anal. Technol. Biomed. Life Sci. 877 (2009) 3257–3260, https://doi.org/10.1016/j.jchromb.2009.08.021.
[25] A. Sousa, F. Sousa, J.A. Queiroz, Differential interactions of plasmid DNA, RNA and genomic DNA with amino acid-based affinity matrices, J. Sep. Sci. 33 (2010) 2610–2618, https://doi.org/10.1002/jssc.201000347.
[26] Z. Wei, W. Huang, J. Li, G. Hou, J. Fang, Z. Yuan, Studies on endotoxin removal mechanism of adsorbents with amino acid ligands, J. Chromatogr. B Anal. Technol. Biomed. Life Sci. 852 (2007) 288–292, https://doi.org/10.1016/j.jchromb.2007.01.038.
[27] C.I. Wooddell, V.M. Subbotin, M.G. Sebestyén, J.B. Griffin, G. Zhang, M. Schleef, S. Braun, T. Huss, J.A. Wolff, Muscle damage after delivery of naked plasmid DNA into skeletal muscles is batch dependent, Hum. Gene Ther. 22 (2011) 225–235, https://doi.org/10.1089/hum.2010.113.
[28] R.P. Bazzani, Y. Cai, H.L. Hebel, S.C. Hyde, D.R. Gill, The significance of plasmid DNA preparations contaminated with bacterial genomic DNA on inflammatory responses following delivery of lipoplexes to the murine lung, Biomaterials 32 (2011) 9854–9865, https://doi.org/10.1016/j.biomaterials.2011.08.092.
[29] G.N.M. Ferreira, Chromatographic approaches in the purification of plasmid DNA for therapy and vaccination, Chem. Eng. Technol. 28 (2005) 1285–1294, https://doi.org/10.1002/ceat.200500158.

Paper VI

The use of size-exclusion chromatography in the isolation of supercoiled minicircle DNA from *Escherichia coli* lysate

A.M. Almeida, D. Eusébio, J.A. Queiroz, F. Sousa, A. Sousa

CICS-UBI – Centro de Investigação em Ciências da Saúde, Universidade da Beira Interior, Av. Infante D. Henrique, 6200-506 Covilhã, Portugal

Journal of Chromatography A 460444

Short description: An original research paper focusing the study of size-exclusion chromatography in the purification of minicircle DNA in its supercoiled isoform

Journal of Chromatography A, 1609 (2020) 460444

Contents lists available at ScienceDirect

Journal of Chromatography A

journal homepage: www.elsevier.com/locate/chroma

The use of size-exclusion chromatography in the isolation of supercoiled minicircle DNA from *Escherichia coli* lysate

A.M. Almeida, D. Eusébio, J.A. Queiroz, F. Sousa*, A. Sousa

CICS-UBI – Centro de Investigação em Ciências da Saúde, Universidade da Beira Interior, Av. Infante D. Henrique, 6200-506 Covilhã, Portugal

ARTICLE INFO

Article history:
Received 19 May 2019
Received in revised form 7 August 2019
Accepted 8 August 2019
Available online 9 August 2019

Keywords:
Minicircle DNA
Sephacryl
Size exclusion chromatography

ABSTRACT

Minicircle DNA (mcDNA) is the new cutting-edge technology which researchers have been exploring for gene therapy and DNA vaccination. Although it presents enormous advantages in comparison to conventional plasmid DNA regarding bioactivity and safety, its challenging isolation from parental plasmid and miniplasmid has been setting back its launching in biomedical sciences. In this work, it is demonstrated the use of a simple size exclusion chromatographic method for the isolation of supercoiled mcDNA. Sephacryl S-1000 SF matrix was explored under different conditions (flow, peak fractionation volume and sample loading) to achieve the best performance and retrieve a mcDNA sample devoid of other bacterial contaminants or plasmid species resultant from the recombination process. This isolation methodology resulted in 66.7% of mcDNA recovery with 98.1% of purity. In addition, to show the robustness of the method, the potential of using this matrix for the isolation of a larger mcDNA was also evaluated. Upon adjusting the flow or the column volume, the larger mcDNA molecule was also successfully isolated. Overall, a simple and effective strategy has been established for the isolation of supercoiled mcDNA, underlining the potential of size exclusion chromatography in mcDNA separation.

1. Introduction

The use of plasmid DNA (pDNA) as a non-viral DNA vector has been undeniably popular in the last decades. From its easy manipulation to its low-cost production, researchers have found this molecule very attractive as a carrier for gene therapy and DNA vaccination. However, this conventional molecule is also known for its limitations comparatively to viral vectors, especially due to lower expression efficiencies. Although this molecule is considered safer than viral vectors, it still presents prokaryotic sequences, which are essential for the recombinant pDNA production but can confer antibiotic resistance to the patient and elicit adverse reactions [1]. Minicircle DNA (mcDNA) is an innovative non-viral DNA vector that is currently being presented as an upgrade to pDNA. The production of this molecule requires an original parental pDNA (PP) molecule that, upon specific induction, recombines to form two different molecules: mcDNA and miniplasmid (mP). While mcDNA presents the former PP eukaryotic sequences necessary for the expression of the target gene, mP contains the prokaryotic sequences required for the selection of transformed bacteria and PP amplification [2]. Also, the mP and PP molecules can present several I-SceI restriction sites that after induction will be recognized and lead these species to degradation [2]. Nonetheless, such *in vivo* recombination and enzyme digestion is not 100% effective, rendering a difficult separation of the mcDNA in its supercoiled (sc) isoform from the other mP and PP species, which present very similar structures and sequences. Up to now, the purification strategies established for mcDNA isolation require the manipulation and insertion of specific sequences in the PP backbone, to improve selectivity, or the utilization of enzymes, adding more costs to the whole process and preventing the use of such techniques in other PP backbones [3–5]. Therefore, the development of an universal strategy for the purification of mcDNA stands as a critical step to implement this promising and innovative DNA vector in the non-viral vectors therapeutic field. So far, Diamantino and co-workers described the single strategy that has been published within these specifications [6]. Such work resorts to the use of a CIM DEAE monolithic disk for the separation of mcDNA through the exploration of ionic conditions. However, the recovery yield of this strategy remains in about 50%, due to mcDNA elution in two different chromatographic steps [6]. In the present work, it is described the size-exclusion chromatography for the isolation of mcDNA from a complex lysate sample, making use of Sephacryl S-1000 SF matrix. This matrix was chosen due to its wide fractionation range (from 5×10^5 to 10^8 molecular

* Corresponding author.
E-mail address: fani.sousa@fcsaude.ubi.pt (F. Sousa).

https://doi.org/10.1016/j.chroma.2019.460444
0021-9673/

weight), which may allow the separation of macromolecules such as genomic DNA (gDNA), PP and mcDNA.

2. Material and methods

2.1. mcDNA production

The ZYCY10P3S2T *E. coli* strains harboring either the pMC.CMV-MCS-EF1-GFP-SV40 PolyA vector (PP) (System Biosciences, USA), with a molecular weight of 7 Kbp, or the pMC.CMV-MCS-EF1-GFP-SV40 PolyA vector modified with the p53 insert (PP 53), with a molecular weight of 8.2 Kbp, were cultured in Terrific Broth medium (20 g/L of tryptone, 24 g/L of yeast extract, 4 mL/L of glycerol, 0.017 M KH_2PO_4, 0.072 M K_2HPO_4) at 42 °C for PP and PP 53 production. Then, for mcDNA formation by inducing the recombination process, 0.01% L-Arabinose was added and the culture was maintained for 3 h at 32 °C, as described by Gaspar and co-workers [2]. Once the induction was completed, cells were recovered by centrifugation and stored at -20 °C.

2.2. Lysate preparation and mcDNA isolation

To retrieve a complex mcDNA-containing lysate sample, the modified alkaline lysis method described by Diogo and co-workers was performed [7]. The resulting lysate sample was directly used for the chromatographic assays, in order to isolate the mcDNA.

All chromatographic experiments were performed in an AKTA Püre system (GE Healthcare, Buckinghamshire, UK), consisting in a compact separation unit and a personal computer with UNICORN™ 6.3 software. A 1.6 cm diameter column (bed height 60 cm) was used to pack 121 mL of Sephacryl S-1000 SF media. An isocratic gradient was kept with 10 mM Tris-HCl, 10 mM EDTA, 150 mM NaCl (pH 7.00) buffer. The sample was injected directly onto the column (2 mL) and experiments were carried out between 0.2 and 0.45 mL/min, at room temperature and the absorbance was continuously monitored at 260 nm. Fractions were recovered, according to the chromatograms, concentrated and desalted with Vivaspin® 6 Centrifugal Concentrator (Vivaproducts, Littleton, MA, USA), for further analysis. All chromatograms were adjusted according to the total void volume and excluded void volume. Selectivity was calculated according to the following equation:

$$\alpha = \frac{tr2 - t0}{tr1 - t0}$$

2.3. mcDNA purity and recovery assessment

To assess the purity and recovery levels of mcDNA present in the fractions collected from the chromatographic assays (n = 3), qPCR was performed in a CFX Connect Real-time System (Bio-Rad Laboratories, Hercules, CA). For PP detection, primers were designed for pUC19 origin (ColE1) (forward [fw]: 5'-TCCTGTTACCAGTGGCTGCT; reverse [rv]: 5'-AGTTCGGTGTAGGTCGTTCG), amplifying a fragment of 151 bp. For mcDNA detection, primers were designed for the GFP gene, (forward [fw]: 5'- ATGGAGAGCGACGAGAGCGG; reverse [rv]: 5'- TTAGCGAGATCCGGTGGAGC), amplifying a fragment of 759 bp. For mP detection, primers were designed for the kanamycin antibiotic resistance gene, (forward [fw]: 5'-TCACGACGAGATCCTCGCCGTC; reverse [rv]: 5'- CGTTAGGTAGAACAAGTTAGTA), amplifying a fragment of 561 bp. A calibration curve for each set of primers in the range of 0.5–50 ng/μL was performed with PP purified with NZYMaxiprep commercial kit (NZYTech, Lisbon, Portugal), according to the manufacturer's instructions. The qPCR was carried out with 20 μL reactions containing 10 μL of SYBR green mastermix, 3 μM of each primer and 1 μL of DNA. Cycling parameters were: denaturation at 95 °C for 10 min; 35 cycles of denaturation at 95 °C for 10 s, annealing at 60 °C for 30 s and extension at 72 °C for 10 s. The content of PP, mP and mcDNA was calculated resorting to the calibration curve. For mP and mcDNA quantification, the PP was subtracted, as similarly reported by Mayrhofer and co-workers [3].

2.4. mcDNA impurity assessment

For gDNA quantification qPCR was performed with Maxima SYBR Green/Fluorescein qPCR Master Mix (Thermo Fisher Scientific), as described by Sousa and co-workers [8]. A calibration curve in the range of 0.005 to 50 ng/μL was constructed by serial dilutions of the *E. coli* gDNA. For endotoxin detection, ToxinSensor™Chromogenic Limulus amoebocyte lysate assay kit from GenScript (USA, Inc.) was used according to the manufacturer's instructions. A calibration curve was constructed with 10 EU/mL stock solution provided by the kit (0.005–0.1 EU/mL). For protein assessment, the Micro-BCA (bicinchoninic acid) protein assay kit from Pierce (Rockford, USA) was used, according to the manufacturer's instructions. A calibration curve was constructed with Bovine Serum Albumin (BSA) as standard protein (0.01–0.1 mg/mL).

3. Results and discussion

With the intent of exploring the Sephacryl matrix ability to isolate minicircle DNA, few conditions were initially tested. At first, the influence of flow rate was evaluated by performing the experiments at 0.45 mL/min and 0.3 mL/min. Such flow rate range was selected after evaluating different studies performed with similar intentions. For instance, Latulippe and co-workers, studied the elution profile of differently sized pDNAs with a Sephacryl column of 35 mL [9]. In this work, a flow rate of 0.2 mL was applied. However, Latulippe results suggest that low flow rates cannot guarantee the isolation of these different pDNAs due to diffusivity and pore accessibility by smaller plasmids [9]. This seemed important, considering the fact that sc mcDNA presents a smaller size than PP molecule. On the other hand, different studies have been performed with Sephacryl for the isolation of sc pDNA from other bacterial contaminants such as RNA or gDNA, which are other impurities that should be accounted for. While Ferreira developed a strategy with a 19 mL Sephacryl column for the isolation of a 4.8 Kbp pDNA at 0.5 mL/min, Li and co-workers studied the use of a 180 mL column at 0.57 mL/min for the purification of a 7.07 Kbp pDNA molecule from a complex sample [10,11]. Considering the flow rates used in previous works, it seemed logical to experiment an intermediate flow rate within the range of the flow rates previously presented, thus the 0.45 mL/min was selected. Fig. 1A presents the chromatogram and the respective electrophoresis, resulting from the assay performed at 0.45 mL/min. Fractions of 4 mL were recovered throughout the whole assay and few key fractions were selected, according to the chromatogram, to proceed for electrophoresis. As it is perceived from Fig. 1A, and as expected in size-exclusion chromatography [9], most high weight or larger molecules began to elute in the first fractions (peak I). Then, mcDNA eluted mostly in fractions 4 and 5, together with some high weight molecules (peak II). Then, a large peak is perceivable, composed mainly by RNA (peak III, fraction 10). The electrophoresis allowed the identification of the species eluting in each peak. In I, it is observed the main elution of gDNA and PP molecules, in peak II the mcDNA elutes, followed by the elution of small molecules such as RNA in III. This approach only allowed the recovery of mcDNA co-eluting with other impurities. Thus, to explore the effect of the flow rate on the separation of biomolecules and to improve peak resolution, expecting a consequent improvement on mcDNA purity, the flow rate of 0.3 mL/min

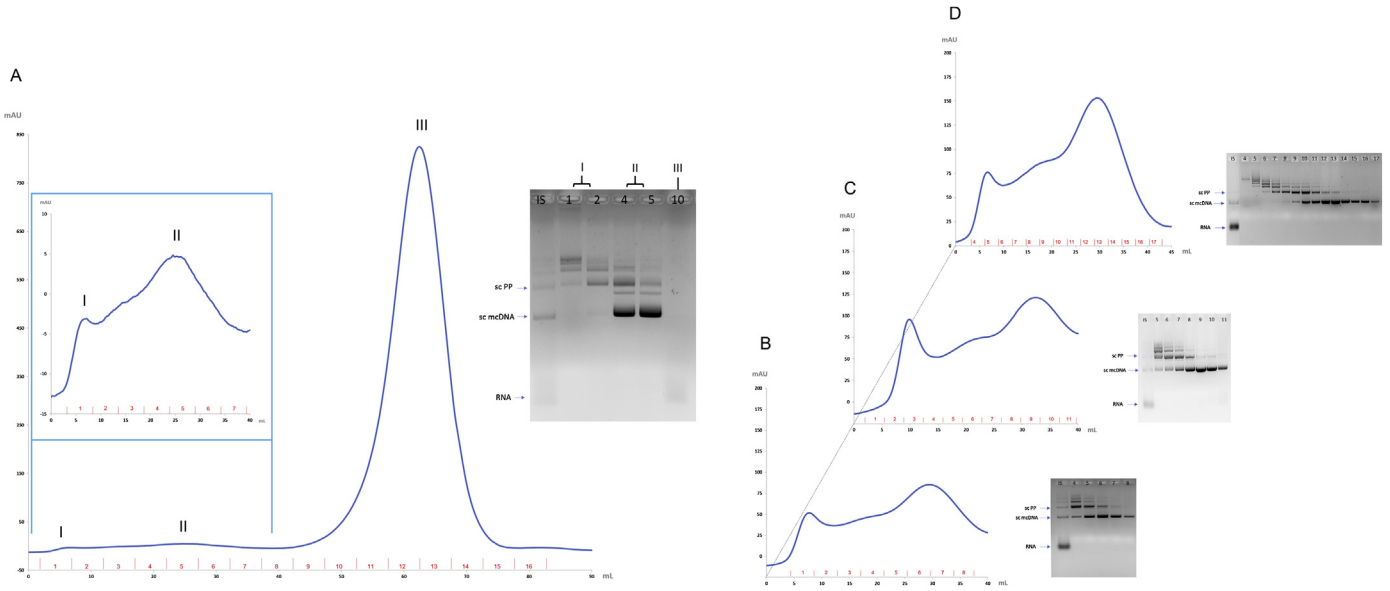

Fig. 1. Establishment of chromatographic conditions for mcDNA isolation using the Sephacryl support. Main elution peaks are marked as I, II and III. Chromatographic profile and corresponding electrophoresis of the selected fractions, using the following conditions: A – flow-rate of 0.45 mL/min, sample loading of 4 mL and fractionation of 4 mL, Vo =85 mL; B – flow-rate of 0.3 mL/min, sample loading of 4 mL and fractionation of 4 mL, Vo =48 mL; C – flow-rate at 0.3 mL/min, sample loading of 2 mL and fractionation of 4 mL, Vo = 38 mL; D – flow-rate at 0.3 mL/min, sample loading of 2 mL and fractionation of 3 mL, Vo =40 mL. IS – Initial Sample; Vo – Void Volume.

was then tested. It is known that in SEC the flow rate is inversely proportional to peak resolution [12,13]. Such phenomenon derives from the fact that, at high flow rates, molecules tend to lose the ability to diffuse in and out of matrix pores [12,13]. In Fig. 1B is presented the chromatogram and electrophoresis obtained in the experiment using 0.3 mL/min. Taking into account that mcDNA elution occurred in peak II of the previous experiment (Fig. 1A), the fractions chosen for electrophoresis were the corresponding to this part of the chromatogram. Here it is perceived that most of mcDNA-containing fractions were less contaminated than the previous assay (fractions 6–8). However, few adjustments were still necessary to improve its recovery with higher purity. As these previous assays were performed with the injection of 4 mL of sample, and given the fact that sample volume has been shown to affect the resolution in SEC [14], the injection of a smaller volume was tested to evaluate its effect in mcDNA isolation. Thus, an assay was performed with 2 mL of sample loading, using 0.3 mL/min as flow-rate. In Fig. 1C is presented the corresponding chromatogram and its electrophoresis. As it is perceived, few impurities are detected in the fractions where mcDNA is mainly eluting (fractions 9–11), suggesting that the reduction of the sample volume was advantageous for mcDNA isolation. Nonetheless, the dilution factor can be considered a main disadvantage of SEC, so in order to reduce this effect and trying to recover a purer and more concentrated mcDNA sample, the fraction size of the recovery was modified. Thus, as all previous assays were performed with 4 mL fraction volume, here it was adjusted to 3 mL. In Fig. 1D is presented the resulting chromatogram and electrophoresis. Here, it can be perceived with more detail the whole elution pattern of the injected complex sample. It is also verified that mcDNA elutes mainly between the fractions 10–17, but in the fractions 10–12 it is detected a high level of impurities. A comparative analysis of the selectivity reached with these different chromatographic conditions was performed regarding mcDNA separation from PP. It was found that the highest selectivity (4. 405) belongs to the last implemented strategy (1D), while the lowest selectivity belongs to the first strategy (1A). This data is supported by the electrophoresis analysis, where mcDNA seems to be almost fully isolated at 0.3 mL/min and with a sample loading of 2 mL. Therefore, fractions 13–17 were selected as the isolated mcDNA for further purity and recovery analysis.

Impurity levels of the sc mcDNA retrieved from Sephacryl matrix were analyzed. Although the criteria have been established for pDNA product, they can be used as a reference for the quality control of mcDNA samples, due to their similar nature and function. In this sample, gDNA levels were found at 0.002 μg /μg mcDNA and endotoxins presented levels of 11 EU/mg mcDNA, while proteins and RNA were undetectable. These data suggest Sephacryl is able to retrieve a pure mcDNA sample, which meets all the impurity criteria established by the competent authorities, such as FDA (under 0.01 μg /μg gDNA/pDNA, protein and RNA content undetectable and under 40 EU/mg endotoxins/pDNA) [15]. The low levels obtained for these impurities might be related with the fact that Sephacryl presents a broad fractionation range. Considering the fact that most proteins and RNA have smaller sizes, coupled with the fact that gDNA is much larger than the remaining molecules, the elimination of these impurities is not surprising. The large size of gDNA renders this molecule unable to interact with the matrix pores, thus first eluting apart from the molecule of interest. On the other hand, proteins and RNA, due to its smaller size, are able to enter into the pores, retarding its elution comparatively to mcDNA. In fact, other studies have highlighted the application of this matrix for the elimination of such impurities [10,16]. The assessment of the impurity levels is crucial when developing a purification strategy for a recombinant therapeutic product, given that the presence of such contaminants may induce adverse effects which can potentially harm the treated individual, by causing inflammation, septic shock or organ failure [17–19].

Also, the recovery (66% ± 4.37%) and purity (98.35% ± 1.56%) levels of mcDNA in comparison to other contaminants (PP and mP) were determined. These values were obtained as an average of three separated experiments, highlighting the reproducibility of this methodology. To obtain such high purity grade, the recovery was slightly sacrificed to avoid mcDNA contamination with other high molecular weight nucleic acids, similarly to other studies that have been designed to obtain pure and safe bioproducts. On the same note, Soares and co-workers reported recovery yield below

40% with the use of an arginine monolith for sc pDNA isolation [21]. Considering the importance of guaranteeing the purity of the target molecule for therapeutic applications, sometimes having a very high recovery is secondary. Moreover, SEC strategies usually contribute to higher dilution levels coupled with less recovery yield. Thus, taking into account the complexity of the sample and the mcDNA novelty, perhaps can be justifiable to maintain the current purification strategy. Other purification strategies have already been established for mcDNA isolation, such as the work conducted by Mayrhofer and co-workers or Alves and co-workers [3,4], but no indication about the recovery yield of their processes are provided. Mayrhofer and co-workers' strategy, which is based on the use of affinity ligands for mcDNA separation, does not allow the separation of mcDNA from PP molecules, and the efficiency of the process totally depends on the complete recombination of PP molecules to form mcDNA and mP. Moreover, this strategy also requires the modification of PP backbone to include the affinity sequence that will be the target for the recognition [3]. On the other hand, Alves and co-workers' study presents the added value of separating mcDNA from other molecules such as mP, PP and bacterial RNA [4]. However, this study describes a lengthy process which requires the use of enzymes before hydrophobic interaction chromatography (HIC). The use of enzymes and high concentration of salts, typically associated with HIC, can represent high costs in the industrial scale-up of this process, thus retrieving a more expensive mcDNA product. Nonetheless, other mcDNA purification strategies have been also published. Hou and co-workers, established a purification strategy resorting to magnetic beads which allows the separation of mcDNA from mP and PP [5]. Although it retrieves a 94–95% recovery yield, it requires the use of streptavidin-coated magnetic beads and the modification of PP backbone for affinity separation [5]. Like the others, this strategy can also be considered a costly approach to scale-up for industry. Notwithstanding, Diamantino and co-workers later published a strategy using a CIM DEAE commercial column (BIAseparations) for mcDNA separation from mP, PP and bacterial RNA. Such study was pioneer in establishing a scalable process for mcDNA purification industry, without added costs such as backbone modification. However, the recovery yield of this

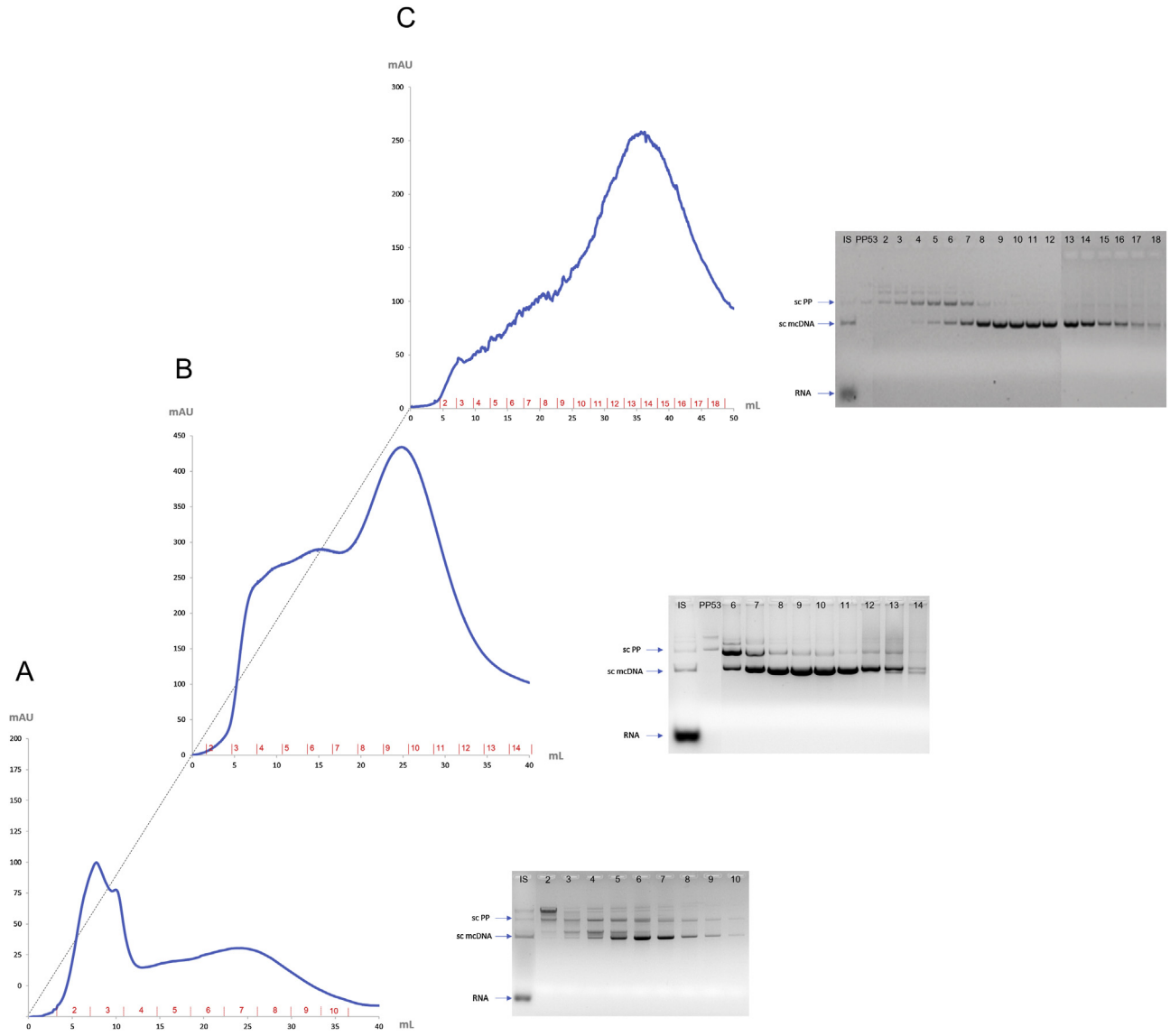

Fig. 2. Optimization of chromatographic conditions for mcDNA-p53 isolation. 2A – Chromatographic profile and corresponding electrophoresis of the selected fractions, using the following conditions: A – 60 cm column, flow-rate at 0.3 mL/min and sample loading of 2 mL, Vo = 38 mL; B – 60 cm column, flow-rate at 0.2 mL/min and sample loading of 2 mL, Vo =43 mL; C – 90 cm column, flow-rate at 0.3 mL/min and sample loading of 2.5 mL, Vo =65 mL. Fractionation was performed with 3 mL for all assays. IS – Initial Sample; Vo – Void Volume.

strategy is about 50%, which should be improved to lower the final biopharmaceutical price. More recently, a study conducted by our research group demonstrated the use of two monoliths for mcDNA purification, each one modified with either lysine or cadaverine ligands [22]. Following the first steps taken by Diamantino and co-workers, this work was designed with the intent of being applicable to different mcDNAs, without resorting to special modification of its backbone. In this study, good results were reported for cadaverine modified monolith, which was able to isolate sc mcDNA with 78.6% recovery yield and 98.4% purity [22]. Monoliths are innovative chromatographic structures that have been under the spotlight in the late years, especially due to the possibility of performing faster assays without loss of peak resolution. However, some limitations have been found. For instance, monoliths are prone to clog with the injection of more complex samples, mainly containing high content of gDNA [23]. The cadaverine-modified monolith strategy reports the injection of 100 μL of initial sample. Although this strategy is much faster than the one described in the current study, it would also require much more assays to obtain the same amount of pure mcDNA as a sole assay in Sephacryl matrix, considering an assay with cadaverine monolith renders only 1.97 μg of pure sc mcDNA while an assay with Sephacryl renders 24.02 μg of pure sc mcDNA. Thus, from an industrial point of view, the utilization of Sephacryl could be cheaper in terms of assays than cadaverine-modified monolith. Nonetheless, cadaverine-modified monolith could be a good approach to explore for the implementation of an analytical method for sc mcDNA assessment.

Thus, the data reported in the present work, allied with what is described in the literature, suggest that Sephacryl can be a lower cost isolation strategy and an improvement on what has been published so far regarding mcDNA downstream processing.

Considering that SEC strategy is mainly dependent on the size of the target product, and due to the need to characterize the robustness of the process, it seemed important to assess its ability to separate mcDNA containing a gene of interest, given that the initial tests were performed with an empty mcDNA vector and the inclusion of a gene will render a larger molecule. Thus, a complex lysate sample of mcDNA encoding the p53 was used. At first, the same conditions used for mcDNA empty vector were applied for mcDNA-p53 isolation. In Fig. 2A it is presented the corresponding chromatogram and electrophoresis. As expected, it was verified the co-elution of mcDNA with high molecular weight impurities (corresponding to PP 53) in a higher extent, when compared with the empty mcDNA sample, under the same conditions. While the empty mcDNA vector has a molecular weight of 3.8 Kbp, mcDNA-p53 has a molecular weight of 5 Kbp. The fact that mcDNA-p53 has a larger size may hamper its isolation from other contaminants, accounting that this molecule will have less distribution to the matrix pores, than smaller molecules, therefore, be more prone to elute concomitantly with larger molecules [24]. Thus, few adjustments in this strategy were still necessary in order to improve the mcDNA-p53 purity. As previously mentioned, the flow rate can affect peak resolution [12,13], while the increase of the column height is also known to be an important factor for the separation of molecules with similar weights. To understand the contribution of both parameters in mcDNA-p53 isolation two assays were performed. The first one consisted in the decrease of the flow rate to 0.2 mL/min and the second one was accomplished in a new column containing Sephacryl S-1000 SF matrix, with an increase of 50% in height, resulting in 90 cm. In Fig. 2B and C are respectively portrayed the resulting chromatograms and electrophoresis. The results achieved by changing the flow-rate (2B) demonstrated that the isolation of mcDNA was improved. Actually, the co-elution of high weight molecules, such as PP, with the mcDNA was reduced, in comparison with the previous flow conditions (2A), thus suggesting that lowering the flow rate can improve the purity of mcDNA. In Fig. 2C, given that the aim was to solely study the effect of column height, the flow was maintained at 0.3 mL/min and the sample loading was accordingly adjusted to column volume (1.65% of the volume). In comparison to Fig. 2A and B, here it is noticeable that mcDNA appears to be further isolated, suggesting that adjusting the column height might be more important and practical for the isolation of higher weight mcDNA molecules than lowering the flow. Selectivity was also analyzed for mcDNA-p53 isolation from PP-p53. Although better sc mcDNA isolation is perceived in the electrophoresis with the increase of the column height and decrease of flow rate, selectivity is lower under these conditions. The highest selectivity value found was 3.49 for the 60 cm column coupled with 0.3 mL/min flow rate (2A), while the lowest selectivity was found for the last strategy studied (2C). The low selectivity results in the loss of peak resolution, which Latulippe and co-workers have found to decrease at lower flow rates [9]. Although low peak resolution is theoretically undesirable, the crucial aim of this work is to recover the isolated target molecule. This achievement is proven by electrophoresis and qPCR, suggesting the low resolution found for the target peak does not impair the implementation of this strategy.

In conclusion, the use of Sephacryl matrix might be a suitable strategy to isolate different mcDNA molecules, regardless their backbone and without resorting to expensive clarification strategies such as the use of enzymes, requiring only the adjustment of the assay conditions accordingly with mcDNA size.

Declaration of Competing Interest

The authors declare that they have no known competing financial interests or personal relationships that could have appeared to influence the work reported in this paper.

Acknowledgements

This work was supported by FEDER funds through the POCI - COMPETE 2020 - Operational Programme Competitiveness and Internationalization in Axis I - Strengthening research, technological development and innovation (Project POCI-01-0145-FEDER-007491) and National Funds by FCT - Foundation for Science and Technology (Project UID/Multi /00709/2013). Also, A.M, Almeida acknowledges a doctoral fellowship (SFRH/BD/102284/2014) from FCT.

References

[1] P. Mayrhofer, M. Schleef, W. Jechlinger, Use of minicircle plasmids for gene therapy, Methods Mol. Biol. 542 (2009) 87–104, http://dx.doi.org/10.1007/978-1-59745-561-9_4.
[2] V.M. Gaspar, C.J. Maia, J.A. Queiroz, C. Pichon, I.J. Correia, F. Sousa, Improved minicircle DNA biosynthesis for gene therapy applications, Hum. Gene Ther. Methods 25 (2014) 93–105, http://dx.doi.org/10.1089/hgtb.2013.020.
[3] P. Mayrhofer, M. Blaesen, M. Schleef, W. Jechlinger, Minicircle-DNA production by site specific recombination and protein-DNA interaction chromatography, J. Gene Med. 10 (2008) 1253–1269, http://dx.doi.org/10.1002/jgm.1243.
[4] C.P.A. Alves, M. Šimčíková, L. Brito, G.A. Monteiro, D.M.F. Prazeres, Development of a nicking endonuclease-assisted method for the purification of minicircles, J. Chromatogr. A 1443 (2016) 136–144, http://dx.doi.org/10.1016/j.chroma.2016.03.035.
[5] X.H. Hou, X.Y. Guo, Y. Chen, C.-Y. He, Z.-Y. Chen, Increasing the minicircle DNA purity using an enhanced triplex DNA technology to eliminate DNA contaminants, Mol. Ther. — Methods Clin. Dev. 1 (2015) 14062, http://dx.doi.org/10.1038/mtm.2014.62.
[6] T. Diamantino, P. Pereira, J.A. Queiroz, Â. Sousa, F. Sousa, Minicircle DNA purification using a CIM® DEAE-1 monolithic support, J. Sep. Sci. 39 (2016) 3544–3549, http://dx.doi.org/10.1002/jssc.201600375.
[7] M.M. Diogo, J. a Queiroz, G. a Monteiro, S. a Martins, G.N. Ferreira, D.M. Prazeres, Purification of a cystic fibrosis plasmid vector for gene therapy using hydrophobic interaction chromatography, Biotechnol. Bioeng. 68 (2000) 576–583, doi:10.1002/(SICI)1097-0290(20000605)68:5<576::AID-BIT13>3.0.CO;2-5 [pii].
[8] A. Sousa, C.T. Tomaz, F. Sousa, J.A. Queiroz, Successful application of monolithic innovative technology using a carbonyldiimidazole disk to purify

supercoiled plasmid DNA suitable for pharmaceutical applications, J. Chromatogr. A 1218 (2011) 8333–8343, http://dx.doi.org/10.1016/j.chroma.2011.09.033.
[9] D.R. Latulippe, A.L. Zydney, Size exclusion chromatography of plasmid DNA isoforms, J. Chromatogr. A (2009), http://dx.doi.org/10.1016/j.chroma.2009.07.009.
[10] G.N.M. Ferreira, J.M.S. Cabral, D.M.F. Prazeres, A comparison of gel filtration chromatographic supports for plasmid purification, Biotechnol. Tech. 11 (1997) 417–420, http://dx.doi.org/10.1023/A:1018420807203.
[11] L.Z. Li, Y. Liu, M.S. Sun, Y.M. Shao, Effect of salt on purification of plasmid DNA using size-exclusion chromatography, J. Chromatogr. A (2007), http://dx.doi.org/10.1016/j.chroma.2006.11.027.
[12] A. Biosciences, Gel-filtration: Principles and Methods, Amersham Biosci. Handbooks, 2006, http://dx.doi.org/10.1038/nmeth0506-411.
[13] C. Ó'Fágáin, P.M. Cummins, B. O'Connor, Gel-filtration chromatography, Methods Mol. Biol. (2017), http://dx.doi.org/10.1007/978-1-4939-6412-3_2.
[14] S. Yamamoto, M. Nomura, Y. Sano, Scaling up of medium-performance gel filtration chromatography of proteins, J. Chem. Eng. Japan 19 (1986) 227–231.
[15] Guidance for industry: considerations for plasmid DNA vaccines for infectious disease indications, Biotechnol. Law Rep. 26 (2008) 641–647, http://dx.doi.org/10.1089/blr.2007.9905.
[16] N.A. Horn, J.A. Meek, G. Budahazi, M. Marquet, Cancer gene therapy using plasmid DNA: purification of DNA for human clinical trials, Hum. Gene Ther. 5 (1995) 565–573, http://dx.doi.org/10.1089/hum.1995.6.5-565.
[17] Z. Wei, W. Huang, J. Li, G. Hou, J. Fang, Z. Yuan, Studies on endotoxin removal mechanism of adsorbents with amino acid ligands, J. Chromatogr. B Anal. Technol. Biomed. Life Sci. 852 (2007) 288–292, http://dx.doi.org/10.1016/j.jchromb.2007.01.038.
[18] C.I. Wooddell, V.M. Subbotin, M.G. Sebestyén, J.B. Griffin, G. Zhang, M. Schleef, S. Braun, T. Huss, J.A. Wolff, Muscle damage after delivery of naked plasmid DNA into skeletal muscles is batch dependent, Hum. Gene Ther. 22 (2011) 225–235, http://dx.doi.org/10.1089/hum.2010.113.
[19] R.P. Bazzani, Y. Cai, H.L. Hebel, S.C. Hyde, D.R. Gill, The significance of plasmid DNA preparations contaminated with bacterial genomic DNA on inflammatory responses following delivery of lipoplexes to the murine lung, Biomaterials 32 (2011) 9854–9865, http://dx.doi.org/10.1016/j.biomaterials.2011.08.092.
[21] A. Soares, J.A. Queiroz, F. Sousa, A. Sousa, Purification of human papillomavirus 16 E6/E7 plasmid deoxyribonucleic acid-based vaccine using an arginine modified monolithic support, J. Chromatogr. A 1320 (2013) 72–79, http://dx.doi.org/10.1016/j.chroma.2013.10.053.
[22] A.M. Almeida, J.A. Queiroz, F. Sousa, A. Sousa, Minicircle DNA purification: performance of chromatographic monoliths bearing lysine and cadaverine ligands, J. Chromatogr. B Anal. Technol. Biomed. Life Sci. 1118–1119 (2019) 7–16, http://dx.doi.org/10.1016/j.jchromb.2019.04.024.
[23] K. Benčina, M. Benčina, A. Podgornik, A. Štrancar, Influence of the methacrylate monolith structure on genomic DNA mechanical degradation, enzymes activity and clogging, J. Chromatogr. A 1160 (2007) 176–183, http://dx.doi.org/10.1016/j.chroma.2007.05.034.
[24] K. Nagy, K. Vékey, Separation methods, Med. Appl. Mass Spectrom. (2008), http://dx.doi.org/10.1016/B978-044451980-1.50007-0.

Paper VII

Quality assessment of supercoiled minicircle DNA by cadaverine-modified analytical chromatographic monolith

A.M. Almeida[a], U. Černigoj[b], J.A. Queiroz[a], F. Sousa[a], A. Sousa[a]

[a]*CICS-UBI – Centro de Investigação em Ciências da Saúde, Universidade da Beira Interior, Av. Infante D. Henrique, 6200-506 Covilhã, Portugal*
[b]*BIA Separations d.o.o., Mirce 21, 5270 Ajdovščina, Slovenia*

Journal of Pharmaceutical and Biomedical Analysis (2019) 180: 113037

Short description: An original research paper describing the implementation of an analytical chromatographic method for the characterization of minicircle DNA content in complex and pure samples.

Journal of Pharmaceutical and Biomedical Analysis 180 (2020) 113037

Contents lists available at ScienceDirect

Journal of Pharmaceutical and Biomedical Analysis

journal homepage: www.elsevier.com/locate/jpba

Quality assessment of supercoiled minicircle DNA by cadaverine-modified analytical chromatographic monolith

A.M. Almeida[a], U. Černigoj[b], J.A. Queiroz[a], F. Sousa[a], A. Sousa[a,*]

[a] CICS-UBI – Centro de Investigação em Ciências da Saúde, Universidade da Beira Interior, Av. Infante D. Henrique, 6200-506 Covilhã, Portugal
[b] BIA Separations d.o.o., Mirce 21, 5270 Ajdovščina, Slovenia

ARTICLE INFO

Article history:
Received 18 September 2019
Received in revised form 5 December 2019
Accepted 7 December 2019
Available online 9 December 2019

Keywords:
Analytical chromatography
Cadaverine-modified monolith
Minicircle DNA assessment
Method validation

ABSTRACT

Minicircle DNA (mcDNA) is the ultimate non-viral DNA vector, presenting higher biosafety and therapeutic effect than conventional plasmid DNA (pDNA). However, given the similarity between mcDNA and its precursor, the parental plasmid (PP), analytical methodologies established for pDNA are unable to distinguish mcDNA from PP. Thus, a new need emerged for the implementation of suitable, rapid and non-expensive analytical methodologies for the characterization of mcDNA samples. Recently, our research group was able to develop a purification strategy for the isolation of supercoiled (sc) mcDNA resorting to cadaverine-modified monolith. Considering the promising results obtained with this strategy, a cadaverine-modified analytical monolith was prepared and explored for mcDNA quantification. Thus, a strategy of three-step increasing NaCl gradient was considered to first elute RNA/protein content, then isolate sc mcDNA and finally eliminate PP and other impurities still bounded to the matrix. A calibration curve was constructed with different sc mcDNA standards within a range of 1–25 μg/mL. Linearity, accuracy, precision and selectivity of this method were validated according to the international guidelines and the limit of detection and the lower limit of quantification were determined as 1 μg/mL. For the first time, to the best of our knowledge, an analytical method for mcDNA quantification is described. Besides ensuring the safety of mcDNA application by assessing the product purity, such methodology can be used in the future to control industrial mcDNA production and purification, perhaps aiding in the establishment of optimized and less expensive biotechnological operations.

1. Introduction

Minicircle DNA (mcDNA) is a DNA vector increasingly considered in gene therapy and DNA vaccines in the past recent years. Such acceptance amongst researchers is based on the fact that this cutting-edge DNA technology renders a molecule devoid of prokaryotic sequences, which are usually associated to adverse effects when administered to patients. The use of specifically modified *E. coli* ZYCY10P3S2T cells allows the PhiC31 integrase and I-SceI endonuclease expression [1]. Upon recombination induction, PhiC31 integrase will recombine parental plasmid (PP) into mcDNA, while I-SceI expression will lead to the degradation of mP and unrecombined PP molecules, which present the I-SceI sites. However, PP residues are still found at the end of this process, most probably due to its incomplete recombination and digestion [2]. So far, no chromatographic methods for mcDNA analysis have been established and many difficulties have been found by scientists in establishing chromatographic strategies for mcDNA isolation that do not resort to specific modifications to the backbone of the PP plasmid or enzymatic digestions.

Taking into account the growing interest of the biotechnological research in the study and application of sc mcDNA, it has become crucial to develop suitable strategies that can guarantee the biosafety and therapeutic effect of this biopharmaceutical, considering its prokaryotic production. Besides the importance of monitoring the production/recombination, extraction and purification of mcDNA throughout the whole process, in the end it is necessary to assure the purity and the host component levels meet the specifications imposed by regulatory agencies. Analytical methods developed so far for pDNA analysis do not present enough selectivity towards the sc mcDNA isolation from oc mcDNA and oc and sc PP isoforms. Beyond the structural similarities of both mcDNA isoforms and the PP isoforms, differing only in size, mcDNA also shares physicochemical properties, as it presents the same sequences of its precursor PP [2,3]. Actually, this represents a big

* Corresponding author at: Centro de Investigação em Ciências da Saúde, Universidade da Beira Interior, Av. Infante D. Henrique, 6200-506 Covilhã, Portugal.
E-mail address: angela@fcsaude.ubi.pt (A. Sousa).

https://doi.org/10.1016/j.jpba.2019.113037
0731-7085/

challenge for the separation of these species and, thus, many efforts have been placed into exploring new chromatographic strategies for mcDNA purification [3–6]. As a matter of fact, our research group has recently published a study describing the use of cadaverine-modified monolith in the isolation and purification of sc mcDNA from a clarified lysate sample [2]. This particular study yielded sc mcDNA with 98.4% purity and 78.6% recovery yield without resorting to PP backbone modification or enzymatic digestion. Such analysis was performed by resorting to real-time PCR, which is an expensive and time-consuming methodology, especially when compared to analytical chromatography.

Considering the potential demonstrated by cadaverine-modified monolith in mcDNA purification and the selectivity achieved for the sc mcDNA isoform, our research group decided to prepare a cadaverine-modified analytical monolith and study the implementation of an analytical method for mcDNA quantification (Fig. 1). Thus, this work describes the validation of a rapid and cheap quantitative methodology for sc mcDNA, following the international guidelines [7].

2. Materials and methods

2.1. Different mcDNA and PP vectors lysate production and purification

To produce mcDNA, PP amplification was first carried out as previously described by Diamantino and co-workers [3]. *E. coli* strain ZYCY10P3S2T was grown in Terrific Broth medium (20 g/L of tryptone, 24 g/L of yeast extract, 4 mL/L of glycerol, 0.017 M KH_2PO_4, 0.072 M K_2HPO_4) at 42 °C, 250 rpm. Recombination of PP into mcDNA was induced through the addition of an induction mixture containing 0.01% L-arabinose diluted in LB medium, supplemented with 0.04 M NaOH. Induction was carried out for 3 h at 32 °C, before recovering cells through centrifugation. To prepare a PP clarified sample, induction step was not performed during the fermentation procedure. Clarified lysate samples of either PP and mcDNA were prepared with the modified alkaline lysis protocol described by Diogo and co-workers [8], followed by a desalting step with PD-10 desalting columns (GE Healthcare, Buckinghamshire, UK). This procedure was applied for the preparation of three different mcDNA-PP pairs. First, the pMC.CMV-MCS-EF1-GFP-SV40 PolyA vector was used as the standard mcDNA-PP pair (3.8 Kbp and 7.06 Kbp). Then, the same vector (pMC.CMV-MCS-EF1-GFP-SV40 PolyA) was subjected to an enzymatic digestion resulting in a smaller mcDNA-PP pair (0.88 Kbp and 4.88 Kbp). Moreover, a new insert (p53 gene) was included in the standard vector (pMC.CMV-MCS-EF1-GFP-SV40 PolyA), allowing the preparation of a larger mcDNA-PP pair (5 Kbp and 8.2 Kbp). To achieve a sc mcDNA purified sample, a strategy previously implemented with cadaverine-modified monolith was used [2].

2.2. Cadaverine modified analytical monolith preparation

A cadaverine-modified analytical monolith was prepared as described by Almeida and co-workers [2]. Briefly, a cadaverine ligand (Alfa Aesar, Karlsruhe, Germany) was immobilized on a 0.1 mL bed volume of a Convective Interaction Media (CIM®) analytical epoxy chromatographic monolith (CIMac™), provided by BIA Separations (Ajdovščina, Slovenia). Cadaverine hydrochloride (0.6 g) was dissolved in water (3.5 mL), followed by 5 M NaOH addition to adjust pH to 10.5. Afterwards, 2 mL of ethanol was added, followed by pumping of the reagent through the monolith channels. Then, the monolith was incubated together with the immobilization solution for 48 h at 60 °C. The quenching of the remaining epoxy groups was carried out with 0.5 M H_2SO_4 (5 h at 65 °C), followed by washing the monoliths with water and storing them in 20% ethanol.

2.3. Analytical chromatographic assays

All chromatographic experiments were carried out using an AKTA Pure system (GE Healthcare, Buckinghamshire, UK), with a computer unit controlled by UNICORN™ 6.3 software. For DNA standards, samples were prepared by consecutive dilution of a stock sc mcDNA sample with the equilibration buffer used in the chromatographic experiments. All final concentrations were confirmed with Ultrospec 3000 UV/Visible Spectrophotometer (Pharmacia Biotech, Cambridge, England). The conditions used to explore the implementation of an analytical method were based on a mcDNA purification strategy previously developed by our research group with cadaverine-modified monolith [2]. Thus, the analytical monolith was first equilibrated with 1.07 M NaCl in 10 mM Tris-EDTA buffer (pH 7.0), followed by sample injection (50 μL). After washing out the unbound species, namely RNA, a salt increase adjustment to 1.16 M NaCl in 10 mM Tris-EDTA buffer (pH 7.0) was performed, for mcDNA elution. Flow-rate was kept at 1 mL/min and UV was monitored at 260 nm. Then, to elute strongly bound PP and other molecules with higher molecular weight, salt concentration was increased to 1.3 M NaCl in 10 mM Tris-EDTA buffer (pH 7.0). All experiments were performed at room temperature (≈25 °C), a parameter that was simultaneously measured together with the conductivity. The conductivity control demonstrated to be crucial, given that it highly influences mcDNA selectivity.

2.4. Agarose gel electrophoresis

All the recovered fractions were desalted and concentrated to 200 μL, by Vivaspin® 6 Centrifugal Concentrator (Vivaproducts, Littleton, MA, USA), before injecting them onto the electrophoresis. The agarose gel was prepared for 0.8%, stained with 0.016 μL/mL Greensafe premium (NZYTech, Lda. - Genes and Enzymes, Lisbon, Portugal), and the horizontal electrophoresis was carried out at 110 V for 30 min in TAE buffer (40 mM Tris base, 20 mM acetic acid and 1 mM EDTA, pH8.0), before visualizing the gel under UV light in a Vilber Lourmat system (ILC Lda, Lisbon, Portugal).

3. Results and discussion

The establishment of an adequate analytical method for the purity assessment of a biotechnological product, such as mcDNA, must comprise the validation of different parameters [7]. Monoliths are becoming the new standard in chromatographic columns, offering the possibility of establishing fast methods with separation independent of flow rate. These features are a consequence of the monolith continuous bed and its interconnectivity between channels, which allow fast mass transfer and increased accessibility of the target molecule without loss of peak resolution [9]. Given the lack of analytical methodologies developed for mcDNA, the discussion will be carried out by taking into account analytical methods established for pDNA quality assessment.

3.1. Selectivity

Considering the fact that the isolation of sc mcDNA with cadaverine-modified monolith had already been established [2], we decided to explore the potential of this chromatographic strategy as an analytical method, but in this work, the loading volume was adjusted from 200 μL to 50 μL to decrease the amount of sample spent per assay. First, it was assessed the selectivity of the analytical monolith modified with the cadaverine ligand. The target molecule

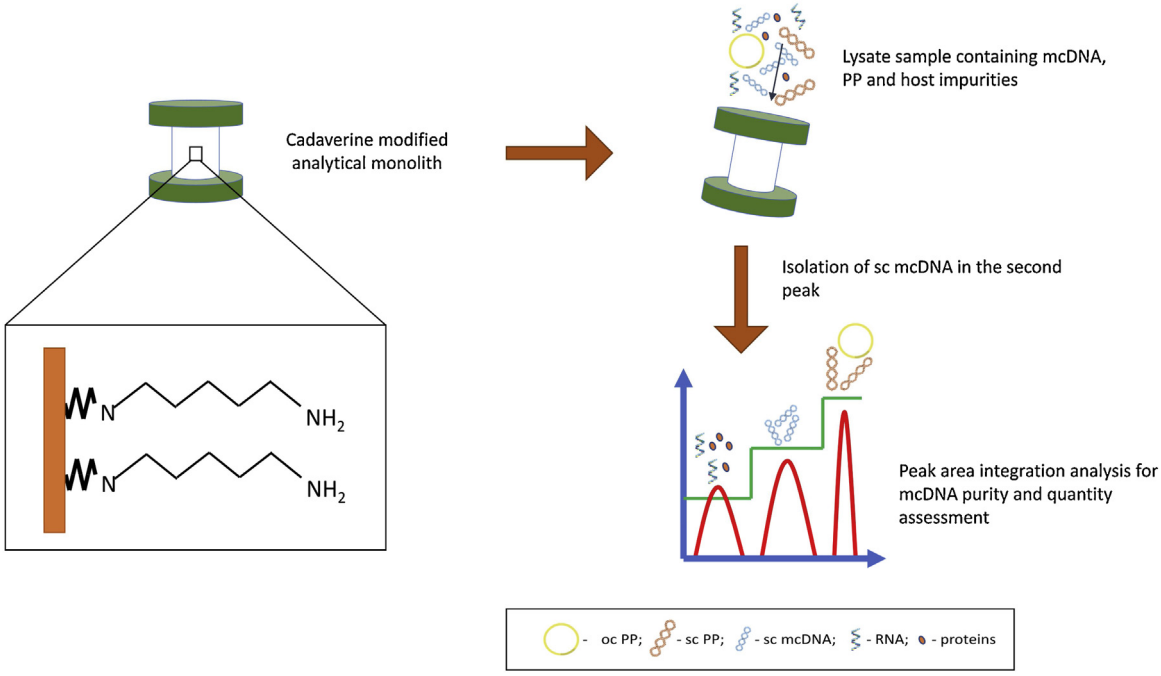

Fig. 1. Graphical representation of chromatographic analytic method for the mcDNA assessment from *E. coli* lysate samples with the cadaverine-modified analytical monolithic column.

should be distinguished from all other contaminants present in the sample, especially PP. To verify the selectivity of cadaverine analytical monolith, three chromatographic experiments were performed with a mcDNA-containing lysate sample (also presenting PP and other bacterial impurities, such as gDNA, RNA, proteins, etc), a PP-enriched lysate sample (containing PP and other bacterial impurities, but in the absence of mcDNA), and a blank sample. The blank was performed by injecting the buffer used for the preparation of the standards (10 mM Tris-EDTA pH 7.0).

In Fig. 2

are represented the respective chromatograms corresponding to each sample: mcDNA lysate (2A), PP lysate (2B) and blank (2C). As portrayed in Fig. 2A and 2B, after injection of 50 μL of sample, the RNA present in each lysate is eluted in the first step at 1.07 M NaCl (peaks 1 and 4). There is a small peak, of similar size, present on all three chromatograms (including blank) at 16.05–16.10 min, just after the second step gradient application, which is considered to be a consequence of an absorbance disturbance due to a sudden buffer change. Such phenomenon has been observed in other studies [10]. Then, different chromatographic profiles can be observed between the different samples. The chromatogram of the mcDNA lysate (Fig. 2A) presents only one peak (2) at retention time (RT) of 18.34 min, occurring in the second-step of the gradient at 1.16 M NaCl and corresponding to mcDNA elution, as observed in lane 2 of the electrophoresis. However, PP lysate (Fig. 2B) reveals only a peak (6), at RT =19.84 min, which does not present nucleic acids elution, as verified in lane 6 of electrophoresis. Interestingly, the mcDNA peak does not begin to elute immediately after the step gradient application, but it is delayed for approximately 2 min (from 16.1 to 18.3 min). This might be related to the fact that a small salt increasing step (from 1.07 to 1.16 M NaCl) creates a semi linear gradient conditions, in the middle of which the mcDNA content elutes. Finally, PP molecules are eluted in the third-step gradient performed at 1.3 M NaCl, as perceivable for both mcDNA and PP lysates (peak 3 and lane 3 of Fig. 2A and peak 7 and lane 7 of Fig. 2B, respectively). At this point, PP lysate presents a larger peak than mcDNA lysate. This is explained by the fact that in the mcDNA-containing lysate, most of PP content belonging to mcDNA lysate has been recombined into mcDNA, thus reducing the PP content. Moreover, molecules of high molecular weight, such as gDNA, are concomitantly eluted with PP (Fig. 2A and 2B). Therefore, it can be concluded that this analytical method presents selectivity towards mcDNA, as it had been previously verified [2].

3.2. Linearity

The establishment of an analytical method for mcDNA quantification started with linearity assessment. Thus, the injection of six different mcDNA concentrations was performed under the chromatographic conditions previously established. A standard curve was prepared by using 3 replicates of 6 known mcDNA concentrations (1, 2.5, 5, 10, 17.5 and 25 μg/mL). In general, pDNA standard curves used in the implementation of analytical methods present higher concentrations than the ones selected for this study. For instance, Mota and co-workers even performed a study considering two different ranges (2–20 μg/mL and 20–200 μg/mL) for different applications [11]. However, in the current scenario, sc mcDNA content in lysate samples is much lower than the amount of pDNA usually observed. Besides the fact that this is a smaller molecule, its production results from an induction process where total PP recombination does not occur, implying a lower mcDNA final content. The standards were obtained by diluting a stock mcDNA solution with 10 mM Tris-EDTA pH 7.0, also used to prepare the chromatographic buffers. The calibration curve was determined by calculating the peak area correspondent to the mcDNA elution (RT = 18.34), obtained in the second-step gradient of each chromatogram (all raw data is available in Supplementary Information 1). The obtained calibration curve, with the equation Y = 0.9416 X – 0.2781, presented a correlation coefficient of 0.999 (the curve is available in Supplementary Information 2). In Fig. 3 the mcDNA chromatographic peaks are shown for all prepared standards. The peak of interest increases proportionally with the concentration

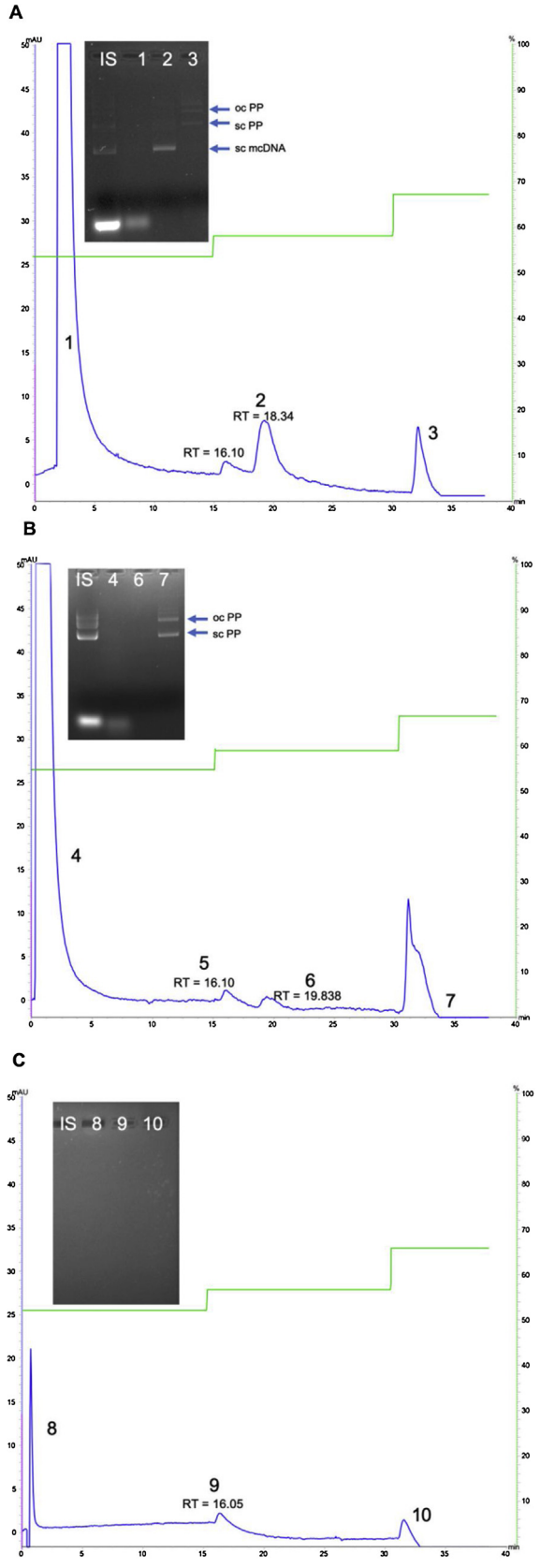

Fig. 2. Selectivity evaluation employing cadaverine-modified chromatographic column. Chromatographic runs performed with 1.07 M NaCl in 10 mM Tris–HCl/EDTA (pH 7.0, 91.01 mS/cm), followed by 1.16 M NaCl in 10 mM Tris–HCl/EDTA (pH 7.0, 96.72 mS/cm) and 1.3 M NaCl in 10 mM Tris–HCl/EDTA (pH 7.0, 106.2 mS/cm). A – Chromatographic run of mcDNA clarified lysate sample, containing also PP and other bacterial impurities (gDNA, RNA, proteins, etc). B – Chromatographic run of PP clarified lysate sample, containing PP and other bacterial impurities (gDNA, RNA, proteins, etc) but without mcDNA, with respective electrophoresis. C – Chromatographic run of blank sample (constituted of 10 mM Tris-EDTA pH 7.0).

Table 1
Accuracy for the assessment of mcDNA in the range of 1–25 μg/mL (n = 3).

Nominal Concentration (μg/mL)	Mean Concentration[a] (μg/mL)	Standard Deviation	CV[b] (%)	Mean relative Error[c] (%)
25	24.97	0.43	1.71	0.14
17.5	17.84	1.51	8.49	1.93
12.5	12.02	0.60	5.03	3.87
10	9.45	0.12	1.24	5.49
5	4.97	0.26	5.22	0.60
2.5	2.67	0.01	0.35	6.83
1	1.10	0.11	10.02	10.19

[a] Calibration curve used (y = mx + b): m = 0.9416; b = - 0.2781; R2 = 0.999.
[b] Coefficient of variation.
[c] ([(Measured concentration)–(nominal concentration)]/(nominal concentration)) x 100.

increase. A "ghost" peak with RT of 16.01 min, described in Fig. 2C due to the buffer exchange, is observed in all samples independently of the mcDNA concentration. The correlation coefficient of 0.999 meets the values found for correlation coefficients of other established pDNA quantification methods, therefore it can be concluded that the linearity requirement was met by this chromatographic strategy [11–15].

3.3. Accuracy

Accuracy was determined by back-calculating the concentration of each standard, using the equation provided by the calibration curve. Also, an intermediate concentration, that was not used for the construction of the calibration curve, was back-calculated (12.5 μg/mL). In Table 1 it is presented the mean concentration values found for each nominal concentration (3 replicates), followed by the corresponding standard deviation, coefficient of variation (CV) and mean relative error. Through Table 1 analysis, we are able to infer that the lowest nominal concentration (1 μg/mL) presents the highest mean relative error (10.19%), as well as the highest coefficient of variation (10.02%). On the other hand, the lowest mean relative error (0.14%) was calculated for the highest nominal concentration (25 μg/mL) while the lowest coefficient of variation was presented by 2.5 μg/mL standard (0.35%). Mota and co-workers were able to establish an analytical method for sc pDNA quantification by resorting to a CIM DEAE monolithic disk [11]. In that study, the coefficients of variation for accuracy were found to vary between 0.65% and 3.68%, while the mean relative error was found in a range from 0.19% and 2.25%. Although higher coefficient of variation and mean relative error values were found in our study, both are within the ± 15% range accepted by the established guidelines [7]. Nonetheless, in the current work, a lower nominal concentration (1 μg/mL) was studied in comparison to other established analytical methods (2 μg/mL) [11,13]. These results are in agreement with data found in other similar studies, as for instance the work developed by Quaak and co-workers, whom established a methodology for the quantification of sc pDNA pDERMATT by resorting to a TSKgel DNA-NPR analytical column [14].

3.4. Limit of detection and limit of quantification

Table 1 also allows to infer the sensitivity of the method by determining the lower limit of quantification (LLOQ), which represents the lowest mcDNA concentration that can be assessed with

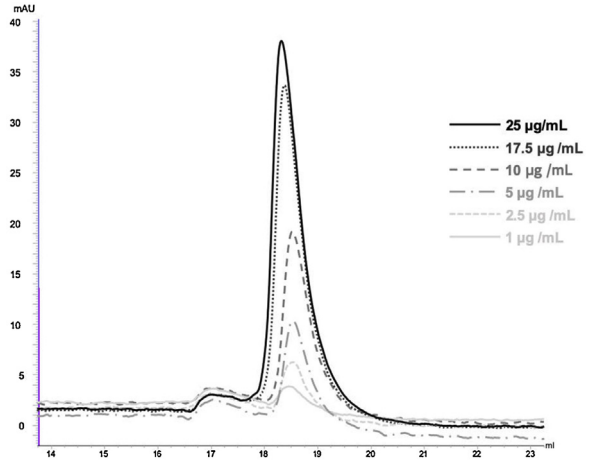

Fig. 3. mcDNA linearity assessment. Second step profile obtained for 6 sc mcDNA standards with the concentration of 1, 2.5, 5, 10, 17.5 and 25 µg/mL. Chromatographic runs performed with 1.07 M NaCl in 10 mM Tris–HCl/EDTA (pH 7.0, 91.01 mS/cm), followed by 1.16 M NaCl in 10 mM Tris–HCl/EDTA (pH 7.0, 96.72 mS/cm) and 1.3 M NaCl in 10 mM Tris–HCl/EDTA (pH 7.0, 106.2 mS/cm).

Table 2
Intra-day precision for the assessment of mcDNA (n = 3).

Nominal Concentration (µg/mL)	Mean Concentration[a] (µg/mL)	Standard Deviation	CV[b] (%)	Mean relative Error[c] (%)
17.5	16.54	0.60	3.60	5.48
5	5.00	0.04	0.90	0.01
2.5	2.67	0.01	0.35	6.83

[a] Calibration curve used (y = mx + b): m = 0.9416; b = - 0.2781; R2 = 0.999.
[b] Coefficient of variation.
[c] ([(Measured concentration)–(nominal concentration)]/(nominal concentration)) x 100.

suitable precision and adequate accuracy (± 20% of the nominal concentration) [7]. Taking into account the data displayed in Table 1, it is possible to establish the LLOQ of this strategy as 1 µg/mL, which presents a coefficient of variation of 10.02% and a mean relative error of 10.19%, lower than the 20% limit range accepted by the guidelines. The limit of detection (LOD), which is described by the guidelines as a signal-to-noise ratio of 3:1 between the measured signals of known low mcDNA concentration samples and the blank samples, was also determined. This allows to establish the minimum concentration limit at which mcDNA can be detected [7]. Thus, the chromatogram of Fig. 2C, corresponding to the blank sample, was integrated and a comparative analysis was performed between the peak area of this assay and the peak area observed for the lowest standard at RT of 18.34 min. Since the blank did not present any peak corresponding to this RT, it was possible to identify 1 µg/mL as the LOD for this method, similarly to what was described by Diogo and co-workers [12]. Despite the fact that the same LOD was verified for both studies, Diogo's work was implemented for total pDNA quantification, and this concentration would correspond to both sc and oc isoforms. In the current study, however, this LOD was observed for mcDNA exclusively in sc conformation.

3.5. Precision

To evaluate the precision of this analytical method, reproducibility and repeatability studies were performed according to the guidelines [7]. The repeatability (or intra-day) assessment for mcDNA quantification is shown in Table 2. Three different standards were injected three consecutive times to evaluate intra-day repeatability. As presented in Table 2, the standard with highest mean relative error was 2.5 µg/mL (6.83%) and the standard with highest variation was 17.5 µg/mL (3.60%). Such values are very close to the ones found by Sousa and co-workers, 6.86% and 3.45% respectively, who were able to develop an analytical method based on arginine-affinity chromatography for oc and sc pDNA isoform separation [13]. Thus, both values remain below the 15% range accepted by the guidelines, consequently highlighting the repeatability of this analytical method [7]. On the other hand, in Table 3 it is portrayed the method's reproducibility (or inter-day) evaluation. To assess this parameter, three different standards were injected throughout three different days. In Table 3, it is possible to analyse that the standard with highest mean relative error (6.74%) and highest coefficient of variation (7.59%) was 2.5 µg/mL. Again, similar values were found by Sousa and co-workers (4.03% and 5.13%, respectively) [13]. These values remain below the 15% range accepted by the guidelines, therefore suggesting this analytical method is reproducible. Thus, both reproducibility and repeatability studies prove and emphasize, respectively, the precision and accuracy presented by this method for mcDNA quantification.

Table 3
Inter-day precision for the assessment of mcDNA (n = 3).

Nominal Concentration (µg/mL)	Mean Concentration[a] (µg/mL)	Standard Deviation	CV[b] (%)	Mean relative Error[c] (%)
17.5	17.13	0.90	5.27	2.10
5	5.04	0.06	1.11	0.70
2.5	2.67	0.20	7.59	6.74

[a] Calibration curve used (y = mx + b): m = 0.9416; b = - 0.2781; R2 = 0.999.
[b] Coefficient of variation.
[c] ([(Measured concentration)–(nominal concentration)]/(nominal concentration)) x 100.

Table 4
Assessment of sc pDNA in lysate samples enriched with sc pDNA in different concentrations (2.5, 5 and 10 µg/mL) (n = 3).

Nominal Concentration (µg/mL)	Mean Concentration[a] (µg/mL)	Standard Deviation	CV[b] (%)	Mean relative Error[c] (%)
10	10.76	0.14	1.31	7.60
5	5.60	0.25	4.45	12.02
2.5	2.50	0.25	10.04	0.17

[a] Calibration curve used (y = mx + b): m = 0.9416; b = - 0.2781; R2 = 0.999.
[b] Coefficient of variation.
[c] ([(Measured concentration)–(nominal concentration)]/(nominal concentration)) x 100.

3.6. mcDNA assessment in process solutions

After completing the validation of the method through these different required parameters, it was necessary to evaluate in a more real context the ability of this chromatographic strategy to assess mcDNA content in a complex sample. In order to verify this, PP clarified lysate samples were prepared and supplemented with known amount of purified sc mcDNA to obtain known mcDNA concentrations in a complex sample (2.5, 5 and 10 µg/mL). The respective chromatograms (4A) and electrophoresis (4B) are collected in Fig. 4. As it is perceivable, RNA is promptly eluted in the first step, followed by mcDNA elution in the second step and elution of high-weight molecules (PP) in the third step. Each of these assays were performed three times for the assessment of mcDNA concentration through peak area, as performed for the accuracy studies. The back-calculated concentrations are gathered in Table 4. The standard with the highest mean relative error (12.02%) was 5 µg/mL, while the standard presenting highest coefficient of variation (10.04%) was 2.5 µg/mL. Mota and co-workers obtained similar

values (8.94% and 11.26%, respectively) to the ones obtained in this study [11]. Such high values might be related with the fact that these samples present a more diversified content, due to the presence of several host impurities. Nonetheless, both values remain below the 15% limit range accepted by the guidelines, therefore suggesting this analytical method can be reliably applied in a complex mixture. Besides proving its application, this assay highlights the selectivity presented by this analytical method for sc mcDNA quantification. Such feature, coupled with the novelty of this mcDNA study, underlines the potential of cadaverine as an amino-acid derivative affinity-chromatography ligand [16].

Further applicability of the discussed methodology was tested in the mcDNA lysate sample, such as the one presented in Fig. 2A. This technique has potential in Process Analytical Technology (PAT) for monitoring the amount of mcDNA and impurities in laboratory and/or industrial upstream and downstream processing. To quantify the amount of mcDNA present in the sample it is essential to use the calibration curve previously obtained, while relative nucleic acid purity is assessed by calculating the area percentage of mcDNA peak versus the total area of all found peaks. By using this approach, it was possible to quantify the presence of 8.9 μg/mL sc mcDNA and determine a purity of 3% in the chromatographic run corresponding to Fig. 2A. Such low purity was expected, accounting for the presence of RNA and PP in the lysate sample. This result reassures the standard curve range was suitably selected, considering this result is within its range (1–25 μg/mL).

3.7. Robustness

The fact that this strategy requires the use of a very specific ionic strength for mcDNA isolation, suggests that this approach is indeed very sensitive and selective. In the beginning of this study it was found that temperature, together with the buffer ionic strength, can affect the final conductivity, increasing the mcDNA molecules retention as a consequence of the temperature increase. This led to the close monitoring of the temperature throughout all assays by working in a controlled and climatized room, with the intention of keeping it at 25 °C. This allowed to achieve reliable results between different assays. Nonetheless, the composition and structure of the target molecule can also interfere with such selectivity [17]. For example, a comparative study based on the injection of different oligonucleotides (differing in size and composition) in different amino acid-based chromatographic matrices (histidine, arginine and lysine) has shown that each one of these ligands interact differently with the diverse oligonucleotides [18]. Also, for the same ligand, different retention patterns were achieved for the oligonucleotides in study, depending on their size and bases composition [18]. Thus, it could be supposed that the selectivity of the ligand and the applicability of the present method could be dependent on the features of the mcDNA molecule. To further prove the robustness of the methodology described in this study, a comparison between mcDNA vectors with different sizes and composition was performed. In Fig. 5A the chromatogram and respective electrophoresis of a mcDNA molecule with 0.88 Kbp is presented, while in Fig. 5B the chromatogram and respective electrophoresis of a mcDNA molecule with 5 Kbp is shown. The same chromatographic conditions were used for 0.88 Kbp and 5 Kbp mcDNA, as they were established for 3.8 Kbp. In Fig. 5A, isolation of the 0.88 Kbp sc mcDNA was achieved with some sc PP contamination, while in Fig. 5B the recovery of 5 Kbp sc mcDNA together with some sc and oc PP content was verified in the main peak 2. For both assays, the electrophoresis suggests no loss of mcDNA, since all mcDNA content is found in the second step of the gradient (peak 2). These results underline the applicability of cadaverine as a ligand for mcDNA isolation, but small adjustments may be required and can be performed when working with different mcDNA samples to maintain the same purity degree. However, the selectivity of cadaverine ligand towards mcDNA isolation is undeniable given its ability to isolate two extremely different mcDNAs (with a 5 times size difference) under the same exact chromatographic conditions. To the best of our knowledge, it is also the first time that it is reported a comparative study of the behaviour of mcDNA molecules with different sizes and composition, through the use of the same purification strategy.

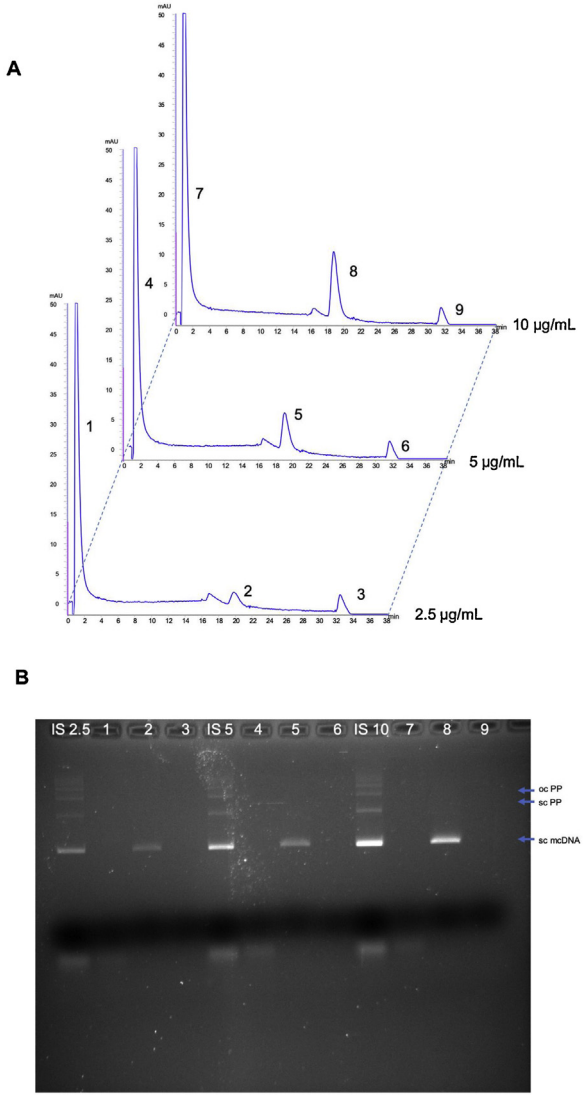

Fig. 4. Chromatographic profile and electrophoresis of the PP clarified *E. coli* lysate supplemented with known mcDNA concentrations in the cadaverine-modified monolith. Chromatographic runs performed with 1.07 M NaCl in 10 mM Tris–HCl/EDTA (pH 7.0, 91.01 mS/cm), followed by 1.16 M NaCl in 10 mM Tris–HCl/EDTA (pH 7.0, 96.72 mS/cm) and 1.3 M NaCl in 10 mM Tris–HCl/EDTA (pH 7.0, 106.2 mS/cm). A) Chromatographic runs for PP clarified lysate sample supplemented with 2.5, 5 and 10 μg/mL. B) Agarose gel electrophoresis of the different peaks. Lane IS 2.5 μg/mL – Initial Sample of PP lysate supplemented with 2.5 μg/mL; Lane 1–3 - Samples corresponding to the respective chromatographic peaks; Lane IS 5 μg/mL – Initial Sample of PP lysate supplemented with 5 μg/mL; Lane 4–6 - Samples corresponding to the respective chromatographic peaks; Lane IS 10 μg/mL – Initial Sample of PP lysate supplemented with 10 μg/mL; Lane 7–9 - Samples corresponding to the respective chromatographic peaks. C) Chromatographic run for mcDNA lysate sample for mcDNA content assessment.

4. Conclusion

In this work, a new methodology for mcDNA quantification and analysis is proposed, resorting to a chromatographic strategy

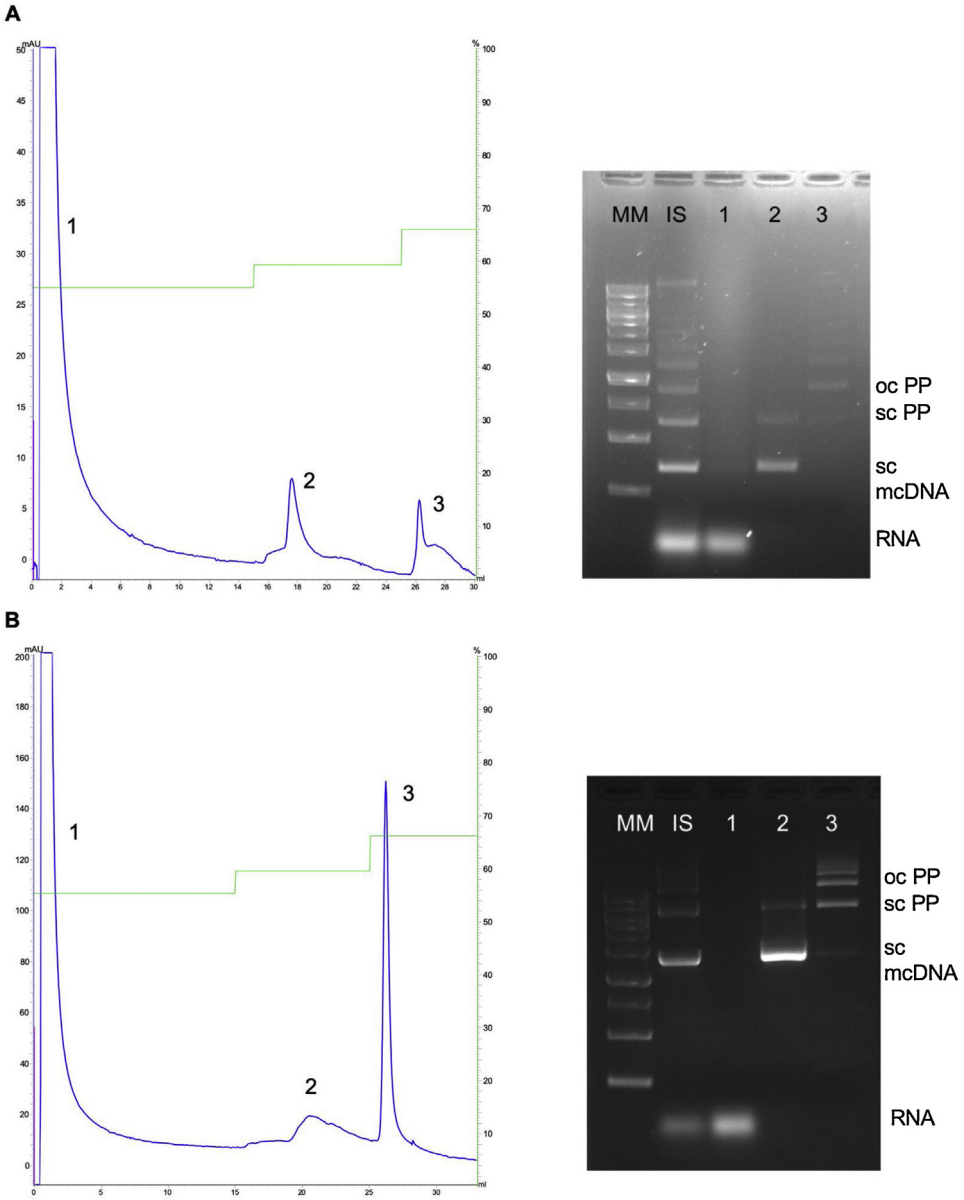

Fig. 5. Chromatographic profile and electrophoresis of the clarified *E. coli* lysate of differently sized mcDNA molecules injected in the analytical cadaverine-modified monolith. Chromatographic runs performed with 1.07 M NaCl in 10 mM Tris-HCl/EDTA (pH 7.0, 91.01 mS/cm), followed by 1.16 M NaCl in 10 mM Tris−HCl/EDTA (pH 7.0, 96.72 mS/cm) and 1.3 M NaCl in 10 mM Tris−HCl/EDTA (pH 7.0, 106.2 mS/cm). A) Chromatographic run for 0.88 Kbp mcDNA clarified *E. coli* lysate and corresponding electrophoresis. B) Chromatographic run for 5 Kbp mcDNA clarified *E. coli* lysate and corresponding electrophoresis. Lane IS – Initial Sample; Lane 1–3 - Samples corresponding to the respective chromatographic peaks.

that had been previously established for mcDNA isolation with cadaverine-modified chromatographic monolith. Linearity, precision and accuracy were proven suitable within 1–25 μg/mL mcDNA concentration range and the LLOQ and LOD were established as 1 μg/mL. Supplementation studies demonstrated the applicability of this method for mcDNA quantification in a complex mixture. Also, for the first time, different mcDNA – PP size pairs (with mcDNAs presenting a size varying from 0.88 to 5 Kbp) were analysed under the same chromatographic conditions to assess its elution tendency, demonstrating the robustness of this new analytical column.

This study demonstrates for the first time the development of a mcDNA quantification chromatographic methodology employing CIM chromatographic monoliths that can be gently adjusted to suit different mcDNA – PP pairs. Contrarily to expensive qPCR methods that have been currently used for mcDNA analysis/quantification, this strategy is more economic and less time-consuming, especially when it is necessary to control mcDNA production and purification. Such achievement might represent in the future a useful tool for the biotechnological industry regarding the preparation of mcDNA biopharmaceuticals.

CRediT authorship contribution statement

A.M. Almeida: Conceptualization, Investigation, Formal analysis, Visualization, Writing - original draft. **U. Černigoj:** Resources, Validation, Writing - review & editing. **J.A. Queiroz:** Writing - review & editing. **F. Sousa:** Supervision, Writing - review & edit-

ing. **A. Sousa:** Conceptualization, Resources, Supervision, Writing - review & editing.

Acknowledgements

This work was supported by FEDER funds through the POCI - COMPETE 2020 - Operational Programme Competitiveness and Internationalization in Axis I - Strengthening research, technological development and innovation (Project POCI-01-0145-FEDER-007491) and National Funds by FCT - Foundation for Science and Technology (Project UID/Multi/00709/2019). Also, A.M. Almeida acknowledges a doctoral fellowship (SFRH/BD/102284/2014) from FCT.

Appendix A. Supplementary data

Supplementary material related to this article can be found, in the online version, at doi:https://doi.org/10.1016/j.jpba.2019.113037.

References

[1] V.M. Gaspar, C.J. Maia, J.A. Queiroz, C. Pichon, I.J. Correia, F. Sousa, Improved minicircle DNA biosynthesis for gene therapy applications, Hum. Gene Ther. Methods 25 (2014) 93–105, http://dx.doi.org/10.1089/hgtb.2013.020.

[2] A.M. Almeida, J.A. Queiroz, F. Sousa, A. Sousa, Minicircle DNA purification: performance of chromatographic monoliths bearing lysine and cadaverine ligands, J. Chromatogr. B Anal. Technol. Biomed. Life Sci. 1118–1119 (2019) 7–16, http://dx.doi.org/10.1016/j.jchromb.2019.04.024.

[3] T. Diamantino, P. Pereira, J.A. Queiroz, Â. Sousa, F. Sousa, Minicircle DNA purification using a CIM® DEAE-1 monolithic support, J. Sep. Sci. 39 (2016) 3544–3549, http://dx.doi.org/10.1002/jssc.201600375.

[4] C.P.A. Alves, M. Šimčíková, L. Brito, G.A. Monteiro, D.M.F. Prazeres, Development of a nicking endonuclease-assisted method for the purification of minicircles, J. Chromatogr. A 1443 (2016) 136–144, http://dx.doi.org/10.1016/j.chroma.2016.03.035.

[5] P. Mayrhofer, M. Blaesen, M. Schleef, W. Jechlinger, Minicircle-DNA production by site specific recombination and protein-DNA interaction chromatography, J. Gene Med. 10 (2008) 1253–1269, http://dx.doi.org/10.1002/jgm.1243.

[6] X.H. Hou, X.Y. Guo, Y. Chen, C.Y. He, Z.Y. Chen, Increasing the minicircle DNA purity using an enhanced triplex DNA technology to eliminate DNA contaminants, Mol. Ther. — Methods Clin. Dev. 1 (2015) 14062, http://dx.doi.org/10.1038/mtm.2014.62.

[7] U.S.F, D. Administration, Guidance for industry: bioanalytical method validation, in: Draft Guidance, 2013, /documents/FDA/FDA-Others/Laboratory/f-507-bioanalytical-4252fnl.pdf http://www.labcompliance.de.

[8] M.M. Diogo, J. a Queiroz, G. a Monteiro, S. a Martins, G.N. Ferreira, D.M. Prazeres, Purification of a cystic fibrosis plasmid vector for gene therapy using hydrophobic interaction chromatography, Biotechnol. Bioeng. 68 (2000) 576–583, http://dx.doi.org/10.1002/(SICI)1097-0290(20000605)68:5<576::AID-BIT13>3.0.CO;2-5 [pii].

[9] Â. Sousa, F. Sousa, J.A. Queiroz, Advances in chromatographic supports for pharmaceutical-grade plasmid DNA purification, J. Sep. Sci. 35 (2012) 3046–3058, http://dx.doi.org/10.1002/jssc.201200307.

[10] A. Sousa, C.T. Tomaz, F. Sousa, J.A. Queiroz, Successful application of monolithic innovative technology using a carbonyldiimidazole disk to purify supercoiled plasmid DNA suitable for pharmaceutical applications, J. Chromatogr. A 1218 (2011) 8333–8343, http://dx.doi.org/10.1016/j.chroma.2011.09.033.

[11] É. Mota, Â. Sousa, U. Černigoj, J.A. Queiroz, C.T. Tomaz, F. Sousa, Rapid quantification of supercoiled plasmid deoxyribonucleic acid using a monolithic ion exchanger, J. Chromatogr. A 1291 (2013) 114–121, http://dx.doi.org/10.1016/j.chroma.2013.03.070.

[12] M.M. Diogo, J.A. Queiroz, D.M.F. Prazeres, Assessment of purity and quantification of plasmid DNA in process solutions using high-performance hydrophobic interaction chromatography, J. Chromatogr. A 998 (2003) 109–117, http://dx.doi.org/10.1016/S0021-9673(03)00618-6.

[13] F. Sousa, J.A. Queiroz, Supercoiled plasmid quality assessment by analytical arginine-affinity chromatography, J. Chromatogr. A 1218 (2011) 124–129, http://dx.doi.org/10.1016/j.chroma.2010.11.002.

[14] S.G.L. Quaak, B. Nuijen, J.B.A.G. Haanen, J.H. Beijnen, Development and validation of an anion-exchange LC-UV method for the quantification and purity determination of the DNA plasmid pDERMATT, J. Pharm. Biomed. Anal. (2009), http://dx.doi.org/10.1016/j.jpba.2008.11.011.

[15] J. Van Loco, M. Elskens, C. Croux, H. Beernaert, Linearity of calibration curves: use and misuse of the correlation coefficient, Accredit. Qual. Assur. (2002), http://dx.doi.org/10.1007/s00769-002-0487-6.

[16] F. Sousa, C. Cruz, J.A. Queiroz, Amino acids-nucleotides biomolecular recognition: from biological occurrence to affinity chromatography, J. Mol. Recognit. (2010), http://dx.doi.org/10.1002/jmr.1053.

[17] Â. Sousa, P. Pereira, F. Sousa, J.A. Queiroz, Binding mechanisms for histamine and agmatine ligands in plasmid deoxyribonucleic acid purifications, J. Chromatogr. A 1366 (2014) 110–119, http://dx.doi.org/10.1016/j.chroma.2014.09.031.

[18] A. Sousa, F. Sousa, J.A. Queiroz, Differential interactions of plasmid DNA, RNA and genomic DNA with amino acid-based affinity matrices, J. Sep. Sci. 33 (2010) 2610–2618, http://dx.doi.org/10.1002/jssc.201000347.

Paper VIII

Silencing Human Papillomaviruses E6 and E7 oncoproteins with a minicircle DNA vector encoding pri-miR-375

A.M. Almeida, J.A. Queiroz, F. Sousa, A. Sousa

CICS-UBI – Centro de Investigação em Ciências da Saúde, Universidade da Beira Interior, Av. Infante D. Henrique, 6200-506 Covilhã, Portugal

(Currently under study)

Short description: An original research paper focusing the construction of a minicircle DNA bearing genetic information for silencing of E6 and E7 oncoproteins and evaluation of its *in vitro* performance

Abstract

The link between the infections caused by Human Papillomaviruses (HPV) and the development of cervical cancer has long been established. HPV high risk types such as HPV16 and HPV18 express E6 and E7 oncoproteins, which interfere with cell cycle regulation and repair mechanisms by downregulating the expression of tumor suppressors such as p53 and pRB, respectively. Due to this problematics, researchers have been focused on innovative treatment options, and the interest in silencing harmful proteins has been rising. Minicircle DNA (mcDNA) is a new vector whose efficacy has been proven to be higher than the highly studied plasmid DNA (pDNA). This work describes the preparation of a mcDNA encoding the pri-miR-375 gene, aiming to increase the microRNA-375 (miR-375) expression in cervical cancer cells to silence HPV E6 and E7 oncoproteins. E6 and E7 transcript levels were assessed and found to be nearly 80% diminished 24 hours after transfection of CaSki cells, a HPV16-infected cervical cancer model. Proliferation studies demonstrated growth arrest for CaSki cells throughout 72 hours, while viability of these cells was also found gradually decreasing for the same time period. Moreover, a comparison between mcDNA and its parental plasmid, the pDNA molecule which originates mcDNA, demonstrated that mcDNA displays higher effect on E6 and E7 transcripts silencing, proving the increased efficacy of this cutting-edge non-viral DNA technology. These results suggest that mcDNA-pri-miR-375 has potential to be further explored in a near future as therapeutic DNA vector in the treatment of HPV-caused cervical cancer.

Keywords

Cervical cancer; Gene silencing; Human Papillomavirus; minicircle DNA; miR-375

1. Introduction

Cervical cancer is a health problem common to a variety of countries, especially underdeveloped ones. Due to lack of health conditions and appropriate vaccine distribution, Eastern and Central Africa remain as the regions most affected worldwide [1]. Human Papillomavirus (HPV) plays a crucial role in cervical cancer development. In fact, HPV DNA has been detected in between 79% to 100% invasive cervical cancer cases worldwide [2,3]. The presence of such viral genome leads to the expression of E6 and E7 oncoproteins, which in turn are responsible for the impairment of cell regulation and proliferation mechanisms [4,5]. These oncoproteins interfere with important tumor suppressor proteins such as p53 and pRB. While E6 is responsible for the low p53 levels by inducing its degradation, E7 binds to pRB inactivating its function as E2F transcription factor regulator [4,5]. Thus, considering the relevance that E6 and E7 have in cervical cancer development, current therapeutic strategies are mainly focused on targeting these proteins [1].

One approach that has recently been gaining a lot of attention is gene silencing. Many efforts have been placed to explore the silencing of these harmful proteins through the use of artificial RNA vectors, such as small-interfering RNA (siRNA), or gene editing technologies, such as clustered regularly interspaced short palindromic repeats (CRISPR) [1]. However, increasing attention has been given to the use of microRNAs (miRNAs) for such goal. MiRNAs are small non-coding RNA molecules, which have been proved to regulate cellular mechanisms, by regulating gene expression at post-transcriptional level. These are first naturally expressed as primary miRNA transcripts (pri-miRNA) in the nucleus, followed by processing into precursor miRNA (pre-miRNA) before being transported to the cytoplasm to be processed into mature miRNA (miR) [1]. In the cytoplasm, miRNAs associated to the RNA-induced silencing complex enable the recognition of mRNAs whose nucleotide sequence is complementary to the miRNA [6]. Then, accordingly to the complementary level displayed between mRNA and miRNA, the targeted mRNA molecule can be inactivated or degraded [6,7]. MiR-375 is a miRNA which has been found down-regulated in cervical cancer [8]. In fact, different studies performed under this context have unveiled the potential of miR-375 as a therapeutic tool for cervical cancer: the overexpression of this miRNA leads to the decrease of E6 and E7 mRNA and protein levels, consequently increasing the p53 and pRB tumor suppressor levels and interfering with the proliferation and invasion of HPV-infected cancer cells [8–10]. Thus, the study of such approach as a therapeutic treatment for cervical cancer seems very interesting and promising.

Minicircle DNA (mcDNA) is an innovative non-viral DNA vector, which is considered safer and more effective than the popular plasmid DNA (pDNA) [11]. This molecule is devoid of bacterial sequences, presenting only the eukaryotic genes necessary for therapeutic purposes. Such structural feature is accomplished through the production of a parental plasmid (PP) molecule, which presents both prokaryotic and eukaryotic sequences required for its production in bacteria, and for the therapeutic effect, respectively [11,12]. However, the PP molecule can

be recombined into two different molecules, originating the miniplasmid (mP), containing the prokaryotic sequences, and the mcDNA molecule, containing the eukaryotic sequences [12]. The elimination of the prokaryotic sequences renders mcDNA as a smaller molecule, which facilitates its entry into the targeting cells. Moreover, the lack of these bacterial sequences increases the expression of the target gene, considering the fact that these sequences have been proven to silence the expression of pDNA due to the formation of repressive heterochromatin [13]. Consequently, mcDNA displays higher expression levels than the conventional pDNA, which can consequently contribute to different therapeutic outcomes [14-16]. Therefore, this work consisted in the construction of a mcDNA vector able to encode the pri-miR-375 for further assessment of its potential in decreasing the expression of E6 and E7 oncoproteins in a HPV-infected cervical cancer cell model. CaSki cell line was selected as the cancer cell model to be used for this study due to its HPV high copy level in comparison to other well-known HPV-infected cervical cancer models such as HeLa or SiHa [17]. For that, a comparison between the efficacy of PP and mcDNA on oncoproteins silencing effect was performed. 2 - Methods

2.1. Construction and production of mcDNA-pri-miR-375

The pMC.CMV-MCS-EF1-GFP-SV40Poly A empty PP vector was amplified by *E. coli* ZYCY10P3S2T bacterial growth in Terrific Broth medium (20 g/L of tryptone, 24 g/L of yeast extract, 4 mL/L of glycerol, 0.017 M KH_2PO_4, 0.072 M K_2HPO_4) supplemented with 50 µg/mL of kanamycin at 250 rpm, 42 ºC. Pri-miR-375-containing pcDNA-3 plasmid was purchased from Genescript Limited (Hong Kong) and used as a template for Polymerase Chain Reaction (PCR) for pri-miR-375 fragment amplification. For PCR, primers pri-miR-375 FW 5'-CGGGACAAGCTCCAAGGCGT and pri-miR-375 RV 5'- TTTCCACCTCCAGAAGGGTT were used. PCR was first carried out at 95 ˚C for 5 min, followed by 30 cycles of 95 ˚C for 40 sec, 60 ˚C for 30 sec and 72 ˚C for 1 min, before proceeding 5 minutes at 72 ˚C. For cloning, XbaI and BamHI enzymes were used to digest PP empty vector and pri-miR-375 fragment before using T4 DNA Ligase (NZYTech – Genes and Enzymes, Portugal), according to the manufacturer's instructions. Through thermal shock, competent *E. coli* ZYCY10P3S2T bacteria were transformed with the resultant cloning mixture. Positive colonies were isolated from LB – agar plates and PP-pri-miR-375 cloning was confirmed by pri-miR-375 PCR. To produce mcDNA-pri-miR-375, PP-pri-miR-375 was amplified, as aforementioned, until an optic density of 5 was attained, followed by PP recombination induction through 0.01% L-Arabinose addition. Induction was carried out for 3 hours at 32 ˚C, before bacteria were recovered through centrifugation and stored at -20 ˚C.

2.2. PP and mcDNA extraction and purification

For PP extraction and purification, NZYMaxiprep commercial kit (NZYTech, Lisbon, Portugal) for pDNA isolation was used according to the manufacturer's instructions. To recover mcDNA from bacteria, given the lack of commercial kits available for mcDNA purification, an alkaline modified lysis was first performed according to Diogo and co-workers [18]. The resulting sample

was desalted with PD-10 desalting columns (GE Healthcare, Buckinghamshire, UK) and the supercoiled (sc) mcDNA isoform was purified from host impurities, other mcDNA isoforms or PP non-recombined molecules, as described by Almeida and co-workers [19]. Briefly, a chromatographic column with a bed height of 60 cm containing 121 mL of Sephacryl SF-1000 matrix was coupled to an AKTA Pŭre system (GE Healthcare, Buckinghamshire, UK). A volume of 2 mL of clarified mcDNA complex sample was injected to the column and separated by size exclusion with a flow of 0.3 mL/min and UV detection at 260 nm. The target peak containing sc mcDNA was concentrated and desalted with Vivaspin® 6 Centrifugal Concentrator (Vivaproducts, Littleton, MA, USA), for further assays.

2.3. Cell culture and transfection

HPV-16 infected cervical cancer (CaSki) and fibroblast cell lines were used for *in vitro* studies. Cell growth was carried out at 37 ˚C, 5% CO_2 with RPMI (CaSki) and DMEM-F12 (fibroblasts) medium supplemented with 10% (v:v) of fetal bovine serum (FBS) and 1% (v:v) of antibiotic mixture of penicillin (100 µg/mL) and streptomycin (100 µg/mL). The day before transfection, cells were deprived from antibiotic. Cell transfection with PP-pri-miR-375 and mcDNA-pri-miR-375 was carried out with Torpedo (Ibidi, Martinsried, Germany), according to manufacturer's instructions (ratio 3:1 - reagent:mcDNA) and, 6 hours later, medium containing antibiotic was re-established.

2.4. FITC staining and mcDNA uptake

To assess mcDNA entry, CaSki cells were grown in 8 µ-slide 8 well (Ibidi, Martinsried, Germany) before 80-90% confluence was reached. Afterwards, purified mcDNA sample was stained as described by Almeida and co-workers [20]. Once the mcDNA was labeled with FITC, complexation with Torpedo (Ibidi, Martinsried, Germany) was performed and CaSki cells were transfected. After 6 hours, cells were fixed with 4% paraformaldehyde, nuclei were stained with Hoescht and the µ-slides were visualized through LSM710 confocal laser scanning microscope (Carl Zeiss, Germany) under a 633 magnification and analyzed with the Zeiss LSM 710 laser scanning confocal microscope (Carl Zeiss SMT, Inc., Oberkochen, Germany).

2.5.RNA extraction, RT-PCR and RT-qPCR

To assess miR-375, E6 and E7 transcripts, CaSki cells were seeded with a density of 6.86 x 10^4 cells/cm^2 in 12-well plates, and after 24 h of transfection, the total RNA extraction of transfected and non-transfected cells was performed resorting to TripleXractor reagent (Grisp Research Solutions, Porto, Portugal), following the manufacturer's instructions. For E6 and E7 transcripts, 1 µg of total RNA was reversed transcribed into cDNA with the Xpert cDNA Synthesis (GRiSP - Research Solutions, Portugal) according to the manufacturer's instructions. For miR-375 transcripts, cDNA was synthetized by using a stem-loop primer specifically designed for miR-375, as described by Wang and co-workers [8]. Afterwards, RT-PCR was carried out with

NZYTaq2x Green MasTerMix (NZYtech, Lisbon, Portugal) at the following conditions: 95 ˚C for 5 minutes, 30 cycles at 95 ˚C for 30 seconds, 60 ˚C for 30 seconds and 72 ˚C for 1 minute and final extension at 72 ˚C for 5 minutes. The primers used for this methodology are the following: miR-375 stem-loop: 5' GTCGTATCCAGTGCAGGGTCCGAGGTATTCGCACTGGATACGACTCACGC; miR-375 FW: 5' GCCGTTTGTTCGTTCGGCT; miR-375 RV: 5' GTGCAGGGTCCGAGGT; E6 FW : 5'-CAGGAGCGACCCAGAAAGTT; E6 RV: 5- GTCATATACCTCACGTCGCAGT; E7 FW: 5'-TCCAGCTGGACAAGCAGAACCGGA; E7 RV: 5'- GCACACAATTCCTAGTGTGCCCAT. On the other hand, RT-qPCR was carried out as previously described by Almeida and co-workers [20]. Primers for GAPDH housekeeping gene were employed for data normalization and its constitution is the following: FW: GAPDH 5'- ATGGGGAAGGTGAAGGTCG; GAPDH RV: 5'-GGGGTCATTGATGGCAACAATA. Statistical analysis was performed with one-way ANOVA, with an N=3, resorting to GraphPad Prism 7.

2.6. Western Blot

To assess protein content, CaSki cells were seeded with a density of 6.86 x 10^4 cells/cm^2 in 6-well plates and western blot was carried out with 40 µg of protein extracted after 24 hours of transfected and non-transfected CaSki cells. Briefly, all samples were quantified by Bradford micro-assay from BioRad (Hemel Hempstead, UK), before injection in vertical polyacrylamide electrophoresis for protein separation. Electroblotting was performed resorting to Trans-Blot Turbo system (BioRad, Hemel Hempstead, UK), throughout 15 minutes with standard SD pre-programmed protocol. Mouse anti-E6 IgG monoclonal antibody or mouse anti-E7 IgG monoclonal antibody (Santa Cruz Biotechnology, Heidelberg, Germany) were incubated with resulting membranes overnight, with a dilution of 1:200. Then, membranes were incubated with goat anti-mouse IgG polyclonal antibody conjugated with alkaline phosphatase (Santa Cruz Biotechnology Heidelberg, Germany), before 5 minutes incubation with enhanced chemofluorescence, (GE Healthcare, Buckinghamshire, United Kingdom) and were visualized in BioRad FX-Pro-plus (Bio-Rad, Hemel Hempstead, UK).

2.7. Proliferation Assays

To evaluate the mcDNA-pri-miR-375 impact in cell growth, proliferation assays were performed throughout 72 hours with CaSki. Briefly, cells were respectively seeded with a density of 6.86 x 10^4 cells/cm^2 in 12-well plates, to normalize the cell density between wells, transfected as aforementioned and trypsinized after 24, 36, 48 and 72 hours. Then, cells were recovered through centrifugation and viable cells were counted resorting to trypan blue and Neubauer chamber. As a control for normal cancer cell growth, non-transfected cells were trypsinized in each time-point and counted concomitantly. All assays were performed with an N=3 and each N was counted 4 times. Statistical analysis was performed with two-way ANOVA, resorting to GraphPad Prism 7.

2.8. Viability studies

To understand the effect of mcDNA-pri-miR-375 in the viability of CaSki and Fibroblasts after transfection, viability studies were performed with resazurin compound. Briefly, cells were seeded with a density of 6.86 x 10^4 cells/cm^2 and 3.33 x 10^4 cells/cm^2, respectively, in 96 well plates and transfections were carried out at 24, 36, 48 and 72 hours. Resazurin was prepared at 0.1% (m/v) and added to each well to a concentration of 20%. After 4 hours incubation, the resazurin-medium mixture was transferred and fluorescence was read in SpectraMAX Gemini EM (Molecular Devices,USA) Microplate Reader at 544 nm excitation and 590 nm emission wavelengths. Non-transfected cells were used as negative control and non-transfected cells treated with 70% ethanol were used as positive control. All assays were performed with an N=4 and statistical analysis was performed with two-way ANOVA test in GraphPad Prism 7.

3. Results and discussion

Despite all the efforts that have been dedicated to the prevention and treatment of HPV infection, the reality is that many countries are still affected by the infection caused by this virus and new therapeutic methodologies should be explored [1].

Considering the potential that miR-375 has shown in silencing HPV oncoproteins, pri-miR-375 gene was synthetized and cloned into PP backbone. After PCR confirmation, bulk production was performed, alongside with recombination and purification, for the attainment of sc mcDNA-pri-miR-375 for further transfection studies, through the use of methodologies previously established by our research group [12,19]. For *in vitro* studies, a commercial transfection agent was chosen, given our aim was to understand the therapeutic effect of the newly constructed mcDNA-pri-miR-375 vector. At first, to guarantee that the transfection conditions suggested by the manufacturer were adequate for mcDNA entry in CaSki cells, fluorescent labeling was performed with FITC and cell entry was detected 6 hours after transfection, as suggested by the manufacturer and presented in figure 1. The presence of labeled-mcDNA inside the nucleus of CaSki cells confirmed the efficacy of the transfection protocol, suggesting that further studies could be performed under these conditions.

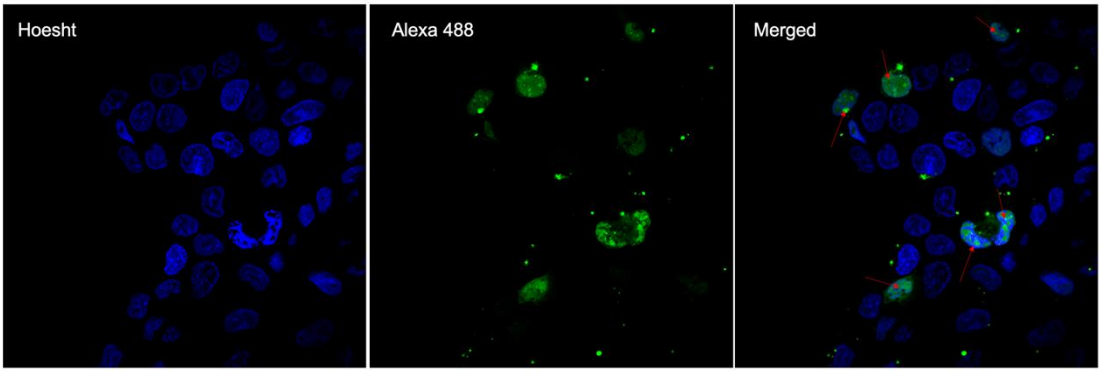

Figure 1 – McDNA transfection of CaSki cells, 6 hours after. The blue staining represents the cell nucleus while the green staining represents FITC-labeled mcDNA.

Therefore, after guaranteeing mcDNA transfection, it was necessary to evaluate the correct expression of pri-miR-375 and its processing into mature miR-375. Thus, after 24 hours of transfection, CaSki cells were harvested and total RNA was extracted before cDNA was synthetized. To correctly synthetize cDNA from miR-375, a protocol described by Wang and colleagues was applied, resorting to the use of a stem-loop primer specifically designed for miR-375 [8]. In figure 2A is presented the electrophoresis performed for miR-375 RT-PCR. As perceivable, band density seems to be less intense in non-transfected cells, comparatively to PP and mcDNA transfected cells. This could be indicative that PP and mcDNA are correctly overexpressing miR-375, comparatively to the natural miR-375 expression in CaSki cells. However, such illation should not be taken right away as a proof of the pri-miR-375 gene effectiveness. It is necessary to evaluate the transcripts of E6 and E7 genes to understand if they present a decreased level in transfected cells. Therefore, the evaluation of E6 and E7 mRNA transcripts were performed by PCR for RNA samples of CaSki cells collected 24 hours after transfection, as presented in figure 2B. It is possible to verify an intense band for non-transfected cells, which naturally express HPV oncoproteins due to the presence of HPV genome, for both E6 and E7 transcripts. However, a difference is notorious for PP and mcDNA samples. For both transcripts, PP presents a very lighter band, comparatively to non-transfected cells, while mcDNA does not present any band. First of all, these data further suggest that pri-miR-375 is correctly being processed into miR-375 and it is acting on E6 and E7 silencing, due to the lighter/none band displayed by transfected cells. Furthermore, it is possible to perceive the different outcome between PP-pri-miR-375 and mcDNA-pri-miR-375 vectors. This difference suggests that mcDNA has a better performance than PP, in accordance with other works performed within this thematic. For instance, Wu and co-workers designed a study to compare the therapeutic outcome of mcDNA and pDNA vectors bearing the liver regeneration/ growth factor ERV1-like (ALR/GFER) gene [16]. In their preliminary studies, higher expression from mcDNA vector, comparatively to pDNA, was detected. This led researchers to adjust the final mcDNA dose, which would be administrated to liver fibrosis disease rats, to 30% of the pDNA final dose. Even with this adjustment, rats treated with mcDNA

demonstrated an increased therapeutic effect than rats treated with pDNA. Thus, it is noticeable the increased potential of mcDNA as a non-viral vector. To further confirm these results, RT-qPCR was performed for analysis of these oncoproteins mRNA expression between PP-, mcDNA-transfected and non-transfected cells. In figure 3A and 3B is portrayed the results obtained for the expression of E6 and E7 mRNA, respectively. As it is shown, E6 and E7 mRNA are found to be significantly decreased, nearly 80%, in cells transfected with PP and mcDNA, comparatively to non-transfected cells, further reinforcing the results obtained for PCR. In E6 mRNA assessment, mcDNA-transfected samples demonstrate to be significantly decreased comparatively to PP-transfected samples. This is also in agreement with the findings of Wu and co-workers [16]. However, no difference was visualized between these samples for E7 mRNA assessment, suggesting more data should be collected.

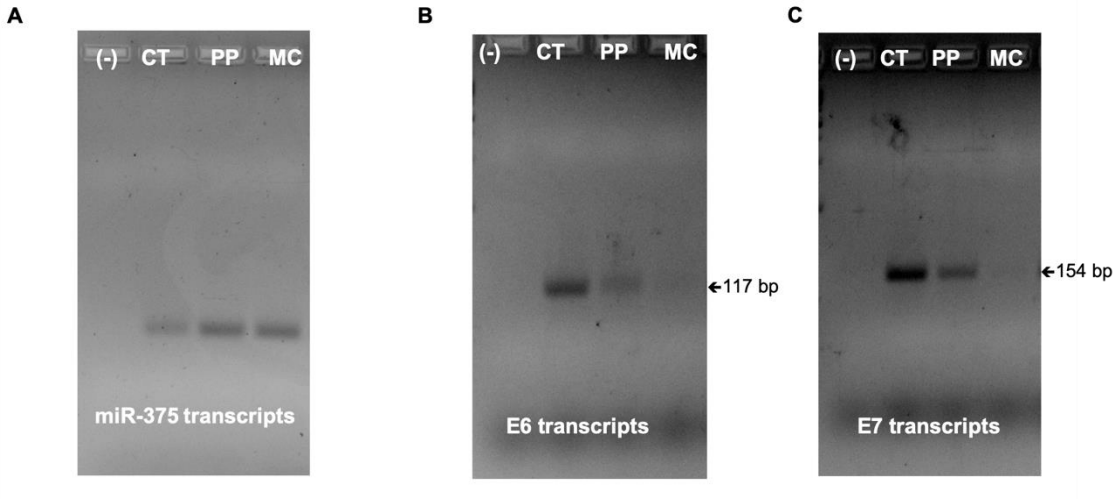

Figure 2 – Electrophoresis RT-PCR result for miR-375 (A), E6 (B) and E7 transcripts (C) after 24 hours transfection of CaSki cells. CT – Non-transfected cells, PP – cells transfected with PP-pri-miR-375, mcDNA – cells transfected with mcDNA-pri-miR-375.

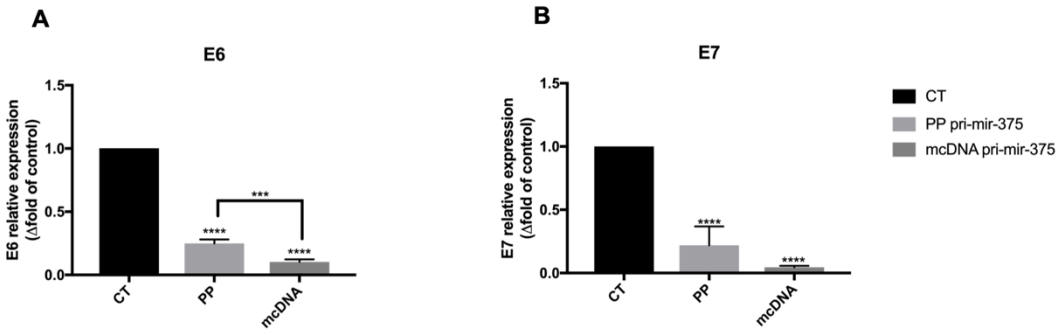

Figure 3 - E6 (A) and E7 (B) mRNA relative expression between PP-, mcDNA-transfected and non-transfected cells, 24 h after transfection (N=3, One-way ANOVA *** P<0.001; **** P<0.0001).

However, it is still necessary to further prove the E6 and E7 decreased expression in the protein content of transfected CaSki cells. Thus, western blot for staining of both proteins was performed for CaSki cells after 24 hours of transfection. In figure 4 is presented the western blot results obtained for E6, E7 and ß-actin proteins. The latter is a housekeeping gene that is normally expressed within cells and is often used for the normalization of western blot techniques. As perceivable, E6 protein content for mcDNA seems to be lower than non-transfected cells and PP protein content. However, such difference is not as notorious as the one observed for E7 protein, where both PP and mcDNA samples demonstrate much lower E7 content than non-transfected cells. These results are in agreement with the data previously obtained by RT-PCR and RT-qPCR. Although this seems very promising, further assays should be performed to obtain more data so that protein quantification can be assessed.

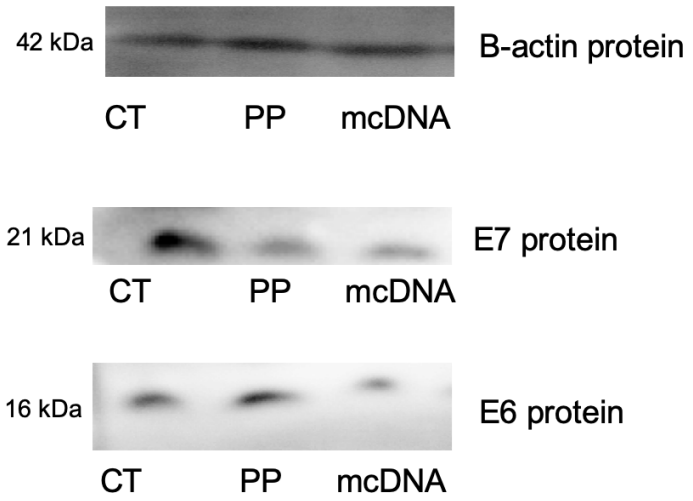

Figure 4 – Western blot results for E6, E7 and ß-actin proteins for 24 hours after transfection of CaSki cells. CT – Non-transfected cells, PP – cells transfected with PP-pri-miR-375, mcDNA – cells transfected with mcDNA-pri-miR-375.

Although E6 and E7 silencing is the general aim of this approach, the influence of this DNA vector in a potential therapeutic effect should be evaluated. This therapeutic effect should rely in the stoppage of cancer cell growth, and perhaps its consequent death. Therefore, proliferation studies were performed with CaSki cells. This assay was based on cell transfection with mcDNA, followed by cell trypsinization at 24, 36, 48 and 72 hours to assess if this vector somehow affected cell growth. In figure 5 is presented the growth curve found for cells transfected with mcDNA (purple), alongside the growth curve obtained for non-transfected cells (blue). It is perceivable that transfected cells present lower proliferation than non-transfected cells. This might be related with the fact that E6 and E7 are being silenced, therefore not being able to trigger the cancer cell mechanism to survive. Thus, with E6 and E7 silencing, tumor suppressors such as p53 and pRB might be rescued from inactivation/degradation, re-

establishing cell repairing mechanism. This hypothesis has been proven by Jung and co-workers, who were able to demonstrate that the increase of miR-375 levels led to the silencing of E6 and E7 proteins and consequent re-establishment of p53 and pRB content in SiHa and HeLa cell lines, cervical cancer models, which are respectively infected by HPV-16 and HPV-18 [9]. Thus, the lower exponential growth displayed by mcDNA transfected cells can be a consequence of the p53 and pRB levels re-establishment, which might be triggering the cell cycle arrest. However, this cannot be proven by proliferation studies, given that other hypothesis could be driving cell quiescence, such as vector toxicity.

Thus, to prove the effect of pri-miR-375 expression in transfected cells is safe for surrounding healthy tissues, viability studies were performed by resorting to resazurin technique. These were carried out in CaSki and fibroblast cell lines to compare the effect this vector presents in malignant and healthy cells, respectively. As perceivable in the results schematized in Figure 6, both cell lines present a significant viability decrease in the first 36 hours. However, from this point on, fibroblasts seem to be able to recover from this viability decrease, being fully restored at 72 hours. On the other hand, CaSki cell line viability loss seems to continue gradually over time, being more significative at 72 hours. This suggests that such loss of viability in fibroblasts might be related with a small influence of the transfection process or some toxicity associated to the transfection reagent, which is known to be slightly aggressive towards cell integrity. In the case of CaSki cells, the viability loss is more evident probably due to the expression of pri-miR-375, which is enabling the silencing of E6 and E7 oncoproteins and re-establishment of p53 and pRB levels.

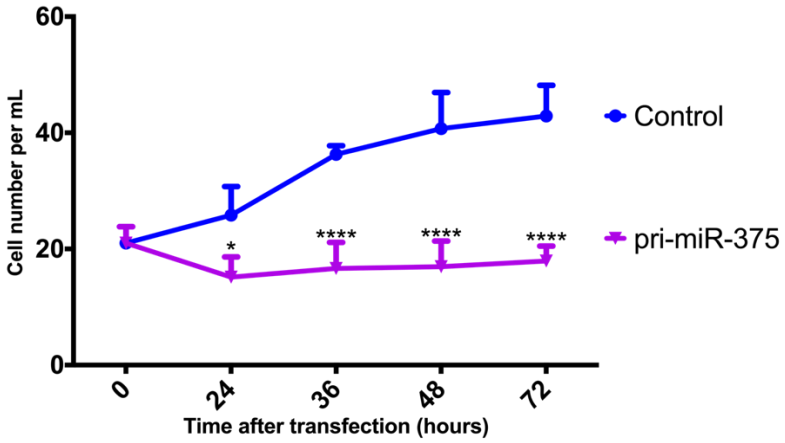

Figure 5 – Proliferation results for non-transfected CaSki cells (blue line) and mcDNA-pri-miR-375 transfected CaSki cells, throughout 72 hours. (N=3, ** $p < 0.05$, **** $p < 0.0001$, compared to non-transfected cells)

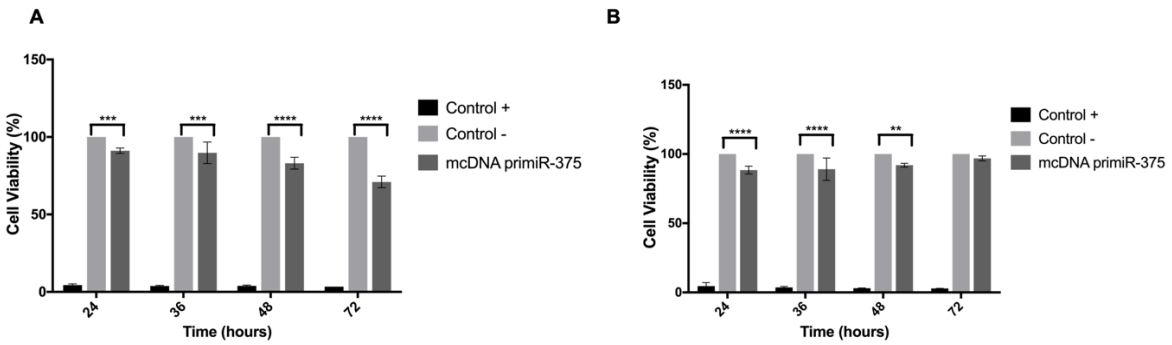

Figure 6 – Viability studies for CaSki (A) and Fibroblast (B) cell lines. Control + – positive control (non-transfected cells incubated with 70% ethanol), Control - – negative control (non-transfected cells), mcDNA-pri-miR-375 – cells transfected with mcDNA-pri-miR-375. (N=3, * $p<0.05$, ** $p< 0.001$, **** $p<0.0001$, compared to negative control)

4. Conclusion and future perspectives

In this study, it was shown that mcDNA-pri-miR-375 vector presents a stronger effect on HPV oncoproteins transcripts silencing, comparatively to PP molecule, highlighting the potential of this innovative non-viral DNA vector. Nonetheless, further assays should be performed to gather significant statistical results to guarantee such effect. Also, this work demonstrated the potential displayed by pri-miR-375 in silencing E6 and E7 proteins, leading to growth arrest in HPV-infected cervical cancer cell line model, CaSki. Also, although fibroblast cell line demonstrated a small viability loss in the first 36 hours after transfection, such viability is recovered and fully re-established by 72 hours. This suggests that the initial loss of viability might be related with commercial transfection reagent toxicity or, perhaps, with the transfection process itself. More studies should be performed to confirm this possibility, such as the administration of the commercial transfection reagent alone. In case this hypothesis is indeed confirmed, it might be concluded that mcDNA-pri-miR-375 does not present a toxic effect towards healthy cells. Nonetheless, to further prove this vector therapeutic effect, p53 and pRB levels should be assessed, followed by apoptosis evaluation.

Acknowledgments

This work was supported by FEDER funds through the POCI - COMPETE 2020 - Operational Programme Competitiveness and Internationalization in Axis I - Strengthening research, technological development and innovation (Project POCI-01-0145-FEDER-007491) and National Funds by FCT - Foundation for Science and Technology (Project UID/Multi/00709/2019). Also, A.M, Almeida acknowledges a doctoral fellowship (SFRH/BD/102284/2014) from FCT.

References

1 Almeida, A.M. et al. (2019) Cervical cancer and HPV infection: ongoing therapeutic research to counteract the action of E6 and E7 oncoproteins. Drug Discov. Today DOI: 10.1016/j.drudis.2019.07.011

2 Rogovskaya, S.I. et al. Human Papillomavirus Prevalence and Type-Distribution, Cervical Cancer Screening Practices and Current Status of Vaccination Implementation in Russian Federation, the Western Countries of the former Soviet Union, Caucasus Region and Central Asia. , Vaccine, 31. (2013)

3 de Sanjose, S. et al. (2010) Human papillomavirus genotype attribution in invasive cervical cancer: a retrospective cross-sectional worldwide study. Lancet Oncol. 11, 1048–1056

4 Vande Pol, S.B. and Klingelhutz, A.J. (2013) Papillomavirus E6 oncoproteins. Virology 445, 115–137

5 Roman, A. and Munger, K. (2013) The papillomavirus E7 proteins. Virology 445, 138–168

6 Pereira, P. et al. Current progress on microRNAs-based therapeutics in neurodegenerative diseases. , Wiley Interdisciplinary Reviews: RNA. (2017)

7 Díaz-González, S.D.M. et al. Utility of MicroRNAs and siRNAs in cervical carcinogenesis. , BioMed Research International. (2015)

8 Wang, F. et al. (2011) MiR-375 is down-regulated in squamous cervical cancer and inhibits cell migration and invasion via targeting transcription factor SP1. Am. J. Pathol. 179, 2580–2588

9 Jung, H.M. et al. (2014) MiR-375 activates p21 and suppresses telomerase activity by coordinately regulating HPV E6/E7, E6AP, CIP2A, and 14-3-3ζ. Mol. Cancer 13,

10 Yu, X. et al. (2016) MiR-375 Affects the Proliferation, Invasion, and Apoptosis of HPV16-Positive Human Cervical Cancer Cells by Targeting IGF-1R. Int. J. Gynecol. Cancer 26, 851–858

11 Mayrhofer, P. et al. (2009) Use of minicircle plasmids for gene therapy. Methods Mol. Biol. 542, 87–104

12 Gaspar, V.M. et al. (2014) Improved Minicircle DNA Biosynthesis for Gene Therapy Applications. Hum. Gene Ther. Methods 25, 93–105

13 Chen, Z.Y. et al. (2008) Silencing of episomal transgene expression in liver by plasmid bacterial backbone DNA is independent of CpG methylation. Mol. Ther. 16, p548-556

14 Chen, Z.Y. et al. (2003) Minicircle DNA vectors devoid of bacterial DNA result in persistent and high-level transgene expression in vivo. Mol. Ther. 8, 495–500

15 Dietz, W.M. et al. (2013) Minicircle DNA is superior to plasmid DNA in eliciting antigen-specific CD8 + T-cell responses. Mol. Ther. 21, 1526–1535

16 Wu, X. et al. (2016) Augmenter of liver regeneration gene therapy using a Novel Minicircle DNA vector alleviates liver fibrosis in rats. Hum. Gene Ther. 27, 880–891

17 Meissner, J.D. (1999) Nucleotide sequences and further characterization of human papillomavirus DNA present in the CaSki, SiHa and HeLa cervical carcinoma cell lines. J.

Gen. Virol. 80, 1725–1733

18 Diogo, M.M. et al. (2000) Purification of a cystic fibrosis plasmid vector for gene therapy using hydrophobic interaction chromatography. Biotechnol. Bioeng. 68, 576–583

19 Almeida, A.M. et al. (2019) The use of size-exclusion chromatography in the isolation of supercoiled minicircle DNA from Escherichia coli lysate. J. Chromatogr. A

20 Almeida, A.M. et al. (2018) HPV-16 targeted DNA vaccine expression: The role of purification. Biotechnol. Prog. 34, 546–551

CHAPTER V

Concluding remarks

This work was designed to explore two different approaches, namely DNA vaccines and gene therapy, by establishing suitable biotechnological platforms for the production of each bioproduct and understanding its potential impact in the treatment of cervical cancer.

In what concerns to the first approach, DNA vaccines, a pDNA molecule containing the genetic information for the expression of E6 and E7 HPV-16 oncoproteins was used. Through the use of a purification strategy previously established by our research group, which resorted to the use of affinity chromatography based on the utilization of a monolithic disk bearing arginine ligands, it was possible to assess the expression efficiency displayed by this vector in *in vitro* studies. Concomitantly, to further comprehend the effect that sc pDNA purity level may exert in the expression of the target proteins, a commercial purification kit was used to obtain the DNA vaccine. *In vitro* studies performed with the DNA vaccine obtained by these two different methods demonstrated that sc content influenced the expression levels displayed by transfected cells. Thus, the sc homogenous DNA vaccine purified by arginine modified monolith exerted a significantly higher expression level than the DNA vaccine obtained by a commercial purification kit, due to the presence of other pDNA isoforms in the latter strategy, highlighting the importance of choosing adequate purification strategies for the maximization of the therapeutic outcome.

Also, a modification of the strategy previously implemented with arginine monolith was explored by preparing an arginine monolith bearing a spacer arm in the purification of this vaccine. This modification was performed with the intention of providing more accessibility of the arginine ligand to the target molecule. The results obtained demonstrate the purification of sc pDNA with binding capacities higher than 1 mg/mL when using a complex lysate sample and 2.53 mg/mL with a pre-purified sc pDNA sample. This data was found to be lower than the one obtained for the previous arginine monolith strategy, possibly due to the occupation of a larger area by the spacer arm, limiting the available arginine ligands. Nonetheless, purity was found to increase in loading conditions due to sample displacement phenomena, as the non-functional isoforms were eluted throughout column loading.

Since DNA vaccines must be efficiently delivered in order to enhance its therapeutic potential, calcium carbonate nano-delivery systems coupled with gelatin were fabricated to encapsulate and deliver the DNA vaccine to dendritic cells. After nanocarrier characterization, *in vitro* studies were carried out to access the ability of this system to promptly deliver the DNA vaccine. After 24 hours, fluorescently labeled pDNA molecules were found within THP-1 dendritic cell line, suggesting transfection occurred with success. This result was later confirmed by RT-PCR detection of E6 transcripts and detection of E6 protein presence in

transfected cells through Western Blot technique, suggesting the DNA vaccine was being correctly expressed. These results suggest that calcium carbonate gelatin nanoplexes are able to efficiently deliver the DNA vaccine to antigen presenting cells, such as dendritic cells, which are cell lines which have been known to be difficult to transfect. This data highlights the potential of said nanocarriers when developing new DNA vaccine strategies.

On the other hand, E6 and E7 protein silencing through gene therapy was also explored for the treatment of cervical cancer with the use of a mcDNA containing genetic information for miR-375 expression. However, before proceeding into the therapeutic evaluation of this vector, it was first necessary to establish suitable strategies for its production and purification. Considering the lack of adequate mcDNA universal purification strategies, a comparison between the utilization of two different monolithic disks was carried out to assess the most promising approach for sc mcDNA purification. Thus, two monolithic disks were prepared, one containing lysine ligands and the other containing cadaverine ligands. It was found that sc mcDNA isolation from a complex sample with cadaverine-modified monolith was the most suitable strategy, allowing the recovery of 78.6% of the injected sc mcDNA, with 98.4% purity and devoid of host components such as genomic DNA, proteins, endotoxins or RNA. The implementation of this strategy without resorting to backbone modification or enzymatic digestion stood as a very promising approach to be scaled-up for industrial mcDNA production. However, it was found that each chromatographic run allowed the purification of a low mcDNA mass (1.97 µg), a feature that could compromise the scale-up of this strategy to a low-cost industrial methodology. With the intention of further improving the obtainment of pure sc mcDNA, size exclusion chromatography was explored.

A column containing Sephacryl SF-1000 matrix was prepared to assess its ability to separate sc mcDNA from a complex sample. After optimizing the necessary chromatographic conditions, the purification of sc mcDNA was successfully achieved with Sephacryl SF-1000, allowing a sc mcDNA yield of 66% and a purity of 98.35%. Also, it was found that host contaminants were within the levels specified by regulatory agencies. Moreover, the use of a larger mcDNA provided insightful information regarding the adjustments that should be performed to obtain pure sc mcDNA with higher sizes, mainly the increase of column size and the lowering of flow rate. Although this strategy allowed the purification of 24.02 µg pure sc mcDNA in a single run, the assays were more time consuming and recovery yield was found to be lower than cadaverine-modified monolith, suggesting that each approach should be applied accordingly with the final aim.

In fact, the results obtained with cadaverine-modified monolith suggested that this strategy could be explored for the implementation of an analytical methodology for mcDNA quality assessment. Currently, few methodologies have been implemented with this finality and are usually expensive or inaccurate. Thus, by making use of the chromatographic conditions previously established for sc mcDNA isolation, an analytical method was implemented resorting

to cadaverine-modified monolith. After thoroughly assessing different parameters necessary for the establishment of an analytical method, a chromatographic quantification methodology was successfully developed and validated for sc mcDNA assessment in pure and complex samples. Moreover, it was possible to verify the robustness of this methodology by assessing its ability in separating differently composed sc mcDNA-PP pairs, requiring only small adjustments to the chromatographic conditions. For the first time, to the best of our knowledge, an analytical chromatographic method was implemented for sc mcDNA assessment, allowing the evaluation of a mcDNA sample within 40 minutes.

Once appropriate conditions were settled for the purification and characterization of sc mcDNA, production of sc mcDNA-pri-miR-375 was carried out for further evaluation of its therapeutic potential in *in vitro* studies. Thus, CaSki, the cervical cancer infected with HPV-16 cell line model, was used to assess the ability of this strategy to suitably silence E6 and E7 oncoproteins. Concomitantly, PP-pri-miR-375 sample was used to compare the expression efficiency of a pDNA-like vector or of a mcDNA. After 24h hours of transfection, cells were retrieved and total RNA was extracted to evaluate miR-375, E6 and E7 transcripts through RT-PCR. It was found that, in comparison to non-transfected cells, both PP and mcDNA samples were able to slightly increase miR-375 content. Moreover, the difference in E6 and E7 transcripts between non-transfected cells and transfected cells was notorious, suggesting miR-375 was indeed being correctly expressed. While non-transfected cells presented a marked band, PP-transfected cells demonstrated a fainter band followed by absence of band for mcDNA-transfected cells. These results seem to highlight the potential displayed by mcDNA in obtaining higher expression efficiencies than conventional pDNA. Afterwards, protein content was assessed to understand if it would corroborate the previously obtained data. Through preliminary western blot analysis, transfected cells also demonstrated lower E6 and E7 content than non-transfected cells. Once the silencing of HPV viral proteins was proven, the impact in cancer cell regulation was evaluated. Proliferation assays were performed to understand if cervical cancer cells, upon silencing E6 and E7 oncoproteins, could maintain the fast proliferation rate associated with cancer cells. It was found that, throughout 72 hours, transfected cells growth would stagnate comparatively to non-transfected cells, suggesting that miR-375 could be re-establishing the mechanisms for cell repairment and growth control. On the other hand, such stagnation could also be synonym that transfection cytotoxicity could be occurring. Thus, viability studies were performed in CaSki and healthy fibroblasts to understand if this behavior was characteristic of cancer cells or if transfection would be affecting non-cancer cells too. It was found that for both cell lines, viability was significantly decreased in the first 36 hours, comparatively to non-transfected cells. However, healthy cells would recover and proliferate afterwards, suggesting that this could be a consequence from the transfection process or toxicity associated to the commercial transfection agent, which is known to be slightly aggressive towards cell integrity.

Overall, this doctoral thesis allowed the study and exploration of two different approaches in the treatment of cervical cancer. In addition, useful and innovative methodologies were developed and established for downstream processing of these biotechnological products, further providing the basis for improvement of other related techniques, especially for mcDNA.

Future trends

To complete the work under preparation in this thesis, and to fully understand miR-375 therapeutic effect in cervical cancer treatment, further *in vitro* studies should be conducted. Besides obtaining more statistical data for E6 and E7 content assessment after transfection, other techniques should be performed to understand the entire impact miR-375 might have in cell regulation of proliferation and death. The use of a scrambled miR will be useful to understand if the obtained results are indeed specific to miR-375 action. Also, the evaluation of tumor suppressor proteins levels, such as p53 and pRB, will allow to confirm that E6 and E7 action has been prevented. Finally, apoptosis evaluation should be performed to assure that controlled cell death is occurring.

On the other hand, different directions can be explored in the future to reach the ultimate approach for developing a suitable cervical cancer treatment. For instance, considering that the presence of CpG motifs in the bacterial backbone of the DNA vaccine might be useful to facilitate the triggering of an immune response, specialized nano-delivery systems should be studied and developed through its functionalization with specific ligands that might direct the delivery of the pDNA vaccine to the antigen presenting cells. This could allow higher antigen expression and, therefore, the elicitation of a stronger immune response with better therapeutic outcome. This therapeutic outcome should ultimately be evaluated resorting to *in vivo* studies with C57BL/6 mice models. Upon injection of cancer cells infected with HPV to induce tumor nodules, the triggering of the therapeutic immune system pathway might be evaluated in these models, followed by tumor regression assessment to comprehend the therapeutic effect displayed by the DNA vaccine.

In what concerns to mcDNA, further methodologies should be expected to rise, given its innovative character. Currently, more upstream and downstream methodologies should be explored to optimize the industrial production of this biotechnological product, since it is the main limitation associated to this vector comparatively to well established pDNA. Moreover, the development of suitably functionalized nano-delivery strategies to cervical cancer cells is imperative, since the more specific the delivery is, the more efficient it will be in expressing the target gene. This will allow to concentrate the therapy used within the tissue area to which it was designed to act, without losing its effect to surrounding tissues. In addition, these delivery systems will allow the protection of mcDNA from degradation, maximizing its delivery and therapeutic action.

Finally, *in vivo* studies should be conducted to understand which of strategies described in this thesis can be more adequate for the treatment of cervical cancer. Eventually, the combination

of both strategies could be performed to assess its potential in maximizing its therapeutic effect against cervical cancer.